

**SYNTHESIS OF FUNCTIONAL LACTIDE COPOLYMERS FOR
USE IN BIOMEDICAL APPLICATIONS**

A Dissertation
Presented to
The Academic Faculty

by

David Edward Noga

In Partial Fulfillment
of the Requirements for the Degree
Doctor of Philosophy in the
School of Chemistry and Biochemistry

Georgia Institute of Technology
August 2008

**SYNTHESIS OF FUNCTIONAL LACTIDE COPOLYMERS FOR
USE IN BIOMEDICAL APPLICATIONS**

Approved by:

Dr. David M. Collard, Advisor
School of Chemistry and Biochemistry
Georgia Institute of Technology

Dr. Marcus Weck
School of Chemistry and Biochemistry
Georgia Institute of Technology

Dr. Andrés J. García
Woodruff School of Mechanical
Engineering
Georgia Institute of Technology

Dr. Laren Tolbert
School of Chemistry and Biochemistry
Georgia Institute of Technology

Dr. Yadong Wang
Department of Biomedical Engineering
Georgia Institute of Technology

Date Approved: June 24, 2008

To my wife, Jill

ACKNOWLEDGEMENTS

I wish to thank Dr. David M. Collard for his invaluable support, advice, and encouragement throughout my time here at Georgia Institute of Technology. The title of “advisor” hardly does him justice, as he has always been so much more to those in his research group. I would also like to thank my two “co-advisors”, Dr. Marcus Weck and Dr. Andrés J. García, for their innumerable contributions, expertise, and their friendship. Special thanks to Dr. Laren Tolbert and Dr. Yadong Wang for their participation in my committee and their insight into my research.

The work found in Chapter 2, in its entirety, was a collaborative effort with Dr. Warren Gerhardt from Dr. Weck’s group. Anjali Kumar provided monomer for use in Chapter 3. The biological ligand studies in Chapter 3 were performed with the assistance of Timothy A. Petrie, and the micro-CT analysis found in Chapter 4 was performed by Abigail M. Wojtowicz, both of whom are from Dr. García’s group. I would also like to acknowledge Dr. Kunsang Yoon and Dr. Yiqing Wang for their synthetic contribution of poly(norbornene) macroinitiator in Chapter 5, and Dr. Alexander Norman of New York University for the characterization (SAXS, WAXS, SEC).

I would like to thank the members of the Collard group (“Team Collard”) past, present, and future for their assistance and for all of the laughter we have shared. I would like to express my appreciation for Dr. Glen Brizius for all he has taught me, Dr. Kurt Knoblock for being patient with me and all of my questions when I was a 1st year student in Boggs, Ms. Jenny E. Raynor for her contributions during group meeting, Rakesh Nambiar for his friendship, Brad Carson for his advice, Ms. Kathy Woody for all she has

done for our lab, and Subodh Jagtap for the promise he shows in sustaining the tradition of excellence in the Collard Group. Special thanks to Kamlesh P. Nair for aiding me in my studies, Dr. Warren Gerhardt for his initial work on this project, Ms. Anjali Kumar for her synthetic contributions, Ms. Whitney Komorner for her support, Ms. Catherine Silvestri for her thought-provoking discussions, Dr. Kunsang Yoon and Dr. Yiqing Wang for all of their help, and Timothy A. Petrie and Abigail M. Wojtowicz for their guidance in all things biochemistry.

I would like to show my appreciation for the faculty and staff of Georgia Institute of Technology for allowing my graduate studies to be both enlightening and enjoyable.

I would also like to thank Dr. Tom Brooks for first piquing my interest in chemistry, Dr. Preston MacDougall for expanding my knowledge, and Dr. Andrienne C. Friedli for further advancing my understanding of organic synthesis.

I am grateful for the support of a wonderful family: my parents, Ken and Michele, and my brothers, Daniel and Capt. Chris. I also appreciate the encouragement received from David and Sue Moyers, my parents away from home.

Most importantly, I would like to thank my wife, Jill, for her love, for being a constant source of encouragement, and for reminding me where my strength comes from.

TABLE OF CONTENTS

	Page
ACKNOWLEDGEMENTS	iv
LIST OF TABLES	xiii
LIST OF FIGURES	xiv
LIST OF SYMBOLS AND ABBREVIATIONS	xix
SUMMARY	xxii
CHAPTER	
1 INTRODUCTION TO POLY(LACTIDE)	1
1.1. Biodegradable Polyesters	1
1.2. PLA	2
1.2.1. PLA Production	2
1.2.2. Methods for PLA Preparation	3
1.2.3. Applications of PLA	4
1.3. Overcoming the Limitations of PLA	5
1.4. Hybrid Scaffolds for Tissue Engineering	5
1.5. Scope of Work	6
1.6. References	8
2 SYNTHESIS OF NEW FUNCTIONAL PLA COPOLYMERS	15
2.1. Introduction	15
2.2. Experimental	17
2.2.1. General Methods	17
2.2.2. Synthesis of Functional Monomers	20
2.2.2.1. 3-Benzyloxy-2-hydroxypropionic acid (4)	20

2.2.2.2. 6-(Benzyloxycarbonylamino)-2-hydroxyhexanoic acid (5)	21
2.2.2.3. 2-Hydroxypentanedioic acid 5-benzyl ester (6)	22
2.2.2.4. 3-(Benzyloxy)-2-(2-bromopropanoyloxy)propanoic acid (7)	23
2.2.2.5. 6-Benzyloxycarbonylamino-2-(2-bromopropionyloxy)hexanoic acid (8)	24
2.2.2.6. 2-(2-Bromo-propionyloxy)pentanedioic acid 5-benzyl ester (9)	25
2.2.2.7. General Procedure for the Halide Exchange	26
2.2.2.8. 3-(Benzyloxymethyl)-6-methyl-1,4-dioxane-2,5-dione (1)	27
2.2.2.9. Benzyl 4-(5-methyl-3,6-dioxo-1,4-dioxan-2-yl)butyl carbamate (2)	29
2.2.2.10 Benzyl 3-(5-methyl-3,6-dioxo-1,4-dioxan-2-yl)propanoate (3)	31
2.2.3. Preparation of Protected Homopolymers	33
2.2.3.1. SnOct ₂ Catalyst Stock Solution	33
2.2.3.2. General Procedure for Homopolymerizations	33
2.2.3.3. Homopolymer P1	33
2.2.3.4. Homopolymer P2	33
2.2.3.5. Homopolymer P3	34
2.2.4. Preparation of Protected PLA Copolymers	35
2.2.4.1. General Procedure for Copolymerizations	35
2.2.4.2. Copolymer CP1	35
2.2.4.3. Copolymer CP2	35
2.2.4.4. Copolymer CP3	36
2.2.5. Preparation of Functional Homopolymers and Copolymers	37
2.2.5.1. General Procedure for Hydrogenolysis Deprotections	37

2.2.5.2. General Procedure for Acidolysis Deprotections of Benzyl Carbamates	38
2.2.5.3. Homopolymer P1a	38
2.2.5.4. Homopolymer P2a	38
2.2.5.5. Homopolymer P3a	38
2.2.5.6. Copolymer CP1a	39
2.2.5.7. Copolymer CP2a	39
2.2.5.8. Copolymer CP3a	39
2.3. Results and Discussion	40
2.3.1. Synthetic Approaches Towards Functional Monomers	40
2.3.2. Synthesis of Protected Functional Homopolymers and PLA Copolymers	46
2.3.3. Protected Functional Homo- and Copolymer Deprotection	49
2.4. Conclusions	52
2.5. References	53
3 MODIFICATION OF FUNCTIONAL PLA WITH BIOLOGICAL LIGANDS	58
3.1. Introduction	58
3.2. Experimental	60
3.2.1. General Methods	60
3.2.2. Synthesis of Dibenzoyloxy-substituted Monomer	62
3.2.2.1. (<i>S</i>) 3-Benzoyloxy-2-hydroxypropionic acid	62
3.2.2.2. (<i>S,S</i>)-3,6-(Benzoyloxymethyl)-1,4-dioxane-2,5-dione (2)	63
3.2.3. Preparation of Protected Copolymers	64
3.2.3.1. Copolymerization of Lactide with Dibenzoyloxy-substituted Monomer 2	64
3.2.4. Preparation of Functional Copolymers	65

3.2.4.1. Deprotection of Copolymer 3 to Afford Hydroxyl-substituted Polymer 4	65
3.2.5. Functional Copolymer Modification	66
3.2.5.1. Modification of Hydroxyl-bearing Copolymer 4 with Succinic Anhydride	66
3.2.6. Film Formation	67
3.2.7. Biotin Coupling	67
3.2.8. RGD-FITC Coupling	67
3.2.9. ELISA	68
3.2.10. Cell Adhesion Assay	69
3.2.11. Statistics	69
3.3. Results and Discussion	69
3.3.1. Synthesis of Protected Functional Monomer	69
3.3.2. Copolymerization, Deprotection, and Modification with Succinic Anhydride	72
3.3.3. Biotin Coupling	77
3.3.4. RGD-peptide Coupling and Control of Cell Adhesion	79
3.4. Conclusions	82
3.5. References	82
4 SYNTHESIS OF PHOTOCROSSLINKABLE PLA SCAFFOLDS	86
4.1. Introduction	86
4.2. Experimental	88
4.2.1. General Methods	88
4.2.2. Synthesis of Dibenzoyloxy-substituted Monomer using DCC/HOBt	90
4.2.2.1. (<i>S,S</i>)-3,6-(Benzyloxymethyl)-1,4-dioxane-2,5-dione (1)	90

4.2.3. Copolymerization of 1 and Lactide, and Deprotection of Copolymer 3	91
4.2.4. Preparation of Cinnamate-modified PLA Copolymers	93
4.2.4.1. Modification of Hydroxyl-bearing Copolymer with Cinnamoyl Chloride	93
4.2.5. Foam Formation	94
4.2.6. Compression Strength Tests	94
4.2.7. Hydrolytic Degradation	94
4.3. Results and Discussion	95
4.3.1. Synthesis of Protected Functional Monomer	95
4.3.2. Copolymerization, Deprotection, and Modification with Cinnamoyl Chloride	97
4.3.3. Photocrosslinking of Cinnamate-substituted PLA Copolymers	99
4.3.4. Cinnamate-substituted Copolymer Foams	102
4.3.5. Hydrolytic Degradation of Copolymer Foams	108
4.3.6. Dye Penetration in Copolymer Foams	109
4.4. Conclusions	111
4.5. References	112
5 SYNTHESIS OF PNb-PLA DIBLOCK COPOLYMERS	118
5.1. Introduction	118
5.2. Experimental	120
5.2.1. General Methods	120
5.2.2. Synthesis of PNb- <i>bl</i> -PLA Diblock Copolymers	124
5.2.2.1. Copolymerization of Lactide using Hydroxyl-terminated PNb Macroinitiator	124
5.2.3. Preparation of h-PNb- <i>bl</i> -PLA	125
5.2.3.1. Hydrogenation of PNb- <i>bl</i> -PLA	125

5.3. Results and Discussion	125
5.3.1. PNb- <i>bl</i> -PLA Diblock Copolymer Synthesis and Hydrogenation	125
5.3.2. Thermal Properties of PNb- <i>bl</i> -PLA	131
5.3.3. Diblock Copolymer Morphology	132
5.4. Conclusions	135
5.5. References	135
6 SUGGESTIONS FOR FUTURE STUDY	137
6.1. Functionalized Hydrogenated PNb- <i>bl</i> -PLA Foams for Tissue Engineering	137
6.2. Functionalized PLA Copolymers for Drug Delivery	139
6.3. References	141
APPENDIX A: KINETIC STUDIES ON THE RING-OPENING POLYMERIZATION OF SUBSTITUTED LACTIDES	143
A.1. Introduction	143
A.2. Experimental	144
A.2.1. General Methods	144
A.2.2. Synthesis of Isopropyl-substituted Lactide Monomer	145
A.2.2.1. 3-Methyl-6-isopropyl-1,4-dioxane-2,5-dione (1)	145
A.2.3. Polymerization of Isopropyl-substituted Lactide Monomer	146
A.2.3.1. Homopolymerization of Monomer 1	146
A.3. Results and Discussion	147
A.3.1. Isopropyl-substituted Lactide Preparation	147
A.3.2. Polymerization of Isopropyl-substituted Lactide	148
A.4. Conclusions	154
A.5. References	154

APPENDIX B: SPECTROSCOPIC CHARACTERIZATION OF SYNTHETIC PRODUCTS	155
VITA	196

LIST OF TABLES

	Page
Table 2.1. Homopolymer Characterization Data.	47
Table 2.2. Copolymer Characterization Data.	47
Table 3.1. GPC and DSC Characterization of Copolymers 3-5 .	77
Table 4.1. GPC and DSC Characterization of Copolymers 3-5 .	99
Table 4.2. MicroCT Characterization Data of Foams of Copolymer 5 .	103
Table 5.1. Hydroxyl-terminated PNB Characterization Data.	121
Table 5.2. Copolymer Characterization Data.	128
Table 5.3. PLA Homopolymer Data.	129
Table 5.4. Thermal Analysis of Copolymers.	132
Table A.1. Degree of Polymerization and End Group Comparison.	151

LIST OF FIGURES

	Page
Figure 1.1. Examples of biodegradable polyesters.	1
Figure 1.2. A simplified view of the PLA life cycle.	2
Figure 1.3. Two common approaches used to synthesize PLA.	3
Figure 1.4. One common approach towards tissue engineering.	6
Figure 1.5. Overview for the fabrication of a self-assembled peptide-immobilized PNB-PLA diblock copolymer scaffold.	7
Figure 2.1. Functional lactide analogues.	17
Figure 2.2. Functional lactide monomers investigated	40
Figure 2.3. Synthesis of cyclic monomers 1 and 2 using an acid chloride coupling.	41
Figure 2.4. Synthesis of cyclic monomers 2 and 3 .	43
Figure 2.5. Crystal structure of monomer 1 .	44
Figure 2.6. One unique structure in the asymmetric unit cell of monomer 2 .	45
Figure 2.7. Homo- and co-polymerizations of 1 , 2 , and 3 .	47
Figure 2.8. Deprotection strategies for protected polymers.	50
Figure 2.9. (A) ¹ H NMR spectra of serine derivatives in <i>d</i> ₆ -acetone: 1) monomer 1 ; 2) homopolymer P1 ; 3) deprotected homopolymer P1a ; (B) ¹ H NMR spectra of glutamic acid derivatives in <i>d</i> ₆ -acetone: 1) monomer 3 ; 2) homopolymer P3 ; 3) deprotected homopolymer P3a .	51
Figure 2.10. ¹ H NMR spectra of lysine derivatives in <i>d</i> ₆ -acetone.	52
Figure 3.1. Synthesis of protected functional monomer 2 .	71
Figure 3.2. ¹ H NMR analysis and X-ray diffraction of cyclic disubstituted dimers.	73
Figure 3.3. Copolymer synthesis, deprotection, and modification with succinic anhydride.	74
Figure 3.4. ¹ H NMR spectra of copolymers: A, benzyloxy-substituted copolymer 3 ; B, deprotected hydroxymethyl bearing copolymer 4 ; C, succinylated copolymer 5 .	76

Figure 3.5. Attachment of an amine-substituted biotin derivative to copolymer films.	78
Figure 3.6. ELISA determination of relative density of amine-substituted biotin on succinylated PLA copolymer: Relative fluorescence indicating biotin attachment to films of copolymer 5 exposed to biotin-amine and biotin carboxylic acid derivatives with and without EDC.	79
Figure 3.7. Relative fluorescence of succinylated PLA copolymer films 5 exposed to RGD at various concentrations with and without EDC (lower data point at 20 $\mu\text{g/mL}$).	80
Figure 3.8. Relative fluorescence indicating cell attachment to films of copolymer 5 exposed to RGD at various concentrations with and without EDC.	81
Figure 4.1. Synthesis of dibenzyloxy-substituted lactide 1 .	96
Figure 4.2. Copolymerization, deprotection and modification with cinnamoyl chloride.	96
Figure 4.3. ^1H NMR spectra of copolymers: A, benzyloxy substituted copolymer; B, deprotected hydroxymethyl bearing copolymer; C, cinnamate modified copolymer.	98
Figure 4.4. Photocrosslinking of cinnamate-modified PLA copolymer 5 .	100
Figure 4.5. ATR-IR spectra of thick films of cinnamate-modified PLA irradiated for 0, 1, 2, 4, and 7 h.	101
Figure 4.6. UV-vis spectra showing a decrease in the absorption maxima of the thin films of copolymer 5 upon irradiation at 300 nm (0, 0.17, 0.33, 0.50, 1, 2, 3, 4, 6, and 18 h).	102
Figure 4.7. SEM images and a micro-CT scan of foams of cinnamate-modified PLA copolymer 5 prepared from benzene solutions (4% (w/v)).	105
Figure 4.8. ATR-IR spectra of nonirradiated (0 h) and irradiated (16 h) foams.	106
Figure 4.9. Typical stress-strain curve of strain-hardening cellular solids.	107
Figure 4.10. Typical stress-strain curves of crosslinked and noncrosslinked foams of PLA copolymer 5 .	108
Figure 4.11. Percent mass recovery of crosslinked and noncrosslinked foams in an accelerated hydrolytic degradation study in PBS at 60 $^\circ\text{C}$.	109
Figure 4.12. Cinnamate-modified PLA copolymer foams used in a dye penetration study.	110

Figure 5.1. The fabrication of robust PLA scaffolds by incorporation of photocrosslinkable groups or phase-separation of a PNb- <i>bl</i> -PLA diblock copolymer.	119
Figure 5.2. Synthesis of PNb- <i>bl</i> -PLA Diblock Copolymers.	126
Figure 5.3. ¹ H NMR spectra of macroinitiator and copolymers: A, hydroxyl-terminated PNb; B, PNb- <i>bl</i> -PLA diblock copolymer; C, Hydrogenated PNb- <i>bl</i> -PLA.	127
Figure 5.4. Hydrogenolysis of PNb- <i>bl</i> -PLA.	128
Figure 5.5. ¹ H NMR spectra showing the end groups of: A, Hydroxyl-terminated PNb; B, PNb- <i>bl</i> -PLA diblock copolymer; C, Hydrogenated PNb- <i>bl</i> -PLA.	130
Figure 5.6. SAXS profile: A, Intensity as a function of scattering vector <i>q</i> ; B, Domain spacing as a function of temperature.	133
Figure 5.7. WAXS 2D (A) and 1D (B) patterns of PNb ₁₂₉ -PLA ₉₃ at various temperatures.	134
Figure 6.1. The fabrication of robust, peptide-modified diblock copolymer foams.	137
Figure 6.2. The synthesis of functional h-PNb- <i>bl</i> -PLA.	138
Figure A.1. Synthesis of monomer 1 .	147
Figure A.2. Polymerization of monomer 1 with SnOct ₂ catalyst and BBA initiator.	148
Figure A.3. Representative ¹ H NMR spectrum used for end group analysis.	149
Figure A.4. The four possible chain propagations in the polymerization of 1 .	149
Figure A.5. Demonstration of decreasing reactivity (from left to right) as the bulkiness of the substituent increases.	152
Figure A.6. Model compounds to explore the kinetics of the ring-opening of 1 .	153
Figure B.1. ¹ H NMR of 3-Benzyloxy-2-hydroxypropionic acid (4).	156
Figure B.2. ¹ H NMR of 6-(Benzyloxycarbonylamino)-2-hydroxyhexanoic acid (5).	157
Figure B.3. ¹ H NMR of 2-Hydroxypentanedioic acid 5-benzyl ester (6).	158
Figure B.4. ¹ H NMR of 3-(Benzyloxy)-2-(2-bromopropanoyloxy)propanoic acid (7).	159

Figure B.5. ^{13}C NMR of 3-(Benzyloxy)-2-(2-bromopropanoyloxy)propanoic acid (7).	160
Figure B.6. ^1H NMR of 6-Benzyloxycarbonylamino-2-(2-bromopropionyloxy)hexanoic acid (8).	161
Figure B.7. ^{13}C NMR of 6-Benzyloxycarbonylamino-2-(2-bromopropionyloxy)hexanoic acid (8).	162
Figure B.8. ^1H NMR of 2-(2-Bromo-propionyloxy)pentanedioic acid 5-benzyl ester (9).	163
Figure B.9. ^{13}C NMR of 2-(2-Bromo-propionyloxy)pentanedioic acid 5-benzyl ester (9).	164
Figure B.10. ^1H NMR of α -iodocarboxylic acid intermediate (10).	165
Figure B.11. ^{13}C NMR of α -iodocarboxylic acid intermediate (10).	166
Figure B.12. ^1H NMR of α -iodocarboxylic acid intermediate (11).	167
Figure B.13. ^1H NMR of α -iodocarboxylic acid intermediate (12).	168
Figure B.14. ^1H NMR of 3-(Benzyloxymethyl)-6-methyl-1,4-dioxane-2,5-dione (1).	169
Figure B.15. ^{13}C NMR of 3-(Benzyloxymethyl)-6-methyl-1,4-dioxane-2,5-dione (1).	170
Figure B.16. ^1H NMR of Benzyl 4-(5-methyl-3,6-dioxo-1,4-dioxan-2-yl)butylcarbamate (2).	171
Figure B.17. ^{13}C NMR of Benzyl 4-(5-methyl-3,6-dioxo-1,4-dioxan-2-yl)butylcarbamate (2).	172
Figure B.18. ^1H NMR of Benzyl 3-(5-methyl-3,6-dioxo-1,4-dioxan-2-yl)propanoate (3).	173
Figure B.19. ^{13}C NMR of Benzyl 3-(5-methyl-3,6-dioxo-1,4-dioxan-2-yl)propanoate (3).	174
Figure B.20. ^1H NMR of (<i>S,S</i>)-3,6-(Benzyloxymethyl)-1,4-dioxane-2,5-dione (2).	175
Figure B.21. ^{13}C NMR of (<i>S,S</i>)-3,6-(Benzyloxymethyl)-1,4-dioxane-2,5-dione (2).	176
Figure B.22. ^1H NMR of dibenzyloxy-substituted PLA copolymer 3 .	177
Figure B.23. ^{13}C NMR of dibenzyloxy-substituted PLA copolymer 3 .	178

Figure B.24. ^1H NMR of hydroxy-bearing PLA copolymer 4 .	179
Figure B.25. ^{13}C NMR of hydroxy-bearing PLA copolymer 4 .	180
Figure B.26. ^1H NMR of succinic anhydride-modified PLA copolymer 5 .	181
Figure B.27. ^{13}C NMR of succinic anhydride-modified PLA copolymer 5 .	182
Figure B.28. ^1H NMR of cinnamate-modified PLA copolymer 5 .	183
Figure B.29. ^{13}C NMR of cinnamate-modified PLA copolymer 5 .	184
Figure B.30. ^1H NMR of hydroxyl-terminated PNb macroinitiator.	185
Figure B.31. ^{13}C NMR of hydroxyl-terminated PNb macroinitiator.	186
Figure B.32. ^1H NMR of PNb- <i>bl</i> -PLA diblock copolymer.	187
Figure B.33. ^{13}C NMR of PNb- <i>bl</i> -PLA diblock copolymer.	188
Figure B.34. ^1H NMR of hydrogenated PNb- <i>bl</i> -PLA diblock copolymer.	189
Figure B.35. ^{13}C NMR of hydrogenated PNb- <i>bl</i> -PLA diblock copolymer.	190
Figure B.36. ATR-IR spectra of (<i>S,S</i>)-3,6-(Benzyloxymethyl)-1,4-dioxane-2,5-dione (2).	191
Figure B.37. ATR-IR spectra of dibenzyloxy-substituted PLA copolymer 3 .	192
Figure B.38. ATR-IR spectra of hydroxy-bearing PLA copolymer 4 .	193
Figure B.39. ATR-IR spectra of succinic anhydride-modified PLA copolymer 5 .	194
Figure B.40. ATR-IR spectra of cinnamate-modified PLA copolymer 5 .	195

LIST OF SYMBOLS AND ABBREVIATIONS

Δ	heat or reflux
δ	chemical shift
PLA	Poly(lactide)
PGA	Poly(glycolide)
PLCL	Poly(ϵ -caprolactone)
kg	kilograms
FDA	Food and Drug Administration
RGD	Arginine-Glycine-Aspartic acid
Arg	Arginine
Gly	Glycine
Asp	Aspartic acid
UV	Ultraviolet
UV-vis	Ultraviolet-visible
PNb	Poly(norbornene)
<i>bl</i>	block
DIEA	N,N-Diisopropylethyl amine
g	grams
mm	millimeters
μm	microns
FT-IR	Fourier-Transform Infrared Spectroscopy
GPC	Gel Permeation Chromatography
DSC	Differential Scanning Calorimetry
mg	milligrams

min	minutes
MHz	megahertz
ppm	parts per million
TFA	trifluoroacetic acid
NMR	Nuclear Magnetic Resonance Spectroscopy
m	multiplet
s	singlet
t	triplet
nm	nanometers
IR	infrared
<i>J</i>	coupling constant
MS	Mass Spectrometry
HRMS	High Resolution Mass Spectrometry
M	molar
mL	milliliters
dd	doublet of doublets
TLC	thin-layer chromatography
HOBt	1-Hydroxybenzotriazole
DCC	N, N'-Dicyclohexylcarbodiimide
DCU	Dicyclohexylurea
M.P.	Melting Point
PDI	polydispersity index
M_w	weight-average molecular weight
M_n	number-average molecular weight
P	Polymer

CP	Copolymer
T_g	glass transition temperature
ELISA	Enzyme-Linked ImmunoSorbent Assay
PEO	poly(ethylene oxide)
NCS	newborn calf serum
FITC	fluorescein isothio-cyanate
MeOH	methanol
LA	Lactic Acid
PBS	phosphate-buffered saline
SDS	sodium dodecyl sulfate
EDC	1-Ethyl-3-(3-dimethylaminopropyl)carbodiimide
NHS	<i>N</i> -hydroxysuccinimide
DI	deionized
EDTA	ethylene diamine tetraacetic acid
MDCK	Madin-Darby canine kidney
TIPS	Thermally Induced Phase Separation
micro-CT	Microcomputed Tomography
SEM	Scanning Electron Microscopy
ATR-IR	Attenuated Total Reflection Infrared Spectroscopy
SEC	size-exclusion chromatography
SAXS	small-angle x-ray scattering
WAXD	wide-angle x-ray diffraction
DP	Degree of Polymerization
d-spacing	domain spacing
q	scattering vector

SUMMARY

The biocompatibility and biodegradability of poly(lactic acid) (PLA) facilitate its use in a variety of biomedical applications, ranging from sutures to drug delivery. However, uncontrolled interactions with cells and insufficient mechanical properties have prevented PLA from reaching its full potential as a scaffold for use in tissue engineering. Methods to improve the mechanical, chemical and biological properties of PLA are limited by the lack of functional groups along the backbone of the polymer. One possible approach towards overcoming these limitations involves the incorporation of functional groups into the backbone of the polymer through the copolymerization of monomers bearing protected functional groups. Deprotection and modification of these functional groups could provide the opportunity to direct the attachment of cells, and enhance to the physical properties of the polymer.

We have developed a general methodology for the synthesis of lactide monomers substituted with protected functional groups (alcohols protected as benzyl ethers, amines protected as benzyl carbamates and carboxylic acids protected as benzyl esters). The monomers were homopolymerized, and copolymerized with lactide, and deprotected to give functional PLA copolymers with pendant hydroxyl, amine, and carboxyl groups.

A thorough investigation of the chemical modification of PLA copolymers bearing functional groups along the polymer backbone was performed on a copolymer prepared by copolymerization of a dibenzyloxy-substituted lactide monomer with lactide followed by reductive debenylation. Reaction of the resulting hydroxyl-substituted PLA with succinic anhydride resulted in an acid-substituted PLA that is amenable to standard

EDC/NHS coupling. The utility of this copolymer was illustrated by coupling with an amine derivative of biotin, and an RGD-containing peptide sequence. The preparation of the biodegradable polyester substituted with RGD, a ubiquitous adhesion peptide, provided us with control over cellular attachment to the hybrid material.

We also explored approaches to make use of the pendant functional groups on PLA to enhance the physical properties of polymer foams. Copolymers with pendant photocrosslinkable cinnamate groups were prepared by reaction of the hydroxyl-substituted PLA copolymers with cinnamoyl chloride. The copolymer was foamed using thermally-induced phase separation (TIPS), and photocrosslinked upon irradiation at 300 nm. Irradiation resulted in an increase in the compressive modulus of the foams. Crosslinking also led to a decrease in the rate of hydrolytic degradation of the foams, thereby demonstrating the potential for use of these strategies in the development of porous scaffolds for bioengineering.

Another potential approach towards the preparation of robust polymer foams is the incorporation of a rigid polymer block which can phase separate during foam formation to provide additional structural integrity. Several poly(norbornene)-PLA diblock copolymer compositions were prepared by the ring-opening of lactide by a hydroxyl-terminated poly(norbornene) macroinitiator. The ability of the diblock copolymer to phase separate at elevated temperature was verified using small-angle x-ray scattering and wide-angle x-ray scattering.

CHAPTER 1

INTRODUCTION TO POLY(LACTIDE)

1.1. Biodegradable Polyesters

Plastics have become so integrated into our every day lives; worldwide production of plastics totaled more than 200 million metric tons in 2006.¹ However, limited landfill space and the acceptance that crude oil is a surely limited resource have forced the consideration of alternative materials as a replacement for petroleum-based plastics.² Of particular interest are biodegradable polymers, specifically linear aliphatic polyesters such as poly(lactide) (PLA), poly(glycolide) (PGA), and poly(ϵ -caprolactone) (PCL), Figure 1.1.³ These polymers contain ester functionalities throughout the backbone which facilitate rapid degradation in a landfill.^{4,5} Such polymers may also be employed as materials for medical applications in which they are hydrolyzed *in vivo*, and converted into non-toxic components that are excreted from the body.^{6,7} The attractive physical properties and biodegradable character of these polylactones have led to their use in a variety of applications ranging from plastic water bottles and food storage containers⁸ to biomedical devices such as sutures.^{9,10}

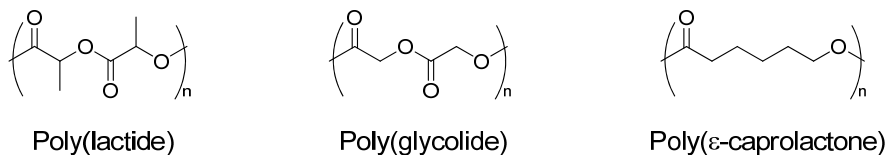


Figure 1.1. Examples of biodegradable polyesters.

1.2. PLA

1.2.1. PLA Production

Poly(lactide), or PLA, has emerged as an attractive biodegradable polyester due to its availability from annually renewable feed stocks. The starch-based constituents found in corn, wheat, potatoes, and food processing waste products can be converted into lactic acid by fermentation and used in the production of PLA, Figure 1.2.¹¹ PLA is hydrolytically and oxidatively degraded into carbon-dioxide and water, where it can re-enter the cycle.¹²

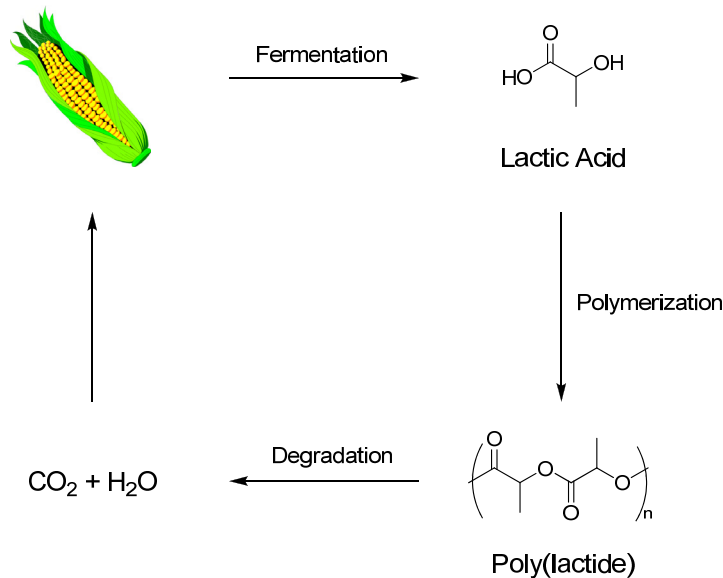


Figure 1.2. A simplified view of the PLA life cycle.

In 1994, Cargill commenced operation of a small PLA development facility in Minnesota capable of producing 5,000 metric tons of PLA per annum. In 2004, Cargill-Dow unveiled a full-scale PLA plant in Nebraska capable of producing 140,000 tons per year.¹³ The manufacture of PLA has not been limited to the United States, and the worldwide production of PLA is expected to reach nearly 400,000 metric tons in 2008.¹⁴

1.2.2. Methods for PLA Preparation

There are two main methods used in the production of PLA from lactic acid, Figure 1.3. The first route involves the step-growth polycondensation of lactic acid which requires high temperatures and results in the formation of lactic acid oligomers with maximum number average molecular weights usually on the order of 30 kg/mol.¹⁵ This process is often limited to the production of low to intermediate molecular weight polymers and can be plagued by side reactions due to excessive temperatures. However, Mitsui Toatsu Chemicals patented a polycondensation method which makes use of the azeotropic removal of water from the polymerization by distillation of a high-boiling solvent to give high molecular weight polymer.¹⁶ The other main strategy used for the synthesis of PLA involves the conversion of lactic acid to the corresponding cyclic dimer known as lactide.¹⁷ The lactide monomer undergoes a ring-opening polymerization under mild conditions with short reaction times to give high molecular weight PLA.¹⁸

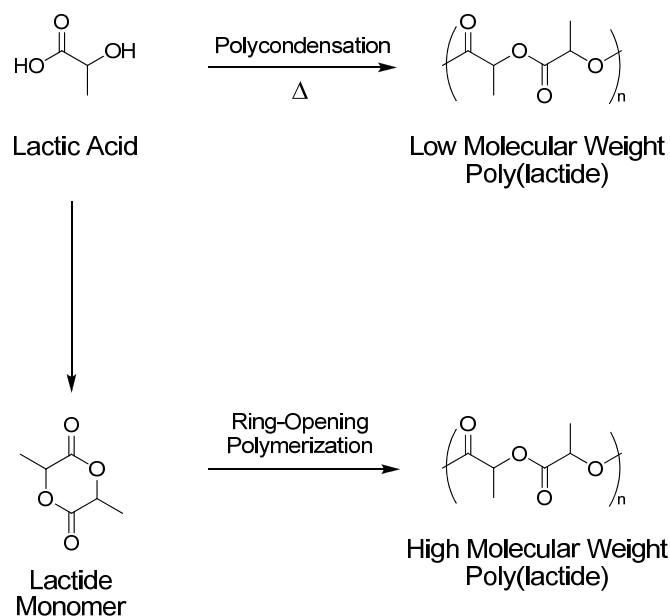


Figure 1.3. Two common approaches used to synthesize PLA.

Cationic,¹⁹⁻²¹ anionic,²²⁻²⁴ and coordination-insertion²⁵⁻²⁷ mechanisms can all be used for the ring-opening polymerization of lactide using a variety of different catalysts. The most common catalyst by far is Sn(II) 2-ethylhexanoate (or stannous octanoate, abbreviated SnOct₂) which has been used extensively in the preparation of high molecular weight PLA.^{28,29} Stannous octanoate is preferred due to its commercial availability, effectiveness, low rate of racemization of the lactide, and low toxicity. Its presence in PLA is accepted by the United States Food and Drug Administration (FDA).³⁰

1.2.3. Applications of PLA

PLA exhibits a diverse range of properties depending on how it is processed. Using standard processing equipment, it can be molded into flexible films for use in plastic wrap and shrink labels, or woven into fibers for use in clothing and carpeting.¹⁴ The biocompatible and bioassimilable nature of PLA allow the use of FDA-approved PLA-PGA copolymers in numerous biomedical applications, including orthopedic devices such as clips and bone pins, sutures, and controlled drug delivery matrices.³¹ All of these applications make use of the physical and biodegradable properties of PLA, which can be affected by the molecular weight, polydispersity, and tacticity of the polymer.⁹ However, PLA is not suited for many applications due to its brittleness, thermal instability, and hydrophobic properties.²

1.3. Overcoming the Limitations of PLA

Much work has focused on tailoring the bulk physical properties of PLA using methods such as incorporating other comonomers into the polymer backbone by ring-opening copolymerization with lactide,³²⁻³⁶ the formation of diblock copolymers,³⁷ blending PLA with other polymers,³⁸ and the addition of plasticizers³⁹ or crosslinking agents.^{40,41} Recently, efforts have focused on incorporating functional groups directly into the polyester backbone of PLA by the copolymerization of protected functional monomers.⁴² Protected functional lactides,⁴³⁻⁴⁵ glycolides,⁴⁶⁻⁴⁹ esteramides,⁵⁰⁻⁵⁵ *N*-carboxyanhydrides,⁵⁶⁻⁵⁹ and lactones⁶⁰⁻⁶⁴ have been copolymerized with lactide monomer to give random copolymers with pendant protected functional groups. Such functional groups could be used to alter the thermal properties of the polymer^{65,66} and thereby provide a means to attach drugs, control the rate of hydrolytic degradation, and to impart hydrophilicity.¹⁵ However, beyond the removal of the protecting group, these approaches have not been thoroughly investigated.

1.4. Hybrid Scaffolds for Tissue Engineering

The field of tissue engineering has emerged as an attractive approach to repairing malfunctioning or lost organs.⁶⁷ In tissue engineering, cells are seeded onto a biologically-modified porous temporary scaffold where they proliferate, secrete extracellular matrices, and promote the formation of tissue, Figure 1.4.⁶⁸ The scaffold, which initially serves as a physical support to guide the formation of the new tissue, degrades and is ultimately eliminated from the body. Requirements for scaffolds for tissue engineering include high porosity to allow proper cell growth, biocompatibility,

biodegradability, and sufficient mechanical properties to prevent premature deformation.^{69,70} Two main types of scaffolds are generally used for tissue engineering; those fabricated from naturally derived polymers, such as collagen, and scaffolds made from synthetic biodegradable polyesters such as PLA.⁷¹ The poor mechanical properties of naturally derived polymers and the inability to control the interactions of cells with hydrophobic biodegradable polyesters have prompted the formation of third class of hybrid foams which combine both synthetic and natural materials.⁷²

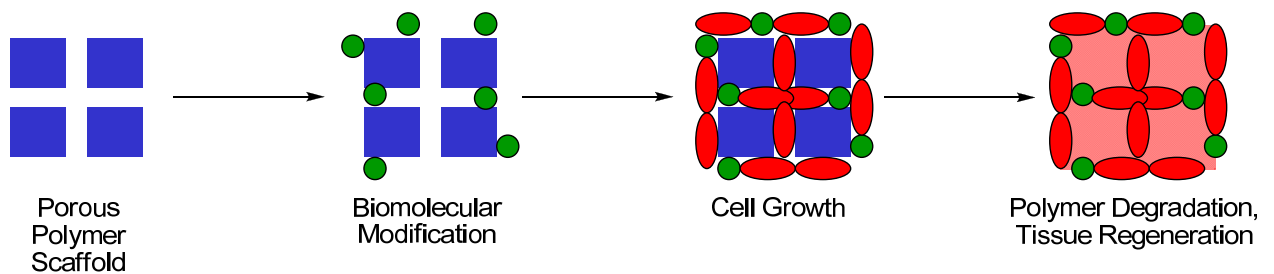


Figure 1.4. One common approach towards tissue engineering.

1.5. Scope of Work

Besides having the potential to improve the physical properties of the polymer,^{65,66} the incorporation of pendant functional groups onto the backbone of PLA could be used to enhance the material's biocompatibility.^{15,49} The peptide sequence RGD (Arg-Gly-Asp) has been shown to improve the cellular attachment and cytocompatibility of a variety of materials.^{73,74} The attachment of biologically relevant motifs such as RGD to PLA could provide the opportunity to control cell adhesion and function.⁵⁰ This combination of synthetic biodegradable polymers with peptides could be used to prepare novel biodegradable hybrid PLA scaffolds ideal for tissue engineering which have the ability to promote specific scaffold-cell interactions.

In this thesis, I describe a series of studies directed towards the development of new PLA based scaffolds for tissue engineering, Figure 1.5.

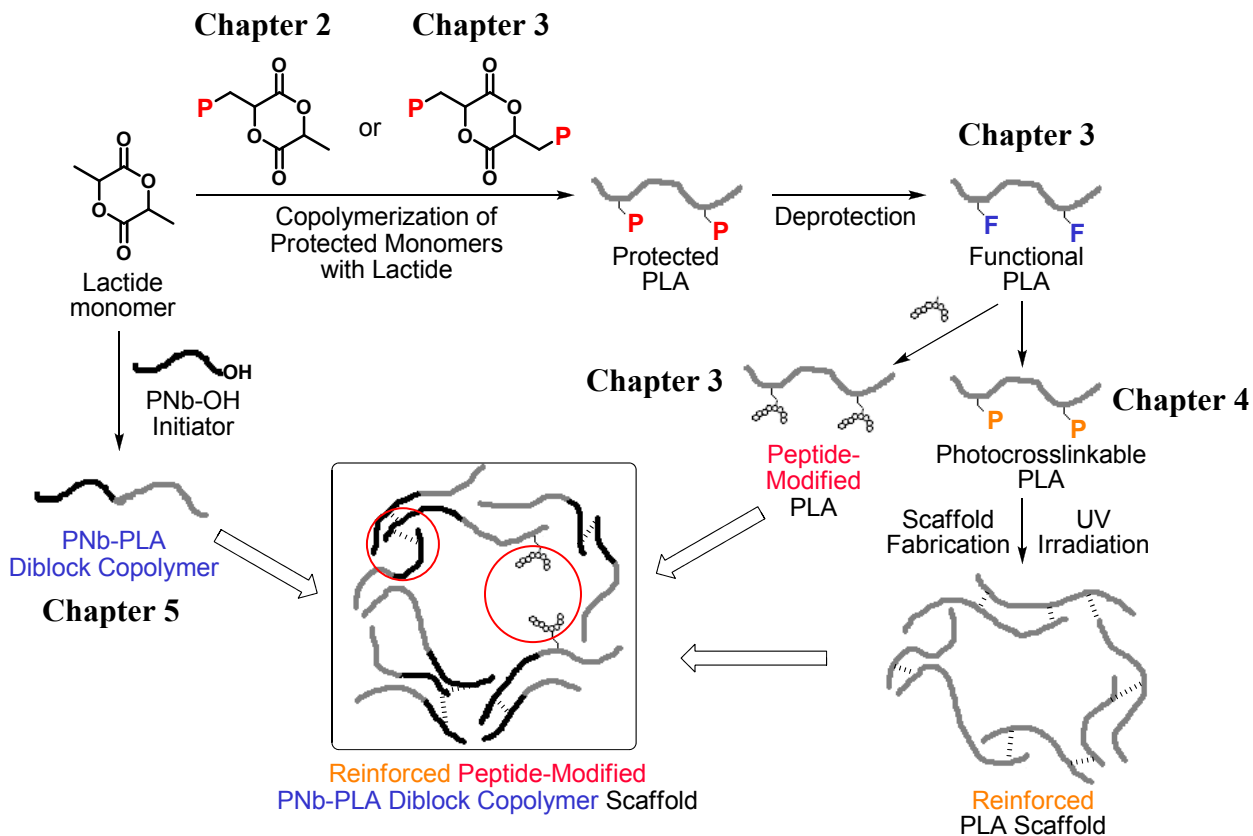


Figure 1.5. Overview for the fabrication of a self-assembled peptide-immobilized PNb-PLA diblock copolymer scaffold.

In Chapter 2, I describe the preparation of protected functional lactide monomers (this work was done in conjunction with Warren Gerhardt from Marcus Weck's group who initially began our study of functional lactides), Figure 1.5. The monomers were homopolymerized and copolymerized with lactide. Subsequently deprotection gave functional PLA copolymers with pendant hydroxyl, amine, and carboxyl groups. We then focused our attention on the modification of functional copolymers with biological

ligands such as RGD. This modification increased the amount of cellular attachment to PLA copolymer films (Chapter 3). Having shown that we could use the pendant functionalities to alter the biological properties of PLA, we next focused on modifying the physical properties of PLA. Chapter 4 describes our efforts to enhance the mechanical properties of PLA films and foams through the attachment of photocrosslinkable groups to the backbone of PLA copolymers. We have also explored an alternative route towards the fabrication of scaffolds with enhanced mechanical properties through development of block copolymers whereby a rigid hydroxyl-terminated poly(norbornene) (PNb) is used as a macroinitiator for the ring-opening of lactide to give PNb-*bl*-PLA diblock copolymers (Chapter 5). Incorporation of the rigid PNb block provides the opportunity for self-assembly and added structural integrity. The information obtained regarding the tethering of peptides, the attachment of photocrosslinkable groups, and the incorporation of semi-rigid PNb blocks can ultimately be used to aid in the design of highly porous polymer scaffolds with enhanced mechanical and cellular properties.

1.6. References

- (1) <http://www.plasticseurope.org> (accessed 6/24/08).
- (2) Williams, C. K., *Chem. Soc. Rev.* **2007**, *36*, 1573-1580.
- (3) Wang, S. G.; Cui, W. J.; Bei, J. Z., *Anal. Bioanal. Chem.* **2005**, *381*, 547-556.
- (4) Ishigaki, T.; Sugano, W.; Nakanishi, A.; Tateda, M.; Ike, M.; Fujita, M., *Chemosphere* **2004**, *54*, 225-233.
- (5) Federle, T. W.; Barlaz, M. A.; Pettigrew, C. A.; Kerr, K. M.; Kemper, J. J.; Nuck, B. A.; Schechtman, L. A., *Biomacromolecules* **2002**, *3*, 813-822.

- (6) Henn, G. G.; Birkinshaw, C.; Buggy, M.; Jones, E., *Macromol. Biosci.* **2001**, *1*, 219-222.
- (7) Bazile, D. V.; Ropert, C.; Huve, P.; Verrecchia, T.; Marland, M.; Frydman, A.; Veillard, M.; Spenleuhauer, G., *Biomaterials* **1992**, *13*, 1093-102.
- (8) <http://www.natureworksllc.com> (accessed 6/24/08).
- (9) Jain, R. A., *Biomaterials* **2000**, *21*, 2475-2490.
- (10) Jain, R.; Shah, N. H.; Malick, A. W.; Rhodes, C. T., *Drug Dev. Ind. Pharm.* **1998**, *24*, 703-727.
- (11) Vaidya, A. N.; Pandey, R. A.; Mudliar, S.; Kumar, M. S.; Chakrabarti, T.; Devotta, S., *Crit. Rev. Environ. Sci. Technol.* **2005**, *35*, 429-467.
- (12) Ragauskas, A. J.; Williams, C. K.; Davison, B. H.; Britovsek, G.; Cairney, J.; Eckert, C. A.; Frederick, W. J.; Hallett, J. P.; Leak, D. J.; Liotta, C. L.; Mielenz, J. R.; Murphy, R.; Templer, R.; Tschaplinski, T., *Science* **2006**, *311*, 484-489.
- (13) Vink, E. T. H.; Rabago, K. R.; Glassner, D. A.; Gruber, P. R., *Polym. Degrad. Stab.* **2003**, *80*, 403-419.
- (14) Mehta, R.; Kumar, V.; Bhunia, H.; Upadhyay, S. N., *J. Macromol. Sci., Polym. Rev.* **2005**, *C45*, 325-349.
- (15) Lou, X. D.; Detrembleur, C.; Jerome, R., *Macromol. Rapid Commun.* **2003**, *24*, 161-172.
- (16) <http://www.mitsuichemicals.com> (accessed 6/24/08).
- (17) Garlotta, D., *J. Polym. Environ.* **2001**, *9*, 63-84.
- (18) Nijenhuis, A. J.; Grijpma, D. W.; Pennings, A. J., *Macromolecules* **1992**, *25*, 6419-6424.

- (19) Kricheldorf, H. R.; Kreiser, I., *Makromol. Chem.* **1987**, *188*, 1861-1873.
- (20) Kricheldorf, H. R.; Sumbel, M., *Eur. Polym. J.* **1989**, *25*, 585-591.
- (21) Dittrich, W.; Schulz, R. C., *Angew. Makromol. Chem.* **1971**, *15*, 109-126.
- (22) Jedlinski, Z.; Walach, W.; Kurcok, P.; Adamus, G., *Makromol. Chem.* **1991**, *192*, 2051-2057.
- (23) Kurcok, P.; Matuszowicz, A.; Jedlinski, Z.; Kricheldorf, H. R.; Dubois, P.; Jerome, R., *Macromol. Rapid Commun.* **1995**, *16*, 513-519.
- (24) Kricheldorf, H. R.; Boettcher, C., *J. Macromol. Sci., Pure Appl. Chem.* **1993**, *A30*, 441-448.
- (25) Kricheldorf, H. R.; Kreiseraunders, I.; Boettcher, C., *Polymer* **1995**, *36*, 1253-1259.
- (26) Kricheldorf, H. R.; Serra, A., *Polym. Bull.* **1985**, *14*, 497-502.
- (27) Stevels, W. M.; Ankone, M. J. K.; Dijkstra, P. J.; Feijen, J., *Macromol. Chem. Phys.* **1995**, *196*, 3687-3694.
- (28) Jalabert, M.; Frascini, C.; Prud'homme, R. E., *J. Polym. Sci., Part A: Polym. Chem.* **2007**, *45*, 1944-1955.
- (29) Degee, P.; Dubois, P.; Jerome, R.; Jacobsen, S.; Fritz, H.-G., *Macromol. Symp.* **1999**, *144*, 289-302.
- (30) Dechy-Cabaret, O.; Martin-Vaca, B.; Bourissou, D., *Chem. Rev.* **2004**, *104*, 6147-6176.
- (31) Albertsson, A. C.; Varma, I. K., *Biomacromolecules* **2003**, *4*, 1466-1486.
- (32) Jiang, X.; Vogel, E. B.; Smith, M. R.; Baker, G. L., *Macromolecules* **2008**, *41*, 1937-1944.

- (33) Lu, X. L.; Cai, W.; Gao, Z. Y., *J. Appl. Polym. Sci.* **2008**, *108*, 1109-1115.
- (34) Park, P. I. P.; Jonnalagadda, S., *J. Appl. Polym. Sci.* **2006**, *100*, 1983-1987.
- (35) Trimaille, T.; Gurny, R.; Moeller, M., *Chimia* **2005**, *59*, 348-352.
- (36) Trimaille, T.; Moeller, M.; Gurny, R., *J. Polym. Sci., Part A: Polym. Chem.* **2004**, *42*, 4379-4391.
- (37) Zalusky, A. S.; Olayo-Valles, R.; Wolf, J. H.; Hillmyer, M. A., *J. Am. Chem. Soc.* **2002**, *124*, 12761-12773.
- (38) Kuo, S.-W.; Huang, C.-F.; Tung, Y.-C.; Chang, F.-C., *J. Appl. Polym. Sci.* **2006**, *100*, 1146-1161.
- (39) Baiardo, M.; Frisoni, G.; Scandola, M.; Rimelen, M.; Lips, D.; Ruffieux, K.; Wintermantel, E., *J. Appl. Polym. Sci.* **2003**, *90*, 1731-1738.
- (40) Hasirci, V.; Lewandrowski, K. U.; Bondre, S. P.; Gresser, J. D.; Trantolo, D. J.; Wise, D. L., *Biomed. Mater. Eng.* **2000**, *10*, 19-29.
- (41) Quynh, T. M.; Mitomo, H.; Nagasawa, N.; Wada, Y.; Yoshii, F.; Tamada, M., *Eur. Polym. J.* **2007**, *43*, 1779-1785.
- (42) Bourissou, D.; Moebs-Sanchez, S.; Martin-Vaca, B., *C. R. Chim.* **2007**, *10*, 775-794.
- (43) Gerhardt, W. W.; Noga, D. E.; Hardcastle, K. I.; Garcia, A. J.; Collard, D. M.; Weck, M., *Biomacromolecules* **2006**, *7*, 1735-1742.
- (44) Marcincinova-Benabdillah, K.; Boustta, M.; Coudane, J.; Vert, M., *Biomacromolecules* **2001**, *2*, 1279-1284.
- (45) Ouchi, T.; Fujino, A., *Makromol. Chem.* **1989**, *190*, 1523-30.

- (46) Kimura, Y.; Shirotani, K.; Yamane, H.; Kitao, T., *Macromolecules* **1988**, *21*, 3338-40.
- (47) Leemhuis, M.; van Nostrum, C. F.; Kruijtzter, J. A. W.; Zhong, Z. Y.; ten Breteler, M. R.; Dijkstra, P. J.; Feijen, J.; Hennink, W. E., *Macromolecules* **2006**, *39*, 3500-3508.
- (48) Leemhuis, M.; van Steenis, J. H.; van Uxem, M. J.; van Nostrum, C. F.; Hennink, W. E., *Eur. J. Org. Chem.* **2003**, 3344-3349.
- (49) Loontjens, C. A. M.; Vermonden, T.; Leemhuis, M.; van Steenberg, M. J.; van Nostrum, C. F.; Hennink, W. E., *Macromolecules* **2007**, *40*, 7208-7216.
- (50) Barrera, D. A.; Zylstra, E.; Lansbury, P. T., Jr.; Langer, R., *J. Am. Chem. Soc.* **1993**, *115*, 11010-11.
- (51) Barrera, D. A.; Zylstra, E.; Lansbury, P. T.; Langer, R., *Macromolecules* **1995**, *28*, 425-32.
- (52) Cook, A. D.; Hrkach, J. S.; Gao, N. N.; Johnson, I. M.; Pajavni, U. B.; Cannizzaro, S. M.; Langer, R., *J. Biomed. Mater. Res.* **1997**, *35*, 513-523.
- (53) Cook, A. D.; Pajvani, U. B.; Hrkach, J. S.; Cannizzaro, S. M.; Langer, R., *Biomaterials* **1997**, *18*, 1417-1424.
- (54) Feng, Y.; Klee, D.; Hocker, H., *Macromol. Chem. Phys.* **2002**, *203*, 819-824.
- (55) In't Veld, P. J. A.; Dijkstra, P. J.; Feijen, J., *Makromol. Chem.* **1992**, *193*, 2713-30.
- (56) Deng, C.; Chen, X.; Yu, H.; Sun, J.; Lu, T.; Jing, X., *Polymer* **2007**, *48*, 139-149.
- (57) Deng, C.; Rong, G.; Tian, H.; Tang, Z.; Chen, X.; Jing, X., *Polymer* **2005**, *46*, 653-659.

- (58) Deng, C.; Tian, H.; Zhang, P.; Sun, J.; Chen, X.; Jing, X., *Biomacromolecules* **2006**, *7*, 590-596.
- (59) Deng, M.; Wang, R.; Rong, G.; Sun, J.; Zhang, X.; Chen, X.; Jing, X., *Biomaterials* **2004**, *25*, 3553-3558.
- (60) Donato, M. T.; Gomez-Lechon, M. J.; Castell, J. V., *Anal. Biochem.* **1993**, *213*, 29-33.
- (61) Mecerreyes, D.; Miller, R. D.; Hedrick, J. L.; Detrembleur, C.; Jerome, R., *J. Polym. Sci., Part A: Polym. Chem.* **2000**, *38*, 870-875.
- (62) Parrish, B.; Breitenkamp, R. B.; Emrick, T., *J. Am. Chem. Soc.* **2005**, *127*, 7404-7410.
- (63) Parrish, B.; Quansah, J. K.; Emrick, T., *J. Polym. Sci., Part A: Polym. Chem.* **2002**, *40*, 1983-1990.
- (64) Riva, R.; Schmeits, S.; Jerome, C.; Jerome, R.; Lecomte, P., *Macromolecules* **2007**, *40*, 796-803.
- (65) Baker, G. L.; Vogel, E. B.; Smith, M. R., *Polym. Rev.* **2008**, *48*, 64-84.
- (66) Jiang, X. W.; Smith, M. R.; Baker, G. L., *Macromolecules* **2008**, *41*, 318-324.
- (67) Langer, R.; Vacanti, J. P., *Science* **1993**, *260*, 920-926.
- (68) Chen, G.; Ushida, T.; Tateishi, T., *Macromol. Biosci.* **2002**, *2*, 67-77.
- (69) Schugens, C.; Maquet, V.; Grandfils, C.; Jerome, R.; Teyssie, P., *J. Biomed. Mater. Res.* **1996**, *30*, 449-461.
- (70) Schugens, C.; Maquet, V.; Grandfils, C.; Jerome, R.; Teyssie, P., *Polymer* **1996**, *37*, 1027-1038.
- (71) Chen, G.; Kawazoe, N.; Tateishi, T.; Tanaka, J., *Mater. Int.* **2007**, *20*, 8-13.

- (72) Chen, G. P.; Ushida, T.; Tateishi, T., *Adv. Mater.* **2000**, *12*, 455-457.
- (73) Wang, D.-A.; Ji, J.; Sun, Y.-H.; Shen, J.-C.; Feng, L.-X.; Elisseeff, J. H.,
Biomacromolecules **2002**, *3*, 1286-1295.
- (74) Fussell, G. W.; Cooper, S. L., *Biomaterials* **2004**, *25*, 2971-2978.

CHAPTER 2

SYNTHESIS OF NEW FUNCTIONAL PLA COPOLYMERS[‡]

2.1. Introduction

With the global production of poly(lactide) PLA expected to reach almost 400,000 tonnes for the year 2008,¹ its impact on the plastics industry is becoming more evident as time progresses.² The biodegradable and biorenewable properties of PLA have contributed to its advancement in several major industries, including use in fibers and packaging,³ and its emerging use in biomedical applications such as implantation devices, sutures, tissue replacement, and as a delivery vehicle.⁴⁻⁶ However, PLA is not well suited for many applications due to its brittleness, hydrophobicity, and lack of pendant functional groups along the backbone of the polymer.⁷ The incorporation of functional groups would provide the means to control the physical properties of PLA, including its degradation rate,⁸ hydrophobicity,^{9,10} and thermal properties.¹¹ Such functional groups could also be used to enhance the biocompatibility of PLA^{12,13} and could be used for the attachment biomolecules to control cell adhesion and function.¹⁴

The main method used for the incorporation of functional groups into the backbone of PLA involves the copolymerization of protected functional glycolides,^{9,10,13,15} esteramides,^{14,16-21} *N*-carboxyanhydrides,²²⁻²⁶ and lactones²⁷⁻³¹ with lactide monomer. Kimura was the first to report on the synthesis of poly(glycolide) copolymers with pendant carboxylic groups based on the copolymerization and deprotection of a protected functional glycolide monomer (Figure 2.1).¹⁵ Other

[‡] The work found in this Chapter was done in collaboration with Dr. Warren W. Gerhardt from the group of Dr. Marcus Weck and certain portions were published in *Biomacromolecules* **2006**, 7, 1735-1742.

functionalized glycolide monomer derivatives followed,³² including one containing a protected gluconic acid sugar.³³ However, poly(glycolide) displays greater hydrophilicity and undergoes more rapid degradation than PLA, which can limit its use in biomedical applications.^{34,35} Other comonomers include morpholine-2,5-dione derivatives (Figure 2.1) which have been copolymerized with lactide to give poly(esteramides).^{14,16-21} However, the dissimilar structures of the amide-containing monomers compared to lactide results in changes in the polymerization and degradation rates of the corresponding copolymers relative to PLA.

These differences in the properties of the functional poly(glycolide) and poly(esteramide) copolymers demonstrate the need to explore the preparation of functional lactide monomers which will more closely resemble the structure of PLA when incorporated into a copolymer. In this work, we examine the synthesis, polymerization, and copolymerization of 6-methyl-1,4-dioxane-2,5-diones bearing a protected functional group at the 3 position that is subject to further modification (Figure 2.1). Though extensive work has been done on the copolymerization of glycolide and morpholine-2,5-dione derivatives with lactide, there are only a few reports regarding the preparation of analogues of the lactide monomer.^{9,10,33,36} Baker³⁷⁻⁴⁰ and Möller⁴¹⁻⁴⁴ have reported on the preparation and copolymerization of alkyl-substituted lactides (i.e., with alkyl substituents on the 3 position) as a method to alter the physical properties of PLA copolymers. However, the resulting copolymers lack the functional groups required for further modification. In an effort to explore the possible advantages of functional lactide copolymers, we have developed a novel strategy for the preparation and polymerization of functional lactide monomers derived from commercially available amino acids. This

methodology could potentially be used with a host of protected amino acid starting materials to provide an array of different protected lactide monomers. Preliminary data shows that the resulting protected lactide monomers can be successfully homo- and copolymerized with lactide to give PLA homo- and copolymers with pendant functional groups which might be used for post-polymerization modification with bioactive ligands.

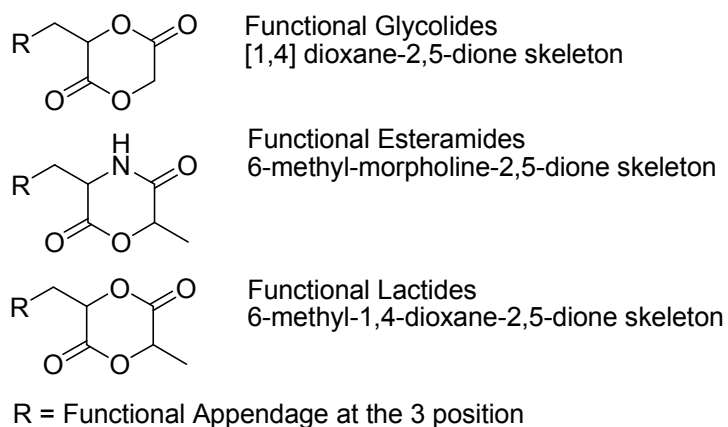


Figure 2.1. Functional lactide analogues.

2.2. Experimental

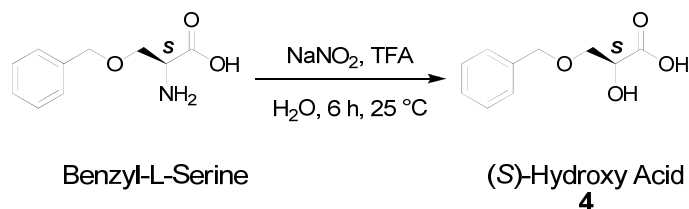
2.2.1. General Methods

H-Ser (Benzyl)-OH was purchased from Indofine Chemical Company. H-Glu(O-Benzyl)-OH was purchased from 3B Medical Systems. H-Lys(Z)-OH was purchased from Fluka. DL lactide was purchased from Aldrich and recrystallized (2x) from dry EtOAc, dissolved in dry benzene, frozen, lyophilized and stored in a nitrogen filled glove box prior to use. N,N-Diisopropylethyl amine (DIEA), Et₂O and benzene were distilled from sodium benzophenone ketyl solutions, EtOAc from CaH₂, acetone from 4Å molecular sieves, and CH₂Cl₂ was dried via passage through Cu₂O and alumina columns.

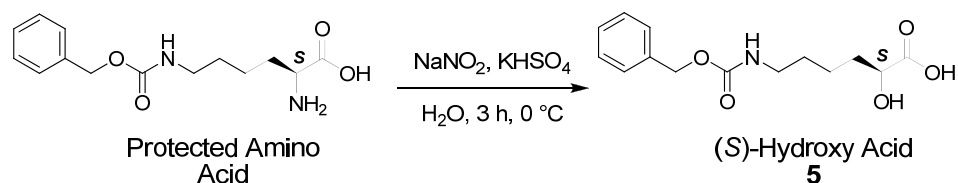
All anhydrous liquids brought into the nitrogen-filled glove box were first degassed with three freeze-pump-thaw cycles using liquid nitrogen at 50 mmHg. Chromatography was performed with Sorbent Tech Premium Grade silica: porosity 60 Å, particle size 40-75 µm (200×400 mesh), surface area 450-550 m²/g, pH range 6-8., decomposition of cyclic monomer **1** was observed during chromatography using Sorbent Tech Standard Grade silica: porosity 60 Å, particle size 32-63 µm (230×450 mesh), surface area 500-600 m²/g, pH range 6.5-7.5. Compounds were analyzed by use of UV light (254 nm), I₂, or a 5% solution of ammonium molybdate in 2 M sulfuric acid. IR spectra were recorded on a Shimadzu FT-IR-8400S. Melting points were determined with a Mel-Temp II apparatus fitted with a Fluke 51^{K/J} digital thermometer and are uncorrected. Molecular weight data were collected on a Shimadzu GPC system consisting of a SCL-10Avp system controller, an LC-10ADvp pump, and a SPD-M10Avp diode array detector. The eluant was methylene chloride, and the columns were American Polymer Standards Corp. AM GPC Gel 10 µm. The molecular weights were determined relative to narrow molecular weight (polydispersity index ≤ 1.05) poly(styrene) standards from American Polymer Standards Corp. Thermal transition data were collected with a Mettler DSC 822^e. The sample size ranged from 6 – 8 mg, and each sample was subjected to two cool-heat-cool cycles from 25 to -50 to 60 °C with a rate of 10 °C/min. NMR spectra were recorded at 298 K on a Varian Mercury spectrometer (300 MHz). Chemical shifts are reported in parts per million (ppm), using residual solvent as an internal standard. Mass spectral analyses were provided by the Georgia Institute of Technology Mass Spectrometry Facility. Elemental analyses were conducted at Atlantic Microlab, Inc. in Norcross, GA. The synthetic procedures described below represent optimized procedures developed in

close collaboration with Warren Gerhardt (Ph.D. thesis, Georgia Institute of Technology, 2007).

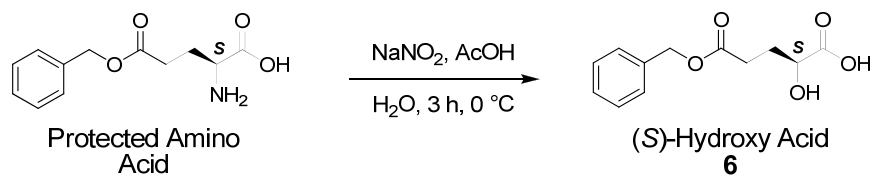
2.2.2. Synthesis of Functional Monomers



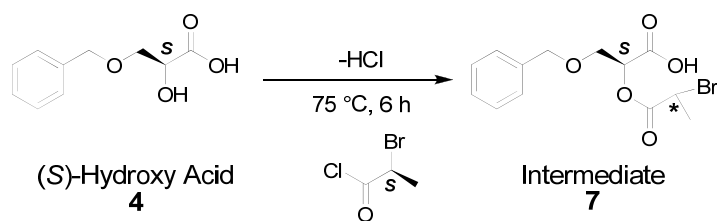
2.2.2.1. 3-Benzyloxy-2-hydroxypropionic acid (4). H-Ser(benzyl)-OH (20.0 g, 102.5 mmol) was dissolved in aq. TFA (0.7 M, 200 mL) and NaNO₂ (10.6 g, 153.7 mmol) in deionized water (100 mL) was added over a period of three hours using a syringe pump at 25 °C. The reaction mixture was stirred for an additional three hours at 25 °C. NaCl (20.0 g) was added to the reaction mixture and the crude product was extracted several times with EtOAc. The combined organic layers were washed with brine, dried over MgSO₄, the solvent removed under reduced pressure, and dried *in vacuo* yielding a yellow oil. The product was further purified by flash column chromatography (silica gel, eluant: 97:2:1 CH₂Cl₂:MeOH:AcOH) and the product was dried *in vacuo* to give a waxy pale yellow solid (15.2 g, 76%). ¹H NMR (300 MHz, CDCl₃) δ: 7.25-7.35 (m, 5H), 4.5 (s, 1H), 4.3 (t, *J* = 3.7, 1H), 3.7-3.8 (m, 2H); ¹³C NMR (300 MHz, CDCl₃) δ: 173.4, 138.8, 128.4, 127.7, 127.6, 73.1, 72.3, 70.8; IR (thin film) ν: 3400, 3028, 2918, 2864, 1716, 1203, 1095, 735, 696 cm⁻¹; MS (EI) *m/z* (relative intensity): 196.1 (M⁺, 29), 107.1 (32), 91.1 (100); HRMS (EI) calcd for C₁₀H₁₂O₄: 196.07356, found: 196.07363.



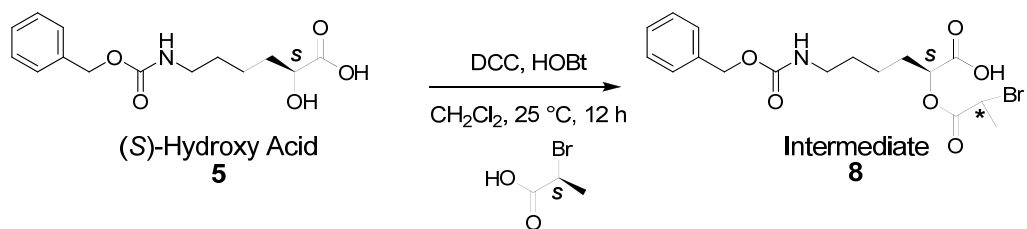
2.2.2.2. 6-(Benzyloxycarbonylamino)-2-hydroxyhexanoic acid (5). A 1 M solution of aq. KHSO₄/CH₃CN was prepared by dissolving KHSO₄ (136.0 g, 1 mole) in deionized water (700 mL) and adding CH₃CN (300 mL). H-Lys(Z)-OH (10.0 g, 35.7 mmol) was dissolved in the solution and it was then cooled to 0 °C and an aqueous solution (100 mL) of NaNO₂ (37.0 g, 535.7 mmol) was added over a period 20 min using a syringe pump. The reaction mixture was kept at 0 °C and stirred for an additional three hours. NaCl (20.0 g) was added to the reaction mixture and the crude product was extracted several times with EtOAc. The combined organic layers were washed with water and brine and dried over MgSO₄. The solvent was removed under reduced pressure and the residue dried *in vacuo* to give a waxy yellow solid. The product was further purified by flash column chromatography (silica gel, eluant: 97:2:1 CH₂Cl₂:MeOH:AcOH) and the product was dried *in vacuo* to give a pale yellow solid (6.0 g, 60%). ¹H NMR (300 MHz, CDCl₃) δ: 7.30-7.50 (m, 5H), 5.5 (s, 2H), 4.2 (dd, *J* = 4.2, 7.5, 1H), 3.7 (m, 2H), 1.85-1.75 (m, 1H), 1.70-1.60 (m, 1H), 1.55-1.30 (m, 4H); ¹³C NMR (300 MHz, CDCl₃) δ: 178.1, 154.0, 132.1, 128.8, 128.7, 128.5, 69.9, 69.8, 40.3, 33.7, 26.2, 22.1; IR (thin film) ν: 3345, 2948, 2936, 1731, 1690, 1609, 1583, 1544, 1272, 748, 731 cm⁻¹; MS (ES⁺): 282.2 (M+1).



2.2.2.3. 2-Hydroxypentanedioic acid 5-benzyl ester (6). This compound was provided by Warren Gerhardt (as synthesized in *Biomacromolecules* **2006**, *7*, 1735-1742).

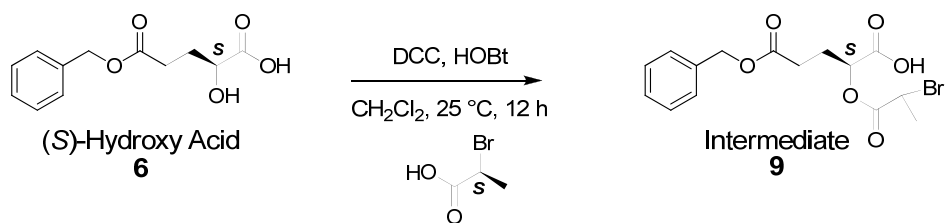


2.2.2.4. 3-(Benzyloxy)-2-(2-bromopropanoyloxy)propanoic acid (7). (S) 2-Bromopropionyl chloride (6.3 mL, 61.2 mmol) was added to **4** (10.0 g, 51 mmol) and the mixture was heated at 70 °C under an argon atmosphere in a three-neck round bottom flask equipped with a NaOH trap. Once the reaction was completed as shown by thin-layer chromatography (TLC) (approx. six hours), the dark brown oil was placed in a Kugelrohr and distilled at 60 °C and 50 mmHg overnight to remove excess 2-bromopropionic acid. Crude **7** was further purified by flash column chromatography (silica gel, eluant: 98:1.5:0.5 CH₂Cl₂:MeOH:AcOH). The solvent was removed *in vacuo* to give a brown oil in 94% yield. Compound **7** was carried on to the halogen exchange step without further purification.

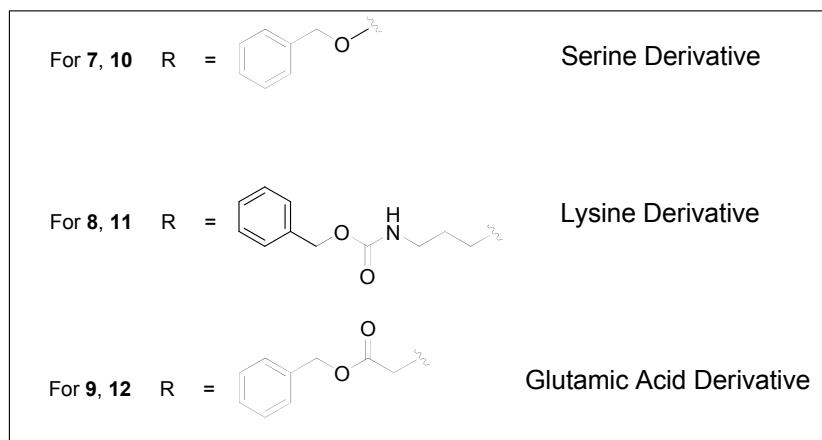
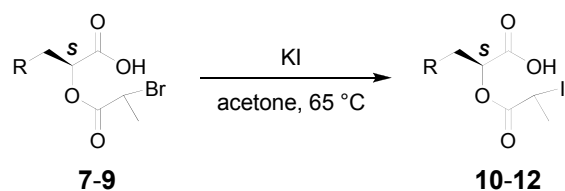


2.2.2.5. 6-Benzyloxycarbonylamino-2-(2-bromopropionyloxy)hexanoic acid

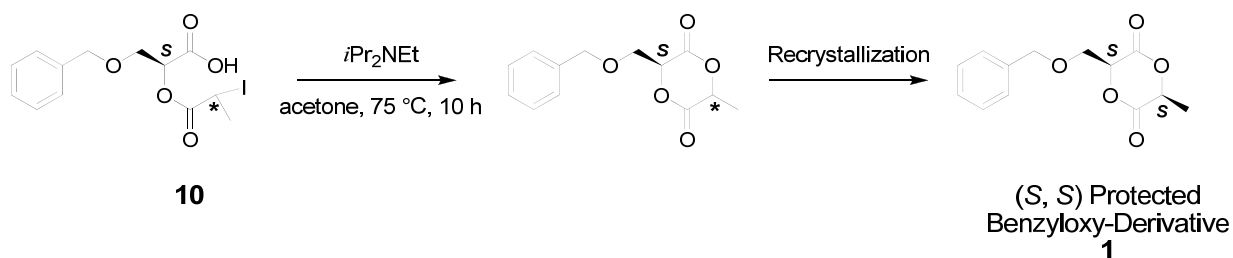
(8). (S) 2-Bromopropionic acid (0.242 mL, 2.7 mmol) and 1-hydroxybenzotriazole (HOBT) (0.32 g, 2.4 mmol) were dissolved in dry CH₂Cl₂ (10 mL). Once homogeneous, the solution was cooled to 0 °C and dicyclohexylcarbodiimide (DCC) (0.42 g, 2.0 mmol) was added in one portion. The reaction was stirred in an ice bath for 5 min and then stirred for an additional 20 min at 25 °C. Dicyclohexylurea (DCU) started to precipitate out instantly upon DCC addition. After a 25 min incubation period, a solution of **5** (0.37 g, 1.3 mmol) in CH₂Cl₂ (15 mL) was added dropwise over 20 min via an addition funnel. The reaction mixture was stirred for twelve hours becoming a dark brown color. It was then filtered through celite to remove DCU. The solvent was removed under reduced pressure and the brown oil redissolved in EtOAc and cooled in a freezer to precipitate out the unreacted DCC which was then filtered off through celite, and washed several times with water to remove most of the HOBT. The solvent was removed under reduced pressure and the dark brown oil was placed in a Kugelrohr and distilled at 60 °C and 50 mmHg overnight to remove excess 2-bromopropionic acid. Crude **8** was further purified by flash column chromatography (silica gel, eluant: 98:1.5:0.5 CH₂Cl₂:MeOH:AcOH). The solvent was removed under reduced pressure and the residue dried *in vacuo* to give a dark brown oil (0.51 g, 93%). Compound **8** was carried on to the halogen exchange step without further purification.



2.2.2.6. 2-(2-Bromo-propionyloxy)pentanedioic acid 5-benzyl ester (9). (S) 2-Bromo-propionic acid (0.24 mL, 2.7 mmol) and 1-hydroxybenzotriazole (HOBT) (0.32 g, 2.4 mmol) were dissolved in dry CH_2Cl_2 (10 mL). The solution was cooled to $0\text{ }^\circ\text{C}$ and dicyclohexylcarbodiimide (DCC) (0.42 g, 2.0 mmol) was added in one portion. The reaction was stirred in an ice bath for 5 min and then stirred for an additional 20 min at $25\text{ }^\circ\text{C}$. Dicyclohexylurea (DCU) started to precipitate out instantly upon DCC addition. After a 25 min incubation period, a solution of **6** (0.32 g, 1.3 mmol) in CH_2Cl_2 (15 mL) was added dropwise over 20 min via an addition funnel. The reaction mixture was stirred for twelve hours becoming a light brown color. It was then filtered through celite to remove the DCU. The solvent was removed under reduced pressure and the brown oil redissolved in EtOAc and cooled in a freezer to precipitate out the unreacted DCC, which was then filtered off through celite, and then washed several times with water to remove most of the HOBT. The solvent was removed under reduced pressure and the dark brown oil was placed in a Kugelrohr and distilled at $60\text{ }^\circ\text{C}$ and 50 mmHg overnight to remove excess 2-bromopropionic acid. Crude **9** was further purified by flash column chromatography (silica gel, eluant: 98:1.5:0.5 CH_2Cl_2 :MeOH:AcOH). The solvent was removed under reduced pressure and the residue dried *in vacuo* to give a brown oil (0.46 g, 91%). Compound **9** was carried on to the halogen exchange step without further purification.

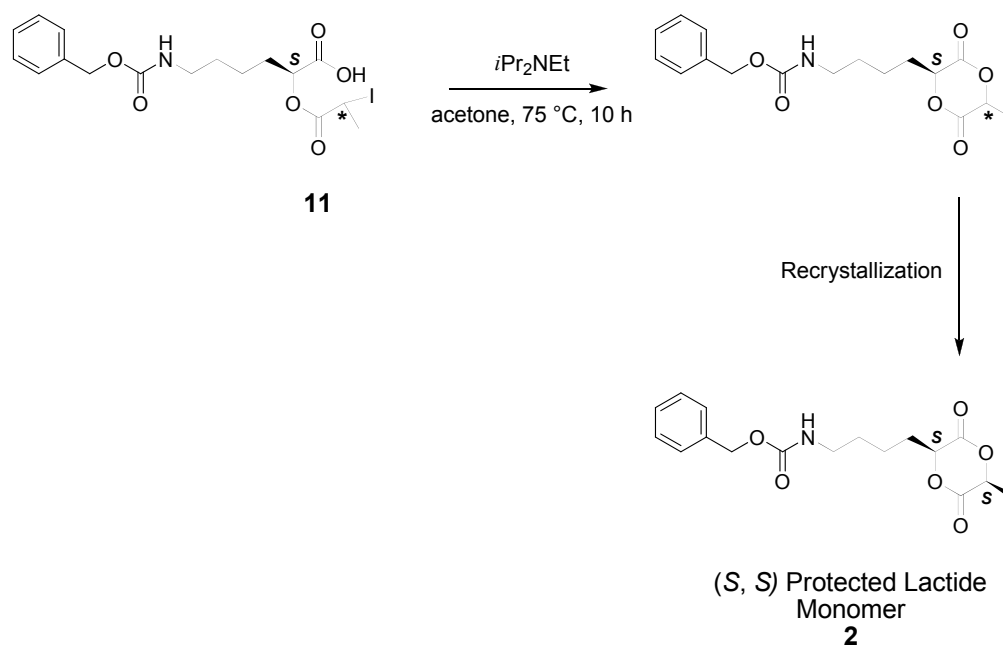


2.2.2.7. General Procedure for the Halide Exchange. A solution of the α -bromocarboxylic acid (**7-9**) in dry acetone (100 mL) was heated to reflux with a large excess of KI (approx. 10 equivalents) under an argon atmosphere. After twelve hours (quantitative conversion by TLC) the reaction mixture was filtered through celite and the solvent was removed under reduced pressure. The residual dark red oil was redissolved in EtOAc and washed several times with a 2 M aq. $\text{Na}_2\text{S}_2\text{O}_3$ solution. After the first wash, the dark red color changed to a pale yellow. The organic layer was dried over MgSO_4 , the solvent was removed under reduced pressure, and the residue was dried *in vacuo*. The α -iodocarboxylic acids (**10-12**) were used without further purification.



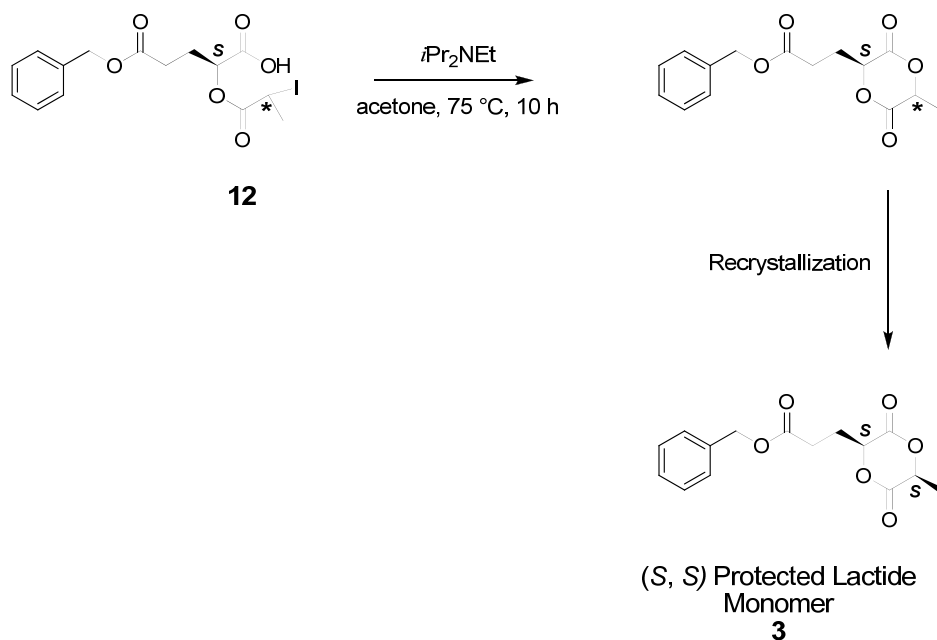
2.2.2.8. 3-(Benzyloxymethyl)-6-methyl-1,4-dioxane-2,5-dione (1). A solution of **10** (5.2 g, 13.9 mmol) in dry CH₂Cl₂ (100 mL) was added slowly over a period of eight hours to a refluxing solution of DIEA (4.6 mL, 27.7 mmol) in dry acetone (1 L) via a syringe pump. After the complete addition of **10** the reaction was stirred for an additional hour at reflux and the solvent was removed under reduced pressure. Et₂O (100 mL) was added to the light brown oil to precipitate out ammonium iodide, which was filtered off through celite and the solvent was removed under reduced pressure. The linear oligomers were removed by passage through a short column of premium grade silica gel (3:1 v/v hexanes:EtOAc) to give the crude diastereomeric mixture as a pale brown oil (1.5 g, 43%). The diastereomers were separated by flash column chromatography (premium grade silica gel, eluant: 80:20 hexanes:EtOAc). The first diastereomer to elute was isolated as a pale brown oil (0.53 g, 36% of mixture). ¹H NMR (300 MHz, CDCl₃) δ: 7.2-7.4 (m, 5H), 5.2 (q, *J* = 7.0 Hz, 1H), 5.0 (dd, *J* = 2.1, 2.5 Hz, 1H), 4.5 (s, 2H), 4.0 (dd, *J* = 2.0, 10.5 Hz, 1H), 3.9 (dd, *J* = 2.6, 10.5 Hz, 1H), 1.6 (d, *J* = 7.0 Hz, 3H). The second diastereomer was recrystallized from Et₂O to give a white crystalline solid (0.93 g, 64% of mixture). ¹H NMR (300 MHz, CDCl₃) δ: 7.2-7.1 (m, 5H), 5.07 (t, *J* = 3.4 Hz, 1H), 5.0 (q, *J* = 6.9 Hz, 1H), 4.6 (s, 2H), 4.0 (d, *J* = 3.5 Hz, 2H), 1.6 (d, *J* = 6.9 Hz, 3H); ¹³C NMR (300 MHz, CDCl₃) δ: 166.0, 164.1, 136.4, 128.4, 128.1, 127.9, 76.0, 74.0, 73.1,

68.6, 17.8; IR (thin film) ν : 3032, 1770, 1749, 1250, 1093 cm^{-1} ; MS (EI) m/z (relative intensity): 250.1 (M^+ , 12), 144 (34), 107 (36), 91.1 (100), 65.1 (11); HRMS (EI) calcd for $\text{C}_{13}\text{H}_{14}\text{O}_5$: 250.08384, found: 250.08412; Elemental analysis: calcd for $\text{C}_{13}\text{H}_{14}\text{O}_5$: C, 62.39; H, 5.64; O, 31.97; found: C, 62.36; H, 5.75; O, 32.00; M.P. 85.4-89.8 $^{\circ}\text{C}$.



2.2.2.9. Benzyl 4-(5-methyl-3,6-dioxo-1,4-dioxan-2-yl)butylcarbamate (2). A solution of **11** (5.8 g, 12.5 mmol) in dry CH_2Cl_2 (100 mL) was added slowly over a period of eight hours to a refluxing solution of DIEA (4.1 mL, 24.9 mmol) in dry acetone (1 L) via a syringe pump. After the complete addition of **11**, the reaction was stirred for an additional hour at reflux and the solvent was removed under reduced pressure. Et_2O (100 mL) was added to the light brown oil to precipitate out ammonium iodide, which was filtered off through celite and the solvent was removed under reduced pressure. The crude product was purified by flash column chromatography (premium grade silica gel, eluant: 80:20 hexanes:EtOAc) to give a clear oil which was recrystallized from EtOAc/hexanes to give a white crystalline solid (3.19 g, 75%). ^1H NMR (300 MHz, CDCl_3) δ : 7.4-7.2 (m, 6H), 5.1 (s, 2H), 4.98 (q, $J = 5$ Hz, 1H), 4.89 (dd, $J = 4.3, 2.8$ Hz, 1H), 4.8 (br. s, 1H), 3.22 (q, $J = 5.7$ Hz, 2H), 2.1 (m, 2H), 1.95 (m, 2H), 1.62 (d, $J = 6.7$ Hz, 3H), 1.6-1.4 (br. s, 4H); ^{13}C NMR (300 MHz, CDCl_3) δ : 167.2, 166.5, 155.2, 136.4,

128.4, 128.0, 127.95, 75.5, 72.3, 66.6, 40.6, 29.55, 29.5, 21.5, 15.9; IR (thin film) ν : 3331, 2943, 2874, 1782, 1749, 1693, 1688, 1537, 1281, 1265, 1227, 696 cm^{-1} ; MS (FAB⁺) m/z (relative intensity): 336.1 (M+1, 100), 292.1 (42), 248.1 (12); HRMS (FAB⁺) calcd for C₁₇H₂₂NO₆: 336.1447, found: 336.14352; Elemental analysis: calcd for C₁₇H₂₁NO₆: C, 60.89; H, 6.31; N, 4.18; O, 28.63; found: C, 60.87; H, 6.33; N, 4.16, O, 28.64; M.P. 94.0-98.6 °C.



2.2.2.10 Benzyl 3-(5-methyl-3,6-dioxo-1,4-dioxan-2-yl)propanoate (**3**). A

solution of **12** (5.5 g, 13.2 mmol) in dry CH_2Cl_2 (100 mL) was added slowly over a period of eight hours to a refluxing solution of DIEA (4.3 mL, 26.3 mmol) in dry acetone (1 L) via a syringe pump. After the complete addition of **12**, the reaction was stirred for an additional hour at reflux and the solvent was removed under reduced pressure. Et_2O (100 mL) was added to the light brown oil to precipitate out ammonium iodide, which was filtered off through celite and the solvent was removed under reduced pressure.

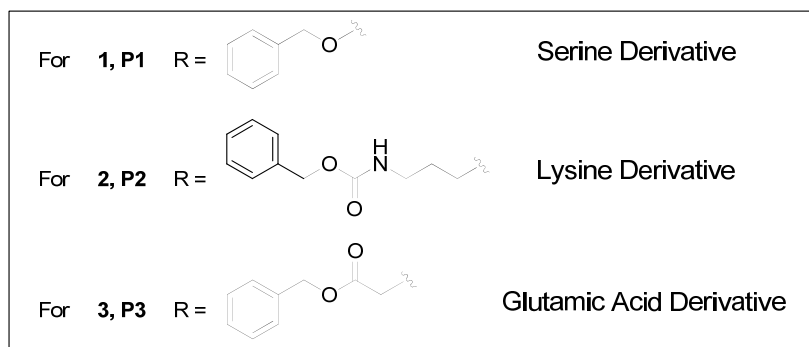
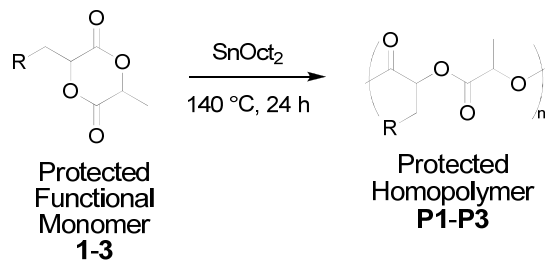
Crude **3** was purified by flash column chromatography (silica gel, eluant: 80:20

hexanes:EtOAc) to give a light brown oil (2.8 g, 73%). ^1H NMR (300 MHz, CDCl_3) δ : 7.34 (m, 5H), 5.12 (s, 2H), 5.09 (t, $J = 3.8$ Hz, 1H), 4.95 (q, $J = 6.7$ Hz, 1H), 2.63 (q, 2H), 2.48 (m, 1H), 2.21 (m, 1H), 1.64 (d, $J = 6.6$ Hz, 3H); ^{13}C NMR (300 MHz, CDCl_3) δ : 171.9, 167.0, 166.5, 135.3, 128.31, 128.07, 127.90, 74.0, 72.1, 66.4, 28.3, 25.0, 15.5; IR ν : (thin film) 3034, 2999, 2947, 1764, 1732, 1246, 1171, 752, 700 cm^{-1} ; HRMS (ESI^+)

calcd for $C_{15}H_{17}O_6$: 293.106425, found: 293.101965; Elemental analysis: calcd for $C_{15}H_{16}O_6$: C, 61.64; H, 5.52; O, 32.84. found: C, 61.49; H, 5.59; O, 32.92.

2.2.3. Preparation of Protected Homopolymers

2.2.3.1. SnOct₂ Catalyst Stock Solution. In a nitrogen-filled glove box, SnOct₂ (0.32 g, 0.8 mmol) was added to a 10 mL volumetric flask that was then filled to the graduation mark with dry, degassed benzene making a 0.8 M solution, this was transferred to a Schlenk flask and stored inside the glove box.



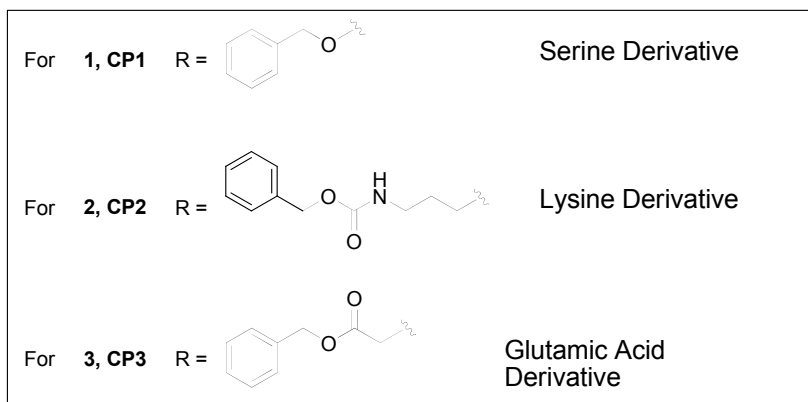
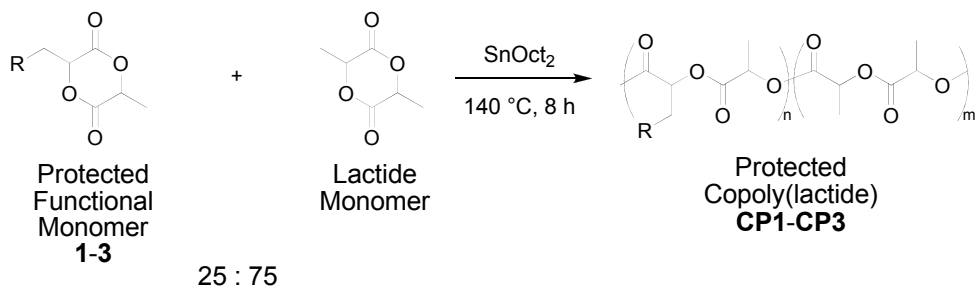
2.2.3.2. General Procedure for Homopolymerizations. Monomers **1-3** were purified and homopolymerized in collaboration with Warren Gerhardt (*Biomacromolecules* **2006**, *7*, 1735-1742).

2.2.3.3. Homopolymer P1. ¹H NMR (300 MHz, CDCl₃) δ: 7.2-7.4 (s, 5H), 5.1-5.5 (m, 2H), 4.4-4.6 (m, 2H), 3.9-4.0 (m, 1H), 3.7-3.9 (m, 1H), 1.4-1.7 (m, 3H); ¹³C NMR (300 MHz, CDCl₃) δ: 169, 166, 164, 138, 129, 128, 73, 72, 69, 68, 67, 32, 17.

2.2.3.4. Homopolymer P2. ¹H NMR (300 MHz, CDCl₃) δ: 7.2-7.4 (m, 5H), 4.8-5.4 (m, 4H), 3.4-3.6 (m, 1H), 3.0-3.2 (m, 1H), 1.4-2.1 (m, 9H); ¹³C NMR (300 MHz, CDCl₃) δ: 169, 168, 156, 137, 129, 128, 72, 69, 66, 40, 30, 29, 22, 16.

2.2.3.5. Homopolymer P3. ^1H NMR (300 MHz, CDCl_3) δ : 7.1-7.4 (m, 5H), 4.9-5.3 (m, 4H), 2.1-2.7 (m, 4H), 1.2-1.6 (m, 3H); ^{13}C NMR (300 MHz, CDCl_3) δ : 176, 172, 169, 168, 136, 135, 129, 128, 75, 72, 69, 67, 66, 31, 29, 27, 26, 16.

2.2.4. Preparation of Protected PLA Copolymers



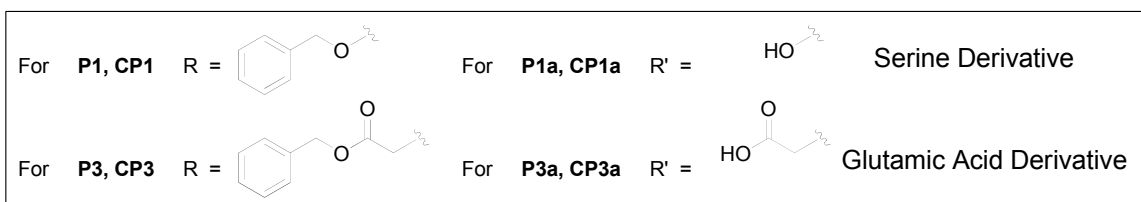
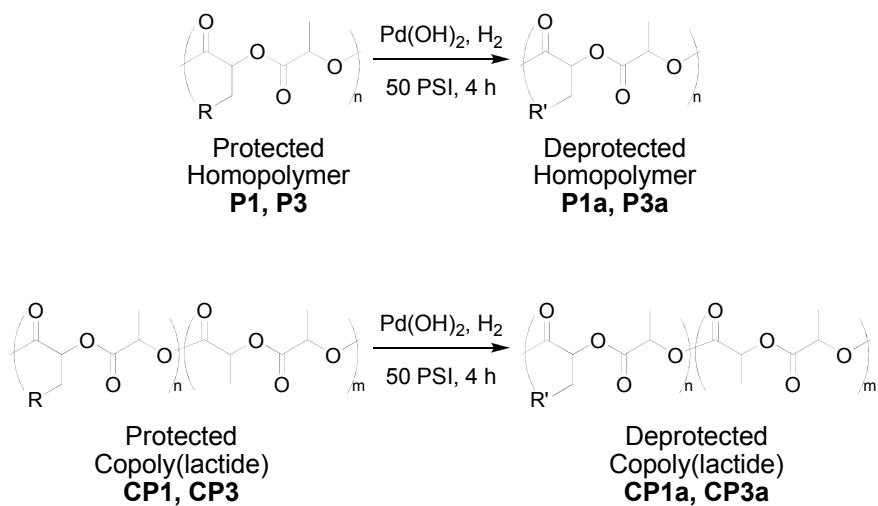
2.2.4.1. General Procedure for Copolymerizations. Monomers **1-3** were copolymerized with lactide in collaboration with Warren Gerhardt (*Biomacromolecules* **2006**, *7*, 1735-1742).

2.2.4.2. Copolymer CP1. $^1\text{H NMR}$ (300 MHz, CDCl_3) δ : 7.2-7.4 (m, 5H), 5.1-5.4 (m, 7H), 4.4-4.60 (m, 2H), 3.8-4.0 (m, 2H), 1.4-1.7 (m, 18H), ; $^{13}\text{C NMR}$ (300 MHz, CDCl_3) δ : 170, 167, 166, 164, 137, 129, 128, 73, 72, 69, 68, 67, 66, 31, 17.

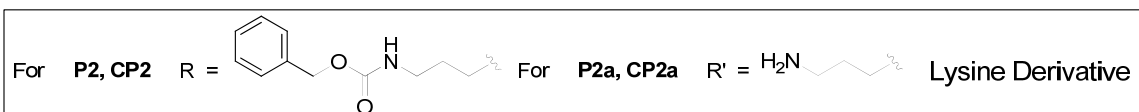
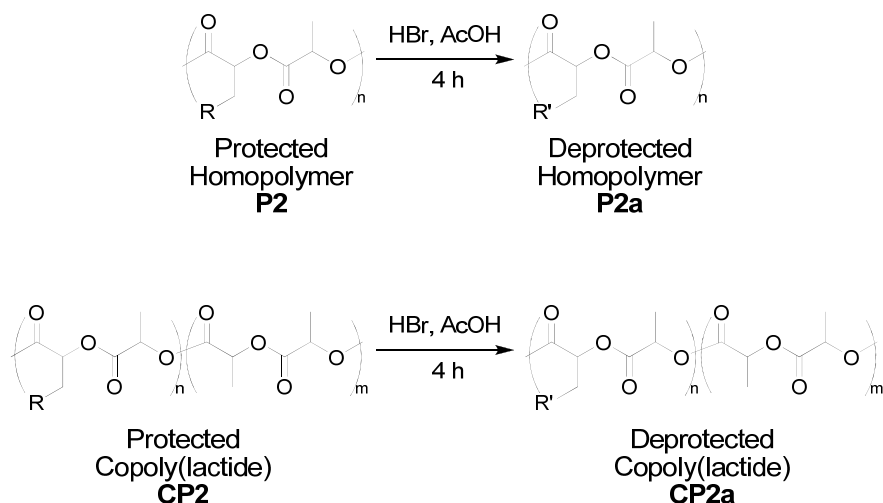
2.2.4.3. Copolymer CP2. $^1\text{H NMR}$ (300 MHz, CDCl_3) δ : 7.2-7.4 (m, 5H), 4.8-5.3 (m, 18H), 3.4-3.5 (m, 1H), 3.0-3.2 (m, 2H), 1.1-2.1 (m, 50H); $^{13}\text{C NMR}$ (300 MHz, CDCl_3) δ : 170, 169, 168, 167, 156, 137, 129, 128, 78, 72, 69, 66, 40, 39, 30, 29, 22, 20, 16.

2.2.4.4. Copolymer CP3. ^1H NMR (300 MHz, CDCl_3) δ : 7.2-7.4 (m, 5H), 4.9-5.3 (m, 10H), 2.2-2.6 (m, 4H), 1.4-1.8 (m, 22H); ^{13}C NMR (300 MHz, CDCl_3) δ : 176, 172, 170, 169, 168, 167, 137, 136, 135, 129, 128, 78, 77, 75, 70, 69, 68, 66, 30, 29, 26, 25, 16.

2.2.5. Preparation of Functional Homopolymers and Copolymers



2.2.5.1. General Procedure for Hydrogenolysis Deprotections. These homo- and copolymers were deprotected in collaboration with Warren Gerhardt (*Biomacromolecules* **2006**, *7*, 1735-1742).



2.2.5.2. General Procedure for Acidolysis Deprotections of Benzyl

Carbamates. These homo- and copolymers were deprotected in collaboration with Warren Gerhardt (*Biomacromolecules* **2006**, *7*, 1735-1742).

2.2.5.3. Homopolymer P1a. ^1H NMR (300 MHz, d_6 -acetone) δ : 5.1-5.4 (m, 2H), 3.9-4.1 (m, 1H), 3.7-3.9 (m, 1H), 3.0-3.2 (m, 1H), 1.8-2.0 (m, 1H), 1.4-1.8 (m, 3H); ^{13}C NMR (300 MHz, d_6 -acetone) δ : 169, 166, 164, 75, 73, 69, 68, 67, 62, 32, 23, 16.

2.2.5.4. Homopolymer P2a. ^1H NMR (300 MHz, d_6 -acetone) δ : 4.8-5.3 (m, 2H), 3.4-3.5 (m, 1H), 3.0-3.3 (m, 1H), 1.8-2.1 (m, 2H), 1.3-1.8 (m, 7H); ^{13}C NMR (300 MHz, d_6 -acetone) δ : 172, 169, 72, 69, 40, 29, 28, 26, 20, 16.

2.2.5.5. Homopolymer P3a. ^1H NMR (300 MHz, d_6 -acetone) δ : 5.1-5.4 (m, 1H), 5.0-5.1 (m, 1H), 2.4-2.8 (m, 2H), 2.2-2.4 (m, 2H), 1.3-1.6 (m, 3H); ^{13}C NMR (300 MHz, d_6 -acetone) δ : 177, 176, 173, 172, 171, 77, 76, 71, 70, 69, 62, 56, 31, 28, 27, 26, 18.

2.2.5.6. Copolymer CP1a. ^1H NMR (300 MHz, CDCl_3) δ : 5.1-5.3 (m, 7H), 3.7-4.0 (m, 2H), 1.3-1.8 (m, 18H); ^{13}C NMR (300 MHz, CDCl_3) δ : 170, 167, 166, 164, 74, 73, 69, 68, 67, 32, 22, 17, 16.

2.2.5.7. Copolymer CP2a. ^1H NMR (300 MHz, CDCl_3) δ : 4.9-5.3 (m, 16H), 3.4-3.5 (m, 1H), 3.0-3.2 (m, 1H), 1.1-2.1 (m, 50H); ^{13}C NMR (300 MHz, CDCl_3) δ : 170, 169, 75, 69, 68, 41, 40, 31, 23, 17.

2.2.5.8. Copolymer CP3a. ^1H NMR (300 MHz, CDCl_3) δ : 5.0-5.3 (m, 8H), 2.4-2.6 (m, 2H), 2.2-2.4 (m, 2H), 1.4-1.7 (22H); ^{13}C NMR (300 MHz, CDCl_3) δ : 180, 174, 173, 172, 170, 169, 167, 72, 70, 69, 68, 66, 30, 29, 26, 25, 16.

2.3. Results and Discussion (Taken from *Biomacromolecules* 2006, 7, 1735-1742)

2.3.1. Synthetic Approaches Towards Functional Monomers

Important to the design of our synthetic strategy is the preservation of the biorenewable character of our functional monomers whereby we make use of commercially available side-chain protected L-amino acids (Figure 2.2). We rationalized that readily available amino acids provide a large diversity of terminal functional groups in their side-chains and that they are available as single enantiomers. To demonstrate the modular character of our functional PLA synthesis based on amino acids, we present the synthesis of three new functional lactide monomers, **1-3**, containing protected amines, carboxylic acids, and alcohols in their side-chains (Figure 2.2) as well as their homopolymerization and copolymerization.

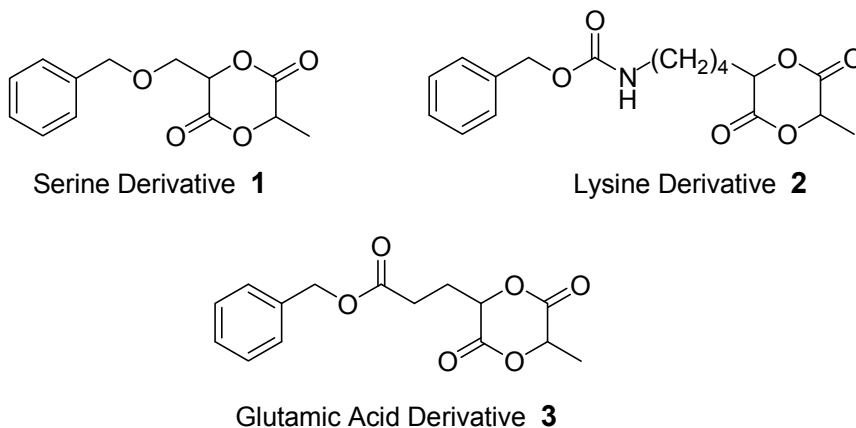


Figure 2.2. Functional lactide monomers investigated.

Our synthetic strategy is based on the simple conversion of amino acids to their corresponding α -hydroxy acids. These are then coupled with either (*S*) 2-bromopropionyl chloride or (*S*) 2-bromopropionic acid and cyclized to provide the monofunctional lactide (Figure 2.3).

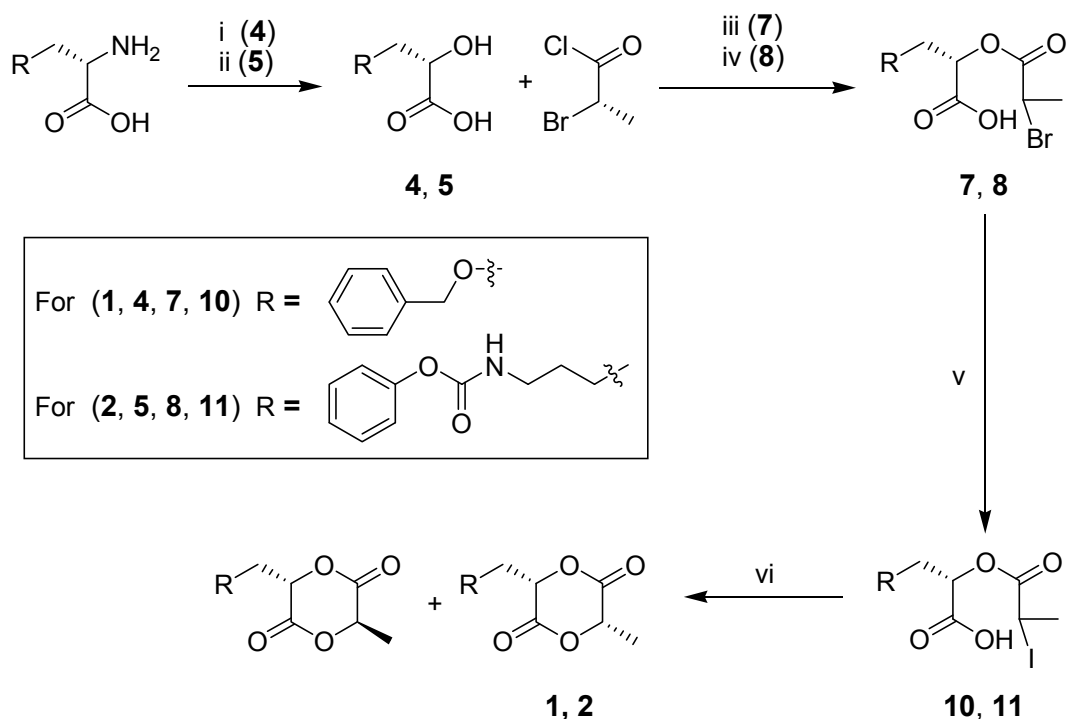


Figure 2.3. Synthesis of cyclic monomers **1** and **2** using an acid chloride coupling. Conditions: (i) NaNO₂, TFA, H₂O, 25 °C, 6 h; (ii) NaNO₂, aq. KHSO₄, 0-25 °C, 3 h; (iii) 75 °C, 6 h; (iv) DIEA, Et₂O, 0-40 °C, 12 h; (v) KI, acetone, 65 °C, 12 h; (vi) DIEA, acetone, 75 °C, 10 h.

Our synthetic strategy commences with the diazotization of the amino acid to the corresponding α -hydroxy acid, with full retention of the stereochemistry.^{45,46} The transformation requires sodium nitrite addition to the amino acid in an aqueous acid solution. As reported by others,⁴⁵ the yields of the diazotization vary widely based on the rate of sodium nitrite addition, choice of acid, and the reaction temperature. The yields shown in Figures 2.3 and 2.4 range from 60% for **5** to 72% for **6**. Since 2-bromopropionyl chloride is only commercially available in the racemic form, we synthesized (*S*) 2-bromopropionyl chloride from L-alanine by diazotization in HBr to provide (*S*) 2-bromopropionic acid, followed by the conversion to the acid chloride with

thionyl chloride.⁴⁷ The conditions for the cyclization of each functionalized α -hydroxy acid with lactic acid to provide the functional cyclic diester varied depending on the lability of each protecting group (Figures 2.3 and 2.4).

The robustness of the benzyl ether protecting group made the synthesis of monomer **1** the most convenient with limited side-reactions throughout the synthetic pathway. Ester **7** was synthesized by treating α -hydroxy-acid **4** with (*S*) 2-bromopropionyl chloride. Racemization of the enolizable acid chloride α -proton in these acidic conditions was expected, and the diastereomeric mixture subjected to halide exchange by a Finkelstein reaction followed by cyclization without separation. The synthesis of **8**, with an acid labile urethane linkage, required the use of lower temperatures and the addition of *N,N*-diisopropylethylamine (DIEA) to scavenge the HCl. However, these conditions were still sufficiently harsh generating persistent byproducts, which were spectroscopically and functionally quite similar to **8**, and therefore difficult to remove. Because the final step is an intramolecular reaction, these unidentified byproducts posed no threat during the cyclization, and the crude monomer precursor was subjected to halide exchange and cyclized, but only low yields of product were obtained. We therefore chose to develop an alternative synthesis of monomer **2** that was also successfully employed for monomer **3**.

Monomers **2** and **3** were prepared by the condensation of functionalized α -hydroxy acids with (*S*) 2-bromopropionic acid using dicyclohexylcarbodiimide (DCC) and 1-hydroxybenzotriazole (HOBt) to provide **8** and **9**. This method circumvented racemization at the new stereocenter through: 1) milder conditions and 2) coupling of an

acid instead of the more readily enolizable acid chloride. These couplings were again followed by a halogen exchange and then cyclization, as outlined in Figure 2.4.

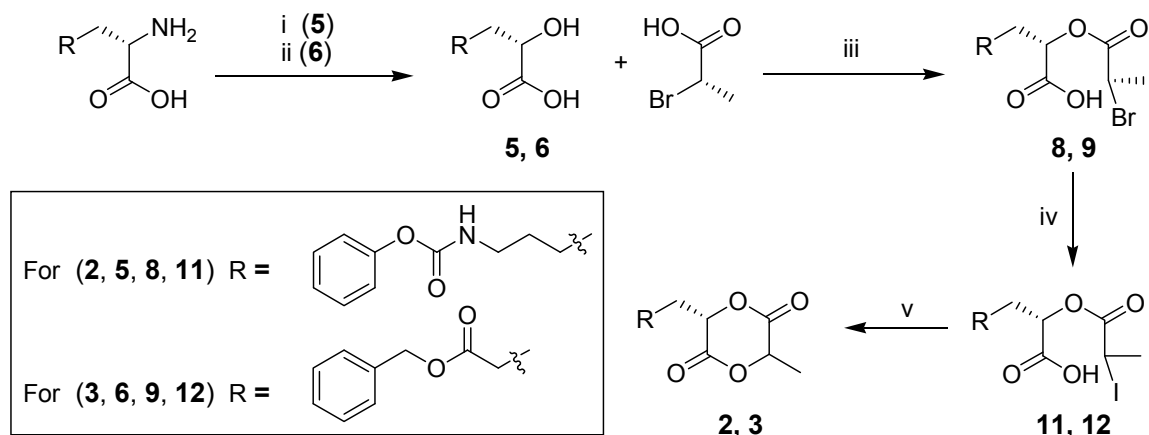


Figure 2.4. Synthesis of cyclic monomers **2** and **3**. Conditions: (i) NaNO_2 , aq. KHSO_4 , 0-25 °C, 3 h; (ii) NaNO_2 , 1:1 $\text{AcOH}/\text{H}_2\text{O}$ (v/v), 0-25 °C, 3 h; (iii) DCC, HOBT, CH_2Cl_2 , 25 °C, 12 h; (iv) KI, acetone, 65 °C, 12 h; (v) DIEA, acetone, 75 °C, 10 h.

The main advantage of the coupling step of α -hydroxy acids **5** or **6** with (*S*)-2-bromopropionic acid is that the yields of the final cyclization are higher due to a clean conversion to the cyclic monomer precursors **8** and **9** versus monomer precursors of **7** and **8** (with persistent byproducts) generated from the acid chloride coupling method of Figure 2.3.

Cyclizations of the functional monomer precursors were carried out by slowly adding uncyclized α -iodocarboxylic acids **10-12** to a dilute solution of DIEA in acetone. Linear oligomers, the primary side-products of this procedure, were easily removed by filtration of a solution of the crude product through a short plug of silica. The cyclization yield of monomer **1** was 43% with an overall yield 30%. Diastereomers of **1** from the

acid chloride method were separated by column chromatography (we found that premium grade silica gel led to significantly higher recovery of product compared to standard grade, which led to decomposition of the cyclized monomers), followed by fractional crystallization from EtOAc/hexanes. The configuration of the stereocenters of the crystalline diastereomer of **1** was shown to be (S,S) as determined by X-ray structural analysis (Figure 2.5). The absolute configuration of cyclic monomer **1** was determined knowing that the stereocenter of the α -hydroxy acid half of the molecule retains the (S) configuration of the protected amino acid precursor under the diazotization conditions.

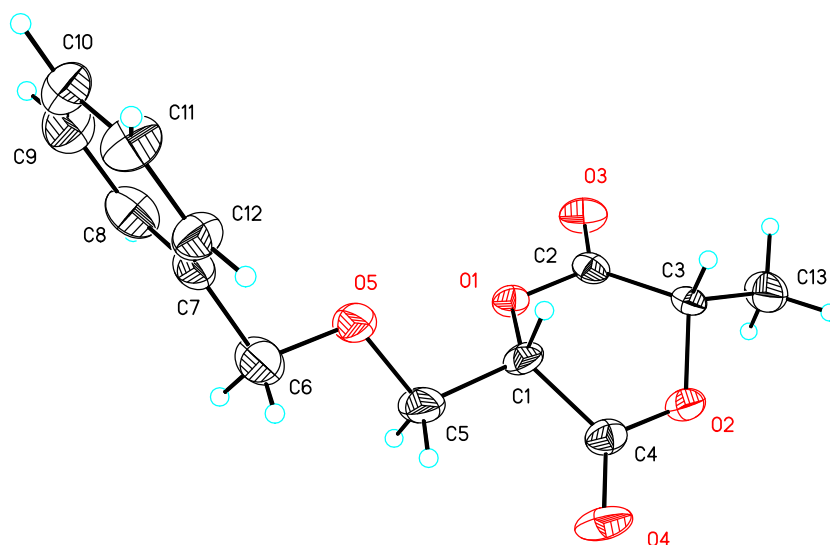


Figure 2.5. Crystal structure of monomer **1**.

As mentioned earlier the DCC/HOBt method eliminated the problem of racemization during the preparation of **8** and **9** thereby allowing for the cyclization to **2** and **3** with a > 95% diastereomeric excess (as shown by $^1\text{H-NMR}$), in yields unprecedented for the cyclization step of any cyclic lactide analogue. These single diastereomers were purified by column chromatography on silica gel, **3** was isolated with

complete control over polymer tacticity and thereby the properties of the resulting material.

2.3.2. *Synthesis of Protected Functional Homopolymers and PLA Copolymers*

To determine if our functionalized monomers could be polymerized, preliminary homo- and co-polymerizations were performed. For this study we restricted our investigation to the use of stannous octoate (SnOct_2) as the catalyst. SnOct_2 has been approved by the FDA as an indirect food additive⁵¹⁻⁵³ and is among the most active and widely used catalyst for the polymerization of lactides and related monomers.²²

All polymerizations were carried out in bulk. The monomers and catalyst were added to the reaction vessels in a nitrogen-filled glove box, along with a solubilizing amount of dry benzene (triply distilled). The reaction vessels were removed from the glove box, the solutions frozen, lyophilized and dried overnight. They were then heated to 140 °C under an atmosphere argon starting the polymerization. Consumption of all monomers occurred within 24 hours for the homopolymers (¹H NMR). For the copolymers conversion plateaued at eight hours, with stirring ceasing for **CP1** and **CP2** after 3-5 hours (Figure 2.7). Longer polymerization times (48 hours) and lower catalyst ratios (0.1%) did not yield higher molecular weight polymers; these same polymerization conditions gave poly(DL lactide) with a M_n of 65,000. Upon cooling, the polymers were purified by precipitation from CH_2Cl_2 into cold methanol (ice-water bath). Yields were based on the mass of each polymer isolated after precipitations. All polymers were characterized by ¹H NMR, ¹³C NMR, GPC, and DSC (homopolymers Table 2.1; copolymers Table 2.2).

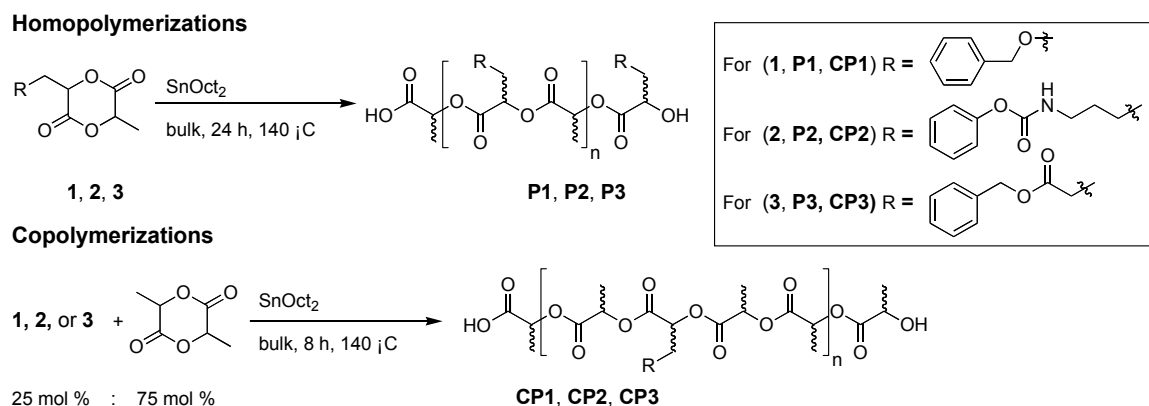


Figure 2.7. Homo- and co-polymerizations of **1**, **2**, and **3**.

Table 2.1. Homopolymer Characterization Data. ^aGPC in CH₂Cl₂ with poly(styrene) standards; ^bidentical for either diastereomer.

Polymer	$M_n (10^{-3})^a$	PDI	$T_g (^\circ\text{C})$	Yield (%)
P1^b	21	1.5	18	79
P2	8	1.4	20	60
P3	3	1.4	10	29

Table 2.2. Copolymer Characterization Data. ^aGPC in CH₂Cl₂ with poly(styrene) standards; ^bpercentage of functional monomer incorporated into the copolymer was determined by ¹H NMR after precipitation; ^cidentical for either diastereomer.

Polymer	$M_n (10^{-3})^a$	PDI	$T_g (^\circ\text{C})$	% copoly ^b	Yield (%)
CP1^c	31	2.0	27	27 %	89
CP2	24	2.1	25	25 %	72
CP3	5	1.4	5	14 %	48

Proton NMR showed broad signals characteristic of a polymer, and gel-permeation chromatography (GPC) confirmed the conversion to high molecular weight polymers for homopolymer **P1** and copolymers **CP1**⁵⁴ and **CP2**. The lower molecular weights of all of these monomers versus lactide is not unexpected owing to the steric bulk of the side-chains, which is known to decrease the ΔG of the polymerization.⁵⁵ However, the low molecular weight of copolymer **CP3** may indicate that the side-chain of monomer **3** has other interactions with the catalyst retarding the polymerization of itself and the lactide component. All of these results are also in agreement with prior reports of the polymerization of other lactide analogs⁴⁰ and substituted morpholine-2,5-dione,²⁰ and the very low molecular weights of all the polymers derived from monomer **3** were also observed in analogs that contain similar functionalities.⁵⁶ Based on the low molecular weights of most of these polymers, the near quantitative conversion of all monomers as measured by ¹H NMR presumably led to low molecular weight oligomers owing to low polymerization rates and/or possible trans esterification reactions.³⁹ However, the incorporation of the functional monomers into their copolymers is in close agreement with the stoichiometric ratio of the monomer:lactide reaction mixtures for **CP1** and **CP2**. Differential-scanning calorimetry of each polymer showed glass-transition temperatures ranging from 5 to 27 °C, which is below the value for poly(lactide) itself. This can be attributed to the presence of the flexible side-chains, which act as internal plasticizers.⁴⁰

These preliminary polymerization results clearly show the potential of monomers **1** and **2** as new functional poly(lactide) analogues. The unsatisfactory results obtained for monomer **3** may be attributed to retardation of the catalyst by coordination of the benzyl

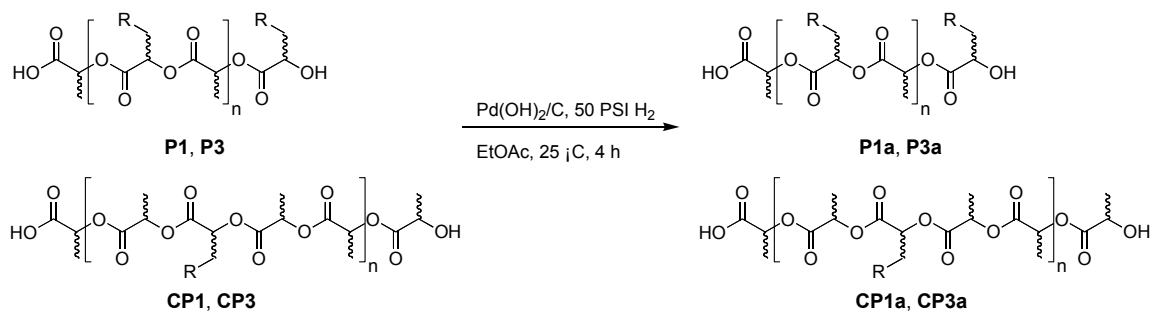
glutamate side-chain. Also, monomer **3** being an oil was harder to purify and dry in contrast to the crystalline monomers, the possible presence of scant amounts of adventitious water, despite rigorous drying procedures, may act as an undesirable initiator limiting molecular weights. Through the screening of an array of catalyst/initiator we are optimistic that higher molecular weights can be obtained for monomers **1** and **2**.

2.3.3. Protected Functional Homo- and Copolymer Deprotection

Deprotection of homo- and co-polymers **P1** and **CP1** derived from serine, and homo- and co-polymers **P3** and **CP3** derived from glutamic acid was accomplished by hydrogenolysis using Pd(OH)₂ as the hydrogenation catalyst revealing the hydroxyl and carboxylic acid functional groups respectively (Figure 2.8A). Clean and quantitative removal of all benzyl ether and ester protecting groups from the homo- and co-polymers was confirmed by the disappearance of the aromatic and benzylic signals from the ¹H NMR and ¹³C NMR spectra. This process did not result in the degradation of the polyester backbone, as shown by the lack of signals between 4.2 - 4.4 ppm associated with the α-hydroxy proton that would be apparent upon the cleavage of the backbone (Figure 2.9), this was also observed in the ¹H NMR spectra of all of the copolymers.

However, homo- and co-polymers **P2** and **CP2** were recalcitrant towards hydrogenolysis and were deprotected using HBr (33%)/AcOH for two hours (Figure 2.8B).

A Benzyl Ether and Benzyl Ester Protected Polymers



B Benzyl Carbamate Protected Polymers

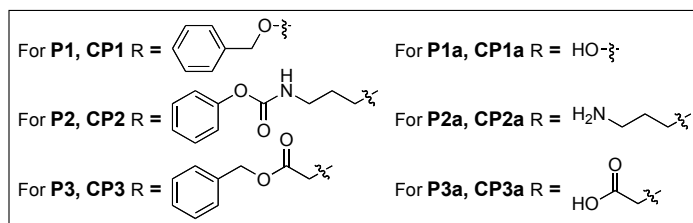
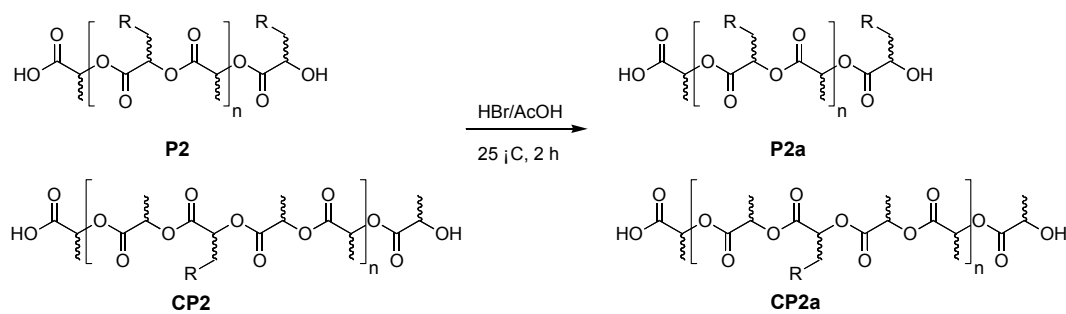


Figure 2.8. Deprotection strategies for protected polymers: (A) Hydrogenolysis of benzyl ethers and esters; (B) Acidolysis of benzyl carbamates.

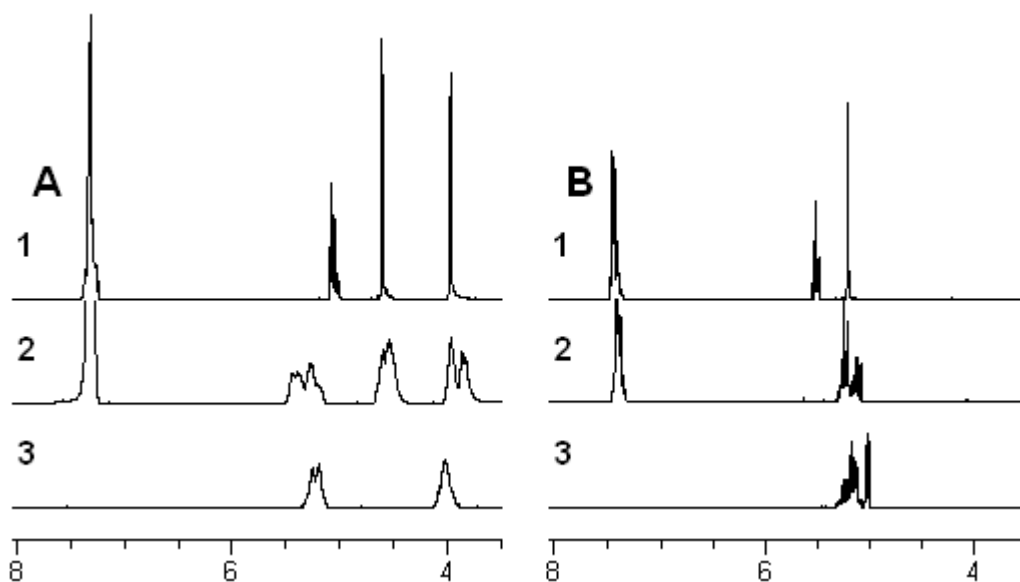


Figure 2.9. (A) ^1H NMR spectra of serine derivatives in d_6 -acetone: 1) monomer **1**; 2) homopolymer **P1**; 3) deprotected homopolymer **P1a**; (B) ^1H NMR spectra of glutamic acid derivatives in d_6 -acetone: 1) monomer **3**; 2) homopolymer **P3**; 3) deprotected homopolymer **P3a**.

Clean and quantitative removal of the benzyl carbamate without backbone degradation was again confirmed by ^1H NMR and ^{13}C NMR, by observing the disappearance of the aromatic and benzylic signals and the absence of a signal in the region of the α -hydroxy proton in the ^1H NMR spectrum (Figure 2.10). Unfortunately, the newly revealed functional groups of all but one of the new homopolymers precluded their characterization by GPC owing to solubility problems of the deprotected homopolymers in CH_2Cl_2 and the different hydrodynamic volumes of the deprotected copolymers. GPC analysis of the deprotected copolymer **CP1a** showed a decrease in molecular weight of approximately 35% corresponding to full cleavage of the benzyl protecting group and no cleavage of the polymer backbone. Also the GPC trace of

poly(DL lactide) with a M_n of 30,000 had the same M_n and peak shape before and after being exposed to each of the deprotection conditions.

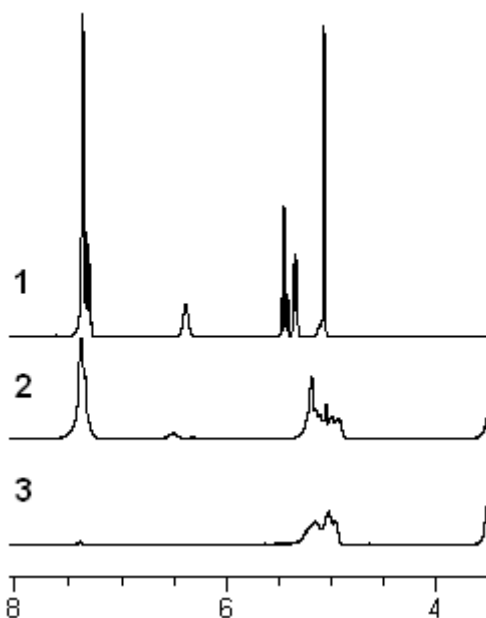


Figure 2.10. ^1H NMR spectra of lysine derivatives in d_6 -acetone: 1) monomer **2**; 2) homopolymer **P2**; 3) deprotected homopolymer **CP2a**.

2.4. Conclusions

In conclusion, we have developed a modular strategy towards the synthesis and polymerization of functional lactides from commercially available protected amino acids. To demonstrate this new strategy, we have synthesized three new functional lactide monomers containing protected amine, alcohol, and carboxylic acid functionalities, we then investigated the homopolymerization behavior using the metal catalyst stannous octoate and then successfully copolymerized each monomer with lactide. Removal of the protecting groups from every polymer was quantitative with no scission of the backbone observed. Monomers **1** and **2** had the most promising polymerization results, upon

deprotection; these new polymers yielded highly functional, biorenewable materials with a multitude of potential applications in the medical field. Optimization of the polymerizations for monomers **1** and **2** will be further investigated, specifically looking at an array of catalysts/initiators. Future work will focus on the development of strategies for post-polymerization modification and decomposition studies of these new functional materials.

2.5. References

- (1) Mehta, R.; Kumar, V.; Bhunia, H.; Upadhyay, S. N., *J. Macromol. Sci., Polym. Rev.* **2005**, *C45*, 325-349.
- (2) Albertsson, A.-C.; Varma, I. K., *Biomacromolecules* **2003**, *4*, 1466-1486.
- (3) Drumright, R. E.; Gruber, P. R.; Henton, D. E., *Adv. Mater.* **2000**, *12*, 1841-1846.
- (4) Dechy-Cabaret, O.; Martin-Vaca, B.; Bourissou, D., *Chem. Rev.* **2004**, *104*, 6147-6176.
- (5) Holy, C. E.; Fialkov, J. A.; Davies, J. E.; Shoichet, M. S., *J. Biomed. Mater. Res., Part A* **2003**, *65A*, 447-453.
- (6) Jin, S.; Gonsalves, K. E., *J. Mater. Sci.: Mater. Med.* **1999**, *10*, 363-368.
- (7) Williams, C. K., *Chem. Soc. Rev.* **2007**, *36*, 1573-1580.
- (8) Kimura, Y.; Shirotani, K.; Yamane, H.; Kitao, T., *Polymer* **1993**, *34*, 1741-8.
- (9) Leemhuis, M.; van Nostrum, C. F.; Kruijtzter, J. A. W.; Zhong, Z. Y.; ten Breteler, M. R.; Dijkstra, P. J.; Feijen, J.; Hennink, W. E., *Macromolecules* **2006**, *39*, 3500-3508.

- (10) Leemhuis, M.; van Steenis, J. H.; van Uxem, M. J.; van Nostrum, C. F.; Hennink, W. E., *Eur. J. Org. Chem.* **2003**, 3344-3349.
- (11) Jiang, X.; Vogel, E. B.; Smith, M. R.; Baker, G. L., *Macromolecules* **2008**, *41*, 1937-1944.
- (12) Lou, X. D.; Detrembleur, C.; Jerome, R., *Macromol. Rapid Commun.* **2003**, *24*, 161-172.
- (13) Loontjens, C. A. M.; Vermonden, T.; Leemhuis, M.; van Steenberg, M. J.; van Nostrum, C. F.; Hennink, W. E., *Macromolecules* **2007**, *40*, 7208-7216.
- (14) Barrera, D. A.; Zylstra, E.; Lansbury, P. T., Jr.; Langer, R., *J. Am. Chem. Soc.* **1993**, *115*, 11010-11.
- (15) Kimura, Y.; Shirotani, K.; Yamane, H.; Kitao, T., *Macromolecules* **1988**, *21*, 3338-40.
- (16) Barrera, D. A.; Zylstra, E.; Lansbury, P. T.; Langer, R., *Macromolecules* **1995**, *28*, 425-32.
- (17) Cook, A. D.; Hrkach, J. S.; Gao, N. N.; Johnson, I. M.; Pajavni, U. B.; Cannizzaro, S. M.; Langer, R., *J. Biomed. Mater. Res.* **1997**, *35*, 513-523.
- (18) Cook, A. D.; Pajvani, U. B.; Hrkach, J. S.; Cannizzaro, S. M.; Langer, R., *Biomaterials* **1997**, *18*, 1417-1424.
- (19) Feng, Y.; Klee, D.; Hocker, H., *Macromol. Chem. Phys.* **2002**, *203*, 819-824.
- (20) In't Veld, P. J. A.; Dijkstra, P. J.; Feijen, J., *Makromol. Chem.* **1992**, *193*, 2713-30.
- (21) Kuo, S.-W.; Huang, C.-F.; Tung, Y.-C.; Chang, F.-C., *J. Appl. Polym. Sci.* **2006**, *100*, 1146-1161.

- (22) Deng, C.; Chen, X.; Yu, H.; Sun, J.; Lu, T.; Jing, X., *Polymer* **2007**, *48*, 139-149.
- (23) Deng, C.; Rong, G.; Tian, H.; Tang, Z.; Chen, X.; Jing, X., *Polymer* **2005**, *46*, 653-659.
- (24) Deng, C.; Tian, H.; Zhang, P.; Sun, J.; Chen, X.; Jing, X., *Biomacromolecules* **2006**, *7*, 590-596.
- (25) Deng, M.; Wang, R.; Rong, G.; Sun, J.; Zhang, X.; Chen, X.; Jing, X., *Biomaterials* **2004**, *25*, 3553-3558.
- (26) Jalabert, M.; Frascini, C.; Prud'homme, R. E., *J. Polym. Sci., Part A: Polym. Chem.* **2007**, *45*, 1944-1955.
- (27) Donato, M. T.; Gomez-Lechon, M. J.; Castell, J. V., *Anal. Biochem.* **1993**, *213*, 29-33.
- (28) Mecerreyes, D.; Miller, R. D.; Hedrick, J. L.; Detrembleur, C.; Jerome, R., *J. Polym. Sci., Part A: Polym. Chem.* **2000**, *38*, 870-875.
- (29) Parrish, B.; Breitenkamp, R. B.; Emrick, T., *J. Am. Chem. Soc.* **2005**, *127*, 7404-7410.
- (30) Parrish, B.; Quansah, J. K.; Emrick, T., *J. Polym. Sci., Part A: Polym. Chem.* **2002**, *40*, 1983-1990.
- (31) Riva, R.; Schmeits, S.; Jerome, C.; Jerome, R.; Lecomte, P., *Macromolecules* **2007**, *40*, 796-803.
- (32) Yang, J.-Y.; Yu, J.; Pan, H.-Z.; Gu, Z.-W.; Cao, W.-X.; Feng, X.-D., *Chin. J. Polym. Sci.* **2001**, *19*, 509-516.
- (33) Marcincinova-Benabdillah, K.; Boustta, M.; Coudane, J.; Vert, M., *Biomacromolecules* **2001**, *2*, 1279-1284.

- (34) Jeong, S. I.; Kim, B.-S.; Lee, Y. M.; Ihn, K. J.; Kim, S. H.; Kim, Y. H., *Biomacromolecules* **2004**, *5*, 1303-1309.
- (35) Uhrich, K. E.; Cannizzaro, S. M.; Langer, R. S.; Shakesheff, K. M., *Chem. Rev.* **1999**, *99*, 3181-3198.
- (36) Ouchi, T.; Fujino, A., *Makromol. Chem.* **1989**, *190*, 1523-30.
- (37) Baker, G. L.; Vogel, E. B.; Smith, M. R., *Polym. Rev.* **2008**, *48*, 64-84.
- (38) Jiang, X. W.; Smith, M. R.; Baker, G. L., *Macromolecules* **2008**, *41*, 318-324.
- (39) Simmons, T. L.; Baker, G. L., *Biomacromolecules* **2001**, *2*, 658-663.
- (40) Yin, M.; Baker, G. L., *Macromolecules* **1999**, *32*, 7711-7718.
- (41) Trimaille, T.; Gurny, R.; Moeller, M., *Chimia* **2005**, *59*, 348-352.
- (42) Trimaille, T.; Gurny, R.; Moller, M., *J. Biomed. Mater. Res., Part A* **2006**, *80A*, 55-65.
- (43) Trimaille, T.; Gurny, R.; Moller, M., *J. Biomed. Mater. Res., Part A* **2007**, *80A*, 55-65.
- (44) Trimaille, T.; Moeller, M.; Gurny, R., *J. Polym. Sci., Part A: Polym. Chem.* **2004**, *42*, 4379-4391.
- (45) Deechongkit, S.; You, S.-L.; Kelly, J. W., *Org. Lett.* **2004**, *6*, 497-500.
- (46) Winitz, M.; Bloch-Frankenthal, L.; Izumiya, N.; Birnbaum, S. M.; Baker, C. G.; Greenstein, J. P., *J. Am. Chem. Soc.* **1956**, *78*, 2423-2430.
- (47) Barrera, D. A.; Zylstra, E.; Lansbury, P. T.; Langer, R., *Macromolecules* **1995**, *28*, 425-432.
- (48) Drumright, R. E.; Gruber, P. R.; Henton, D. E., *Adv. Mater* **2000**, *12*, 1841-1846.

- (49) Chamberlain, B. M.; Cheng, M.; Moore, D. R.; Ovitt, T. M.; Lobkovsky, E. B.; Coates, G. W., *J. Am. Chem. Soc.* **2001**, *123*, 3229-3238.
- (50) O'Keefe, B. J.; Hillmyer, M. A.; Tolman, W. B., *J. Chem. Soc., Dalton Trans.* **2001**, 2215-2224.
- (51) Dechy-Cabaret, O.; Martin-Vaca, B.; Bourissou, D., *Chem. Rev.* **2004**, *104*, 6147-6176.
- (52) Uhrich, K. E.; Cannizzaro, S. M.; Langer, R. S.; Shakesheff, K. M., *Chem. Rev.* **1999**, *99*, 3181-3198.
- (53) US Food and Drug Administration. The List of "Indirect" Additives Used in Food Contact Substances. <http://www.cfsan.fda.gov/~dms/opa-indt.html> (accessed 6/24/08).
- (54) Yang, J.-y.; Yu, J.; Li, M.; Gu, Z.-w.; Feng, X.-d., *Chin. J. Polym. Sci.* **2002**, *20*, 413-417.
- (55) Johns, D. B.; Lenz, R. W.; Luecke, A., *Ring-Opening Polymerization*. Elsevier Applied Science Publisher: London, 1984; Vol. 1, p 461-521.
- (56) Ouchi, T.; Fujino, A., *Makromol. Chem.* **1989**, *190*, 1523-1530.

CHAPTER 3

MODIFICATION OF FUNCTIONAL PLA WITH BIOLOGICAL LIGANDS[‡]

3.1. Introduction

The use of biodegradable polyesters such as poly(lactic acid) (PLA), poly(glycolic acid), and polylactones, in biomedical applications has increased significantly over the past decade.¹⁻⁴ These materials are used in various forms (films, fibers, foams) for a diverse set of applications ranging from drug delivery to sutures.⁵⁻⁷ While the ester functional groups in the backbone contribute to a set of attractive physical properties and facilitate biodegradation, the absence of pendant functional groups limits the versatility of these materials. The incorporation of reactive sites that are amenable to modification with a wide-variety of biologically relevant ligands would provide a host of opportunities to control cell adhesion and function.⁸ For example, a combination of synthetic biodegradable polymers with peptide ligands may provide hybrid scaffolds for use in tissue engineering with control over scaffold-cell interactions as well as targeted drug delivery.⁹ Specifically, the attachment of peptides with the RGD (Arg-Gly-Asp) sequence has been shown to improve the cytocompatibility and cellular attachment characteristics of a variety of materials.¹⁰⁻¹³

The main strategy employed to incorporate pendant functional groups into PLA involves the copolymerization of cyclic lactide monomer with comonomers¹⁴ such as functional glycolides,¹⁵⁻¹⁹ esteramides,²⁰⁻²⁵ *N*-carboxyanhydrides,²⁶⁻²⁹ and lactides.^{16,30-33}

[‡] The ELISA and cell adhesion assays in this chapter were performed with the assistance of Timothy A. Petrie from the group of Dr. Andrés J. García; *Biomacromolecules* **2008**, in press.

While we³⁴ and others³⁵ have reported the successful copolymerization of lactide monomers containing protected functional groups followed by deprotection to provide PLA copolymers bearing new chemical functionality (alcohols, amines and carboxylic acids), these materials have not been subjected to further post-polymerization modification.

Here we demonstrate the ring-opening copolymerization of cyclic lactide and a new dibenzyloxy-substituted lactide, followed by debenylation to afford a hydroxy-substituted copolyester. Reaction of the functional copolymer with succinic anhydride provides a material that presents carboxylic acid functionality to allow standard carbodiimide coupling to attach amine-containing biological molecules. We chose this route to prepare carboxylic acid bearing copolylactides over the incorporation of a protected carboxylic acid containing monomer owing to the ease of monomer synthesis and previous difficulties in polymerizing the protected acid containing lactide.³⁴ We posited that incorporation of a small amount of functional comonomer (5 mol%) would be sufficient to allow for modification with biomolecules without adversely affecting the thermal properties of the copolymer. As proof-of-concept, succinylated films of our new functional PLA copolymer were treated with an amine-bearing biotin derivative and an Enzyme-Linked ImmunoSorbent Assay (ELISA) was used to demonstrate successful coupling. Given the wide interest in interactions between synthetic polymeric materials and biological matrices we tethered an RGD-containing peptide sequence (GGRGDSPGGK) to the copolymer films. A fluorescence assay of succinylated films indicated that the amount of tethered RGD can be controlled by treatment with various concentrations of peptide. The function of these films was demonstrated by the enhanced

adhesion of mammalian cells to RDG-modified PLA copolymers relative to unmodified PLA. This study clearly indicates that the functional groups of the polymer are accessible and can be used for the attachment of bioactive ligands to control surface-cell interactions. Thus, this presents a versatile approach to functionalizing PLA with biomolecules and provides the opportunity to mediate cellular adhesion and impart new biological functionality leading to tailorable biodegradable, biocompatible materials with numerous potential applications.

3.2. Experimental

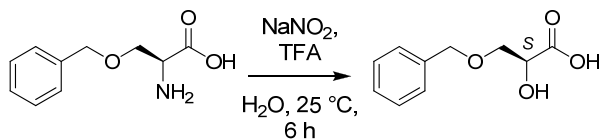
3.2.1. General Methods

Benzyl-L-serine was purchased from Indofine Chemical Company. L-lactide was purchased from Aldrich and recrystallized twice from dry EtOAc. Dry benzene was purchased from VWR and stored in a glovebox. Biotin-PEO-LC-amine was obtained from Pierce Chemical Company (product # 21347). Newborn calf serum (NCS) was obtained from Hyclone Laboratories (product # SH30118.03). Anti-biotin antibody (BN-34) was obtained from Aldrich (product # A6561). The fluorescent peptide sequence GGRGDSPGGK-FITC (the FITC was attached to the lysine residue) was synthesized by the Emory University Microchemical Facility.

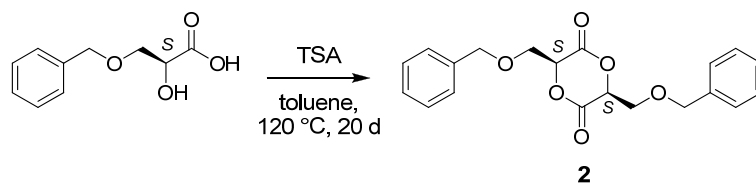
IR spectra were recorded on a Bruker Vector 22 spectrometer. Melting points were determined using a Mel-Temp II apparatus. Molecular weight data was collected using three Waters Styragel columns (5- μ m beads: HR 1, 100 Å; HR 3, 1,000 Å; HR 4, 10,000 Å) connected to a Waters 2690 Separations Module with a Waters 2487 Refractive Index Detector. The eluant was THF (1 mL/min, 303 K) and the molecular

weights were determined relative to six narrow polystyrene standards in THF. Thermal transitions were determined on a Mettler DSC 822. The sample sizes were approximately 4 mg and each sample was subjected to thermal cycles from 0 to 200 °C at a rate of 10 °C per minute. NMR spectra were recorded at room temperature using a Varian Mercury spectrometer (300 MHz) or a Bruker AMX spectrometer (400 MHz). Mass spectral analyses were performed on a VG Instruments 70SE mass spectrometer. The fluorescence intensity of the ELISA samples and RGD assays were recorded using a Perkin Elmer HTS 7000 Plus Bio Assay Reader.

3.2.2. Synthesis of Dibenzoyloxy-substituted Monomer

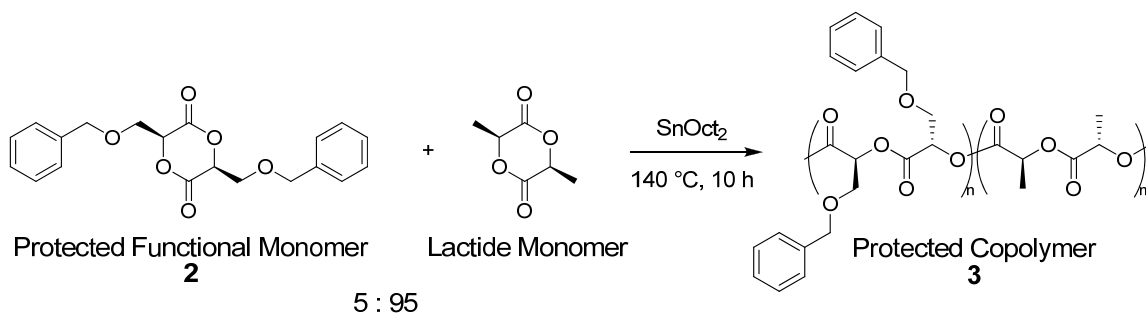


3.2.2.1. (S) 3-Benzyloxy-2-hydroxypropionic acid.³⁶ The hydroxy acid was prepared according to the general method reported by Deechongkit et al.³⁴ A solution of NaNO₂ (10.6 g, 154 mmol) in H₂O (100 mL) was added over 3 h to a solution of *O*-benzyl-L-serine (20.0 g, 103 mmol) in 0.7 M aqueous solution of trifluoroacetic acid (200 mL). The mixture was stirred for 3 h, NaCl (20 g) was added, and the mixture was extracted with EtOAc (3 x 200 mL). The organic layers were combined and dried over MgSO₄. The solvent was removed, and the residue was dried under vacuum overnight to give (*S*)-hydroxy acid as a waxy yellow oil (19.52 g, 97%), which was used without further purification.



3.2.2.2. (*S,S*)-3,6-(Benzyloxymethyl)-1,4-dioxane-2,5-dione (2**).** A mixture of (*S*) 3-benzyloxy-2-hydroxypropionic acid (10 g, 51 mmol) and *p*-toluenesulfonic acid monohydrate (0.2 g, 1.1 mmol) in toluene (1.5 L) was heated at reflux, and water was removed by azeotropic distillation using a Dean-Stark apparatus. After 20 d, the mixture was cooled and washed with H₂O (6 x 500 mL), dried over MgSO₄, and the solvent was removed. The residue was recrystallized from anhydrous Et₂O to give **2** as a white crystalline solid (1.78 g, 21%). m.p. 70.2-73.2 °C. ¹H NMR (300 MHz, CDCl₃) δ 7.25-7.35 (m, 10H), 5.13 (t, *J* = 4.1, -CH-, 2H), 4.49 (d, *J* = 11.8, diast. -OCH₂Ph, 2H), 4.44 (d, *J* = 11.6, diast. -OCH₂Ph, 2H), 3.89 (d, *J* = 4.1, -CH₂-, 4H). ¹³C NMR (133 MHz, CDCl₃) δ 163.4, 136.7, 128.5, 128.1, 128.0, 76.5, 73.7, 69.9. IR (thin film) ν: 3024 (weak, aromatic C-H), 2920, 1757, 1247, 1101 cm⁻¹. MS (EI) *m/z* (relative intensity): 265.1 (M-PhCH₂, 28%), 91.1 (tropylium, 100%) HRMS calcd for C₂₀H₁₉O₆ (M-1): 355.11816, found: 355.11705 (Δ = 3.1 ppm).

3.2.3. Preparation of Protected Copolymers

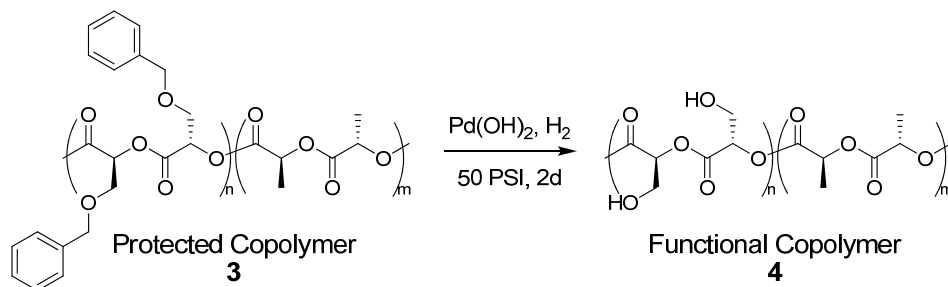


3.2.3.1. Copolymerization of Lactide with Dibenzoyloxy-substituted Monomer

2. A solution of twice-recrystallized lactide (3.8 g, 27 mmol), comonomer **2** (0.50 g, 1.4 mmol) and SnOct₂ (34 μ L of a 0.8 M stock solution in benzene) in benzene (75 mL) was prepared in a dry-box and freeze-dried overnight. The mixture was heated to 140 $^{\circ}$ C for 10 h and poured into MeOH (1 L). The precipitate was collected by filtration and dried under vacuum overnight to give protected copolymer **3** as a white solid (3.69 g, 85%).

¹H NMR (300 MHz, CDCl₃) δ 7.20-7.40 (10 H, -C₆H₅), 5.3-5.5 (2 H, -CH- of benzyloxy-substituted repeat unit), 5.0-5.3 (-CH- of LA unit), 4.4-4.6 (4 H, -OCH₂C₆H₅), 3.8-4.0 (4 H, -CH₂OCH₂C₆H₅), 1.4-1.8 (-CH₃ of LA unit). ¹³C NMR (133 MHz, CDCl₃) δ 169.6, 137.4, 128.4, 127.8, 127.7, 73.4, 69.0, 68.4, 16.6. IR (thin film) 3016 (weak, aromatic C-H), 2991, 1748, 1178, 1080 cm⁻¹.

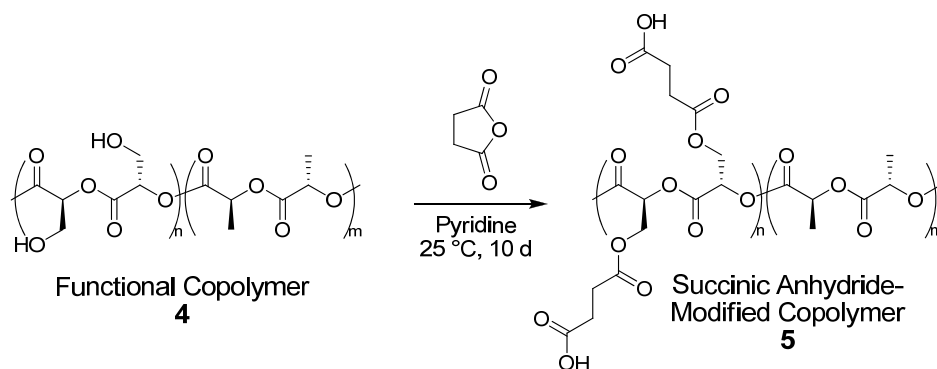
3.2.4. Preparation of Functional Copolymers



3.2.4.1. Deprotection of Copolymer 3 to Afford Hydroxyl-substituted

Polymer 4. Protected copolymer **3** (1.82 g) was dissolved in a 4:1 (v:v) mixture of EtOAc and CH₂Cl₂ and an equal mass of Pd(OH)₂ was added. The solution was placed on a hydrogenator and charged to 50 PSI of H₂ for 48 h. The catalyst was removed by filtration and the solvent was removed to give functional copolymer **4** (1.50 g, 82%). ¹H NMR (300 MHz, CDCl₃) δ 5.0-5.4 (-CH- of functional repeat unit and LA unit), 4.1-4.3 (-CH₂OH of functional repeat unit), 3.9-4.1 (-CH₂OH of functional repeat unit), 1.4-1.8 (-CH₃ of LA unit). ¹³C NMR (133 MHz, CDCl₃) δ 169.6, 69.0, 67.0, 16.6. IR (thin film) 2993, 2943, 1748, 1179, 1082 cm⁻¹.

3.2.5. Functional Copolymer Modification



3.2.5.1. Modification of Hydroxyl-bearing Copolymer **4** with Succinic

Anhydride. Functional copolymer **4** (1.50 g) was treated with succinic anhydride (0.517 g, 5.17 mmol) (5 equiv. of succinic anhydride per mol of hydroxyl side chain) and pyridine (0.5 mL, 6 mmol) (6 equiv. per mol of hydroxyl side chain) in CH₂Cl₂ (90 mL). The reaction mixture was stirred for 10 d, the solvent was removed and the polymer was precipitated into MeOH (250 mL) to give carboxylic acid-functionalized copolymer **5** (1.2 g, 80%). ¹H NMR (300 MHz, CDCl₃) δ 5.3-5.5 (2 H, -CH- of succinate repeat unit), 5.0-5.3 (-CH- of LA unit), 4.4-4.8 (4 H, -CH₂OCOCH₂CH₂COOH), 2.6-2.8 (8 H, -CH₂OCOCH₂CH₂COOH), 1.4-1.8 (-CH₃ of LA). ¹³C NMR (400 MHz, CDCl₃) δ 169.6, 69.0, 28.7, 16.6. IR (thin film) 2995, 2958, 1753, 1710 (weak, -CO₂H), 1182, 1085 cm⁻¹.

3.2.6. *Film Formation*

Films were spin-coated at 2200 rpm on glass discs by applying several drops of a 25 mg/mL solution of copolymer **5** in a 1:1 (v:v) mixture of toluene and CH₂Cl₂. The glass slides containing the films were placed into the wells of a 24-well plastic plate.

3.2.7. *Biotin Coupling*

Biotin stock solution (600 μL of a solution containing 16 mg biotin-PEO-LC-amine and 0.9 mg EDC in 14 mL of a 0.1 M aqueous *N*-morpholinoethane sulfonic acid buffer solution adjusted to a pH of 5.5 using NaOH) was added to each well and the samples were incubated for 2.5 h at room temperature. The biotin solution was removed from the wells by aspiration, and the samples were sequentially incubated in phosphate-buffered saline (PBS) (no Ca/Mg) for 1 h, a 0.1% (w/v) solution of sodium dodecyl sulfate (SDS) in PBS (no Ca/Mg) for 5 min, and DI water at 25 °C to remove any physically adsorbed biotin.

3.2.8. *RGD-FITC Coupling*

Films were treated with 2 mM EDC and 5 mM NHS in a 0.1 M aqueous 2-(*N*-morpho)-ethanesulfonic acid and 0.5 M NaCl solution (pH 5.5) for 30 min at room temperature to activate the carboxylic acids to amidation. Surfaces were subsequently immersed in a 20 mM solution of 2-mercaptoethanol in deionized water to quench any unreacted EDC,³⁷ leaving activate NHS esters on the PLA films. Films were then exposed to various concentrations of the fluorescent peptide GGRGDSPGGK-FITC in PBS for 30 min at room temperature in the dark. The free amines on this peptide were

covalently tethered to the films using the surface NHS esters as leaving groups. The peptide solution was removed from the wells by aspiration, and the samples were incubated in 20 mM glycine for 10 min to quench any unreacted NHS esters. After carefully transferring the slides to a new set of wells, the films were rinsed three times with PBS to remove weakly bound, physically adsorbed RGD-FITC, and the discs were subsequently incubated in PBS for 30 min to further reduce non-specific peptide adsorption. The solution was removed by aspiration, fresh PBS was added, and the fluorescence intensity was measured and quantified.

3.2.9. ELISA

The glass discs were incubated in the plastic wells (24-well plastic plates obtained from Corning, product # 3526) in newborn calf serum (NCS) for 1 h at 37 °C to block the surfaces and washed three times with DI water. A solution of anti-biotin (BN-34, Sigma-Aldrich) or anti-FITC alkaline-phosphatase conjugated antibody (Sigma-Aldrich) (300 μ L of a solution composed of 7 μ L EDTA, 33 μ L of a 10 % NaN_3 solution, 3 μ L of a 1% heat-denatured bovine serum albumin solution in PBS, 10 mL DI water and 5 μ L BN-34) was added to each well and the samples were incubated for 1 h at 37 °C. The glass discs were transferred to a new set of wells to minimize the response caused by the adsorption of antibody onto the wells. The dishes were washed five times with DI water, incubated in NCS for 10 minutes at 25 °C, and rinsed again five times with DI water. A solution of methylumbelliferyl phosphate (300 μ L of a solution composed of 7.5 mL DI water, 2 mL 5X diluted diethanolamine, 500 μ L 0.1 M NaHCO_3 , and 0.6 mg of methylumbelliferyl phosphate) was added to each well and the samples were incubated at 37 °C for 1 h in the

dark. A 50 μ L aliquot from each well was transferred into the corresponding well of a black Dynex 96-well plate, and the fluorescence intensity was recorded.

3.2.10. Cell Adhesion Assay

A wash assay was used to measure relative adhesion of cells adhered to peptide-functionalized and unfunctionalized film surfaces. MDCK cells were labeled with 4 mM calcein-AM in a 2mM dextrose-PBS solution for 20 min and resuspended in α -MEM media (1% penicillin-streptomycin). Cells were seeded onto films at a density of 200 cells/ mm^2 , and allowed to adhere at 37 $^{\circ}$ C for 1 h. Wells were then subjected to three gentle washes with media to detach loosely bound and unbound cells. After a gentle aspiration, post-wash fluorescence was quantified using an HTS 7000 Plus plate reader. The post-wash fluorescence levels correlate with the number of adhered cells.

3.2.11. Statistics.

Data are reported as mean \pm standard error. Results were analyzed by one-way ANOVA using SYSTAT 8.0 (SPSS). If treatment level differences were determined to be significant, pair-wise comparisons were performed using a Tukey post-hoc test. A 95% confidence level was considered significant.

3.3. Results and Discussion

3.3.1. Synthesis of Protected Functional Monomer

We have previously reported that benzyl ether-protected lactide **1** is subject to copolymerization and reductive debenylation to afford hydroxyl-bearing PLA copolymers.³⁴ In the current study, we chose to adopt a different strategy whereby we

prepared the symmetrically di-substituted lactide monomer **2**. This makes use of the robustness of the benzyl ether protecting group and provides a protected functional monomer in fewer synthetic steps. It also provides straightforward access to a single enantiomer of the protected functional monomer. Commercially available *O*-benzyl-L-serine was converted to (*S*)-3-(benzyloxy)-2-hydroxypropanoic acid by diazotization (NaNO_2 , TFA) followed by hydrolysis, Figure 3.1.³⁶ Optimization of the reaction conditions and simple extraction of the product from the aqueous reaction mixture into ethyl acetate gave near quantitative yields of product with full retention of the stereochemistry.

The cyclocondensation of the (*S*)-hydroxy acid was catalyzed by *p*-toluenesulfonic acid, and water was removed from the reaction mixture using a Dean-Stark trap (20 d). The condensation reaction also provides linear oligomers and conversion to the cyclic dimer was typically limited to ca. 40%, which is comparable to conversions previously reported for self-condensation reactions for the preparation of analogous substituted glycolides.³⁸ Attempts to separate **2** from the linear oligomers by column chromatography on silica gel led to ring-opening. However, recrystallization proved effective in affording pure protected functional monomer **2**. This resulted in lower yields (21%) than those found in the literature for the synthesis of alkyl-substituted lactides using the same method.^{30,33} However, while analogous uncyclized alkyl-substituted oligomers can be thermally cracked at high temperature in the presence of a ZnO (a good transesterification catalyst) and vacuum distilled to give cyclic dimer,³⁰ our attempts to transform the benzyloxy-substituted oligomers in this fashion led to decomposition arising from the high temperatures necessitated by the low volatility of **2**.

In relation to the preparation of mono-substituted benzyl ether-protected lactide **1**, this yield is acceptable as the synthetic method has fewer reaction steps, results in the formation of a single diastereomer of monomer **2**, and yields a dibenzyloxy-protected lactide monomer with two potential functional groups per monomer.

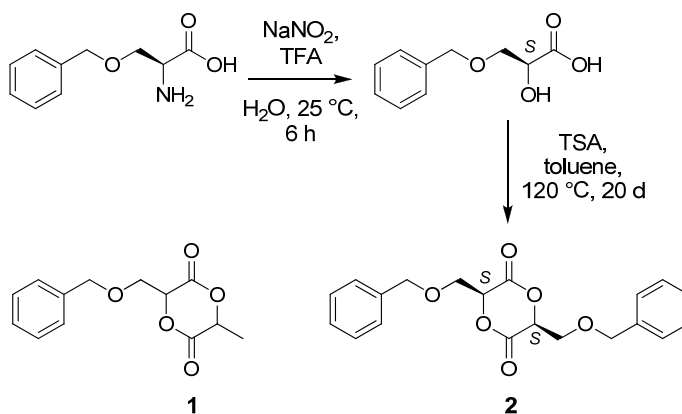


Figure 3.1. Synthesis of protected functional monomer **2**.

^1H NMR analysis was used to verify the stereochemistry of protected functional monomer **2**. The methine protons of **2** appear as a triplet at 5.14 ppm ($J = 4.1$ Hz for coupling of the methine hydrogen to the neighboring pair of diastereotopic hydrogen atoms) corresponding to a single (*S,S*) stereoisomer, Figure 3.2a. In a separate experiment, when a racemic mixture of 3-(benzyloxy)-2-hydroxypropanoic acid (prepared from *rac* *O*-benzyl-serine) was cyclodimerized, two overlapping triplets were observed in the ^1H NMR spectrum, one at 5.14 ppm ($J = 4.1$ Hz) corresponding to the (*S,S*) and (*R,R*) enantiomers, and the other at 5.12 ppm ($J = 2.8$ Hz) corresponding to the meso (*R,S*) compound, Figure 3.2b. An X-ray structure of the benzyl-protected functional (*S,S*) monomer **2** is provided in Figure 3.2c, that shows a pseudo-chair conformation of

the 1,4-dioxane-2,5-dione ring with the benzyloxymethyl side chains occupying equatorial positions.

3.3.2. Copolymerization, Deprotection, and Modification with Succinic Anhydride

A 5:95 mixture of protected monomer **2** and L-lactide monomer, (*S,S*)-3,6-dimethyl-1,4-dioxane-2,5-dione), was copolymerized using stannous octoate (SnOct_2) as the catalyst and residual water as the initiator (Figure 3.3).³⁴ The reaction mixture was heated to 140 °C to facilitate the ring-opening of monomer **2** as higher temperatures are often required to obtain high conversions in the polymerization of substituted lactides.^{33,38} ¹H NMR analysis of the crude copolymerization mixture showed high conversion of both cyclic monomers to linear polyester (~90% by integration of the PLA peaks relative to lactide monomer). The reaction mixture was poured into methanol to precipitate the polymer, which was filtered and dried under vacuum. ¹H NMR spectroscopy of the resulting material verified that the copolymer (**3**) included 5% of protected monomer **2**. The agreement between the amount of protect comonomer and lactide incorporated into the polymer and present in the original polymerization mixture confirms that comonomer **2** polymerized with an equally high conversion as the lactide monomer (although the

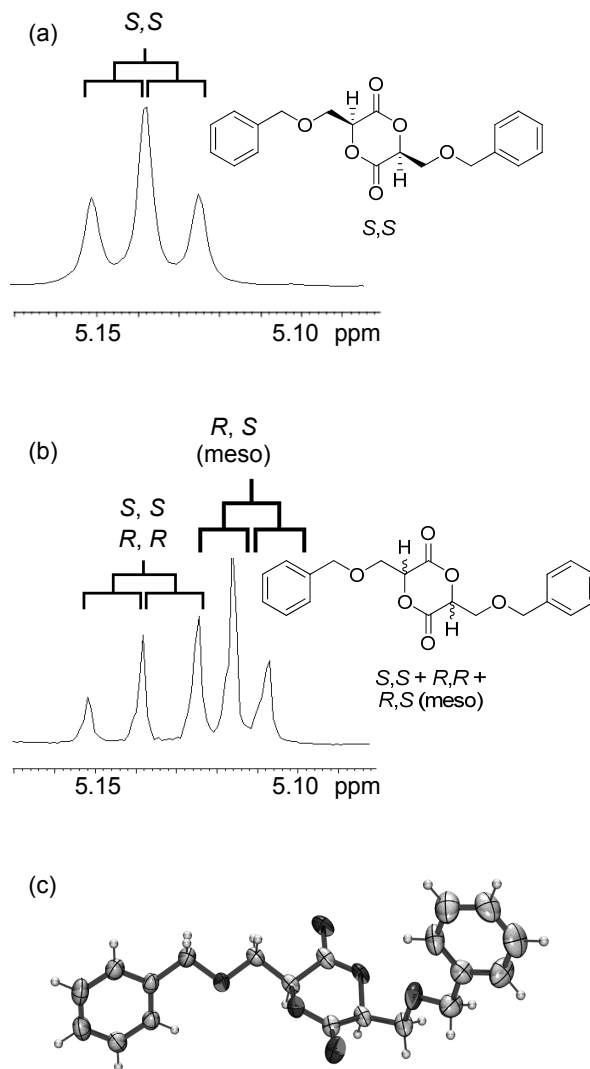


Figure 3.2. ^1H NMR analysis and X-ray diffraction of cyclic disubstituted dimers: (a) ^1H NMR spectrum of the methine protons of (S,S) isomer **2**; (b) ^1H NMR spectrum of a diastereomeric mixture of cyclic dimers obtained from *rac*-hydroxy acid; and (c) X-ray crystal structure of **2**.

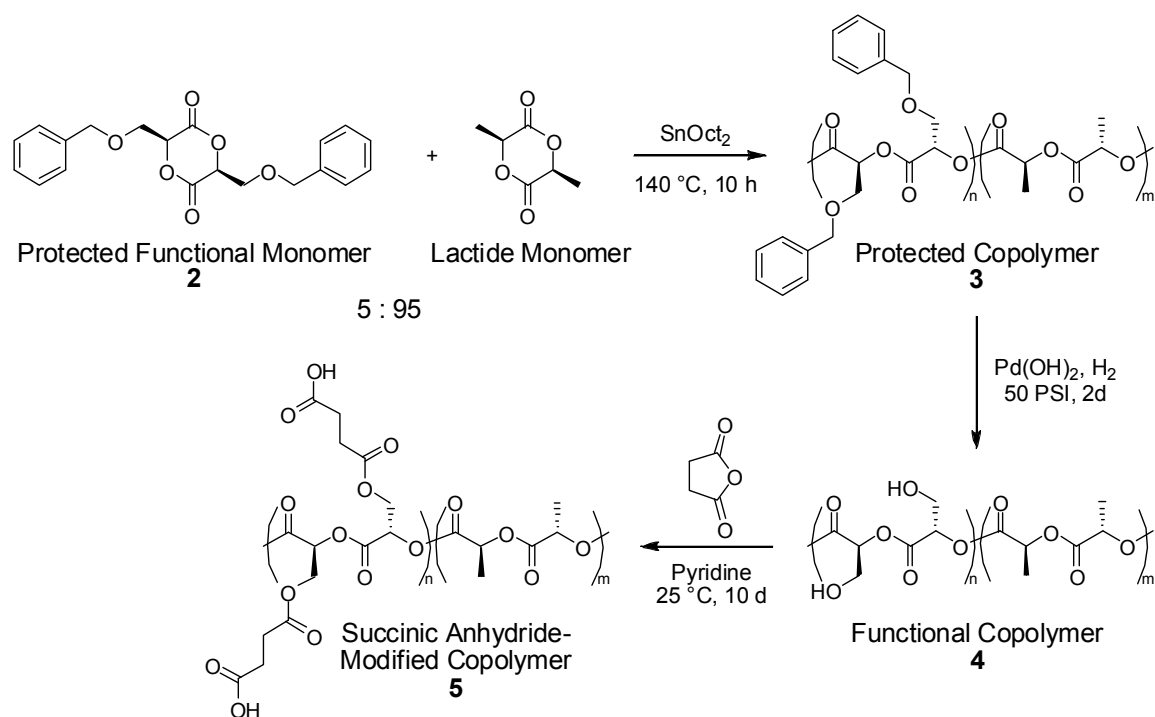


Figure 3.3. Copolymer synthesis, deprotection, and modification with succinic anhydride.

small amount of unreacted monomer **2** in the crude reaction mixture could not be determined directly due to overlap of the signals with those for polymer). While it is expected that the substituted protected lactide comonomer has a lower reactivity than lactide itself,³⁹ the effect of this on the ratio of comonomers incorporated would only be relevant at low conversions. In the current context, we performed polymerizations to high conversion with a resulting copolymer with a composition that matched the ratio of monomers in the reaction mixture. Gel permeation chromatography (GPC, using polystyrene calibration standards) indicated a number average molecular weight of 1.5×10^4 g/mol. This value is comparable to molecular weights found in the literature for the homopolymerization of alkyl-substituted lactides,³³ and the copolymerization of

protected functional mono-substituted lactides with lactide monomer.^{34,35} Though molecular weights up to 7.7×10^4 g/mol could be obtained, the molecular weight of this particular sample could be attributed to the presence of trace amounts of impurities in the monomer or catalyst acting as initiators.

The benzyl protecting groups of copolymer **3** were removed by hydrogenolysis over Pd(OH)₂ (50 PSI of H₂ in a 4:1 (v:v) mixture of EtOAc and CH₂Cl₂) to give functional copolymer **4** with pendent hydroxyl groups. Complete removal of the protecting group was verified by ¹H NMR spectroscopy by the disappearance of the peaks for the phenyl protons at ~7.3 ppm and the appearance of separate one-proton signals at δ 4.0 and 4.2 ppm for the diastereotopic protons of the methylene group (Figure 3.4B, peaks labeled *d*). The deprotection of copolymer **3** was also confirmed by the disappearance of the aromatic C-H stretching vibration at 3016 cm⁻¹ in the infrared (IR) spectrum. While the polymer is soluble in EtOAc alone, repeated attempted reductive debenylation in the absence of added CH₂Cl₂ failed to go to completion.

The hydroxymethyl-substituted copolymer **4** was treated with succinic anhydride to give the acid functionalized copolymer, **5**. The progress of the succinylation reaction was monitored by ¹H NMR spectroscopy. The protons of the methylene group of the hydroxymethyl-substituted copolymer **4** shift downfield to δ 4.6 ppm upon esterification, with simultaneous formation of peaks attributed to the succinate monoester at 2.7 ppm (Figure 3.4C, peaks *d* and *f* respectively). The succinylation was also confirmed by the appearance of a weak peak at 1710 cm⁻¹ in the IR spectrum for the C=O stretching vibration carboxylic acid group. GPC analysis (Table 3.1) indicated that the amount of

polymer degradation of the polyester backbone throughout the deprotection and succinylation steps was minimal, as observed by a slight decrease in the

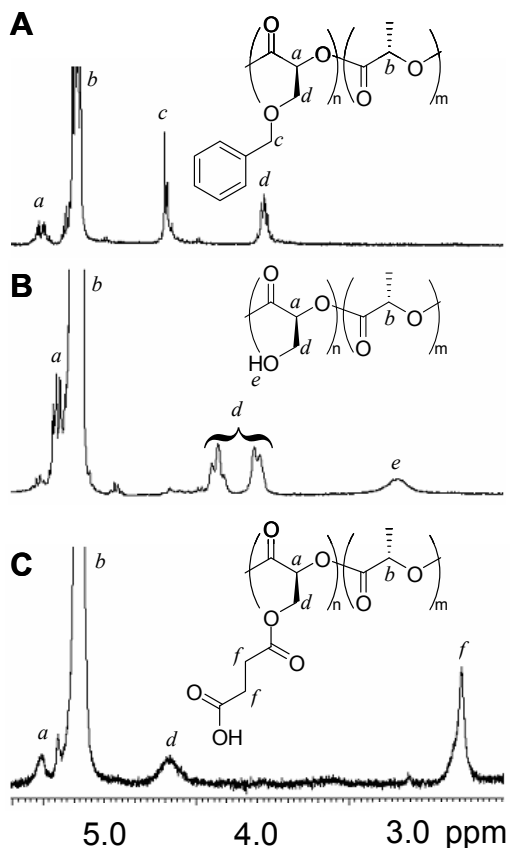


Figure 3.4. ^1H NMR spectra of copolymers: A, benzyloxy-substituted copolymer **3**; B, deprotected hydroxymethyl bearing copolymer **4**; C, succinylated copolymer **5**.

molecular weight. NMR spectroscopy confirmed the preservation of the polymer structure and that the polymers had not broken down into monomeric components. The copolymers were also characterized by differential scanning calorimetry (DSC), Table 3.1. Copolymers **3-5** displayed similar glass transition temperatures, and lower melting temperatures than literature values for semicrystalline PLA homopolymers derived from the ring-opening polymerization of L-lactide.⁴⁰ This shows that the low level

incorporation of difunctional comonomer (5 mol%) does not significantly affect the glass transition or melting point of the PLA copolymer. This is in contrast to our previous report where greater amounts (25%) of monofunctional monomer **1** incorporated into the polymer backbone resulted in a significant decrease in the T_g .³⁴ Copolymer **3** displays a strong cold crystallization on first heating, and copolymer **4** was completely amorphous after the first heating and cooling cycle.

Table 3.1. GPC and DSC Characterization of Copolymers **3-5**.

Copolymer	M_n (kg/mol)	M_w (kg/mol)	PDI	T_g (°C)	T_m (°C)	ΔH_m (J/g)
3	15	33	2.2	56	149	9
4	14	28	2.0	57	152	49
5	11	21	1.9	61	152	25

3.3.3. Biotin Coupling

The pendant carboxylic acids of **5** provide the opportunity to use standard carbodiimide chemistry for attachment of amines. As proof of concept, we coupled an amine-substituted biotin derivative to the copolymer films (Figure 3.5). Films of succinylated copolymer **5** were prepared by spin-coating a solution (25 mg/mL) of the copolymer in a 1:1 (v:v) mixture of toluene and dichloromethane onto glass discs. The discs were then placed into wells in a 24-count polystyrene plate and subjected to conditions for amidation. To verify the attachment of biotin, we performed an ELISA using an alkaline phosphatase enzyme-conjugated anti-biotin antibody. After extensive rinsing to remove weakly adhered antibody, a solution of 4-methylumbelliferyl phosphate

was added and the fluorescence resulting from the formation of the methylumbelliferone anion was quantified and used as a relative measure of the amount of biotin. Films treated with the amine-substituted biotin in the presence of EDC show increased fluorescence relative to control samples which had been treated with the biotin-amine in the absence of EDC ($p < 0.005$), or treated with a carboxylic acid substituted biotin (with [$p < 0.008$]

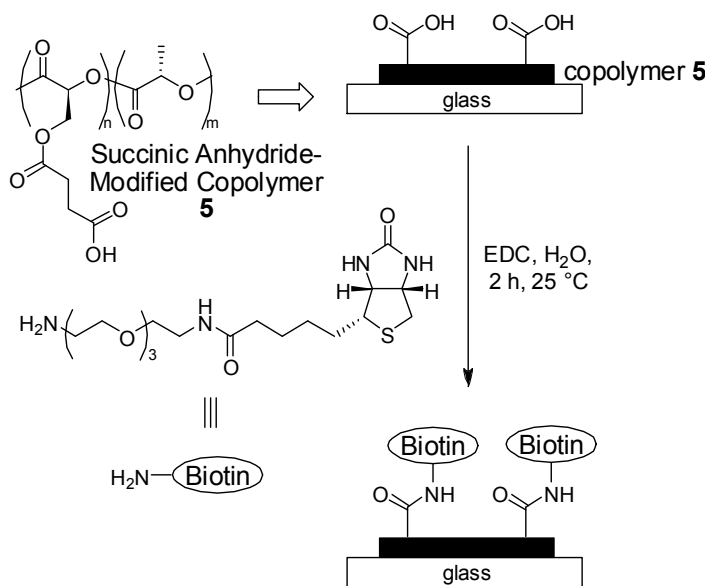


Figure 3.5. Attachment of an amine-substituted biotin derivative to copolymer films.

in the presence of EDC, and [$p < 0.003$] in the absence of EDC), Figure 3.6. The ELISA method is not quantitative - the fluorescence intensity is not linearly related to the density of antigen (biotin). This arises, in part, from the relative size of the antibody and antigen, whereby the fluorescence intensity will saturate at levels far below 5% biotin incorporation. The slightly elevated fluorescence levels of the sample treated with the biotin-carboxylic acid and EDC relative to the other control experiments can be attributed to coupling to small amounts of hydroxyl side chains still present in the sample of

succinylated copolymer **5** (which in this case had failed to react completely with succinic anhydride).

3.3.4. RGD-peptide Coupling and Control of Cell Adhesion

We also treated the succinylated polymer films with an RGD-containing peptide (GGRGDSPGGK) conjugated to a fluorescein derivative (FITC) to demonstrate control over the density of tethered bioactive ligand and its subsequent effect on surface-cell interactions. The green fluorescence of the FITC was quantified to determine the effect

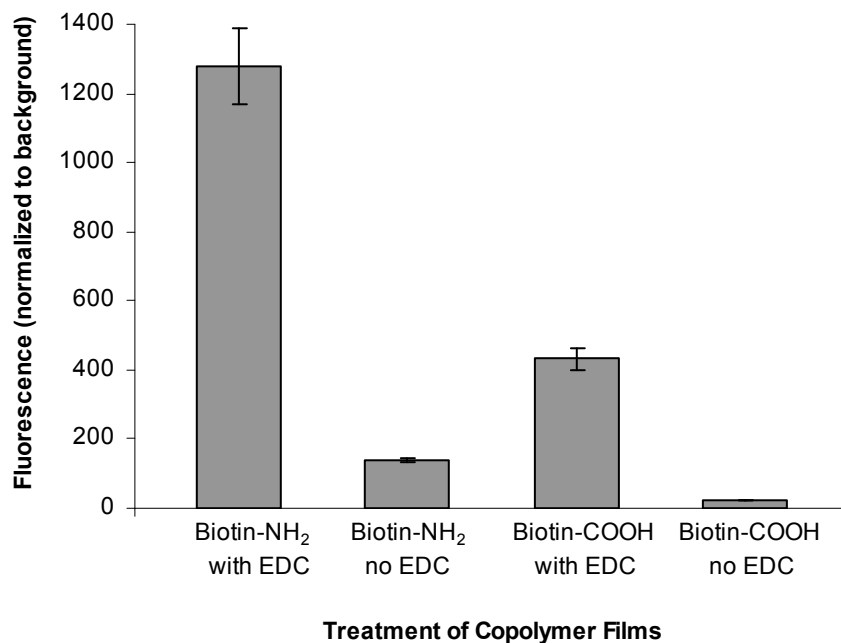


Figure 3.6. ELISA determination of relative density of amine-substituted biotin on succinylated PLA copolymer: Relative fluorescence indicating biotin attachment to films of copolymer **5** exposed to biotin-amine and biotin-carboxylic acid derivatives with and without EDC [Data collected in conjunction with Timothy A. Petrie, School of Biomedical Engineering].

of concentration of the peptide in standard NHS/EDC coupling reactions on the density of immobilized peptide. Films coupled with RGD-FITC showed increased levels of fluorescence, Figure 3.7. Films exhibited increased fluorescence when treated with higher concentrations of RGD-FITC and low fluorescence in the absence of EDC activation (data point at 20 $\mu\text{g/mL}$ RGD-FITC). This clearly demonstrates the ability to control tethered surface density of bioactive RGD ligand by varying coating concentration.

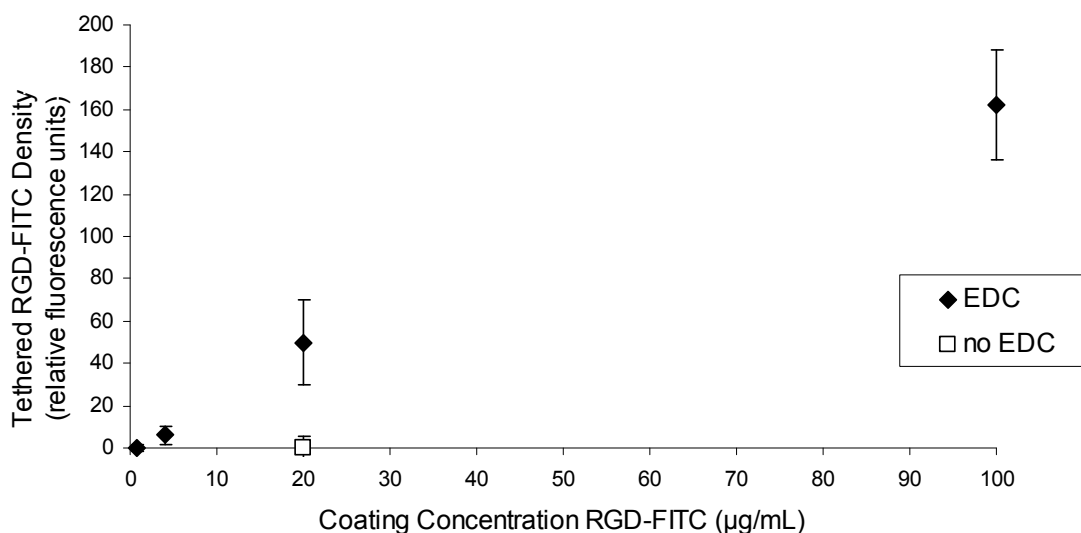


Figure 3.7. Relative fluorescence of succinylated PLA copolymer films **5** exposed to RGD at various concentrations with and without EDC (lower data point at 20 $\mu\text{g/mL}$)

[Data collected in conjunction with Timothy A. Petrie, School of Biomedical Engineering].

Functionalization of the copolymer films with peptides containing the RGD sequence, which is a ubiquitous cell adhesion-promoting sequence, should offer control over cell adhesion. To validate this assertion, we subjected both RGD-functionalized and unfunctionalized copolymer films to a simple adhesion assay using epithelial MDCK cells in serum-free media. Films of polymers were exposed for 1 h to MDCK cells labeled with calcein-AM, a membrane-permeable green fluorescent-dye. Gentle washes with media were performed to dislodge weakly bound cells and post-wash fluorescence was recorded to determine the density of cells adhered to the surface. More cells adhere to the RGD-tethered films than the unfunctionalized films ($p < 0.008$), and adhesion is

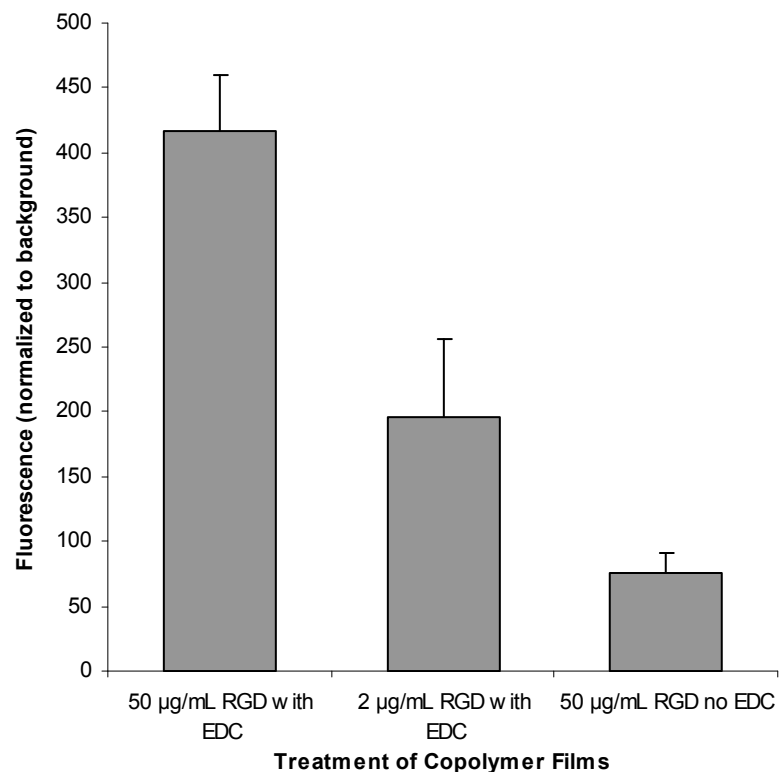


Figure 3.8. Relative fluorescence indicating cell attachment to films of copolymer 5 exposed to RGD at various concentrations with and without EDC [Data collected in conjunction with Timothy A. Petrie, School of Biomedical Engineering].

dependent on RGD-surface density ($p < 0.04$), Figure 3.8. Taken together, these data demonstrate the ability to functionalize PLA films with bioactive ligands and subsequently promote cell adhesion.

3.4. Conclusions

In conclusion, we have synthesized a new protected functional lactide monomer and successfully copolymerized it with lactide to give random copolymers that contain protected functional groups along the backbone. The copolymers were deprotected and used in the ring-opening of succinic anhydride, showing that the functional groups are accessible and amenable further modification. Films of the carboxylic acid functionalized copolymer were treated with a biotin-amine derivative and the coupling was verified using ELISA, showing that the carboxylic acid-functionalized copolymers can be modified with amine-terminated biomolecules. Use of a fluorescently labeled RGD-containing peptide sequence allowed us to verify control over the amount of peptide immobilized onto the succinylated copolymer films. Finally, a cell assay was performed which showed enhanced cell adhesion to RGD-containing films. This provides a general strategy whereby a variety of biomolecules can be attached to functionalized PLA copolymers using standard peptide coupling protocols, thereby leading to novel materials with numerous potential biomedical applications.

3.5. References

- (1) Trimaille, T.; Gurny, R.; Moeller, M., *Chimia* **2005**, *59*, 348-352.

- (2) Holy, C. E.; Fialkov, J. A.; Davies, J. E.; Shoichet, M. S., *J. Biomed. Mater. Res., Part A* **2003**, *65A*, 447-453.
- (3) Parrish, B.; Breitenkamp, R. B.; Emrick, T., *J. Am. Chem. Soc.* **2005**, *127*, 7404-7410.
- (4) Mecerreyes, D.; Miller, R. D.; Hedrick, J. L.; Detrembleur, C.; Jerome, R., *J. Polym. Sci., Part A: Polym. Chem.* **2000**, *38*, 870-875.
- (5) Albertsson, A.-C.; Varma, I. K., *Biomacromolecules* **2003**, *4*, 1466-1486.
- (6) Zurita, R.; Puiggali, J.; Rodriguez-Galan, A., *Macromol. Biosci.* **2006**, *6*, 767-775.
- (7) Trimaille, T.; Gurny, R.; Moller, M., *J. Biomed. Mater. Res., Part A* **2007**, *80A*, 55-65.
- (8) Wang, S.; Cui, W.; Bei, J., *Anal. Bioanal. Chem.* **2005**, *381*, 547-556.
- (9) Chen, G.; Ushida, T.; Tateishi, T., *Adv. Mater.* **2000**, *12*, 455-457.
- (10) Fussell, G. W.; Cooper, S. L., *Biomaterials* **2004**, *25*, 2971-2978.
- (11) Schmedlen, R. H.; Masters, K. S.; West, J. L., *Biomaterials* **2002**, *23*, 4325-4332.
- (12) Stile, R. A.; Healy, K. E., *Biomacromolecules* **2001**, *2*, 185-194.
- (13) Wang, D.-a.; Ji, J.; Sun, Y.-h.; Shen, J.-c.; Feng, L.-x.; Elisseeff, J. H., *Biomacromolecules* **2002**, *3*, 1286-1295.
- (14) Bourissou, D.; Moebs-Sanchez, S.; Martin-Vaca, B., *C. R. Chim.* **2007**, *10*, 775-794.
- (15) Kimura, Y.; Shirotani, K.; Yamane, H.; Kitao, T., *Macromolecules* **1988**, *21*, 3338-40.
- (16) Marcincinova-Benabdillah, K.; Boustta, M.; Coudane, J.; Vert, M., *Biomacromolecules* **2001**, *2*, 1279-1284.

- (17) Yang, J.-Y.; Yu, J.; Li, M.; Gu, Z.-W.; Feng, X.-D., *Chin. J. Polym. Sci.* **2002**, *20*, 413-417.
- (18) Yang, J.-Y.; Yu, J.; Pan, H.-Z.; Gu, Z.-W.; Cao, W.-X.; Feng, X.-D., *Chin. J. Polym. Sci.* **2001**, *19*, 509-516.
- (19) Yamaoka, T.; Hotta, Y.; Kobayashi, K.; Kimura, Y., *Int. J. Biol. Macromol.* **1999**, *25*, 265-271.
- (20) Barrera, D. A.; Zylstra, E.; Lansbury, P. T.; Langer, R., *Macromolecules* **1995**, *28*, 425-32.
- (21) Cook, A. D.; Hrkach, J. S.; Gao, N. N.; Johnson, I. M.; Pajavni, U. B.; Cannizzaro, S. M.; Langer, R., *J. Biomed. Mater. Res.* **1997**, *35*, 513-523.
- (22) Cook, A. D.; Pajvani, U. B.; Hrkach, J. S.; Cannizzaro, S. M.; Langer, R., *Biomaterials* **1997**, *18*, 1417-1424.
- (23) Barrera, D. A.; Zylstra, E.; Lansbury, P. T., Jr.; Langer, R., *J. Am. Chem. Soc.* **1993**, *115*, 11010-11.
- (24) Feng, Y.; Klee, D.; Hocker, H., *Macromol. Chem. Phys.* **2002**, *203*, 819-824.
- (25) In't Veld, P. J. A.; Dijkstra, P. J.; Feijen, J., *Makromol. Chem.* **1992**, *193*, 2713-30.
- (26) Deng, C.; Chen, X.; Yu, H.; Sun, J.; Lu, T.; Jing, X., *Polymer* **2007**, *48*, 139-149.
- (27) Deng, C.; Rong, G.; Tian, H.; Tang, Z.; Chen, X.; Jing, X., *Polymer* **2005**, *46*, 653-659.
- (28) Deng, C.; Tian, H.; Zhang, P.; Sun, J.; Chen, X.; Jing, X., *Biomacromolecules* **2006**, *7*, 590-596.

- (29) Deng, M.; Wang, R.; Rong, G.; Sun, J.; Zhang, X.; Chen, X.; Jing, X., *Biomaterials* **2004**, *25*, 3553-3558.
- (30) Yin, M.; Baker, G. L., *Macromolecules* **1999**, *32*, 7711-7718.
- (31) Leemhuis, M.; van Steenis, J. H.; van Uxem, M. J.; van Nostrum, C. F.; Hennink, W. E., *Eur. J. Org. Chem.* **2003**, 3344-3349.
- (32) Ouchi, T.; Fujino, A., *Makromol. Chem.* **1989**, *190*, 1523-30.
- (33) Trimaille, T.; Moeller, M.; Gurny, R., *J. Polym. Sci., Part A: Polym. Chem.* **2004**, *42*, 4379-4391.
- (34) Gerhardt, W. W.; Noga, D. E.; Hardcastle, K. I.; Garcia, A. J.; Collard, D. M.; Weck, M., *Biomacromolecules* **2006**, *7*, 1735-1742.
- (35) Leemhuis, M.; van Nostrum, C. F.; Kruijtzter, J. A. W.; Zhong, Z. Y.; ten Breteleur, M. R.; Dijkstra, P. J.; Feijen, J.; Hennink, W. E., *Macromolecules* **2006**, *39*, 3500-3508.
- (36) Deechongkit, S.; You, S.-L.; Kelly, J. W., *Org. Lett.* **2004**, *6*, 497-500.
- (37) Grabarek, Z.; Gergely, J., *Anal. Biochem.* **1990**, *185*, 131-135.
- (38) Simmons, T. L.; Baker, G. L., *Biomacromolecules* **2001**, *2*, 658-663.
- (39) Jing, F.; Smith, M. R.; Baker, G. L., *Macromolecules* **2007**, *40*, 9304-9312.
- (40) Radano, C. P.; Baker, G. L.; Smith, M. R., *J. Am. Chem. Soc.* **2000**, *122*, 1552-1553.

CHAPTER 4

SYNTHESIS OF PHOTOCROSSLINKABLE PLA SCAFFOLDS[‡]

4.1. Introduction

Biodegradable polyesters such as poly(lactic acid) (PLA), poly(glycolic acid), and poly(ϵ -caprolactone) show great promise as materials for use in biomedical applications ranging from drug delivery¹⁻⁴ to scaffolds for tissue engineering.⁵⁻⁸ PLA has gained particular attention due to the availability of feedstock monomers from annually renewable resources,⁹ and its controlled degradation into nontoxic products (lactic acid, CO₂).^{10,11}

Polymer scaffolds for tissue growth should be biocompatible, biodegradable, highly porous, and have sufficient mechanical properties including a combination of toughness and flexibility.^{12,13} Although the biodegradation of PLA makes it attractive for use in biomedical applications, the ability to control the mechanical strength of the polymer is crucial in the development of scaffolds.^{14,15} Methods for modifying the physical properties of PLA include the incorporation of other monomers in random copolymers (eg., glycolide,^{16,17} alkyl-substituted lactides,^{1,18,19} ϵ -caprolactone²⁰), formation of PLA diblock copolymers (eg., with polystyrene²¹), blending PLA with other polymers (eg., ϵ -caprolactone²²), and the addition of plasticizers²³ and crosslinking agents.^{24,25} However, not all of these techniques are applicable for the synthesis of porous scaffolds with suitable mechanical properties for tissue engineering.

[‡] The Micro-CT data found in this chapter was obtained and analyzed by Abigail M. Wojtowicz from the group of Dr. Andrés J. García.

In addition to tailoring the mechanical properties of PLA, there are numerous approaches to incorporate chemical functionality that will allow for the immobilization of peptide sequences to provide control over interactions between the scaffolds and adhered cells. These include the copolymerization of protected functional lactides,²⁶⁻²⁹ glycolides,³⁰⁻³³ esteramides,³⁴⁻³⁹ *N*-carboxyanhydrides,⁴⁰⁻⁴³ and lactones⁴⁴⁻⁴⁷ with lactide monomer to afford functional copolymers to which peptide sequences are attached.^{34,36,40,42} We have previously reported on the synthesis of PLA copolymers with pendant functionalities which were used for the attachment of an RGD-containing peptide sequence. In this paper we shift our attention from modifying the cellular properties of PLA and instead make use of the functional groups to prepare PLA copolymers with pendant photocrosslinkable groups.

Incorporating photocrosslinkable groups into the backbone of PLA could provide a useful method to alter the properties of the polymer. The fabrication of linear and star-shaped poly(lactide) copolymers with terminal photocrosslinkable acrylate groups has been reported.⁴⁸⁻⁵² However, there are only a few reports involving the covalent attachment of photocrosslinkable groups directly onto the backbone of PLA,⁵³ and the foaming of such materials for use in biodegradable scaffolding has yet to be thoroughly explored.

Of the many different methods used to make porous polymer foams, thermally induced phase separation (TIPS) has emerged as a facile route towards the fabrication interconnected macroporous scaffolds.⁵⁴ The parameters of the TIPS process (solvent, concentration, temperature) can be easily varied to control pore size, and the method has been applied to the preparation of foams from a variety of different polymers.⁵⁵ The

combination of TIPS and the potential to enhance the mechanical properties of the polymer by photocrosslinking could be used to overcome many of the shortcomings of polymer foams, and provide a route to highly porous, reinforced scaffolds with the mechanical properties suitable for tissue engineering.

Here we describe the synthesis of a PLA copolymer bearing photocrosslinkable cinnamate side chains. The copolymer was foamed using TIPS to give a highly porous, biodegradable scaffold with pore sizes large enough to accommodate cell proliferation. The UV-irradiation of films and foams of the copolymers resulted in photocrosslinking of the cinnamate groups, leading to an increase in the compressive modulus of the foams, and a decrease in the rate of hydrolytic degradation. This presents a novel, facile route towards well-defined, porous biodegradable scaffolds with limitless potential for use in a variety of biomedical applications.

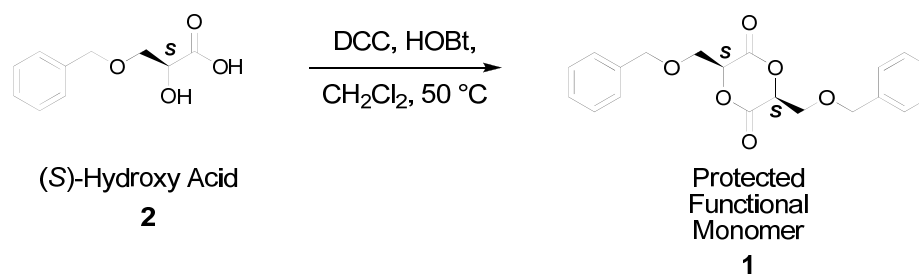
4.2. Experimental

4.2.1. General Methods

L-lactide was purchased from Aldrich and recrystallized twice from dry EtOAc. 3-Benzyloxy-2-hydroxypropionic acid⁵⁶ was prepared as previously reported.²⁶ N, N'-Dicyclohexylcarbodiimide (DCC) (product # A10973) and cinnamoyl chloride (product #A12016) were purchased from Alfa Aesar and used as received. 1-Hydroxybenzotriazole (HOBt) (product #00581) was purchased from Chem-Impex International and used without further purification. Dry benzene was purchased from VWR and stored in a glovebox. Stannous octanoate (SnOct₂) was purchased from Aldrich (product #S3252) and distilled prior to use.

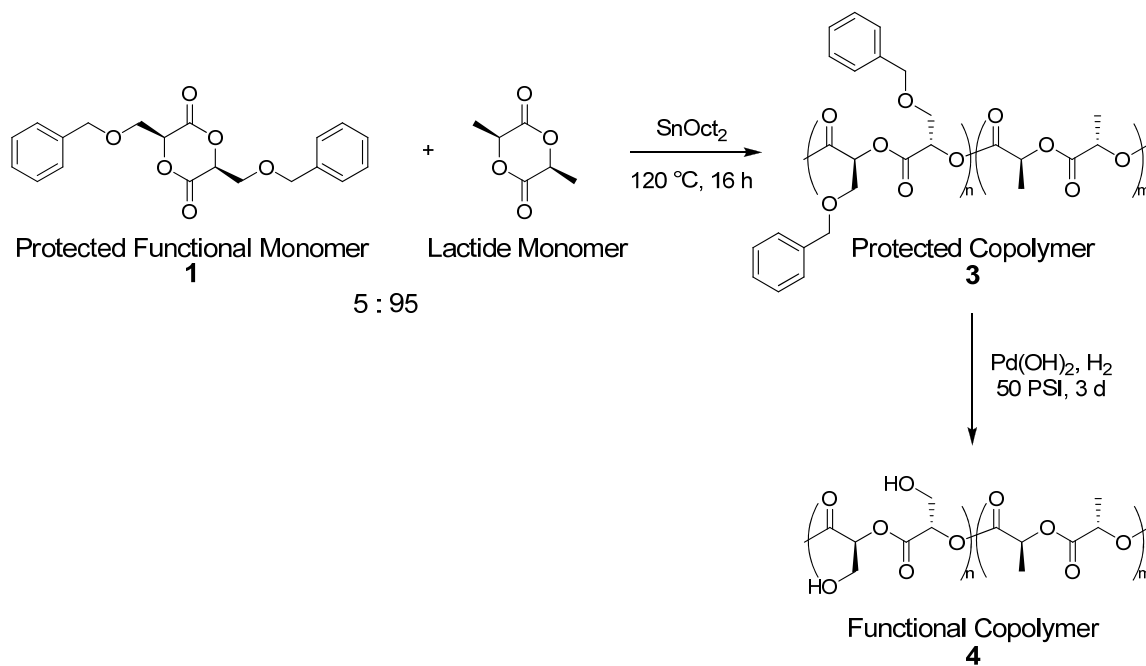
IR spectra were recorded on a Bruker Vector 22 spectrometer. Melting points were determined using a Mel-Temp II apparatus. Molecular weight data was collected using three Waters Styragel columns (5- μm beads: HR 1, 100 Å; HR 3, 1,000 Å; HR 4, 10,000 Å) connected to a Waters 2690 Separations Module with a Waters 2487 Refractive Index Detector. The eluant was THF (1 mL/min, 303 K) and the molecular weights were determined relative to six narrow polystyrene standards in THF. Thermal transitions were determined on a Mettler DSC 822. The sample sizes were approximately 4 mg and each sample was subjected to thermal cycles from 0 to 200 °C at a rate of 10 °C per minute. NMR spectra were recorded at room temperature using a Varian Mercury spectrometer (300 MHz) or a Bruker AMX spectrometer (400 MHz). Mass spectral analyses were performed on a VG Instruments 70SE mass spectrometer. SEM images were obtained from Hitachi S-800. Microcomputed tomography (micro-CT) images were obtained by Abigail M. Wojtowicz using a Scanco Medical CT 40 imaging system and linear attenuation data was reconstructed to generate 3-dimensional images. Samples (~240 μm thick sections) were scanned at 6 micron resolution with an integration time of 300 ms to quantify pore volume. All cross-linking experiments were performed in a Rayonet Photochemical reactor (RPR-100) equipped with a cooling fan. Compressive mechanical properties of scaffolds were tested using an Instron 5566 instrument.

4.2.2. Synthesis of Dibenzylloxy-substituted Monomer using DCC/HOBt



4.2.2.1. (S,S)-3,6-(Benzyloxymethyl)-1,4-dioxane-2,5-dione (1). (S)-Hydroxy acid **2** (15 g, 76 mmol) was dissolved in 700 mL dry CH₂Cl₂ and added dropwise to a mixture of dicyclohexylcarbodiimide (20 g, 97 mmol) and 1-hydroxybenzotriazole (13 g, 97 mmol) over a period of 6 h at 50 °C. After 2 d the solution was cooled to 0 °C and the dicyclohexylurea precipitate was removed by filtration. The solvent was removed, and the resulting oily solid was dissolved in ethyl acetate (200 mL). The mixture was washed with H₂O (3 x 100 mL), dried over MgSO₄, and the solvent was removed. The residue was recrystallized from anhydrous Et₂O to give **1** as a white crystalline solid (4.03 g, 28%). The spectra of the product matched published data.²⁹

4.2.3. Copolymerization of **1** and Lactide, and Deprotection of Copolymer **3**

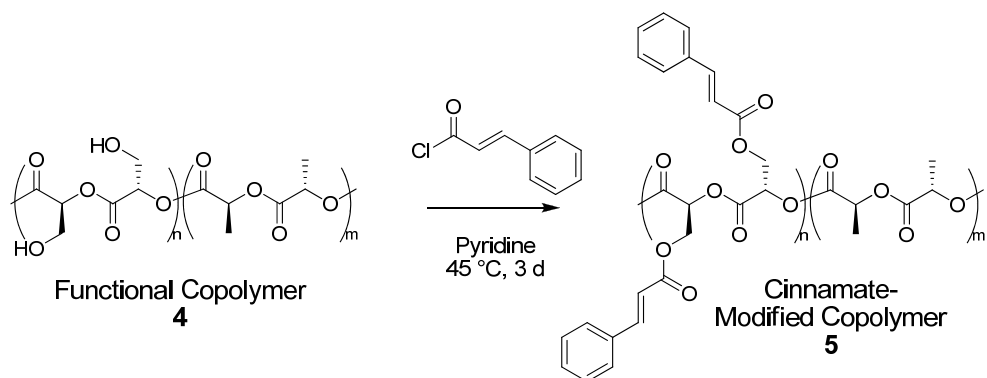


The synthesis and deprotection of protected copolymer **3** was performed as previously reported²⁹ with some minor modifications. Lactide monomer, monomer **1**, and SnOct₂ were added to an oven-dried reaction vessel inside a glove box. The vessel was removed from the glove box and heated to 120 °C for 16 h. The mixture was dissolved in chloroform (100 mL) and poured into cold MeOH (1 L). The precipitate was collected by filtration and dried under vacuum overnight to give protected copolymer **3** as a white solid. The spectra of the protected copolymer **3** matched published data.²⁹

Protected copolymer **3** was dissolved in a 4:1 (v:v) mixture of EtOAc and CH₂Cl₂ and an equal mass of Pd(OH)₂ was added. The solution was placed on a hydrogenator and charged to 50 PSI of H₂ for 3 d. The catalyst was removed by filtration and the solvent was removed under reduced pressure. The resulting solid was dissolved in dichloromethane (100 mL), precipitated into methanol (1L), and dried under vacuum to

give functional copolymer **4**. The spectra of functional copolymer **4** matched published data.²⁹

4.2.4. Preparation of Cinnamate-modified PLA Copolymers



4.2.4.1. Modification of Hydroxyl-bearing Copolymer with Cinnamoyl

Chloride. Functional copolymer **4** (4.0 g) was treated with cinnamoyl chloride (4.6 g, 27 mmol) (10 equiv. of cinnamoyl chloride per mol of hydroxyl side chain) and pyridine (2.2 mL, 27 mmol) (10 equiv. per mol of hydroxyl side chain) in CH_2Cl_2 (200 mL). The reaction mixture was stirred for 3 d at 45 °C, the solvent was removed and the polymer was precipitated twice into MeOH (1 mL) to give cinnamate-modified copolymer **5** (4.1 g, 93%). ^1H NMR (300 MHz, CDCl_3) δ 7.6-7.8 (2 H, -CH- of alkene of cinnamate repeat unit), 7.4-7.6 (4 H, -CH- of phenyl ring of cinnamate repeat unit), 7.2-7.4 (6 H, -CH- of phenyl ring of cinnamate repeat unit), 6.3-6.5 (2 H, -CH- of alkene of cinnamate repeat unit), 5.4-5.6 (-CH- of backbone of cinnamate repeat unit), 5.0-5.3 (-CH- of backbone of LA unit), 4.5-4.8 (- CH_2 - of cinnamate repeat unit), 1.4-1.8 (- CH_3 of LA). ^{13}C NMR (100 MHz, CDCl_3) δ 169.4 (carbonyl of LA unit), 165.9 (carbonyl of cinnamate ester side chain), 145.8 (alkene of cinnamate), 134.0, 130.3, 128.7, 128.0 (phenyl ring of cinnamate repeat unit), 116.8 (alkene of cinnamate), 69.6, 68.8 (-CH- of backbone of LA unit), 62.0, 16.5. IR (thin film) 2993, 2962, 1751, 1722, 1637, 1180, 1080 cm^{-1} .

4.2.5. Foam Formation

Foams of cinnamate-modified PLA copolymer **5** were prepared using the thermally-induced phase separation (TIPS) technique. Either 0.6 mL (to make thinner foams) or 1.0 mL (to make thicker foams for compression studies) of a 40 mg/mL solution of copolymer **5** in benzene was placed in a half dram vial. The vials were then placed in a freezer at -5 °C overnight. The vials were removed from the freezer and placed in liquid nitrogen for approximately 30 s. The vials were removed from the liquid nitrogen, and vacuum was applied for 24 h during which the sample remained solid as the solvent was removed by sublimation. The resulting foams were removed from the vials, and the tops of the foams were cut off (to eliminate the U-shaped feature caused by the meniscus of the frozen solution) to give disc-shaped foams of copolymer **5** with a height of ~3 mm and a diameter of ~ 8 mm (from the 0.6 mL polymer solutions) or a height of ~6 mm and a diameter of ~8 mm (from the 1 mL solutions).

4.2.6. Compression Strength Tests

The compressive properties of foams of copolymer **5** were tested using an Instron 5566 operated at a cross-head speed of 1 mm/min using a 10-N load cell. Six specimens were measured for each type of sample and the average compression modulus along with the standard deviation were calculated.

4.2.7. Hydrolytic Degradation

Foams of copolymer **5** were weighed (~30 mg), immersed in separate vials containing PBS and heated to 60 °C with gentle stirring. Three different crosslinked and

non-crosslinked foams were removed at nine week intervals. The foams were soaked in DI water, dried to a constant weight and the average percent mass recovery was recorded.

4.3. Results and Discussion

4.3.1. Synthesis of Protected Functional Monomer

We have established facile methods towards the preparation of polylactide copolymers bearing functional groups by the copolymerization of lactide with monomers substituted with protected functional groups. We have previously reported the copolymerization of mono- and disubstituted and deprotection to afford PLA copolymers with pendant alcohol, amine and carboxylic acid functional groups.^{26,29} We investigated the synthesis of dibenzyloxy-substituted lactide monomer **1** by the cyclodimerization of (*S*)-3-benzyloxy-2-hydroxypropanoic acid **2** using a variety of conditions for esterification, Figure 4.1. The acid-catalyzed condensation of the (*S*)-hydroxy acid using *p*-toluenesulfonic acid (TSA) results in the formation of cyclic dimer and linear oligomers. Though monomer **1** was easily isolated from the oligomers by recrystallization, this procedure resulted in low conversions of the hydroxyl acid (~40%) and resulted in low yields (18%) of product.

Using an alternate method, (*S*)-3-Benzyloxy-2-hydroxypropanoic acid **2** can be cyclodimerized using dicyclohexylcarbodiimide (DCC) and 1-hydroxybenzotriazole (HOBT), Figure 4.1. In this approach, we are using carbodiimide chemistry to obtain complete ring closure. The resulting yields (28%) were much higher than those obtained using the acid-catalyzed condensation reaction (18%) performed on the same scale (15 g hydroxyl acid **2**). This could be attributed to lower reaction temperature (50 °C) which

led to the formation of a smaller amount of linear oligomers as determined by ^1H NMR spectroscopy. The DCC/HOBt reaction also had the added advantage of a shorter reaction time (2 d as opposed to 20 d) and a higher conversion ($\sim 80\%$). Both methods resulted in the formation of a single diastereomer of the dibenzyloxy-substituted lactide, which was confirmed using ^1H NMR spectroscopy and X-ray structural analysis.

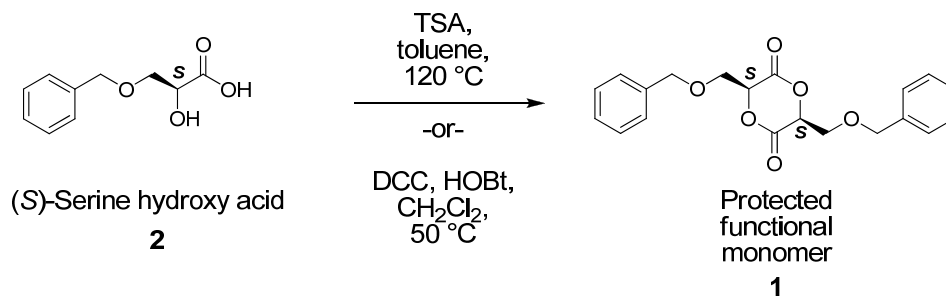


Figure 4.1. Synthesis of dibenzyloxy-substituted lactide 1.

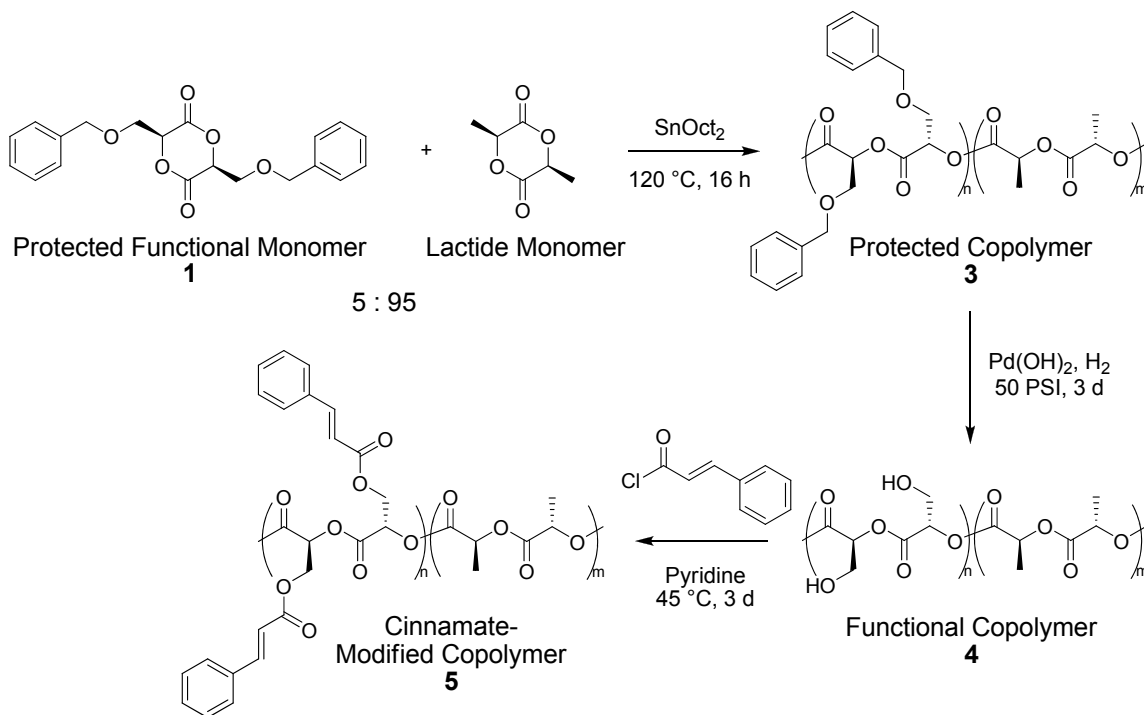


Figure 4.2. Copolymerization, deprotection and modification with cinnamoyl chloride.

4.3.2. Copolymerization, Deprotection, and Modification with Cinnamoyl Chloride

Dibenzyloxy-substituted lactide **1** was copolymerized with L-lactide monomer [(*S,S*)-3,6-dimethyl-1,4-dioxane-2,5-dione] in a 5:95 mol ratio with catalytic stannous octanoate at 120 °C in the absence of solvent, Figure 4.2. A small sample was taken from the copolymerization mixture and the product was analyzed by ¹H NMR spectroscopy. Integration of the methine protons of the lactide monomer (5.0-5.3 ppm) relative to the methine protons of the polymer (5.3-5.5 ppm) indicated a high conversion (89 %). The mixture was poured into a large volume of methanol to precipitate the copolymer and separate any unreacted monomer. ¹H NMR analysis of the resulting copolymer showed the complete removal of the monomer starting material, and integration of the benzylic (4.4-4.6 ppm, protons *j*, Figure 4.3A) and methylene side chain protons (3.8-4.0 ppm, protons *h*, Figure 4.3A) of the copolymer confirmed that 5% protected functional monomer **1** had been incorporated into copolymer **3**. Gel permeation chromatography (GPC, using polystyrene calibration standards) verified the formation of polymers with a narrow polydispersity (PDI = 1.2) and a molecular weight of 2.4×10^4 g/mol.

The benzyl protecting groups of copolymer **3** were removed by hydrogenolysis over Pd(OH)₂ (50 PSI of H₂ in a 3:1 (v:v) mixture of EtOAc and CH₂Cl₂). Complete removal of the protecting groups was confirmed using ¹H NMR spectroscopy by the disappearance of the peaks at 7.3 ppm (phenyl protons *b-d*) and 4.6 ppm (-OCH₂-, protons *j*). Debenzylation also resulted in a downfield shift of the diastereotopic methylene protons of the side chain, with separation of the 2H peak at ~3.9 ppm for the benzyoxy methylene group (Fig 4.3A, signal *h*) into two separate one-proton peaks at 4.1 and 4.3 ppm (Fig 4.3B, signal *h*). Infrared (IR) spectroscopy also confirmed the removal

of the protecting groups by the disappearance of the aromatic C-H stretching vibration at 3016 cm^{-1} .

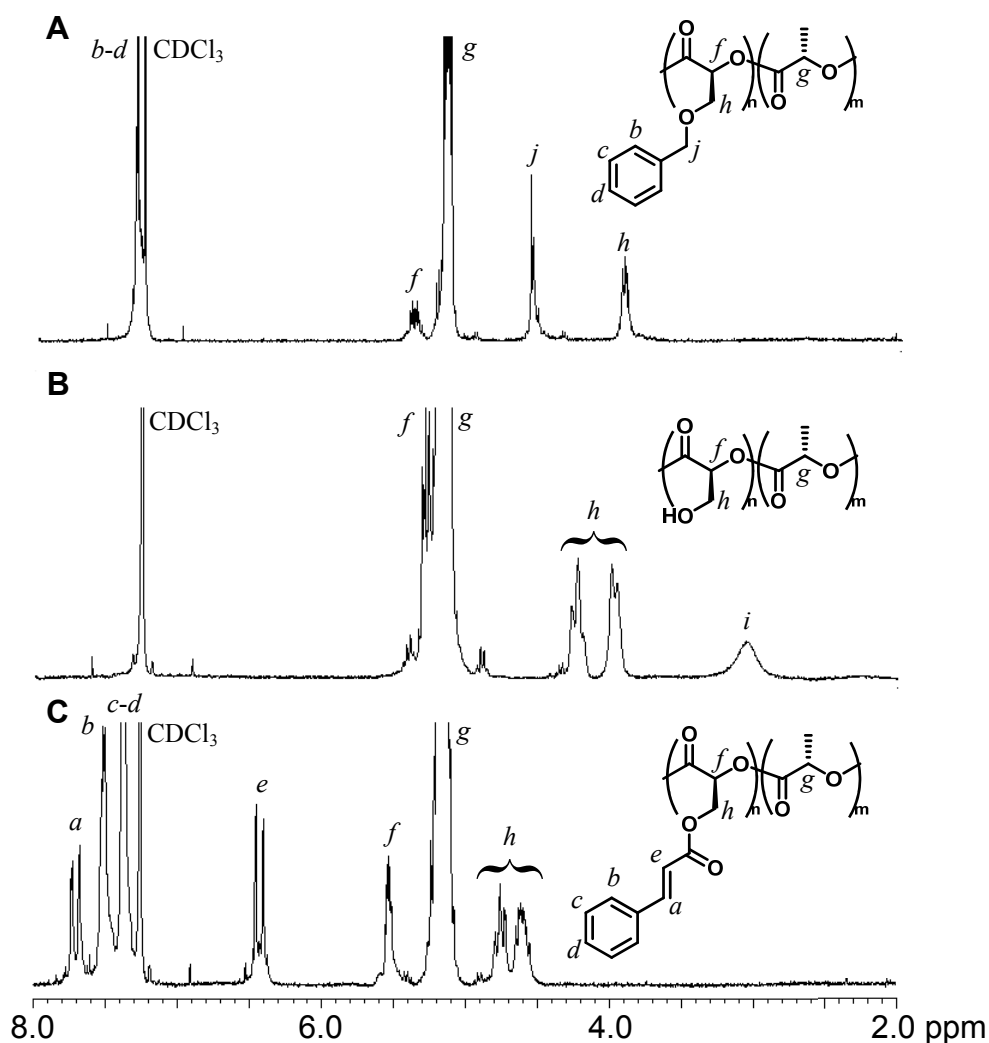


Figure 4.3. ^1H NMR spectra of copolymers: A, benzyloxy substituted copolymer; B, deprotected hydroxymethyl bearing copolymer; C, cinnamate modified copolymer.

The functional PLA copolymer **3** was treated with cinnamoyl chloride in the presence of pyridine at $45\text{ }^\circ\text{C}$ in dichloromethane to give cinnamate ester-modified PLA copolymer **4**. The progress of the reaction was monitored by recording ^1H NMR spectra of aliquots taken from the reaction mixture. The diastereotopic methylene protons of the

side chains (Fig 4.3B, protons *h*) shifted further downfield to 4.6 and 4.8 ppm (Fig 4.3C) upon esterification. Peaks corresponding to the cinnamate ester were observed near 6.5 and 7.5 ppm (Fig 4.3C, protons *a-e*). Complete conversion was obtained after 3d as observed by ¹H NMR spectroscopy. The excess reagents were removed from the reaction mixture by precipitation into methanol followed by filtration to give copolymer **4**. IR spectroscopy indicated the appearance of a characteristic double bond band at 1637 cm⁻¹ for the C=C and a new shoulder on the peak for the carbonyls of the esters in the backbone (1749 cm⁻¹) at 1722 cm⁻¹ arising from the C=O stretching vibration of the cinnamate ester side chains.⁵⁷ GPC analysis confirmed that the polyester backbone remained intact during deprotection and modification with cinnamoyl chloride, Table 4.1. The random copolymers were also characterized by differential scanning calorimetry (DSC), and displayed similar thermal properties to semicrystalline PLA homopolymers⁵⁸ and PLA copolymers prepared in our previous report.²⁶

Table 4.1. GPC and DSC Characterization of Copolymers **3-5**.

Copolymer	M_n (kg/mol)	M_w (kg/mol)	PDI	T_g (°C)	T_m (°C)	ΔH_m (J/g)
3	24	29	1.2	60	151	19
4	28	32	1.1	67	159	17
5	26	30	1.2	69	151	20

4.3.3. Photocrosslinking of Cinnamate-substituted PLA Copolymers

Incorporation of the cinnamate moieties provides the opportunity to crosslink the polymer chains via the photodimerization of the cinnamate side chains by irradiation with UV light, Figure 4.4.⁵⁹

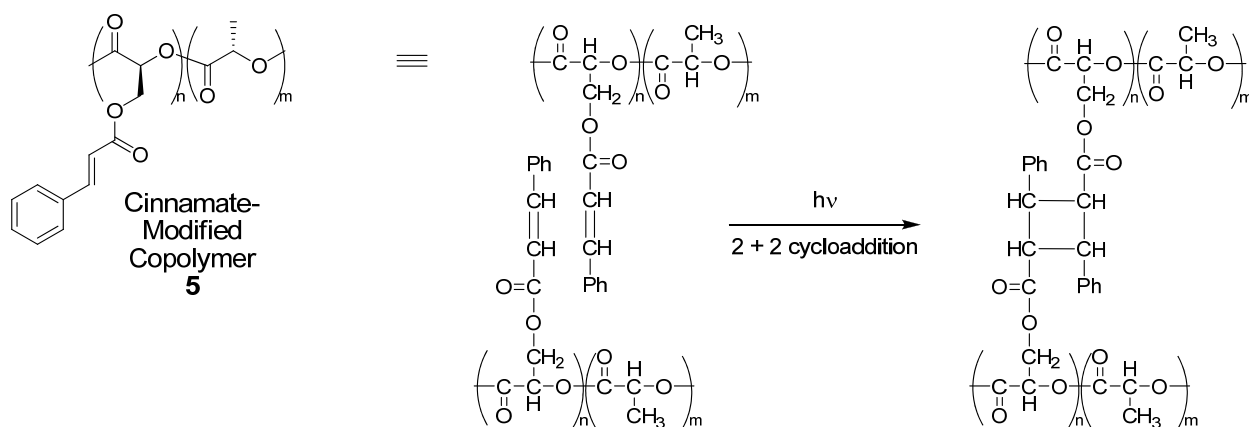


Figure 4.4. Photocrosslinking of cinnamate-modified PLA copolymer **5**.

Free-standing films of cinnamate-modified PLA were prepared by solvent-casting a solution of copolymer **5** in solvent (20 mg/mL) into a glass dish and allowing the solvent to slowly evaporate. The resulting film was cut into 2 cm x 2 cm pieces and mounted on quartz slides. The films were then irradiated in a Rayonet Photochemical reactor (RPR-100) at 300 nm for various times. The progress of the cross-linking reaction was monitored using ATR-IR spectroscopy after 0, 1, 2, 4, and 7 h, Figure 4.5. A decrease in intensity of the band at 1637 cm^{-1} for the C-C double bond was observed as the cinnamate side chains undergo photodimerization to the corresponding cyclobutane derivative.⁵⁷ The disappearance of a shoulder at 1722 cm^{-1} , attributed to the C=O absorption of the cinnamate ester groups, was also observed. Crosslinking was also confirmed by solubility tests. Films irradiated overnight at 300 nm were rendered insoluble in dichloromethane, whereas unirradiated films quickly dissolved in the solvent.

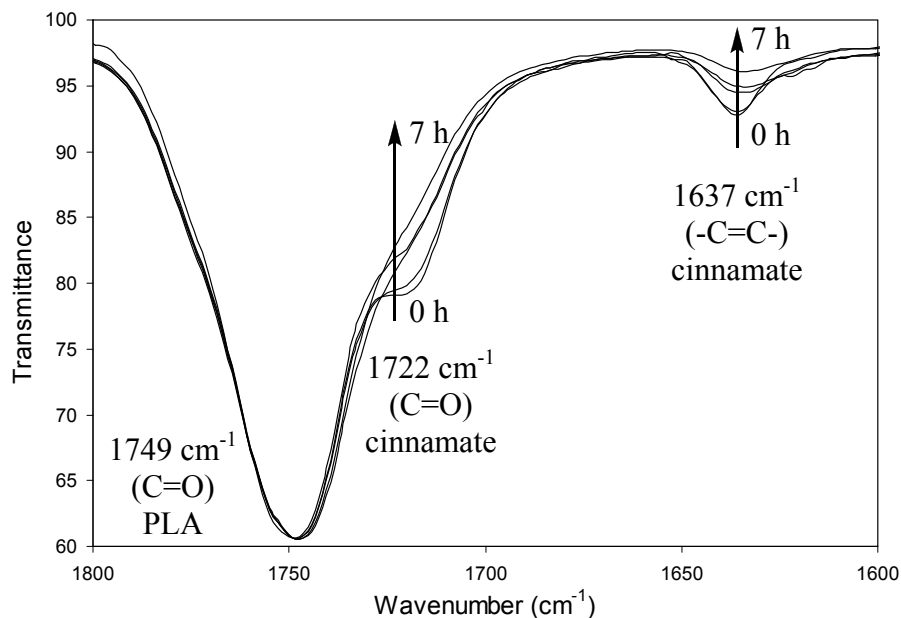


Figure 4.5. ATR-IR spectra of thick films of cinnamate-modified PLA irradiated for 0, 1, 2, 4, and 7 h. Spectra were normalized to the C=O stretching vibration of the PLA polyester backbone at 1749 cm⁻¹.

The photocrosslinking of cinnamate-modified PLA was also demonstrated by changes in the UV-vis spectra. A thin film of the copolymer was prepared by spin-coating a solution (10 mg copolymer in 0.8 mL CH₂Cl₂) directly onto a quartz slide. The sample was then irradiated for selected times (0, 0.17, 0.33, 0.50, 1, 2, 3, 4, 6, and 18 h) and the progress of the reaction was monitored using UV-vis spectroscopy. Increased irradiation time results in a decrease in the π - π^* absorbance of the cinnamate chromophore at 275 nm, Figure 4.6.⁶⁰

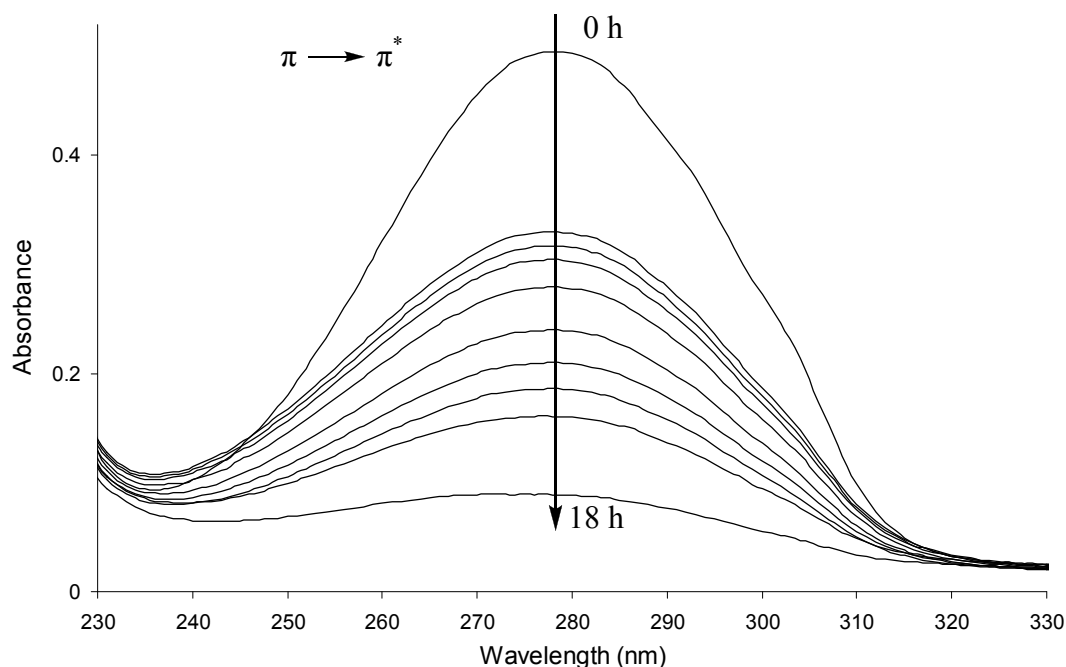


Figure 4.6. UV-vis spectra showing a decrease in the absorption maxima of the thin films of copolymer **5** upon irradiation at 300 nm (0, 0.17, 0.33, 0.50, 1, 2, 3, 4, 6, and 18 h).

4.3.4. Cinnamate-substituted Copolymer Foams

Foams were prepared using a modified thermally-induced phase separation (TIPS) method, whereby the polymer aggregation and solvent segregation that occurs during the freeze-drying of a polymer solution results in the formation of a porous polymer matrix.⁶¹ A solution of copolymer **5** in benzene (40 mg/mL) was heated to 60 °C to aid dissolution. The solution was transferred to vials, which were capped and placed in a -5 °C freezer overnight. The vials were removed from the freezer and exposed to liquid nitrogen for 30 s. The caps were removed, and the vials were placed in a dessicator which was cooled in an ice bath (this was done to ensure the solutions remained frozen throughout the removal of the solvent). The dessicator was subsequently placed under vacuum. After 24 h, the vials were taken out of the dessicator and the copolymer foams

were removed. Initial attempts to fabricate foams of copolymer **5** by a ternary system (15% (w/v) copolymer dissolved in an 87/13 (v/v) dioxane/water) led to ill-defined foams. This led us to shift our attention to phase separation involving a simpler binary system composed of copolymer **5** and benzene.⁶² By decreasing the concentration of the polymer solution to 4% (w/v) and using benzene as the solvent, well-defined foams of copolymer **5** with pore sizes suitable for cellular proliferation (~70 μm) were obtained, as demonstrated by microcomputed tomography (micro-CT), Table 4.2. Six smaller-disc shaped foams (3 mm height, 8 mm diameter) and three larger foams (6 mm height, 8 mm diameter) were analyzed. Micro-CT measurements revealed that the smaller disc-shaped foams showed a similar average porosity, pore size, strut thickness, and connectivity (within the standard deviation) to the larger foams which were later used in the compression strength tests.

Table 4.2. MicroCT Characterization Data of Foams of Copolymer **5**.^a

Sample	foam dimensions		% porosity	pore size (μm)	strut thickness (μm)	% connectivity
	height (mm)	diameter (mm)				
1	3	8	88.2	57	17	>99
2	3	8	84.2	66	19	>99
3	3	8	88.8	74	18	>99
4	3	8	89.4	61	16	>99
5	3	8	84.1	71	20	>99
6	3	8	86.8	73	20	>99
		Mean	86.9 \pm 2.3	67 \pm 7	18 \pm 2	>99
7	6	8	88.6	64	18	>99
8	6	8	79.9	79	22	>99
9	6	8	82.2	83	22	>99
		Mean	83.6 \pm 4.5	75 \pm 10	21 \pm 2	>99
1'	3	8	86.8	56	16	>99
2'	3	8	83.3	61	19	>99
3'	3	8	82.9	71	20	>99
		Mean	84.3 \pm 2.1	63 \pm 8	18 \pm 2	>99

^a Data recorded by Abigail M. Wojtowicz, Georgia Inst. of Tech., Dept. of Biomed. Eng.

' After irradiation

The foams of copolymer **5** were also characterized using scanning electron microscopy (SEM) (Figure 4.7). It was found that contact between the foams and the glass vials during the foaming process resulted in interesting features on the surface of foam. For example, SEM images taken of the bottom of the foams (which were in contact with the bottom of the glass vials during foaming) resulted in either the formation of large tubular pores on the order of 200 μm (Figure 4.7A) or a skin which covered the highly porous surface of the foam (Figure 4.7 B). Shearing off the top surface of the foam revealed a highly porous interior with pore sizes on the order of ~ 70 μm (Figure 4.7 C). This is consistent with the data (Table 4.2) and cross-sectional images (Figure 4.7D) obtained from micro-CT.

The porous foams fabricated using TIPS were irradiated in a Rayonet Photochemical Reactor (RPR-100) at 300 nm for 16 h. MicroCT analysis of Samples 1-3 showed negligible changes in the average porosity, pore size, strut thickness, and connectivity of the foams upon irradiation (Samples 1'-3', Table 4.2). ATR-IR of the crosslinked foams showed complete disappearance of bands arising from the C=O and C=C bonds of the pendant cinnamate groups, Figure 4.8. The photocrosslinking of the cinnamate-modified PLA foams was also confirmed using solubility tests. The initial mass of the irradiated foams were recorded, and the foams were placed in dichloromethane for one hour. The foams were removed from the solvent, dried under vacuum, and the final mass was recorded. By dividing the final mass by the initial mass and multiplying by one hundred, we were able to determine the percent mass recovery.

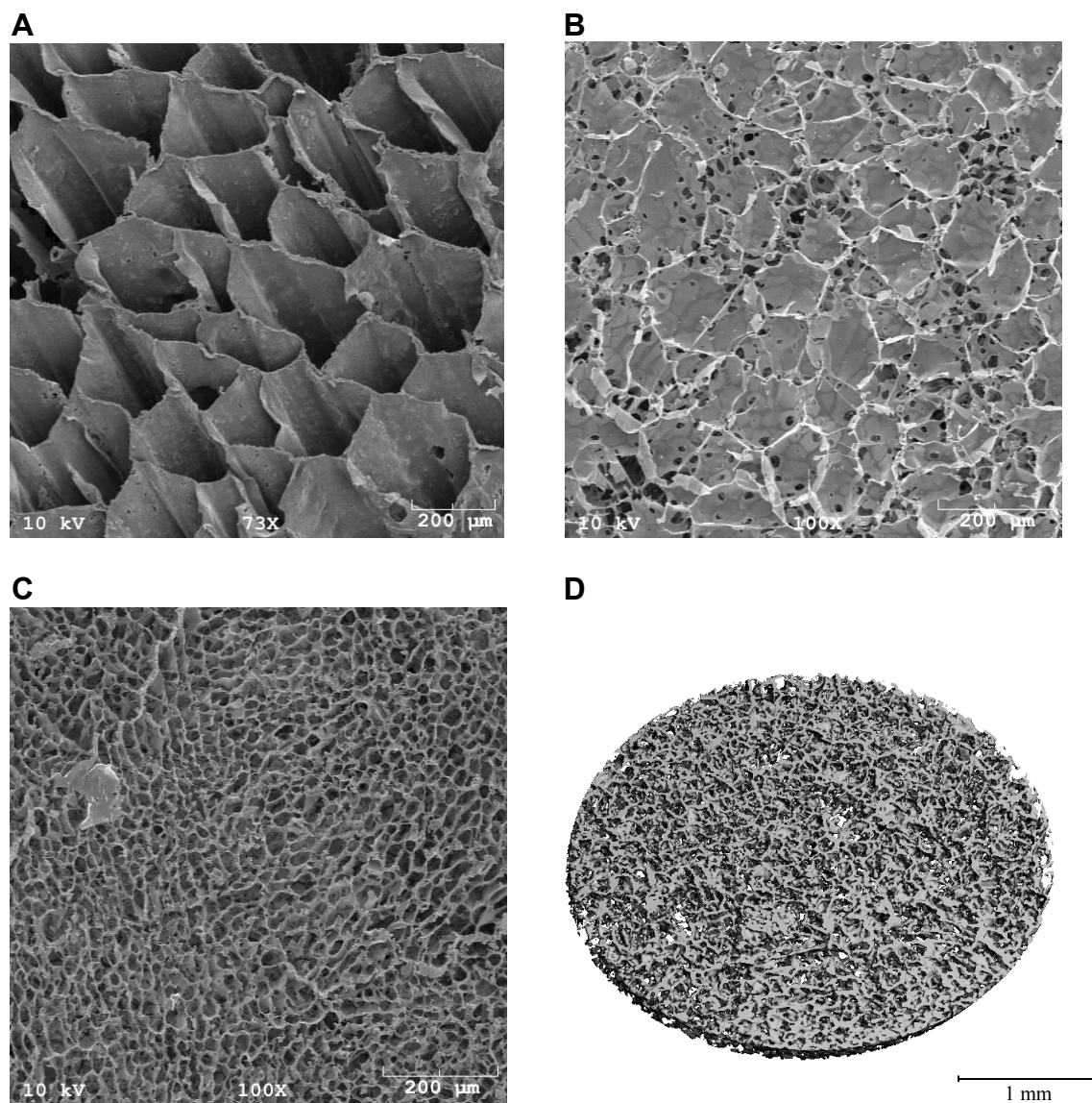


Figure 4.7. SEM images and a micro-CT scan of foams of cinnamate-modified PLA copolymer **5** prepared from benzene solutions (4%): A, Image of the bottom surface of one of the larger foams (6 mm height, 8 mm diameter); B, Image of the bottom of Sample 3; C, Image of the top of Sample 4 (after shearing off the meniscus). D, Micro-CT scan of a 240 μm thick section of Sample 2 taken at 6 micron resolution [SEM data from Yiqing Wang, School of Chemistry and from Amal Raj Puthur Jayapalan, School of Civil and

Environmental Engineering; micro-CT data from Abigail M. Wojtowicz, School of Biomedical Engineering].

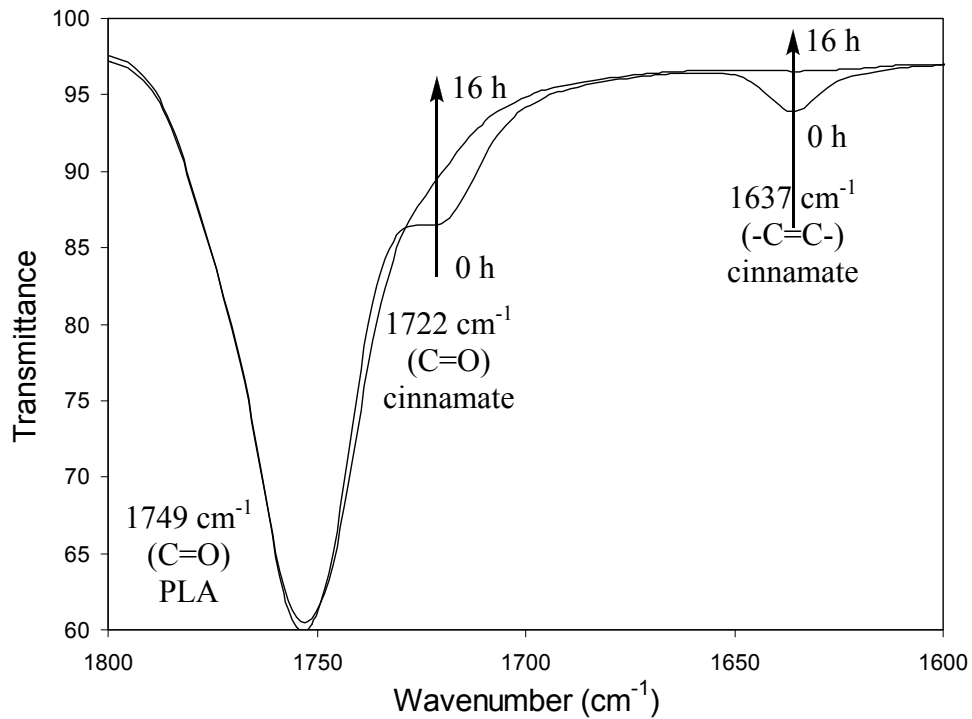


Figure 4.8. ATR-IR spectra of nonirradiated (0 h) and irradiated (16 h) foams.

While nonirradiated foams completely dissolved in the dichloromethane in a matter of seconds, the irradiated foams resulted in 80% mass recovery which shows that the foams are crosslinked during irradiation.

Compression strength tests were performed on the irradiated and unirradiated PLA foams to determine the effect of crosslinking on their mechanical properties. Cylindrical foams with a height of 6 mm and a diameter of 8 mm were prepared to avoid buckling during compression.⁶³ The compressive mechanical properties were measured

using an Instron 5566 instrument. The foams displayed typical stress-strain curves for cellular solids with strain-hardening characteristics⁶⁴ which include a linear elastic region, an increasing plateau region where pore collapse occurs, and a densification region where the stress rises steeply as the foam is further compressed, Figure 4.9.

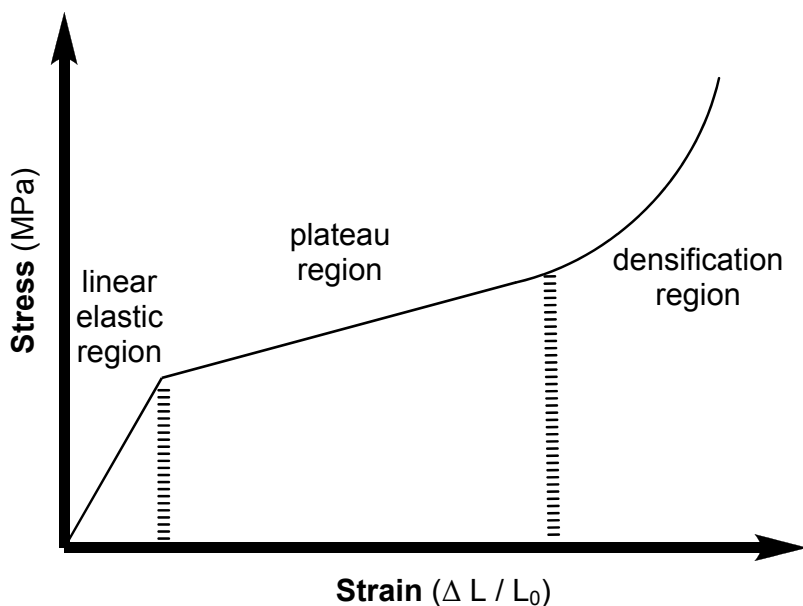


Figure 4.9. Typical stress-strain curve of strain-hardening cellular solids.

The compressive modulus was determined from the slope of the initial linear regime of the stress-strain curve, Figure 4.10.⁶⁵ The arrows indicate inflection points as the compressed foams make the transition between the linear elastic region and the plateau region. The average compressive modulus of crosslinked foams of cinnamate-modified PLA copolymer **5** was higher (1.46 ± 0.25 MPa) than foams which were not crosslinked (0.84 ± 0.15 MPa). From these results, we can conclude that the photocrosslinking of the cinnamate moieties has a significant effect on the compressive modulus and overall mechanical properties of the PLA foams.

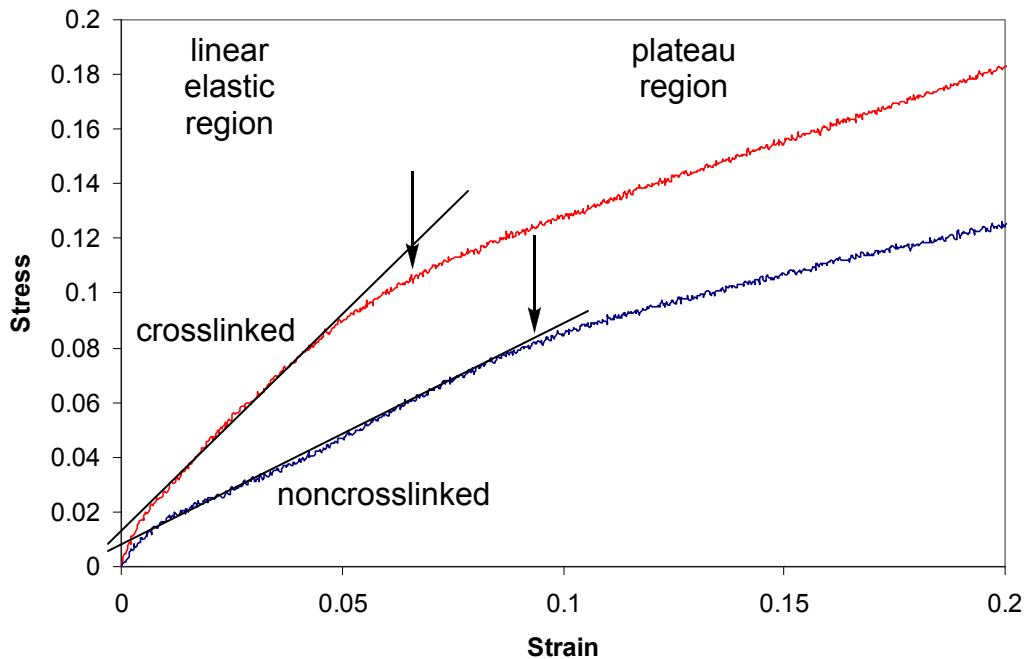


Figure 4.10. Typical stress-strain curves of crosslinked and noncrosslinked foams of PLA copolymer 5.

4.3.5. Hydrolytic Degradation of Copolymer Foams

An accelerated hydrolytic degradation study was performed using crosslinked and noncrosslinked cinnamate-modified PLA foams in order to determine the effect of crosslinking on the degradation rate. Copolymer foams (~ 30 mg) were weighed and placed in phosphate-buffered saline (PBS) at 60 °C with gentle stirring. At selected intervals, three irradiated and unirradiated foams were removed, soaked in deionized water, and dried under vacuum to a constant weight. The mass was recorded and used to calculate the average percent mass recovery as a function of degradation time, Figure 4.11. The data is reported as the mean percent mass recovery of three foams \pm the standard deviation. Foams of copolymer 5 which were crosslinked showed enhanced

hydrolytic stability as shown by a high average percent mass recovery (98-99%) after 7, 9, 18, and 27 weeks. Foams which were not photocrosslinked showed a steady decrease in the average percent mass recovery with time, dropping from 92% to 32% as the hydrolytic degradation time progressed from 18 to 27 weeks.

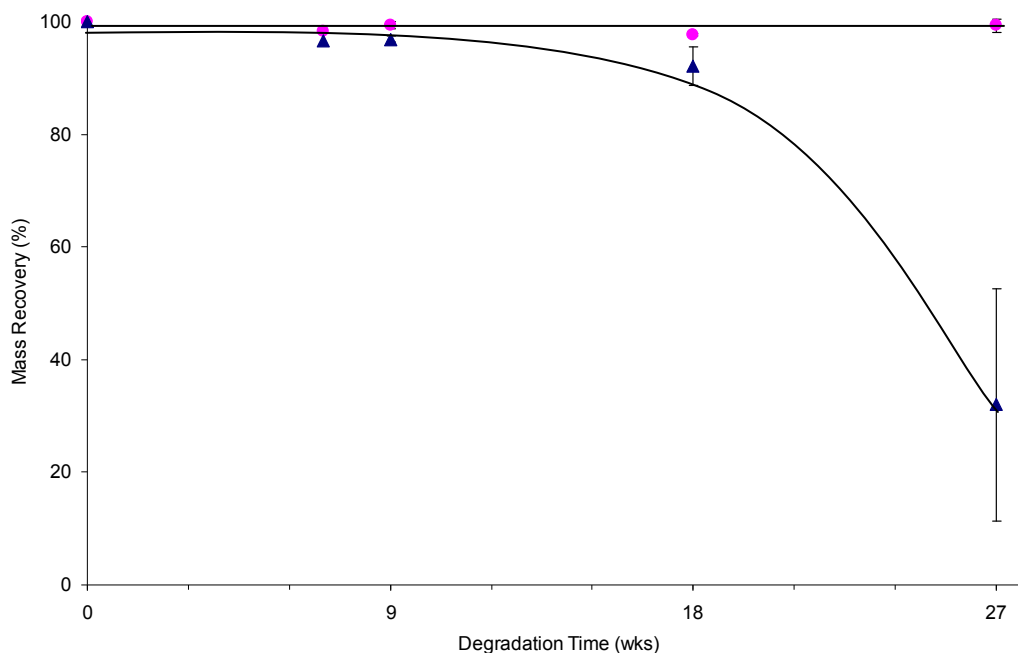


Figure 4.11. Percent mass recovery of crosslinked (●) and noncrosslinked (▲) foams in an accelerated hydrolytic degradation study in PBS at 60 °C. Curves are to guide the eye.

4.3.6. Dye Penetration in Copolymer Foams

Scaffolds used in tissue engineering must be highly porous to facilitate proper cell growth¹⁵ and the transport of nutrients and metabolic waste.⁶⁶ In order to verify the interconnectivity and porosity of our foams and to explore whether or not the porous structures are sufficient for the transport of small molecules, dye penetration studies were performed using aqueous FD&C Red #40 dye (disodium 6-hydroxy-5-[(2-methoxy-5-

methyl-4-sulfophenyl)azo]-2-naphthalene-sulfonate). Foams of cinnamate-modified PLA copolymer **5** were prewet by immersion into 100% ethanol, a 50:50 ethanol:PBS solution, and a 100% PBS solution with sonication (~1 min) in each solution. The foams were then submerged in a solution of Red #40. After 10 minutes, the foams were red, indicating penetration of the dye (Figure 4.12 B). Foams cut along the axial position after dye exposure showed complete penetration of the dye into the interior of the foam (Figure 4.12 E). The foams were then placed in a solution of PBS, and the dye was allowed to diffuse out of the foams. After 10 min, the foams showed a substantial loss of color (Figure 4.12 C), showing that the dye is also able to diffuse out of the foams. Finally, the foams were placed in a solution of PBS for 1 min with sonication, which resulted in an even greater loss of color (Figure 4.12 D).

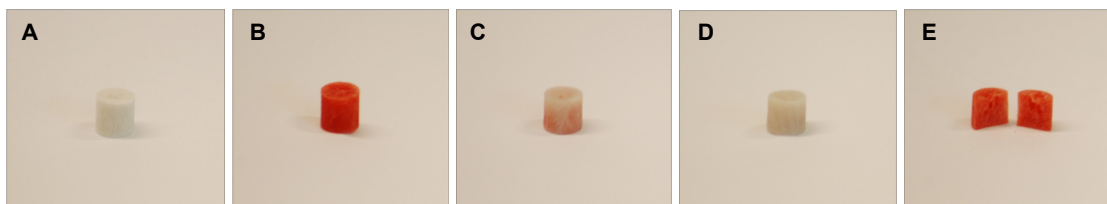


Figure 4.12. Cinnamate-modified PLA copolymer foams used in a dye penetration study: A, dry foam; B, after pre-wetting in ethanol, 50:50 ethanol:PBS, and PBS (with sonication in each solution for 1 min) followed by immersion in a solution of red dye #40 for 10 min; C, after soaking the dyed foam in PBS for 10 min; D, after soaking the foam in PBS for 1 min with sonication; E, Axial cut of the dyed foam showing penetration of the dye into the interior of the foam.

Prewetting with ethanol followed by solvent exchange was important to the success of this process. Foams which were placed directly in a dye solution overnight without prewetting showed a little dye absorption on the exterior, and very little penetration into the interior.

These results not only confirm the feasibility of using these porous foams as scaffolds for cell growth, but also provide a method by which reagents might be infused into porous foams of carboxylic acid-functionalized PLA copolymers to facilitate modification with peptides (Chap. 3).

4.4. Conclusions

In conclusion, we have prepared PLA copolymers with pendant functional groups by the copolymerization of lactide with a protected functional monomer. Copolymer deprotection and modification with cinnamoyl chloride afforded a PLA copolymer with photocrosslinkable side chains. The crosslinking of thin films and of foams was demonstrated by IR and UV-vis spectroscopy. Crosslinking of cinnamate-modified PLA foams resulted in a 74 % increase in the compression modulus. Crosslinking also led to a slower hydrolytic decomposition of the foams. This novel photocrosslinkable, biodegradable PLA copolymer shows great promise as a material for use in host of biomedical applications ranging from scaffolding for tissue engineering to a biodegradable matrix for use in drug delivery.

4.5. References

- (1) Trimaille, T.; Gurny, R.; Moller, M., *J. Biomed. Mater. Res., Part A* **2006**, *80A*, 55-65.
- (2) Kranz, H.; Bodmeier, R., *Int. J. Pharm.* **2007**, *332*, 107-114.
- (3) Grayson, A. C. R.; Voskerician, G.; Lynn, A.; Anderson, J. M.; Cima, M. J.; Langer, R., *J. Biomater. Sci., Polym. Ed.* **2004**, *15*, 1281-1304.
- (4) Gu, M.-q.; Yuan, X.-b.; Kang, C.-s.; Zhao, Y.-h.; Tian, N.-j.; Pu, P.-y.; Sheng, J., *Carbohydr. Polym.* **2007**, *67*, 417-426.
- (5) Zhang, R.; Xiong, Z.; Wang, L., *Cailiao Yanjiu Xuebao* **2003**, *17*, 145-150.
- (6) Holy, C. E.; Fialkov, J. A.; Davies, J. E.; Shoichet, M. S., **2003**, *65A*, 447-453.
- (7) Martina, M.; Hutmacher, D. W., *Polym. Int.* **2007**, *56*, 145-157.
- (8) Cheung, H.-Y.; Lau, K.-T.; Lu, T.-P.; Hui, D., *Composites, Part B* **2007**, *38B*, 291-300.
- (9) Datta, R.; Henry, M., *J. Chem. Technol. Biotechnol.* **2006**, *81*, 1119-1129.
- (10) Ganjyal, G. M.; Weber, R.; Hanna, M. A., *Bioresour. Technol.* **2007**, *98*, 3176-9.
- (11) Bazile, D. V.; Ropert, C.; Huve, P.; Verrecchia, T.; Marlard, M.; Frydman, A.; Veillard, M.; Spenlehauer, G., *Biomaterials* **1992**, *13*, 1093-102.
- (12) Schugens, C.; Maquet, V.; Grandfils, C.; Jerome, R.; Teyssie, P., *J. Biomed. Mater. Res.* **1996**, *30*, 449-461.
- (13) Schugens, C.; Maquet, V.; Grandfils, C.; Jerome, R.; Teyssie, P., *Polymer* **1996**, *37*, 1027-1038.
- (14) Li, S. R.; La Carrubba, V.; Piccarolo, S.; Sannino, D.; Brucato, V., *Polym. Int.* **2004**, *53*, 2079-2085.

- (15) Shin, K. C.; Kim, B. S.; Kim, J. H.; Park, T. G.; Do Nam, J.; Lee, D. S., *Polymer* **2005**, *46*, 3801-3808.
- (16) Jiang, X.; Vogel, E. B.; Smith, M. R.; Baker, G. L., *Macromolecules* **2008**, *41*, 1937-1944.
- (17) Park, P. I. P.; Jonnalagadda, S., *J. Appl. Polym. Sci.* **2006**, *100*, 1983-1987.
- (18) Trimaille, T.; Gurny, R.; Moeller, M., *Chimia* **2005**, *59*, 348-352.
- (19) Trimaille, T.; Moeller, M.; Gurny, R., *J. Polym. Sci., Part A: Polym. Chem.* **2004**, *42*, 4379-4391.
- (20) Lu, X. L.; Cai, W.; Gao, Z. Y., *J. Appl. Polym. Sci.* **2008**, *108*, 1109-1115.
- (21) Zalusky, A. S.; Olayo-Valles, R.; Wolf, J. H.; Hillmyer, M. A., *J. Am. Chem. Soc.* **2002**, *124*, 12761-12773.
- (22) Kuo, S.-W.; Huang, C.-F.; Tung, Y.-C.; Chang, F.-C., *J. Appl. Polym. Sci.* **2006**, *100*, 1146-1161.
- (23) Baiardo, M.; Frisoni, G.; Scandola, M.; Rimelen, M.; Lips, D.; Ruffieux, K.; Wintermantel, E., *J. Appl. Polym. Sci.* **2003**, *90*, 1731-1738.
- (24) Hasirci, V.; Lewandrowski, K. U.; Bondre, S. P.; Gresser, J. D.; Trantolo, D. J.; Wise, D. L., *Biomed. Mater. Eng.* **2000**, *10*, 19-29.
- (25) Quynh, T. M.; Mitomo, H.; Nagasawa, N.; Wada, Y.; Yoshii, F.; Tamada, M., *Eur. Polym. J.* **2007**, *43*, 1779-1785.
- (26) Gerhardt, W. W.; Noga, D. E.; Hardcastle, K. I.; Garcia, A. J.; Collard, D. M.; Weck, M., *Biomacromolecules* **2006**, *7*, 1735-1742.
- (27) Ouchi, T.; Fujino, A., *Makromol. Chem.* **1989**, *190*, 1523-30.

- (28) Marcincinova-Benabdillah, K.; Boustta, M.; Coudane, J.; Vert, M., *Biomacromolecules* **2001**, *2*, 1279-1284.
- (29) Noga, D. E. P., T. A.; Kumar, A.; Weck, M.; García, A. J.; Collard, D. M., *Biomacromolecules*, in submission.
- (30) Loontjens, C. A. M.; Vermonden, T.; Leemhuis, M.; van Steenberg, M. J.; van Nostrum, C. F.; Hennink, W. E., *Macromolecules* **2007**, *40*, 7208-7216.
- (31) Kimura, Y.; Shirotani, K.; Yamane, H.; Kitao, T., *Macromolecules* **1988**, *21*, 3338-40.
- (32) Leemhuis, M.; van Nostrum, C. F.; Kruijtzter, J. A. W.; Zhong, Z. Y.; ten Breteleur, M. R.; Dijkstra, P. J.; Feijen, J.; Hennink, W. E., *Macromolecules* **2006**, *39*, 3500-3508.
- (33) Leemhuis, M.; van Steenis, J. H.; van Uxem, M. J.; van Nostrum, C. F.; Hennink, W. E., *Eur. J. Org. Chem.* **2003**, 3344-3349.
- (34) Barrera, D. A.; Zylstra, E.; Lansbury, P. T., Jr.; Langer, R., *J. Am. Chem. Soc.* **1993**, *115*, 11010-11.
- (35) Barrera, D. A.; Zylstra, E.; Lansbury, P. T.; Langer, R., *Macromolecules* **1995**, *28*, 425-32.
- (36) Cook, A. D.; Hrkach, J. S.; Gao, N. N.; Johnson, I. M.; Pajavni, U. B.; Cannizzaro, S. M.; Langer, R., *J. Biomed. Mater. Res.* **1997**, *35*, 513-523.
- (37) Cook, A. D.; Pajvani, U. B.; Hrkach, J. S.; Cannizzaro, S. M.; Langer, R., *Biomaterials* **1997**, *18*, 1417-1424.
- (38) Feng, Y.; Klee, D.; Hocker, H., *Macromol. Chem. Phys.* **2002**, *203*, 819-824.

- (39) In't Veld, P. J. A.; Dijkstra, P. J.; Feijen, J., *Makromol. Chem.* **1992**, *193*, 2713-30.
- (40) Deng, C.; Chen, X.; Yu, H.; Sun, J.; Lu, T.; Jing, X., *Polymer* **2007**, *48*, 139-149.
- (41) Deng, C.; Rong, G.; Tian, H.; Tang, Z.; Chen, X.; Jing, X., *Polymer* **2005**, *46*, 653-659.
- (42) Deng, C.; Tian, H.; Zhang, P.; Sun, J.; Chen, X.; Jing, X., *Biomacromolecules* **2006**, *7*, 590-596.
- (43) Deng, M.; Wang, R.; Rong, G.; Sun, J.; Zhang, X.; Chen, X.; Jing, X., *Biomaterials* **2004**, *25*, 3553-3558.
- (44) Parrish, B.; Breitenkamp, R. B.; Emrick, T., *J. Am. Chem. Soc.* **2005**, *127*, 7404-7410.
- (45) Riva, R.; Schmeits, S.; Jerome, C.; Jerome, R.; Lecomte, P., *Macromolecules* **2007**, *40*, 796-803.
- (46) Mecerreyes, D.; Miller, R. D.; Hedrick, J. L.; Detrembleur, C.; Jerome, R., *J. Polym. Sci., Part A: Polym. Chem.* **2000**, *38*, 870-875.
- (47) Parrish, B.; Quansah, J. K.; Emrick, T., *J. Polym. Sci., Part A: Polym. Chem.* **2002**, *40*, 1983-1990.
- (48) Clapper, J. D.; Skeie, J. M.; Mullins, R. F.; Guymon, C. A., *Polymer* **2007**, *48*, 6554-6564.
- (49) Amsden, B. G.; Misra, G.; Gu, F.; Younes, H. M., *Biomacromolecules* **2004**, *5*, 2479-2486.
- (50) Chan-Park, M. B.; Zhu, A. P.; Shen, J. Y.; Fan, A. L., *Macromol. Biosci.* **2004**, *4*, 665-673.

- (51) Karikari, A. S.; Edwards, W. F.; Mecham, J. B.; Long, T. E., *Biomacromolecules* **2005**, *6*, 2866-2874.
- (52) Storey, R. F.; Warren, S. C.; Allison, C. J.; Puckett, A. D., *Polymer* **1997**, *38*, 6295-6301.
- (53) John, G.; Morita, M., *Macromolecules* **1999**, *32*, 1853-1858.
- (54) Chen, V. J.; Ma, P. X., *Scaff. Tiss. Eng.* **2006**, 125-137.
- (55) Kim, H. D.; Bae, E. H.; Kwon, I. C.; Pal, R. R.; Nam, J. D.; Lee, D. S., *Biomaterials* **2004**, *25*, 2319-2329.
- (56) Deechongkit, S.; You, S.-L.; Kelly, J. W., *Org. Lett.* **2004**, *6*, 497-500.
- (57) Haramina, T.; Kirchheim, R., *Macromolecules* **2007**, *40*, 4211-4216.
- (58) Park, J. W.; Lee, D. J.; Yoo, E. S.; Im, S. S.; Kim, S. H.; Kim, Y. H., *Korea Polym. J.* **1999**, *7*, 93-101.
- (59) Fujiwara, T.; Iwata, T.; Kimura, Y., *J. Polym. Sci., Part A: Polym. Chem.* **2001**, *39*, 4249-4254.
- (60) Ali, A. H.; Srinivasan, K. S. V., *J. Appl. Polym. Sci.* **1998**, *67*, 441-448.
- (61) Nam, Y. S.; Park, T. G., *Biomaterials* **1999**, *20*, 1783-1790.
- (62) Ma, P. X.; Zhang, R. Y., *J. Biomed. Mater. Res.* **2001**, *56*, 469-477.
- (63) Charles-Harris, M.; del Valle, S.; Hentges, E.; Bleuet, P.; Lacroix, D.; Planell, J. A., *Biomaterials* **2007**, *28*, 4429-4438.
- (64) Li, Q. M.; Magkiriadis, I.; Harrigan, J. J., *J. Cell. Plast.* **2006**, *42*, 371-392.
- (65) Wan, Y.; Fang, Y.; Wu, H.; Cao, X. Y., *J. Biomed. Mater. Res., Part A* **2007**, *80A*, 776-789.

- (66) Venugopal, J.; Vadgama, P.; Kumar, T. S. S.; Ramakrishna, S., *Nanotechnology* **2007**, *18*.

CHAPTER 5

SYNTHESIS OF PNB-PLA DIBLOCK COPOLYMERS[‡]

5.1. Introduction

Block copolymers composed of two or more different polymer chains joined together to make a single molecule represent a new class of materials with unique structural and physical properties.¹ Block copolymers have been incorporated into everyday applications ranging from packaging tape to asphalt.² Interactions between the different blocks and the immiscibility of the components can lead to phase separation on the nanometer scale into various ordered structures, including cubic packed spheres, hexagonal packed cylinders, double gyroid, and lamellar morphologies.³ Though many of the current applications of block copolymers do not require the formation of ordered morphologies,⁴ emerging interest in the preparation of ordered nanoporous polymeric materials for applications such as nanolithography⁵ have prompted the investigation of block copolymer nanoscale phase separation.

Biodegradable implants offer an attractive alternative to other implants since they avoid a second invasive surgery for removal.⁶ However, biodegradable implants often lack the required mechanical properties, and are prone to warping and hollowing during degradation.⁷ Methods to improve mechanical strength include the addition of reinforcing elements such as polymer fibers,⁸ and particles such as hydroxyapatite^{9,10} and bioglass.^{11,12}

[‡] Hydroxyl-terminated poly(norbornene) was synthesized by Dr. Kunsang Yoon and Dr. Yiqing Wang. Characterization (SEC, SAXS, WAXD) provided by Dr. Alexander Norman of NYU.

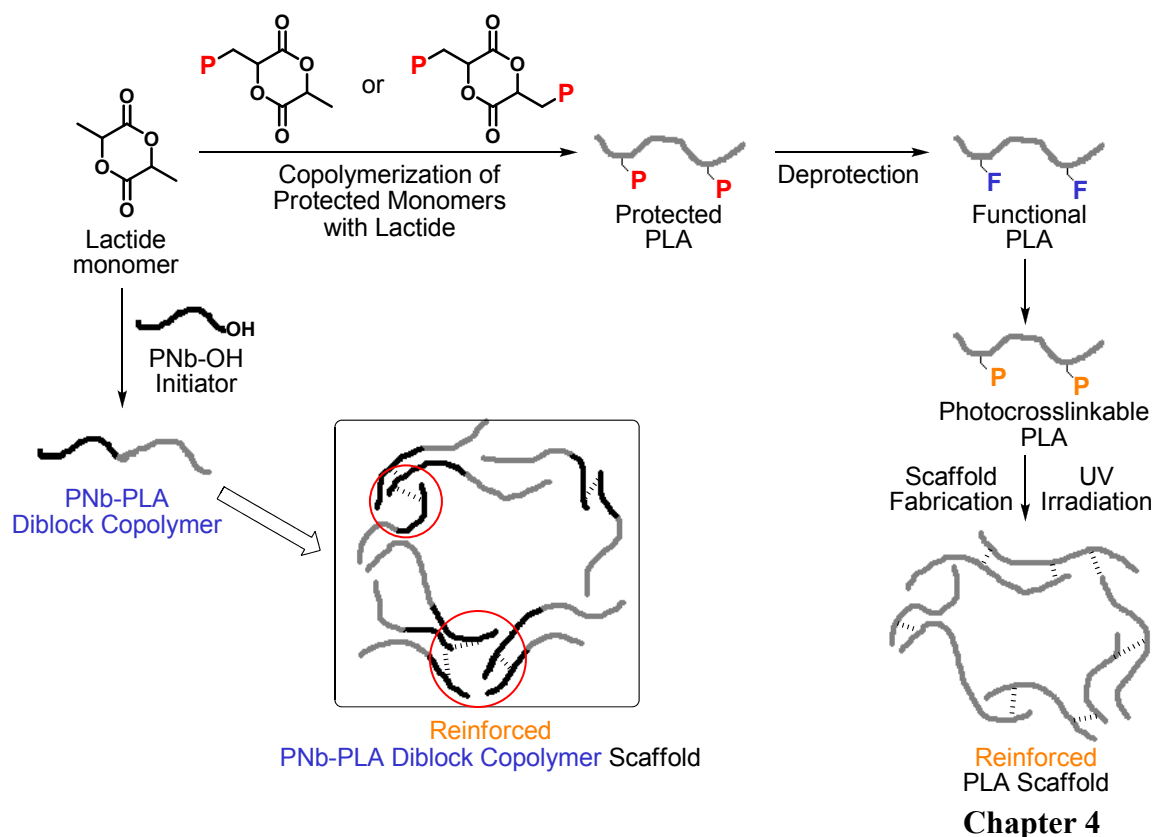


Figure 5.1. The fabrication of robust PLA scaffolds by incorporation of photocrosslinkable groups or phase-separation of a PNB-*bl*-PLA diblock copolymer.

In Chapter 4 we discussed the preparation of PLA copolymers with pendant photocrosslinkable groups, Figure 5.1. Irradiation led to crosslinking via the 2 + 2 cyclodimerization of the cinnamate moieties and resulted in an increase in the compressive modulus of polymer foams. This methodology provides a facile route towards the preparation of PLA scaffolds with enhanced mechanical properties. Another possible route towards the fabrication of mechanically robust foams involves the synthesis of a PLA diblock copolymers, where the additional block is composed of a rigid polymer which phase separates to form a non-covalent crosslink and thereby

provides added structural integrity, Figure 5.1.¹³ In an effort to explore this possibility, polynorbornene-*block*-poly(lactic acid) (PNb-*bl*-PLA) diblock copolymers were prepared and the thermal and morphological properties of the copolymer were studied. PNb was chosen as the rigid block because of its semi-rigid backbone, its ability to phase separate,¹⁴ ease of synthesis in a controlled fashion,¹⁵ and its emerging use in biomedical applications.¹⁶ The PNb-*bl*-PLA diblock copolymers were synthesized using a hydroxyl-terminated polynorbornene as a macroinitiator for the ring opening copolymerization of lactide monomer. One PNb-*bl*-PLA diblock copolymer composition was hydrogenated to give h-PNb-*bl*-PLA in order to explore the effect of the rigid alkene of the PNb block on the properties of the copolymer. The rigid polynorbornene blocks have the potential to offer mechanical reinforcement by aggregating during the foaming process, and could provide a further method for the incorporation of photocrosslinkable groups by modification of the norbornene monomer.¹⁵ Such materials could have potential for use in a variety of applications which extend beyond the strengthening of implant scaffolds to the preparation of novel ordered nanoporous materials.

5.2. Experimental

5.2.1. General Methods

L-lactide was obtained from Aldrich and recrystallized twice from dry EtOAc and stored in a dry-box. Hydroxyl-terminated PNb¹⁵ (Table 5.1) was prepared by Kunsang Yoon and Yiqing Wang from the Weck group as previously reported.¹⁷ Dry benzene was purchased from VWR and stored in a glovebox. Stannous octanoate (SnOct₂) was purchased from Aldrich (product # 287172-250G) and distilled prior to use.

Table 5.1. Hydroxyl-terminated PNb Characterization Data^a

Hydroxyl-terminated PNb	DP (¹ H NMR)	M_n (g/mol) (¹ H NMR)	M_n (g/mol) (GPC)	M_w (g/mol) (GPC)	PDI (GPC)
PNb ₁₈₀	180	27 400	26 100	37 900	1.45
PNb ₁₂₂	122	18 500	18 500	33 200	1.79
PNb ₁₂₉	129	19 600	15 200	23 000	1.51

^aGPCs in THF with poly(styrene) standards

The molecular weight data of the hydroxyl-terminated PNb macroinitiators was determined by gel permeation chromatography (GPC) using three Waters Styragel columns (5- μ m beads: HR 1, 100 Å; HR 3, 1,000 Å; HR 4, 10,000 Å) connected to a Waters 2690 Separations Module with a Waters 2487 Refractive Index Detector. The eluant was THF (1 mL/min, 303 K) and the molecular weights were determined relative to six narrow polystyrene standards in THF.

The molecular weights and polydispersities of the PNb-*b*l-PLA diblock copolymers were determined by size-exclusion chromatography (SEC) using a dual column Rheodyne injector equipped with an Agilent UV/Vis detector, a Wyatt DAWN Heleos light scattering detector and a WYATT OptiPLEX ReX refractive index detector. Thermal analysis was conducted using a Perkin Elmer 600 DSC. All thermal and molecular weight analysis and SAXS and WAXD measurements of the copolymers were performed by Dr. Alexander Norman of New York University. SAXS and WAXD measurements were carried out on beamline X10A of the National Synchrotron Light Source at Brookhaven National Laboratory, Upton, New York. The storage ring provides stored electron beam energy of 2.8 GeV with a maximum operating current of 300 mA, which has an approximate lifetime of 20 hours. The wavelength of the incident radiation used, λ was 1.093 Å (Energy, $E = 11$ keV), providing a beam flux of greater than 10^{12}

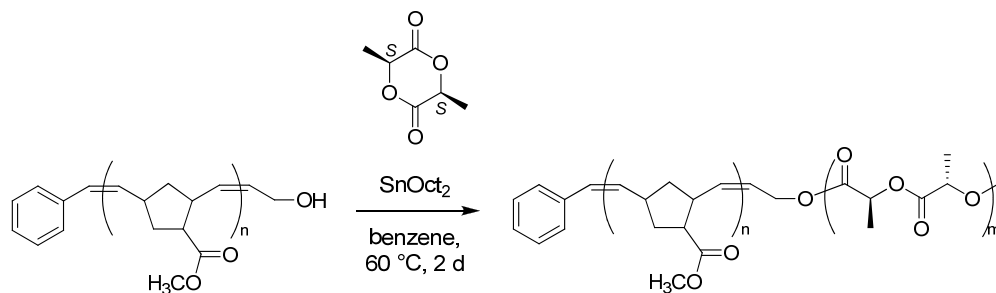
photons/sec. The samples were loaded with polyimide (Kapton) windows into a Mettler Toledo FP99A hotstage which was mounted vertically between the entrance window and the detector. The Bruker CCD camera (has an area of 10.2 x 10.2 cm (1024 pixels x 1024 pixels)) was placed 14.5 cm from the sample (for WAXD measurements) and 2.05 m from the sample (for SAXS measurements). For SAXS measurements, a flight-tube was placed in between the sample holder and the detector. This flight tube was flushed with a steady flow of Argon, minimizing air scatter. The motors, CCD camera and Mettler hotstage were controlled from outside the hutch with a DSP-6002 crate controller running SPEC data acquisition software on a UNIX system.

The degree of crystallinity and crystallographic form were first investigated by WAXD for all samples. The samples were heated from room temperature to 260 °C at a controlled rate of 5 °C/min and cooled back to 30 °C at the same rate. The 2D WAXD patterns were collected for 30 seconds and then corrected for the dark image and unwarped using the Bruker software SMART. Pixel number was converted to a 2θ scale by collecting the WAXD pattern of a known standard: high-density poly(ethylene) (HDPE) where the positions of the (110) and (200) reflections are known. The images of every dataset were converted to the BSL file format using XCONV (part of the software suite FiberFix for Windows). A background subtraction was applied to all datasets and the 2D data were collapsed to a $I(2\theta)$ vs. 2θ plot by performing both equatorial and meridional integrations (horizontal and vertical “slices”).

The microphase separation was then investigated by SAXS. The same heating and cooling rates were applied as those for WAXD. The data were reduced and collapsed in exactly the same way. The 1D data were plotted as $I(q)$ vs. q , where q is the scattering

vector and is related to the scattering angle by $q = 4\pi \sin \theta / \lambda$. Silver Behenate was used as the SAXS calibrant to convert pixel number to q . The extent of microphase separation was determined from the relative peak intensities and the domain spacing between the phase separated regions, d is given by: $d = 2\pi / q$.

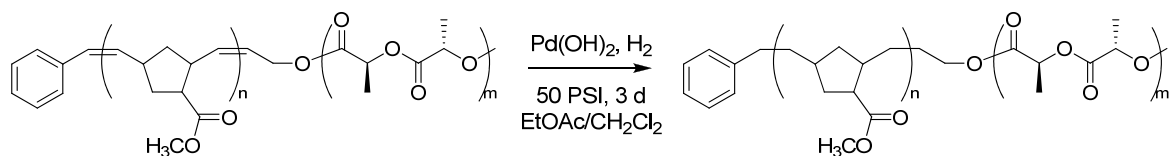
5.2.2. Synthesis of PNb-*bl*-PLA Diblock Copolymers



5.2.2.1 Copolymerization of Lactide using Hydroxyl-terminated PNb

Macroinitiator. In a typical polymerization, hydroxyl-terminated PNb (0.50 g, for PNb₁₈₀ $M_n = 26,100$ g/mol, $M_w = 37,900$ g/mol, PDI = 1.45, 0.018 mmol hydroxyl chain ends), twice-recrystallized lactide (0.47 g, 3.3 mmol) (an equimolar amount of lactide monomer to PNb repeat unit), and SnOct₂ (23 μ L of a 0.8 M stock solution in benzene; 1 mol SnOct₂ per mol of hydroxyl-initiator) in benzene was prepared in a dry-box. The mixture was removed from the glove-box, heated to 60 °C for 2 d, and poured into MeOH (400 mL) cooled in an acetone/dry ice bath. The precipitate was collected by filtration and dried under vacuum overnight to give PNb-*bl*-PLA diblock copolymer as a white solid (0.95 g, 98%). ¹H NMR (300 MHz, CDCl₃) δ 5.3-5.5 (alkene -CH- of PNb repeat unit), 5.1-5.3 (-CH- of PLA repeat unit), 3.5-3.7 (-COOCH₃ of PNb unit), 2.3-3.3 (vinylic -CH- and -CHCOOCH₃ of PNb unit), 1.0-2.2 (-CH₂- of PNb unit), 1.5-1.7 (-CH₃- of PLA unit). ¹³C NMR (133 MHz, CDCl₃) δ 176.3, 174.9 (C=O of PNb), 169.5 (C=O of PLA), 134.4, 133.5, 132.5, 130.9 (alkene C-H of PNb) 68.9 (-CH of PLA), 51.4, 49.4 (COOCH₃ of PNb) 48.2, 47.3, 45.2, 42.4, 41.5 40.6, 36.0 (other -CH and -CH₂- of PNb), 16.6 (-CH₃ PLA).

5.2.3. Preparation of *h*-PNb-*bl*-PLA



5.2.3.1. Hydrogenation of PNb-*bl*-PLA. PNb-*bl*-PLA (1.00 g) was dissolved in a 4:1 (v:v) mixture of EtOAc and CH₂Cl₂ and an equal mass of Pd(OH)₂ relative to the mass of the PNb block (~0.60 g) was added. The solution was placed on a hydrogenator and charged to 50 PSI of H₂ for 3 d. The catalyst was removed by filtration and the solvent was removed. The polymer was dissolved in CH₂Cl₂ (15 mL) and precipitated into ice cold MeOH (500 mL) to give *h*-PNb-*bl*-PLA (0.65 g, 65%). ¹H NMR (300 MHz, CDCl₃) δ 5.1-5.3 (-CH- of PLA repeat unit), 3.5-3.7 (-COOCH₃ of PNb unit), 2.2-2.9 (-CHCOOCH₃ of PNb unit), 1.0-2.2 (other -CH- and -CH₂- of PNb). ¹³C NMR (133 MHz, CDCl₃) δ 177.2, 176.1 (C=O of PNb), 169.4 (C=O of PLA), 68.8 (-CH of PLA), 51.4, 49.1 (COOCH₃ of PNb), 46.7, 44.4, 40.2, 39.0, 36.2, 36.0, 34.7, 34.4 (other -CH and -CH₂- of PNb), 16.5 (-CH₃ PLA).

5.3. Results and Discussion

5.3.1 PNb-*bl*-PLA Diblock Copolymer Synthesis and Hydrogenation

PNb-*bl*-PLA diblock copolymers were prepared by the ring-opening polymerization of lactide using a hydroxyl-terminated PNb macroinitiator and stannous octoate (SnOct₂) as the catalyst, Figure 5.2. An equimolar amount of lactide monomer to

PNb repeat unit was added, and the solution polymerization in benzene was generally allowed to proceed for 2 d. The diblock copolymers were separated from the unreacted monomer by precipitation into methanol. The absence of monomer was demonstrated by ^1H NMR spectroscopy, which showed the disappearance of peaks at ~ 5.0 ppm and ~ 1.7 ppm corresponding to the lactide monomer. The polymerization of lactide was confirmed by the appearance of two additional peaks at 5.1 and 1.6 ppm (Figure 5.3B, peaks *f* and *g*) from the PLA. The copolymer structure was also verified by ^{13}C NMR spectroscopy by the appearance of peaks at 169.5, 68.9, and 16.6 ppm from the PLA block. By varying the chain length of the PNb macroinitiator and the reaction time, several diblock copolymer compositions were obtained, Table 5.2.

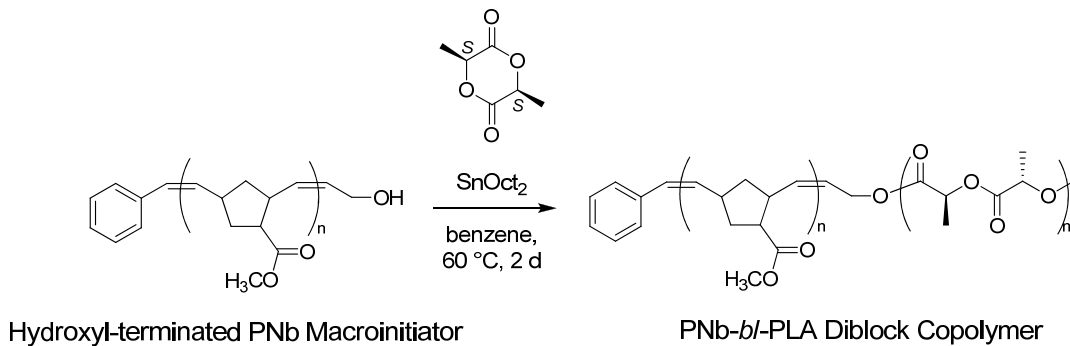


Figure 5.2. Synthesis of PNb-*bl*-PLA Diblock Copolymers.

The PNb backbone of one particular sample was hydrogenated over $\text{Pd}(\text{OH})_2$ (50 PSI of H_2 in a 4:1 (v:v) mixture of EtOAc and CH_2Cl_2) to give a hydrogenated PNb-*bl*-PLA copolymer, h-PNb-*bl*-PLA Figure 5.4. Complete conversion was shown by the disappearance of the peak corresponding to the vinylic protons in the ^1H NMR spectrum of the PNb block (Figure 5.3B, protons *a*) and appearance of a new signal for the protons

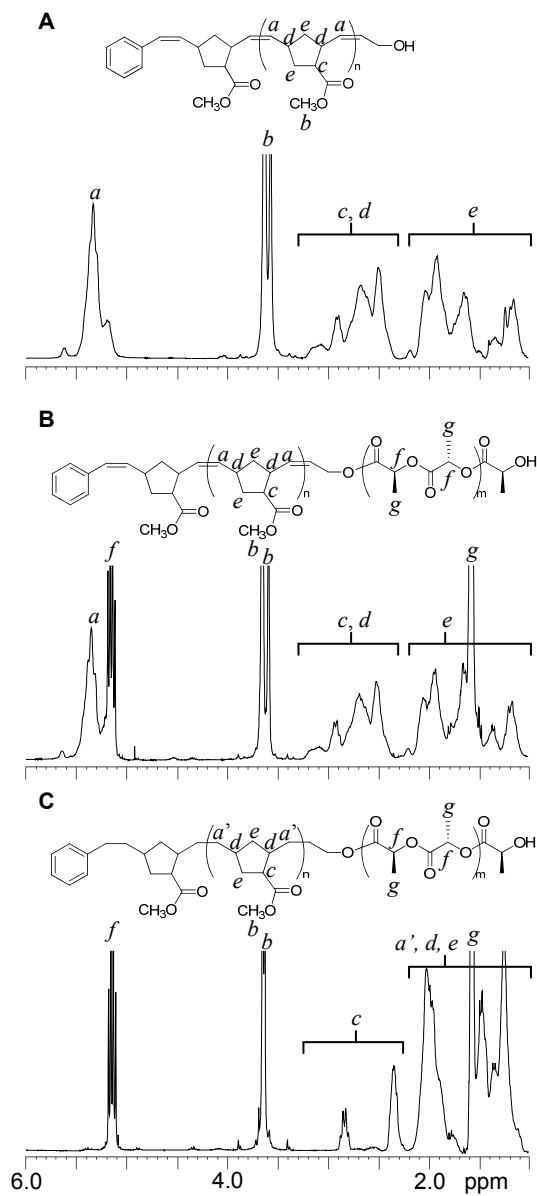


Figure 5.3. ^1H NMR spectra of macroinitiator and copolymers: A, hydroxyl-terminated PNB; B, PNB-*bl*-PLA diblock copolymer; C, Hydrogenated PNB-*bl*-PLA.

of the ethylene (-CH₂CH₂-) units (Figure 5.3C, protons *a'*). An upfield shift of protons *d* was also observed upon hydrogenation. The hydrogenation of the PNb block was also shown by ¹³C NMR spectroscopy which showed the complete disappearance of the alkene carbons near 134 ppm.

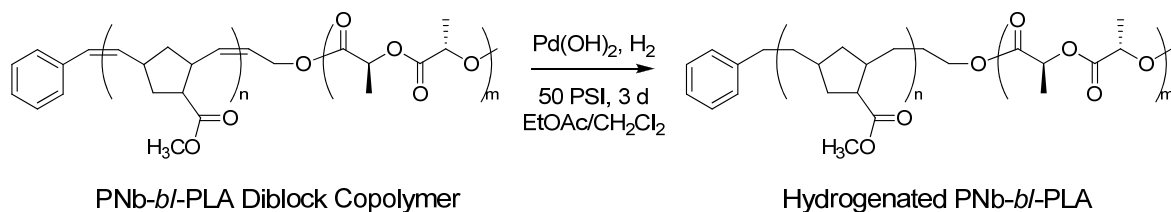


Figure 5.4. Hydrogenolysis of PNb-*bI*-PLA.

Table 5.2. Copolymer Characterization Data^{a,b}

Block Copolymer	<i>M_n</i> (g/mol) (¹ H NMR)	<i>M_n</i> (g/mol) (SEC)	<i>M_w</i> (g/mol) (SEC)	PDI (SEC)	<i>M_n</i> (g/mol) (after DSC)	<i>M_w</i> (g/mol) (after DSC)	PDI (after DSC)
PNb ₁₈₀ -PLA ₂₃	30 800	37 000	41 700	1.13	32 400	41 800	1.29
50 mol% PNb ₁₈₀ -PLA ₄₅ + 50 mol% PLA ₄₅	34 000	23 400	45 700	1.95	19 000	41 100	2.16
75 mol% PNb ₁₈₀ -PLA ₉₃ + 25 mol% PLA ₉₃	41 700	45 800	53 500	1.17	41 300	51 000	1.24
PNb ₁₈₀ -PLA ₉₉	41 700	45 800	53 500	1.17	41 000	51 000	1.24
75 mol% PNb ₁₈₀ -PLA ₁₅₇ + 25 mol% PLA ₁₅₇	50 000	58 200	75 000	1.29	38 000	56 400	1.48
PNb ₁₂₂ -PLA ₉₉	33 000	44 600	51 400	1.15	39 100	47 300	1.2
83 mol% PNb ₁₂₉ -PLA ₉₃ + 17 mol% PLA ₉₃	33 000	47 400	72 500	1.52	/	/	/
83 mol% h-PNb ₁₂₉ -PLA ₉₃ + 17 mol% PLA ₉₃	33 000	38 600	68 500	1.77	/	/	/

^a Characterization data from Alexander Norman

^b GPCs in THF with poly(styrene) standards

The composition of the PNb-PLA diblock copolymers was determined by end group analysis by ¹H NMR by comparison of the alkene protons adjacent to the phenyl

end group of the PNb chain (Figure 5.5B, protons *h*), the methylene protons adjacent to the hydroxyl initiator of the polynorbornene (protons *i* ') and the end group of the PLA chain (protons *j*). By dividing the end group protons by those of the repeat unit for the PNb and PLA chains, the DP for each block was calculated and used to estimate the molecular weight. In most cases, the ratio of protons *h* : *i* ' : *j* showed good agreement (a ratio of 2:2:1) within the error associated with the integration of the small end group peaks (10 % of the integral value). However, in some samples, there was an excess of the PLA end group proton *j* relative to protons *h* and *i* ' of the PNb. This was attributed to the presence of PLA homopolymer in the sample arising from trace amounts of water in the reaction acting as initiator. Therefore, based on the assumption that the PLA homopolymer has the same DP as the PLA block of the PNb-*bl*-PLA copolymer, the relative amount of PLA homopolymer was calculated (Table 5.3).

Table 5.3. PLA Homopolymer Data

Block Copolymer	mol % homoPLA ^a
PNb ₁₈₀ -PLA ₂₃	0
PNb ₁₈₀ -PLA ₄₅	50
PNb ₁₈₀ -PLA ₉₃	25
PNb ₁₈₀ -PLA ₉₉	0
PNb ₁₈₀ -PLA ₁₅₇	25
PNb ₁₂₂ -PLA ₉₉	0
PNb ₁₂₉ -PLA ₉₃	17
h-PNb ₁₂₉ -PLA ₉₃	17

^a Calculated using ¹H NMR spectroscopy

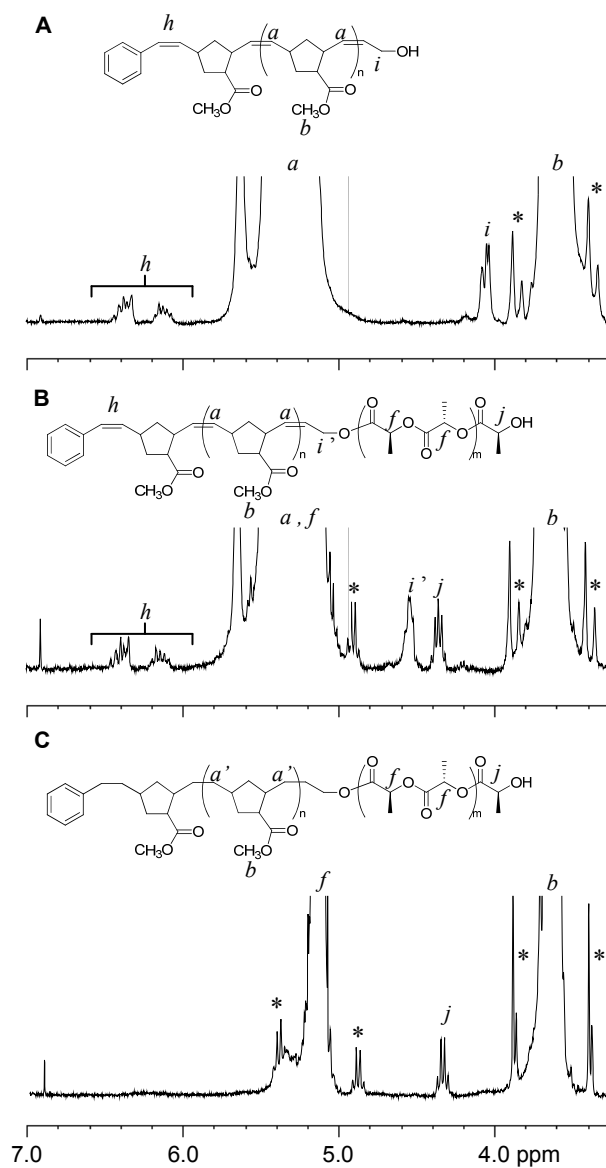


Figure 5.5. ^1H NMR spectra showing the end groups of: A, hydroxyl-terminated PNb; B, PNb-*bl*-PLA diblock copolymer; C, Hydrogenated PNb-*bl*-PLA. *Spinning sidebands

5.3.2. Thermal Properties of PNB-bl-PLA

The T_g , T_c and T_m of the diblocks were determined using DSC, Table 5.4. Very little difference was observed in the thermal properties of the compositions: The T_g and T_m were similar to those found in the literature for PLA homopolymer (T_g and T_m values from various sources: 55, 170 °C¹⁸ ; 57, 169 °C¹⁹). PNB is generally completely amorphous and displays a T_g near 35 °C.^{20,21} Though no evidence for phase separation was observed (such as the observance of two T_g or T_m) we did not rule out the possibility due to the similar T_g of PLA and PNB which might be overlapping in the thermogram and the amorphous behavior of PNB which would prevent the appearance of a second T_m .

Hydrogenolysis of the PNB₁₂₉-PLA₉₃ sample to give h-PNB₁₂₉-PLA₉₃ resulted in a decrease of the T_g to 45 °C and a decrease in the T_m to 149 °C. This value is similar to melting temperatures found in the literature for hydrogenated PNB homopolymers (143 °C²², 141 °C²¹) and is attributed to the formation of a crystalline material upon saturation of the PNB backbone.

The molecular weight of the copolymer compositions were characterized by SEC before and after the first DSC thermal cycle, Table 5.2. This analysis indicates that there is very little degradation to the polymer backbone upon heating (M_n and M_w decrease by less than 20 %), which is important if we are to study the interplay of temperature and morphology of the polymer.

Table 5.4. Thermal Analysis of Copolymers^a

Block Copolymer	T_g (°C)	T_c (°C)	T_m (°C)
PNb ₁₈₀ -PLA ₂₃	59	Not observed	157
50 mol% PNb ₁₈₀ -PLA ₄₅ + 50 mol% PLA ₄₅	Not observed	Not observed	159
75 mol% PNb ₁₈₀ -PLA ₉₃ + 25 mol% PLA ₉₃	58	102	155
PNb ₁₈₀ -PLA ₉₉	60	107	150
75 mol% PNb ₁₈₀ -PLA ₁₅₇ + 25 mol% PLA ₁₅₇	62	Not observed	162
PNb ₁₂₂ -PLA ₉₉	59	112	159
83 mol% PNb ₁₂₉ -PLA ₉₃ + 17 mol% PLA ₉₃	57	109	152
83 mol% h-PNb ₁₂₉ - PLA ₉₃ + 17 mol% PLA ₉₃	45	100	149

^a Characterization data from Alexander Norman

5.3.3. Diblock Copolymer Morphology

The microphase separation of the PNb₁₂₉-PLA₉₃ composition was studied using small-angle x-ray scattering (SAXS) and wide-angle x-ray diffraction (WAXD) by Dr. Alexander Norman of New York University. The SAXS profile (Figure 5.6A) shows a peak which becomes more pronounced as the sample is heated (up to about 130 °C). This was attributed to the crystallization of the PLA block upon heating, which was also confirmed by the presence a cold crystallization peak in the DSC trace. It is expected that this crystallization results in enhanced microphase separation, which is supported by the preservation of the domain spacing (Figure 5.6B). As the temperature is further increased above the T_m , the intensity of the peak (Figure 5.6A) continues to decrease, but is still present even at higher temperatures. Also, a decrease in the domain spacing (d-spacing) occurs as the sample melts (Figure 5.6B), but the sample still shows order even at

temperatures of 180 °C. Both of these results serve as evidence for phase separation even after the material has melted.

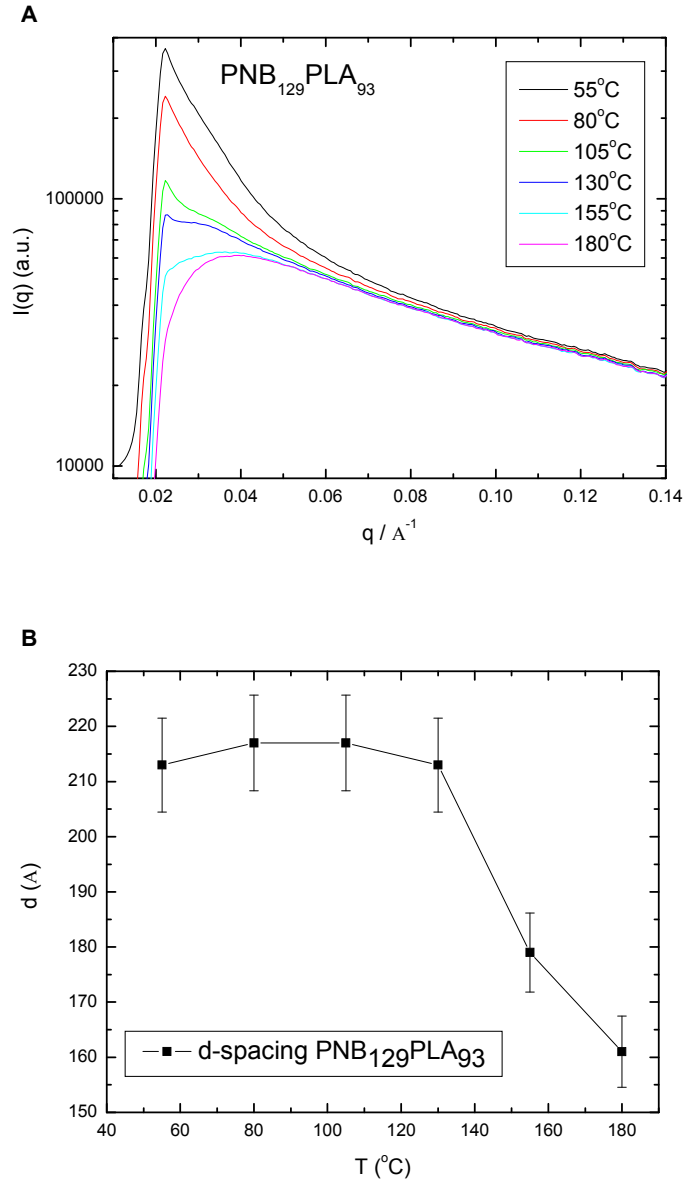


Figure 5.6. SAXS profile: A, Intensity as a function of scattering vector q ; B, Domain spacing as a function of temperature [Data from Alexander Norman, Department of Chemistry, NYU].

WAXD further confirmed the crystallization of the sample upon heating by the appearance of sharp Bragg peaks which disappear as the sample is heated above the T_m , as shown in the powder diffraction patterns (Figure 5.7A) and the 1D meridional integration of the WAXD profile (Figure 5.7B).

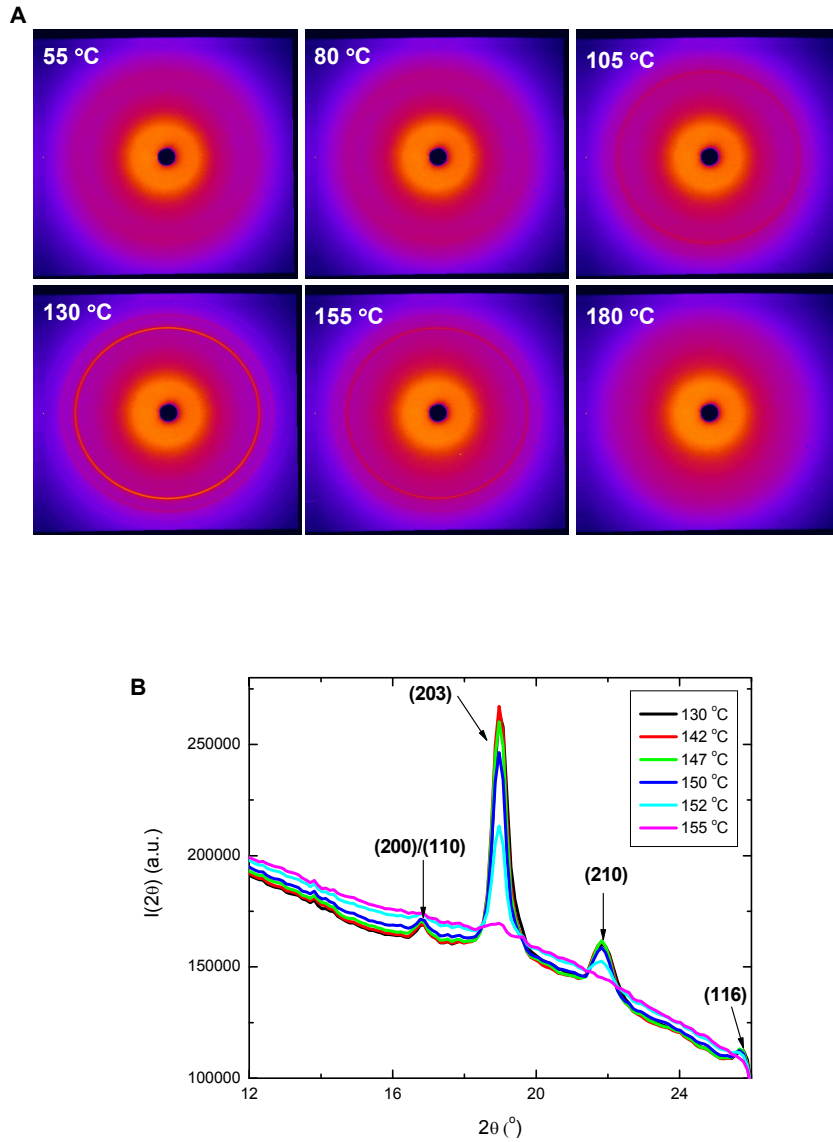


Figure 5.7. WAXD 2D (A) and 1D (B) patterns of PNB₁₂₉-PLA₉₃ at various temperatures

[Data from Alexander Norman, Department of Chemistry, NYU].

5.4. Conclusions

Novel PNB-*bl*-PLA Diblock copolymers were synthesized by the ring-opening polymerization of lactide monomer using hydroxyl-terminated PNB macroinitiators. The thermal properties of the copolymers were studied along with the morphological properties of one particular copolymer composition. SAXS and WAXD showed evidence for the crystallization and phase separation of the copolymer upon heating. The ability of this material to phase separate could ultimately be used in applications ranging from the fabrication of PNB-*bl*-PLA foams with enhanced mechanical properties to the preparation of ordered nanoporous monoliths.

5.5. References

- (1) Nandan, B.; Hsu, J. Y.; Chen, H. L., *Polym. Rev.* **2006**, *46*, 143-172.
- (2) Zalusky, A. S.; Olayo-Valles, R.; Wolf, J. H.; Hillmyer, M. A., *J. Am. Chem. Soc.* **2002**, *124*, 12761-12773.
- (3) Abetz, V.; Simon, P. F. W., *Adv. Polym. Sci.* **2005**, *189*, 125-212.
- (4) Lodge, T. P., *Macromol. Chem. Phys.* **2003**, *204*, 265-273.
- (5) Guo, S. W.; Rzayev, J.; Bailey, T. S.; Zalusky, A. S.; Olayo-Valles, R.; Hillmyer, M. A., *Chem. Mater.* **2006**, *18*, 1719-1721.
- (6) Cordewener, F. W.; Schmitz, J. P., *Tissue Eng.* **2000**, *6*, 413-424.
- (7) Hasirci, V.; Lewandrowski, K. U.; Bondre, S. P.; Gresser, J. D.; Trantolo, D. J.; Wise, D. L., *Biomed. Mater. Eng.* **2000**, *10*, 19-29.
- (8) Tormala, P.; Vasenius, J.; Vainionpaa, S.; Laiho, J.; Pohjonen, T.; Rokkanen, P., *J. Biomed. Mater. Res.* **1991**, *25*, 1-22.

- (9) Xi, J.; Zhang, L.; Zheng, Z. H.; Chen, G. Q.; Gong, Y. D.; Zhao, N. M.; Zhang, X. F., *J. Biomater. Appl.* **2008**, *22*, 293-307.
- (10) Thomson, R. C.; Yaszemski, M. J.; Powers, J. M.; Mikos, A. G., *Biomaterials* **1998**, *19*, 1935-1943.
- (11) Helen, W.; Merry, C. L. R.; Blaker, J. J.; Gough, J. E., *Biomaterials* **2007**, *28*, 2010-2020.
- (12) Blaker, J. J.; Gough, J. E.; Maquet, V.; Notingher, I.; Boccaccini, A. R., *J. Biomed. Mater. Res., Part A* **2003**, *67A*, 1401-1411.
- (13) Zhang, L.; Jeon, H. K.; Malsam, J.; Herrington, R.; Macosko, C. W., *Polymer* **2007**, *48*, 6656-6667.
- (14) Stelzer, F.; Grubbs, R. H.; Leising, G., *Polymer* **1991**, *32*, 1851-6.
- (15) Bielawski, C. W.; Benitez, D.; Morita, T.; Grubbs, R. H., *Macromolecules* **2001**, *34*, 8610-8618.
- (16) Weiss, R. A.; Izzo, E.; Mandelbaum, S., *Macromolecules* **2008**, *41*, 2978-2980.
- (17) Wang, Y.; Noga, D. E.; Yoon, K.; Wojtowicz, A. M.; Lin, A. S. P.; García, A. J.; Collard, D. M.; Weck, M., *Adv. Funct. Mater.* **2008**, in submission.
- (18) Radano, C. P.; Baker, G. L.; Smith, M. R., *J. Am. Chem. Soc.* **2000**, *122*, 1552-1553.
- (19) Park, J. W.; Lee, D. J.; Yoo, E. S.; Im, S. S.; Kim, S. H.; Kim, Y. H., *Korea Polymer Journal* **1999**, *7*, 93-101.
- (20) Hatjopoulos, J. D.; Register, R. A., *Macromolecules* **2005**, *38*, 10320-10322.
- (21) Cataldo, F., *Polym. Int.* **1994**, *34*, 49-57.
- (22) Lee, L. B. W.; Register, R. A., *Macromolecules* **2005**, *38*, 1216-1222.

CHAPTER 6

SUGGESTIONS FOR FUTURE STUDY

6.1. Functionalized Hydrogenated PNB-*bl*-PLA Foams for Tissue Engineering

In Chapter 3, the attachment of biological ligands to succinic anhydride modified PLA copolymer films was explored. In Chapter 4, photocrosslinkable PLA copolymer scaffolds were foamed using TIPS to give highly porous polymer structures which showed improved mechanical strength upon crosslinking. Future challenges include combining what we have learned regarding the biological modification of functional PLA films and the strengthening of polymer foams through crosslinking or diblock

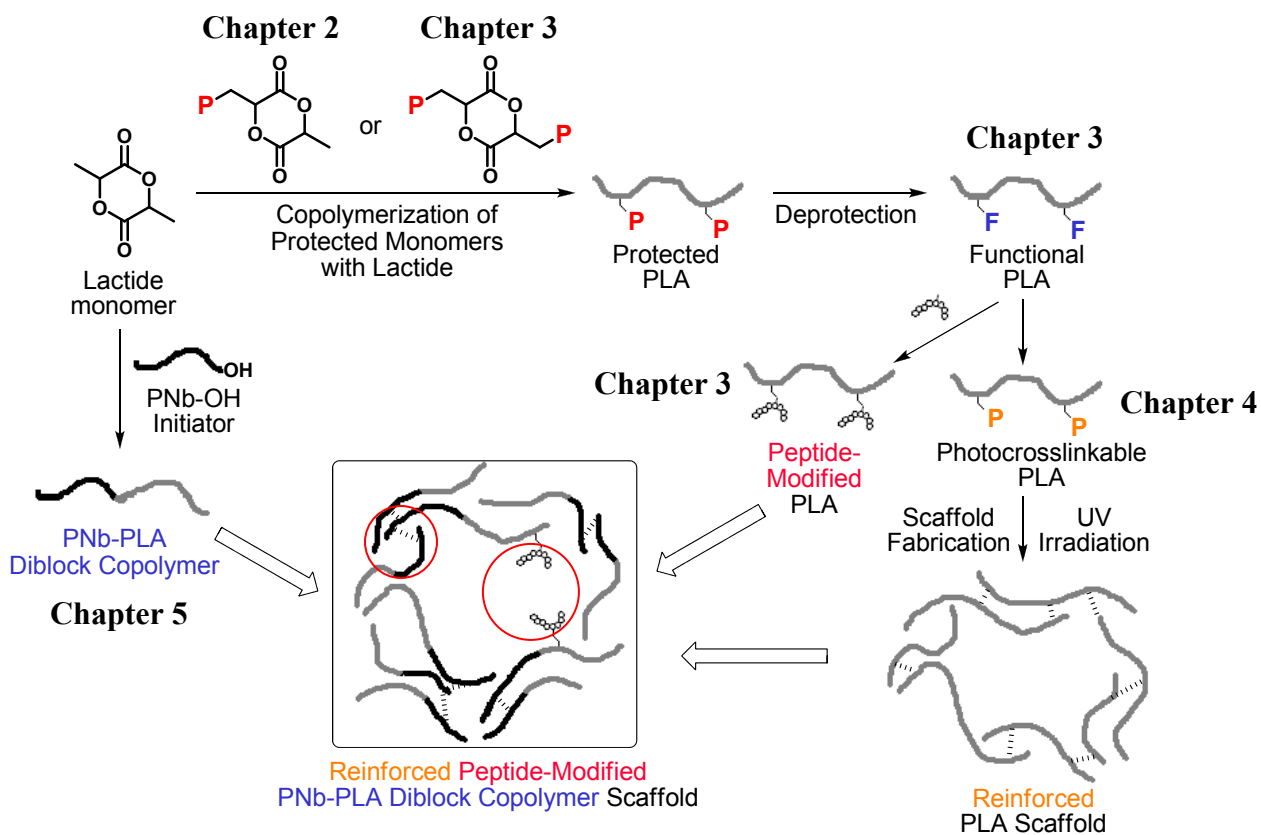


Figure 6.1. The fabrication of robust, peptide-modified diblock copolymer foams.

incorporation to provide polymer scaffolds with superior mechanical and biological properties, Figure 6.1.

Such materials could be easily fabricated by building on techniques from our previous work, Figure 6.2. A protected functional PNB-*bl*-PLA diblock could easily be synthesized by the copolymerization of dibenzyloxy-substituted lactide (Chap. 3) and lactide using a hydroxyl-terminated PNB initiator (Chap. 4). Deprotection, followed by modification with succinic anhydride could lead to a hydrogenated PNB-*bl*-PLA diblock copolymer with carboxylic acid functional groups located along the backbone of the PLA block. This material has the potential to phase separate during foaming for added stability and has pendant carboxyl groups which can be modified with peptides to control cellular interactions.

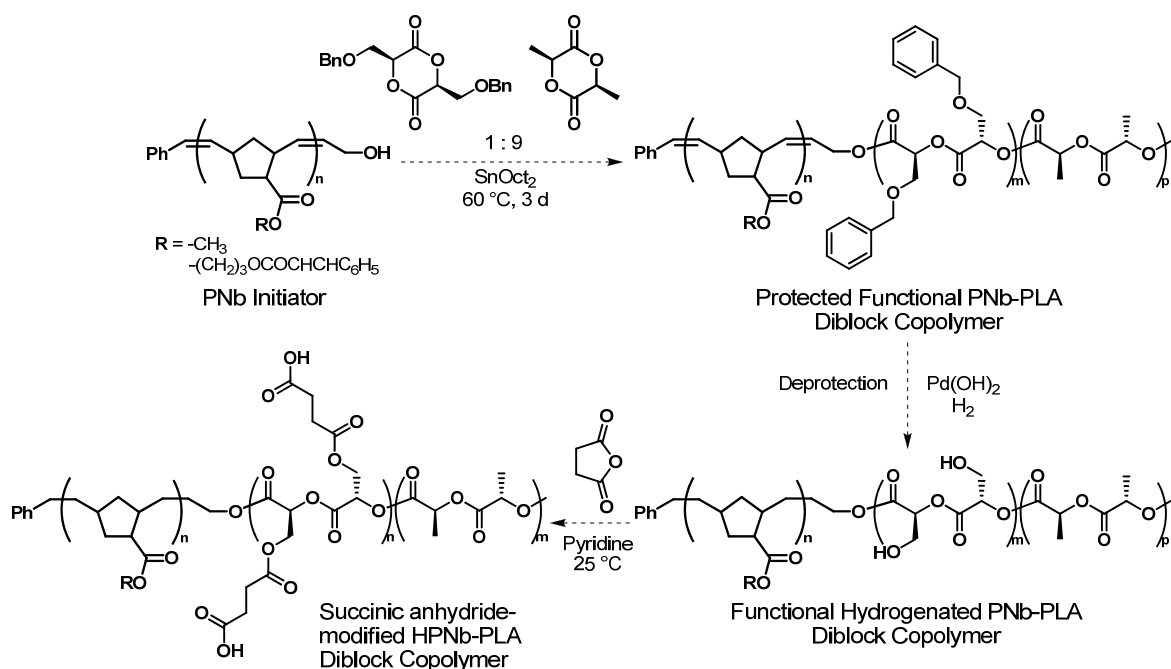


Figure 6.2. The synthesis of functional h-PNB-*bl*-PLA.

Preliminary experiments on the attachment of peptide to porous PLA scaffolds could be carried out using the succinic anhydride-modified functional PLA copolymer without the PNb block for the sake of simplicity. The copolymer would have to first be foamed using TIPS, and the conditions would have to be optimized to provide a material with pore sized suitable for cell migration (>50 μm). Efforts would then focus on developing methods where a peptide/EDC solution could effectively permeate and subsequently be removed from the foams prior to exposure to cells. In the same way, solutions containing cells would have to be able to penetrate the foams, and at the end of the experiment, unattached cells would ultimately have to be removed in order to determine the effect of the peptide on cell adhesion. The complexity of such a task (where variables such as the pore size, type of peptide, and type of cells used all play a role¹) compounded by its lack of precedence in the literature may seem futile. However the wealth of information acquired through the exploration of such a material warrants further investigation.

6.2. Functionalized PLA Copolymers for Drug Delivery

Besides the field of tissue engineering, PLA also show promise for use in drug delivery applications due to its biocompatible and degradable properties.² A variety of factors can affect the drug release behavior of PLA including the molecular weight, crystallinity, and the T_g of the polymer.³ However, even after optimizing the aforementioned conditions, drug release from a PLA matrix can be slow.⁴ Many methods focus on increasing rate of drug release through the addition of small molecules.⁵ Low molecular weight esters were added during the preparation of PLA films and resulted in a

decrease in the T_g and in increase in the degradation rate.⁶ Hydroxyesters such as diethyltartrate (DET) were added to PLA films which showed enhanced drug release relative to unmodified films. Molecular weight analysis of the PLA films with the added DET revealed that the increased rate of drug release was not due to increased hydrolysis from the hydroxyl functional groups of the DET. Further testing of the DET modified films showed that the enhanced degradation was caused by an increase in the amount of water uptake and the formation of open pored structure.

Another possible approach to modifying the drug release behavior of PLA which is not based on the addition of small molecules involves the modification of the side chains our functional PLA copolymers. We have already shown that incorporating pendant protected functional groups into PLA in high mol percentages (Chap.2) can be used to decrease the T_g of the copolymer. This should result in an increase in the degradation rate of the copolymer relative to PLA homopolymer.⁶ Directly attaching various hydrophobic or hydrophilic groups to the functional side chains could also be used as a means to alter the rate of degradation of PLA. For example, incorporation of hydrophobic side chains into the copolymer could lead to phase separation during film formation and enhanced loading and release of hydrophobic drugs.⁵ On the other hand, incorporation of a hydrophilic segment, such as a poly(ethylene glycol) oligomer or a ring-opened sugar could result in an increase in the water uptake and degradation rate.³

We have previously shown (Chap. 4) that the photocrosslinking of PLA scaffolds led to a decrease in the rate of hydrolytic degradation. Such effects should carry over to polymer films, which could be loaded with drugs and used in the development of long-term drug delivery materials or hydrogel applications.⁷ The photocrosslinking of PLA

films might also be used to prevent the initial burst of excess drug from the surface that is often associated with implants.⁸

The fabrication of the aforementioned materials would require synthetic procedures which are mere extensions of work we have previously performed, and confirms the necessity for further exploration towards the advancement of these materials for use in future biomedical applications.

6.3. References

- (1) Shin, K. C.; Kim, B. S.; Kim, J. H.; Park, T. G.; Do Nam, J.; Lee, D. S., *Polymer* **2005**, *46*, 3801-3808.
- (2) Mehta, R.; Kumar, V.; Bhunia, H.; Upadhyay, S. N., *J. Macromol. Sci., Polym. Rev.* **2005**, *C45*, 325-349.
- (3) Mochizuki, A.; Niikawa, T.; Omura, I.; Yamashita, S., *J. Appl. Polym. Sci.* **2008**, *108*, 3353-3360.
- (4) Sharkawi, T.; Leyni-Barbaz, D.; Chikh, N.; McMullen, J. N., *J. Bioact. Compat. Pol.* **2005**, *20*, 153-168.
- (5) Kakinoki, S.; Yasuda, C.; Kaetsu, I.; Uchida, K.; Yukutake, K.; Nakayama, M.; Fujiie, S.; Kuroda, D.; Kato, M.; Ohyanagi, H., *Eur. J. Pharm. Biopharm.* **2003**, *55*, 155-160.
- (6) Labrecque, L. V.; Kumar, R. A.; Dave, V.; Gross, R. A.; McCarthy, S. P., *J. Appl. Polym. Sci.* **1997**, *66*, 1507-1513.
- (7) John, G.; Morita, M., *Macromolecules* **1999**, *32*, 1853-1858.

- (8) Grayson, A. C. R.; Voskerician, G.; Lynn, A.; Anderson, J. M.; Cima, M. J.; Langer, R., *J. Biomater. Sci., Polym. Ed.* **2004**, *15*, 1281-1304.

APPENDIX A

**KINETIC STUDIES ON THE RING-OPENING POLYMERIZATION OF
SUBSTITUTED LACTIDES**

A.1. Introduction

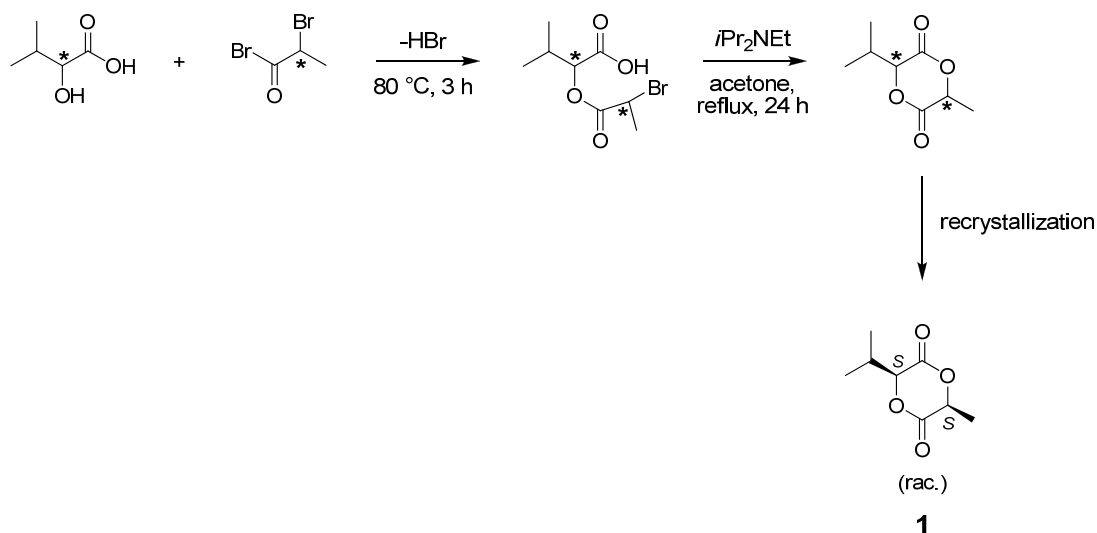
The copolymerization of substituted lactides with lactide monomer has proved to be a facile method to altering the properties of PLA.¹ However, issues concerning the slower reactivity of monomers with bulky substituents relative to lactide prompted us to initiate an investigation of the relative rates of ring-opening polymerization of substituted lactides.^{2,3} We set out to synthesize an isopropyl-substituted monomer and study the effect of the bulky isopropyl substituent on the polymerization kinetics. Our initial goal was not necessarily to quantitatively determine the rate constant or relative reactivity ratio of the monomer, but instead gain a general understanding of the role of the isopropyl-substituent in the coordination-insertion mechanism of the stannous octanoate catalyst and the subsequent ring-opening of the monomer. The polymerization was monitored using ¹H NMR spectroscopy. Analysis of end groups by ¹H NMR as the reaction proceeded allowed us to gain some insight to which carbonyl of the cyclic ester monomer the catalyst of the propagating chain end preferentially coordinated and inserted. Future work involving the synthesis of model compounds which resembled the active chain ends present during the polymerization was initially proposed in order to support the results obtained from the polymer end group analysis. However, a sudden surge of interest in the area^{4,5} led us to ultimately abandon our study and shift our attention from substituted lactides to protected functional lactides (Chp.2).

A.2. Experimental

A.2.1. General Methods

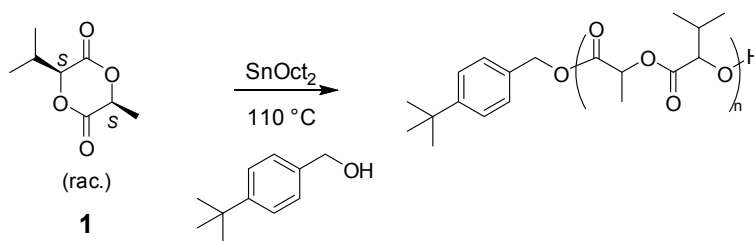
2-Hydroxy-3-methylbutyric acid (product # 219835-5G) and 2-bromopropionyl bromide (product #249785-100G) were purchased from Aldrich and used as received. *N*-ethyl-diisopropylamine (product # A11801) was obtained from Alfa Aesar and used without further purification. Stannous octanoate (SnOct_2) (product # 287172-250G) and 4-*tert*-butylbenzyl alcohol (BBA) (product # 184268) were purchased from Aldrich and the SnOct_2 was distilled prior to use. $^1\text{H-NMR}$ spectra were recorded at 298 K on a Varian Mercury spectrometer (300 MHz).

A.2.2. Synthesis of Isopropyl-substituted Lactide Monomer



A.2.2.1. 3-Methyl-6-isopropyl-1,4-dioxane-2,5-dione (1). Compound **1** was prepared as previously reported in the literature.⁴ 2-Hydroxy-3-methylbutyric acid (10 g, 85 mmol) and 2-bromopropionyl bromide (10 mL, 95 mmol) were stirred for 3 h at 80 °C. The reaction mixture was then dissolved in 200 mL of dry acetone and added dropwise to a solution of *N*-ethyldiisopropylamine (30 mL, 170 mmol) in refluxing acetone (100 mL) over a period of 6 hours, after which the reaction was allowed to proceed overnight. The ethyldiisopropylammonium salt was removed from the mixture by filtration, and the solvent was removed. The mixture was re-dissolved in dichloromethane (20 mL), washed with H₂O (3 × 100 mL), dried over MgSO₄, and the solvent was removed. The resulting oil was recrystallized from Et₂O (20 mL) to give a racemic mixture of **1** as a white crystalline solid (5.2 g, 36%). The spectra of the product matched published data.⁴

A.2.3. Polymerization of Isopropyl-substituted Lactide Monomer



A.2.3.1. Homopolymerization of Monomer 1. Isopropyl-substituted lactide **1** (0.1978 g, 1.15 mmol) and SnOct₂ catalyst (50 μ L of a 0.34 M solution in toluene; 1.5 mol % to monomer) were added to a dry flask and heated to 110 °C. 4-*tert*-butylbenzyl alcohol (BBA) initiator (50 μ L of a 1.52 M solution in toluene; 0.076 mmol; M:I ratio of 15:1) was added, and the timing of the reaction began. At selected intervals, an aliquot was quickly removed, placed in a vial, and dissolved in deuterated chloroform for ¹H NMR end group analysis.

A.3. Results and Discussion

A.3.1. Isopropyl-substituted Lactide Preparation

Monomer **1** was synthesized by the reaction of 2-hydroxy-3-methylbutyric acid with 2-bromopropionyl bromide, Figure A.1. The initial reaction of the hydroxyl group of the hydroxy acid with the acyl bromide was quick, taking only 3 h for the hydroxy acid to be consumed as determined using ^1H NMR analysis. In the following step, the intermediate was slowly added dropwise to a solution of *N*-ethyl-diisopropyl amine to promote the formation of cyclized product rather than linear oligomer. Ring closure under basic conditions followed by selective recrystallization afforded a single set of enantiomers (*S,S* and *R,R* as determined using x-ray crystallography) with reasonable yields (36 %) considering the nature of the reaction and the potential formation of linear oligomers.

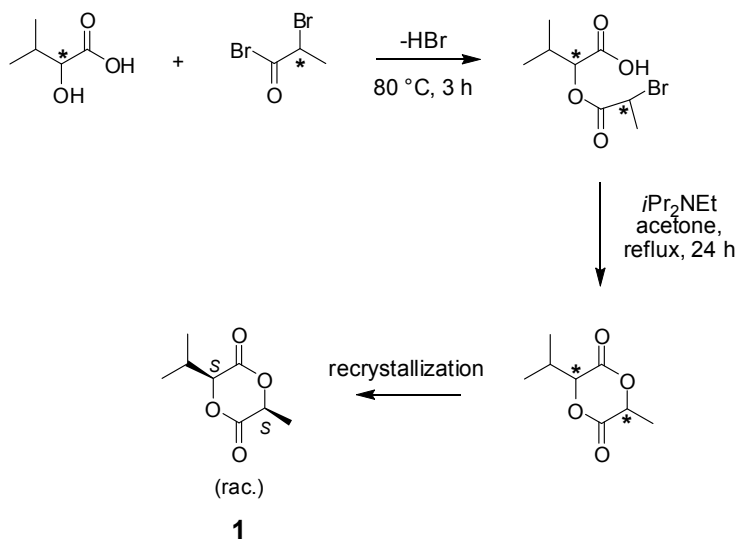


Figure A.1. Synthesis of monomer **1**.

A.3.2. Polymerization of Isopropyl-substituted Lactide

The bulk polymerization of monomer **1** was carried out using stannous octanoate as the catalyst and *t*-butyl benzyl alcohol as the initiator. The polymerization was carried out at 110 °C to facilitate the rapid ring-opening of the substituted lactide within a reasonable amount of time. At various times, an aliquot was removed from the polymerization mixture and dissolved in deuterated chloroform for ¹H NMR analysis.

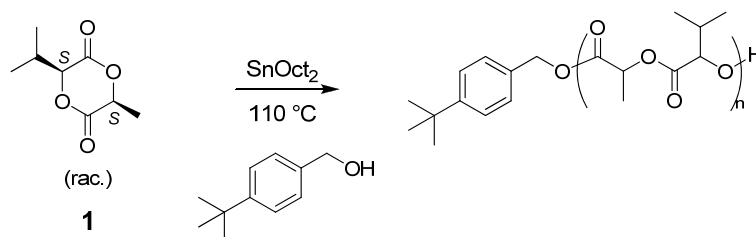


Figure A.2. Polymerization of monomer **1** with SnOct₂ catalyst and BBA initiator.

The ratio of isopropyl and methyl end groups (*i*-Pr_{eg}:Me_{eg}) was monitored as a function of time using ¹H NMR spectroscopy (Figure A.3) in an attempt to gain insight into the relative reactivity of the esters of the alkyl-substituted monomer and the two types of chain ends, Figure A.4. The kinetics of the polymerization are described by rate constants k_1 , k_2 , k_3 and k_4 , Figure A.4.

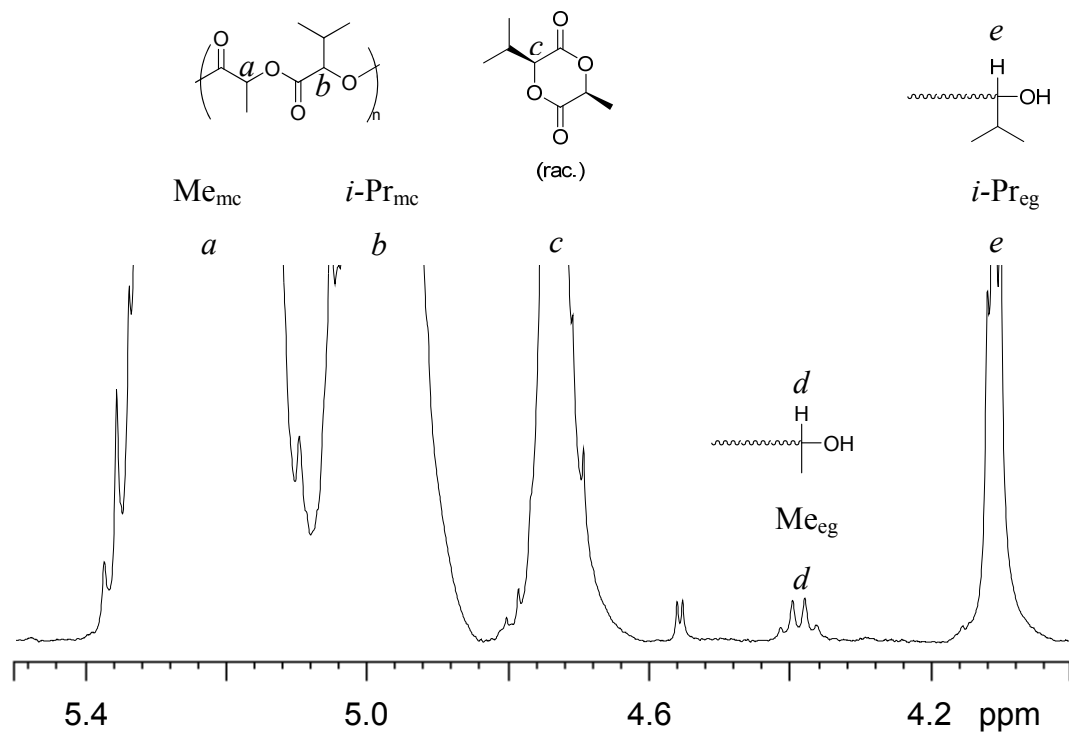


Figure A.3. Representative ^1H NMR spectrum used for end group analysis.

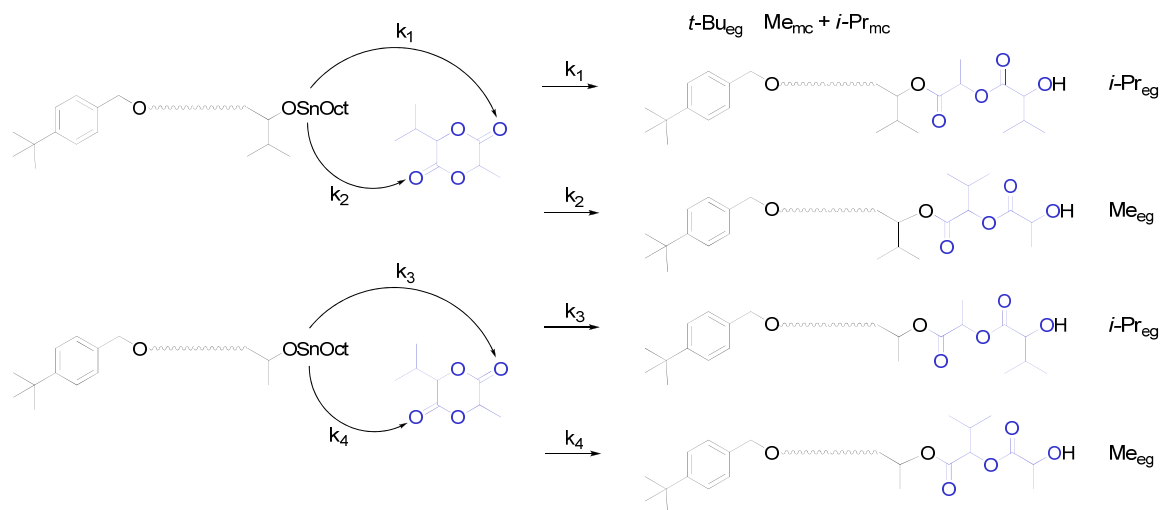


Figure A.4. The four possible chain propagations in the polymerization of **1**.

The relative amounts of methyl (Me_{mc}) and isopropyl ($i\text{-Pr}_{\text{mc}}$) repeat units of the main chain and the *t*-butyl end group ($t\text{-Bu}_{\text{eg}}$) were monitored by ^1H NMR spectroscopy. This allowed for calculation of the degree of polymerization (DP):

$$(1) \quad \text{DP} = \frac{[\text{Me}_{\text{mc}}] + [i - \text{Pr}_{\text{mc}}]}{[t - \text{Bu}_{\text{eg}}]}$$

Alternatively, comparing the rates of the main chain units and the isopropyl and methyl substituted alcohol end groups ($i\text{-Pr}_{\text{eg}}$, Me_{eg}) could also be used to calculate the DP:

$$(2) \quad \text{DP} = \frac{[\text{Me}_{\text{mc}}] + [i - \text{Pr}_{\text{mc}}]}{[\text{Me}_{\text{eg}}] + [i - \text{Pr}_{\text{eg}}]}$$

The ratio of monomer to initiator (M/I) was calculated by dividing the amount of monomer (and reacted polymer) by the amount of *t*-butyl end group. The M/I ratio was multiplied by the percent conversion for calculation of the DP:

$$(3) \quad \text{DP} = \frac{[\text{M}]}{[\text{I}]} \times \% \text{ conversion}$$

For the most part, the percent conversion increased with time (within the $\pm 2\%$ error associated with the ^1H NMR integration of the unconsumed monomer and polymer main chain peaks), Table A.1. The DP values show good agreement (within ± 2 repeat units due to error associated with the integration of the ^1H NMR peaks) except for

outliers at the beginning and end of the reaction. This indicates that residual water was sufficiently removed from the system. Initial experiments which were contaminated with trace amounts of water resulted in the formation of additional methyl and isopropyl end groups (compared to the *t*-butyl end groups). This is due to the ability of water to act as an initiator in a manner analogous to the *t*-butyl benzyl alcohol. Since the water produced extra methyl and isopropyl end groups, yet the amount of *t*-butylbenzyl initiator end groups remained unchanged, different values for the DP were obtained when using equations 1 and 2. The results cast doubt on previous works where the DP was calculated using only the *t*-butyl end group (eq. 2).

Table A.1. Degree of Polymerization and End Group Comparison

Time	% Conversion	DP ^a (<i>i</i> -Pr _{eg} + Me _{eg})	DP ^b (<i>t</i> -Bu _{eg})	DP ^c % Conversion*(M/I)	[<i>i</i> -Pr _{eg}] [Me _{eg}]
0.5 h	63	12	6	8	8.5
1 h	87	8	8	10	6.8
1.5 h	93	14	11	13	7.1
2 h	91	14	12	13	6
2.5 h	95	14	13	14	5.8
3 h	97	14	13	14	4.6
3.5 h	96	14	14	16	5.1
4 h	89	13	9	11	4.8

^a DP calculated from dividing the protons of the main chain repeat units by the isopropyl and methyl end groups of the polymer

^b DP calculated from the *t*-butyl end groups of the polymer

^c DP calculated from the % conversion multiplied by the M/I ratio

From the four possible chain propagations mechanisms (Figure A.4), k_1 and k_3 result in the formation of an isopropyl end group (*i*-Pr_{eg}) and k_2 and k_4 result in the formation of a methyl end group (Me_{eg}). By integrating the protons associated with the isopropyl and methyl end groups throughout the polymerization (Figure A.3), we can draw conclusions regarding the corresponding rate constants:

$$(4) \quad \frac{[k_1 + k_3]}{[k_2 + k_4]} = \frac{[i - \text{Pr}_{\text{eg}}]}{[\text{Me}_{\text{eg}}]}$$

The ratio of isopropyl: methyl end groups is approximately 8:1 throughout the early stages of the reaction (< 90 % conversion) which suggests that the SnOct₂ coordination-insertion catalyst shows preference toward coordinating with the carbonyl adjacent to the less sterically hindered methyl group of the monomer (k_1 , k_3) over the carbonyl adjacent to the bulky isopropyl group (k_2 , k_4). These results are consistent with similar experiments found in the literature involving the polymerization of mono- and di-substituted lactides, Figure A.5.⁵ It has been shown that if the methyl groups of lactide are replaced by groups which can provide a relatively greater amount of steric hindrance (such as isopropyl, cyclohexyl, or phenyl³ groups), this leads to a decrease in the reactivity of the monomer during ring-opening polymerization with stannous octanoate.

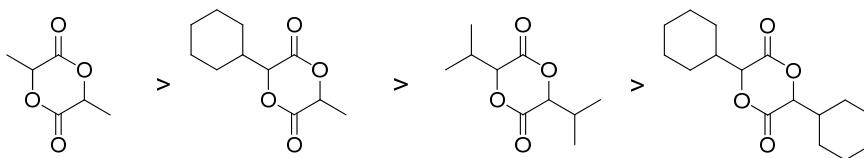


Figure A.5. Demonstration of decreasing reactivity (from left to right) as the bulkiness of the substituent increases.

The decrease of the isopropyl: methyl end group ratio towards the end of the reaction (>90%) could be attributed to competing depolymerization reactions involving the isopropyl and methyl substituted alcohol end groups. These depolymerization reactions, which proceed through a transesterification mechanism rather than the coordination-insertion propagation mechanism, perhaps favor the formation of an equal

ratio of isopropyl to methyl end groups and therefore result in a decrease in the isopropyl:methyl end group ratio as it tends towards a value of 1.

The reaction of model compounds which contain functional groups similar to the propagating chain ends offers a different approach to determine relative rates to gain insight into the kinetics of the polymerization reaction, Figure A.6. In order to explore the kinetics of how a propagating chain end adjacent to a methyl group attacks the monomer (Figure A.3; k_3 , k_4), an excess of commercially available 3-hydroxy-2-butanone **2** was combined with isopropyl-substituted lactide **1** and stannous octoate. The reaction mixture was heated at 110 °C for 10 min. The ^1H NMR spectrum showed an isopropyl:methyl end group ratio of approximately 2:1 ($k_3 > k_4$), confirming once again the coordination of the catalyst to the less sterically hindered carbonyl.

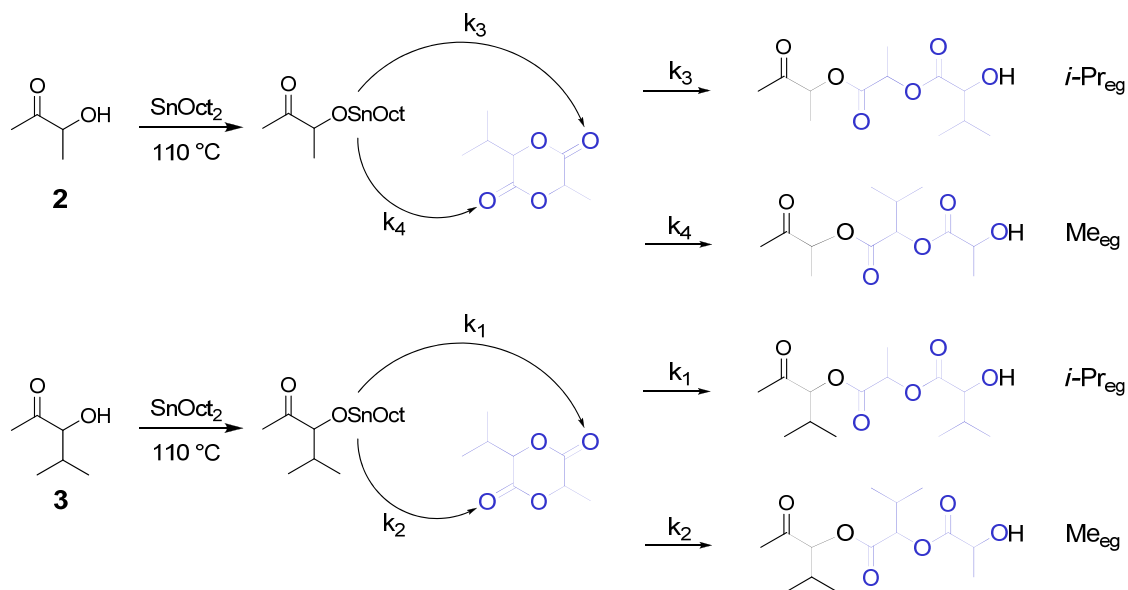


Figure A.6. Model compounds to explore the kinetics of the ring-opening of **1**.

4-Methyl-3-hydroxy-2-pentanone **3** (Figure A.5) would have been our choice to serve as a model for the isopropyl substituted chain ends (Figure A.3; k_1 , k_2). However,

the appearance of new work⁴ in the literature led us to focus instead on the synthesis of protected functional lactides (Chp.2).

A.4. Conclusions

An isopropyl-substituted lactide was synthesized and used to study the effect of the presence of bulky substituent on the ring-opening of the monomer. ¹H NMR end group analysis showed that the SnOct₂ catalyst preferred coordinating to the less sterically-hindered carbonyl, confirming that the presence of the bulky isopropyl groups does play a role in the polymerization kinetics.

A.5. References

- (1) Baker, G. L.; Vogel, E. B.; Smith, M. R., *Polym. Rev.* **2008**, *48*, 64-84.
- (2) Yin, M.; Baker, G. L., *Macromolecules* **1999**, *32*, 7711-7718.
- (3) Simmons, T. L.; Baker, G. L., *Biomacromolecules* **2001**, *2*, 658-663.
- (4) Trimaille, T.; Moeller, M.; Gurny, R., *J. Polym. Sci., Part A: Polym. Chem.* **2004**, *42*, 4379-4391.
- (5) Jing, F.; Smith, M. R.; Baker, G. L., *Macromolecules* **2007**, *40*, 9304-9312.

APPENDIX B

SPECTROSCOPIC CHARACTERIZATION OF SYNTHETIC PRODUCTS

^1H NMR spectra were recorded at room temperature using a Varian Mercury spectrometer (300 MHz), and the ^{13}C NMR spectra were obtained at 100 MHz using a Bruker AMX spectrometer. IR spectra were recorded on a Bruker Vector 22 spectrometer.

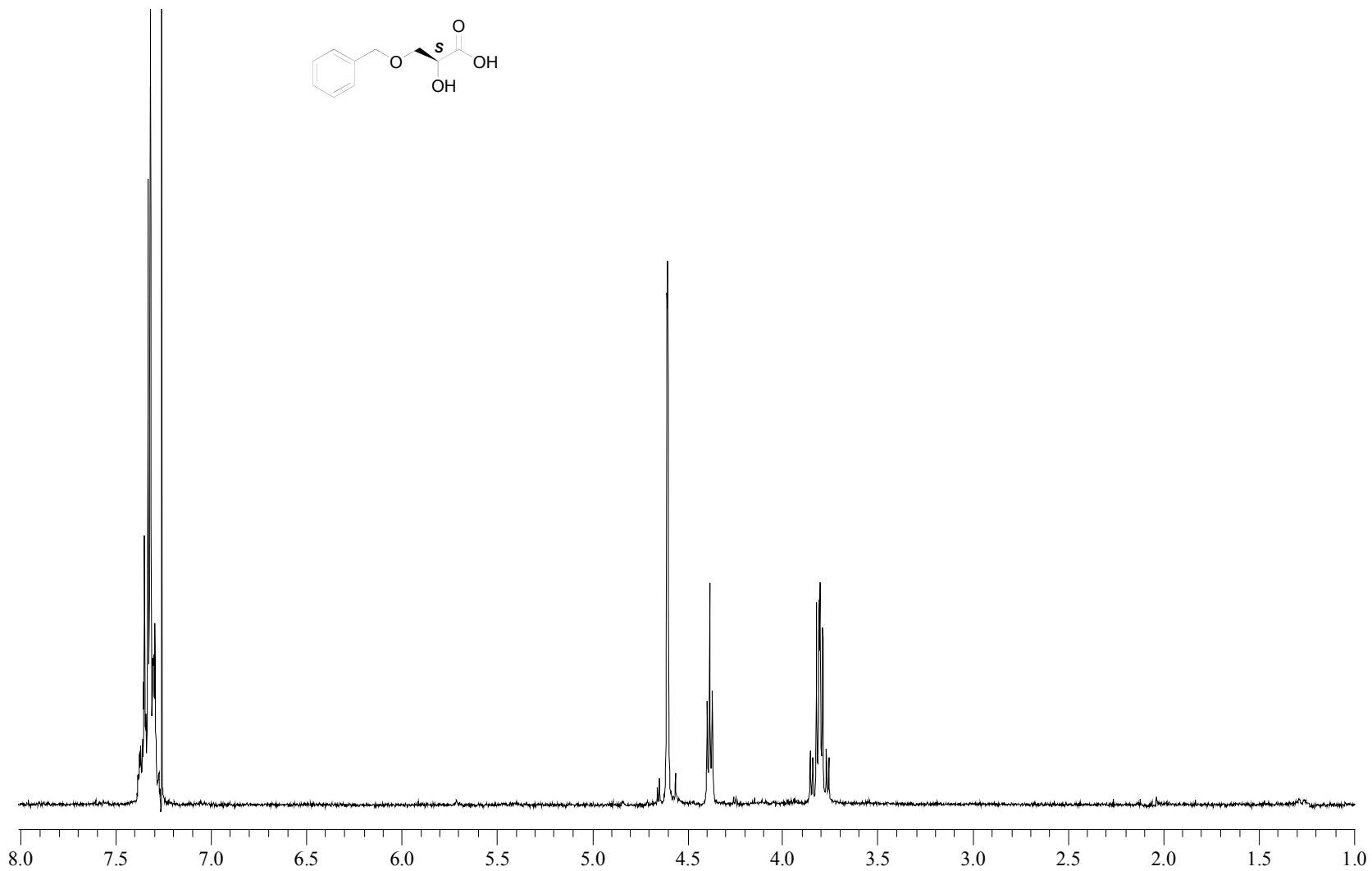


Figure B.1. ^1H NMR of 3-Benzyloxy-2-hydroxypropionic acid (**4**).

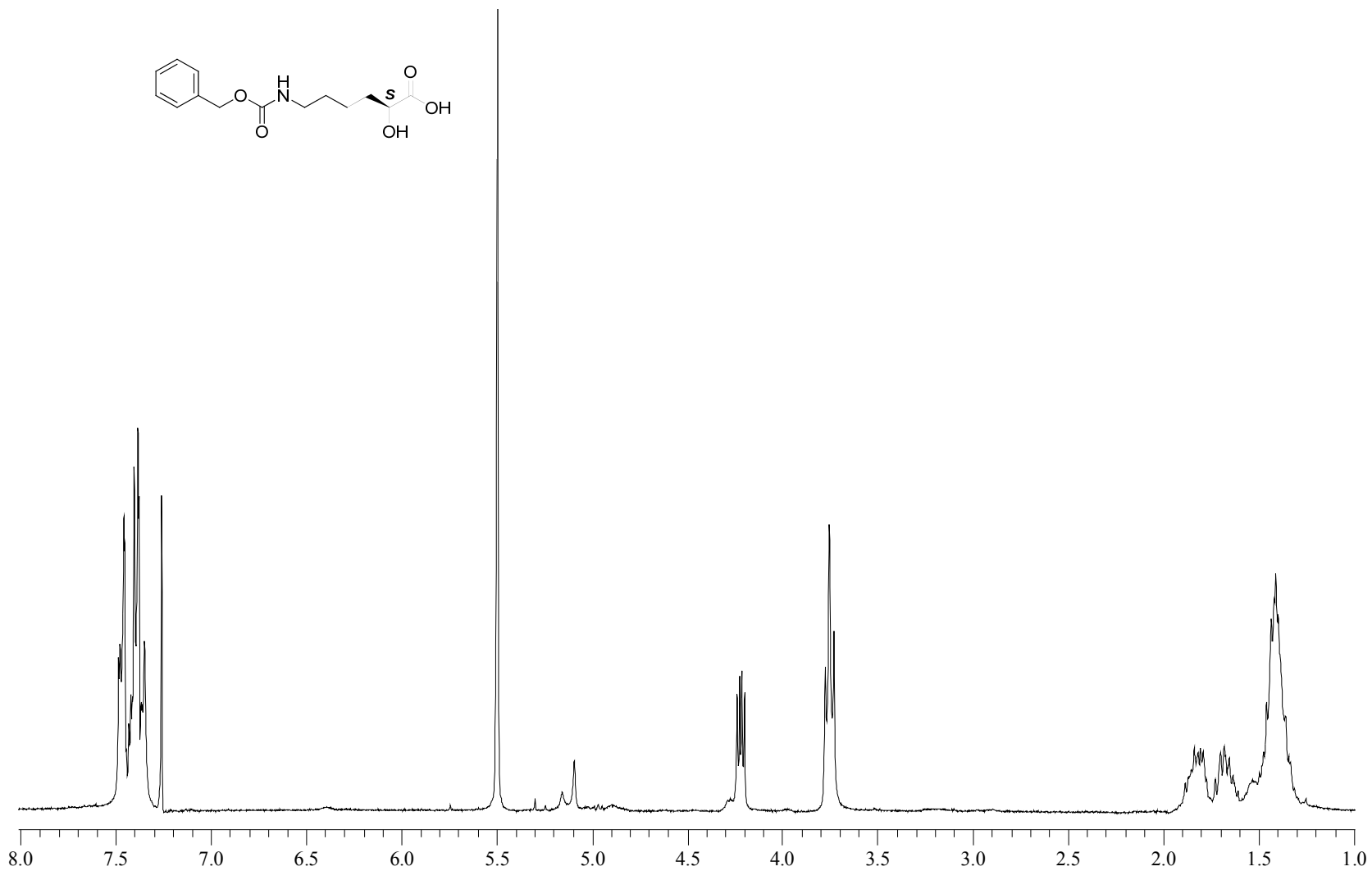


Figure B.2. ¹H NMR of 6-(Benzyloxycarbonylamino)-2-hydroxyhexanoic acid (5).

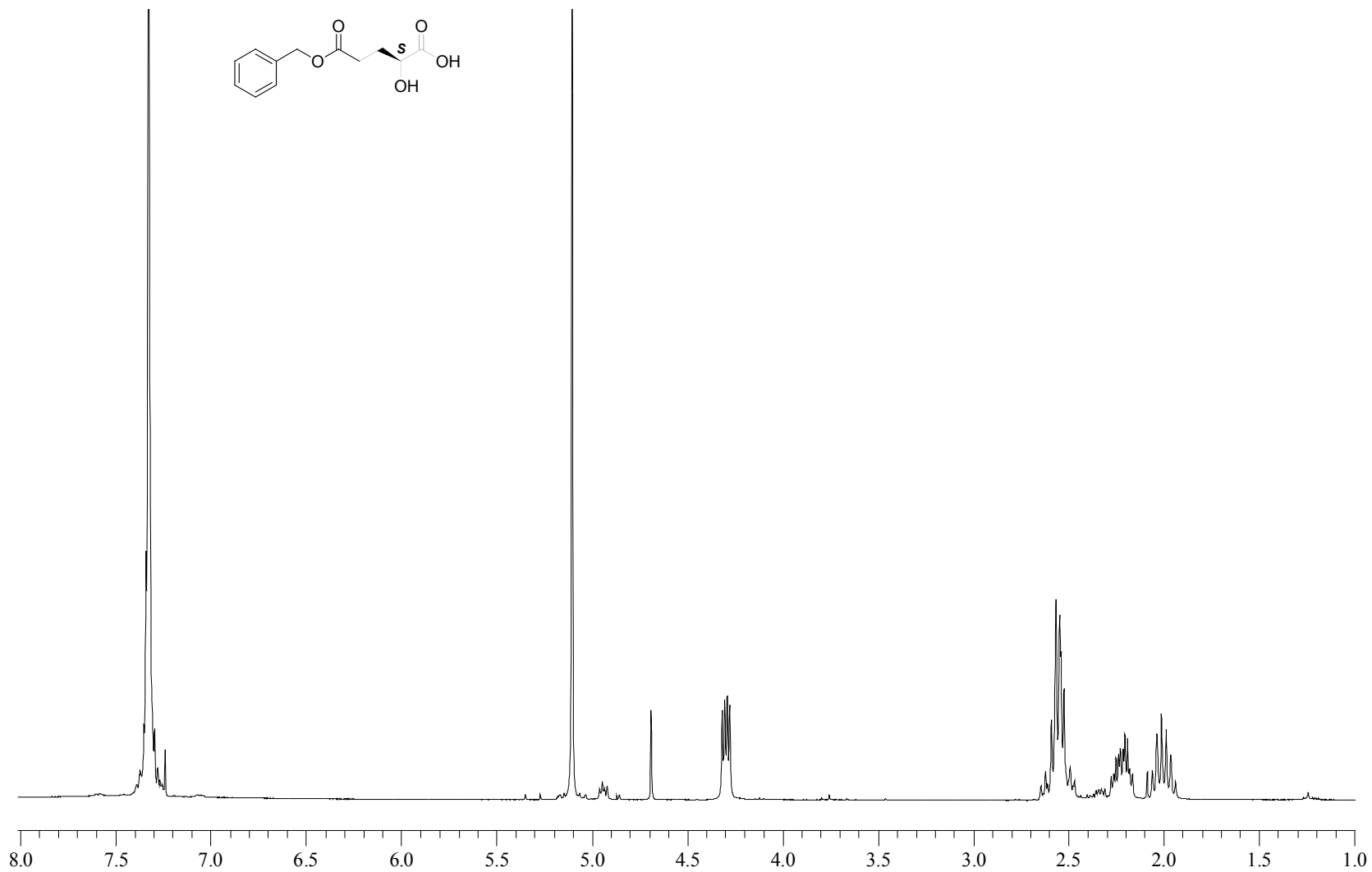


Figure B.3. ^1H NMR of 2-Hydroxypentanedioic acid 5-benzyl ester (**6**).

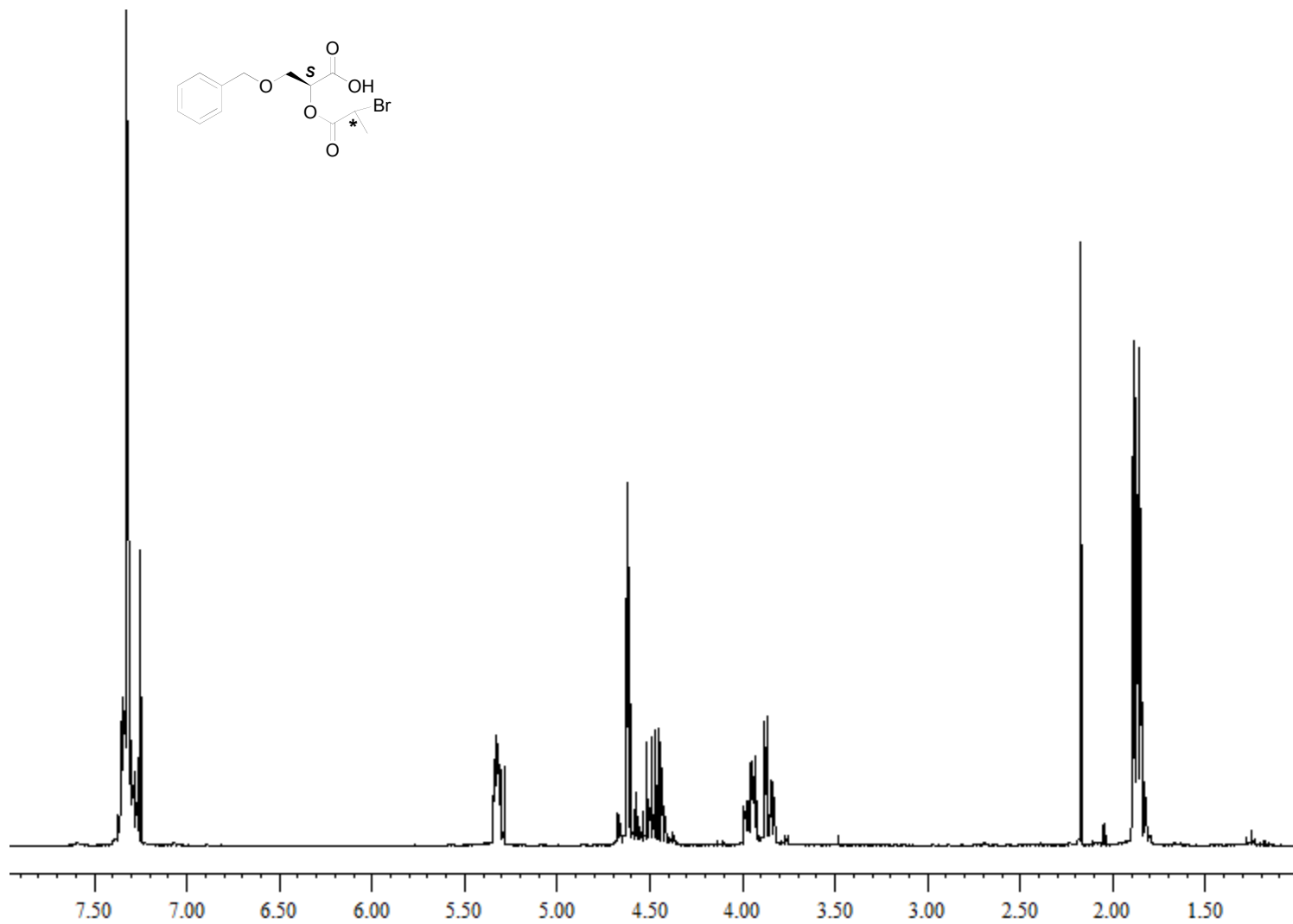


Figure B.4. ^1H NMR of 3-(Benzyloxy)-2-(2-bromopropanoyloxy)propanoic acid (7).

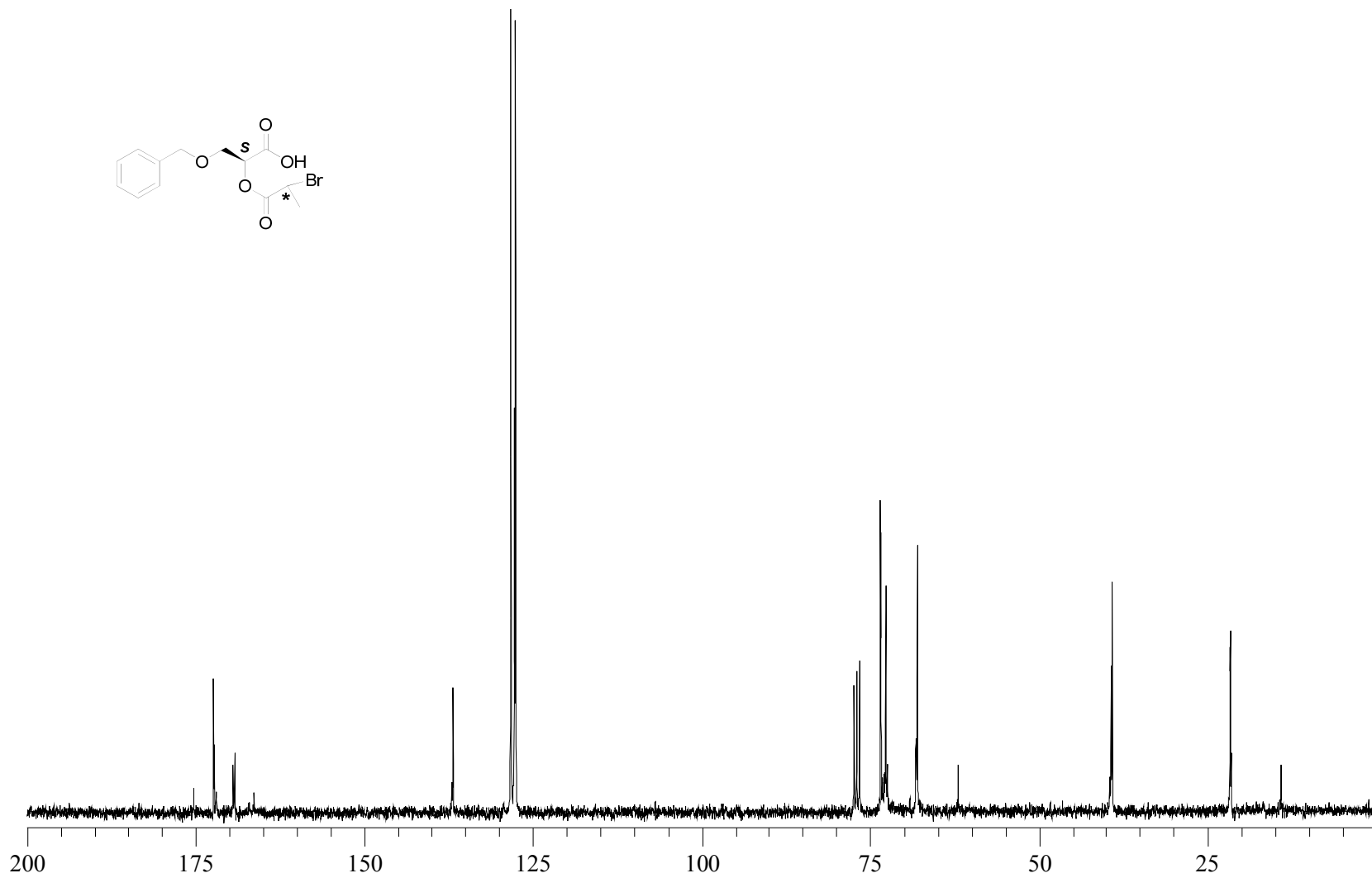


Figure B.5. ^{13}C NMR of 3-(Benzyloxy)-2-(2-bromopropanoyloxy)propanoic acid (7).

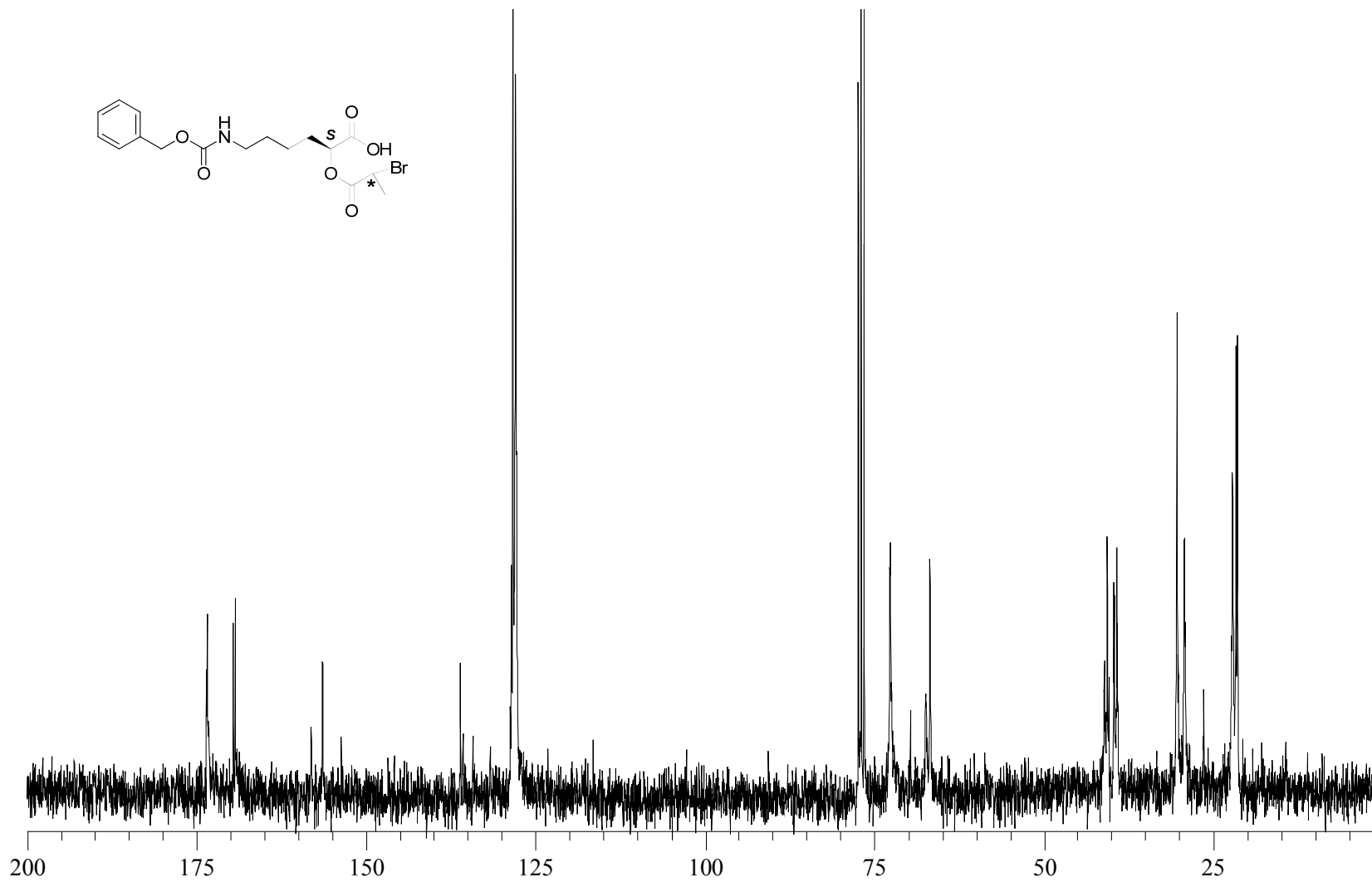


Figure B.7. ^{13}C NMR of 6-Benzyloxycarbonylamino-2-(2-bromopropionyloxy)hexanoic acid (**8**).

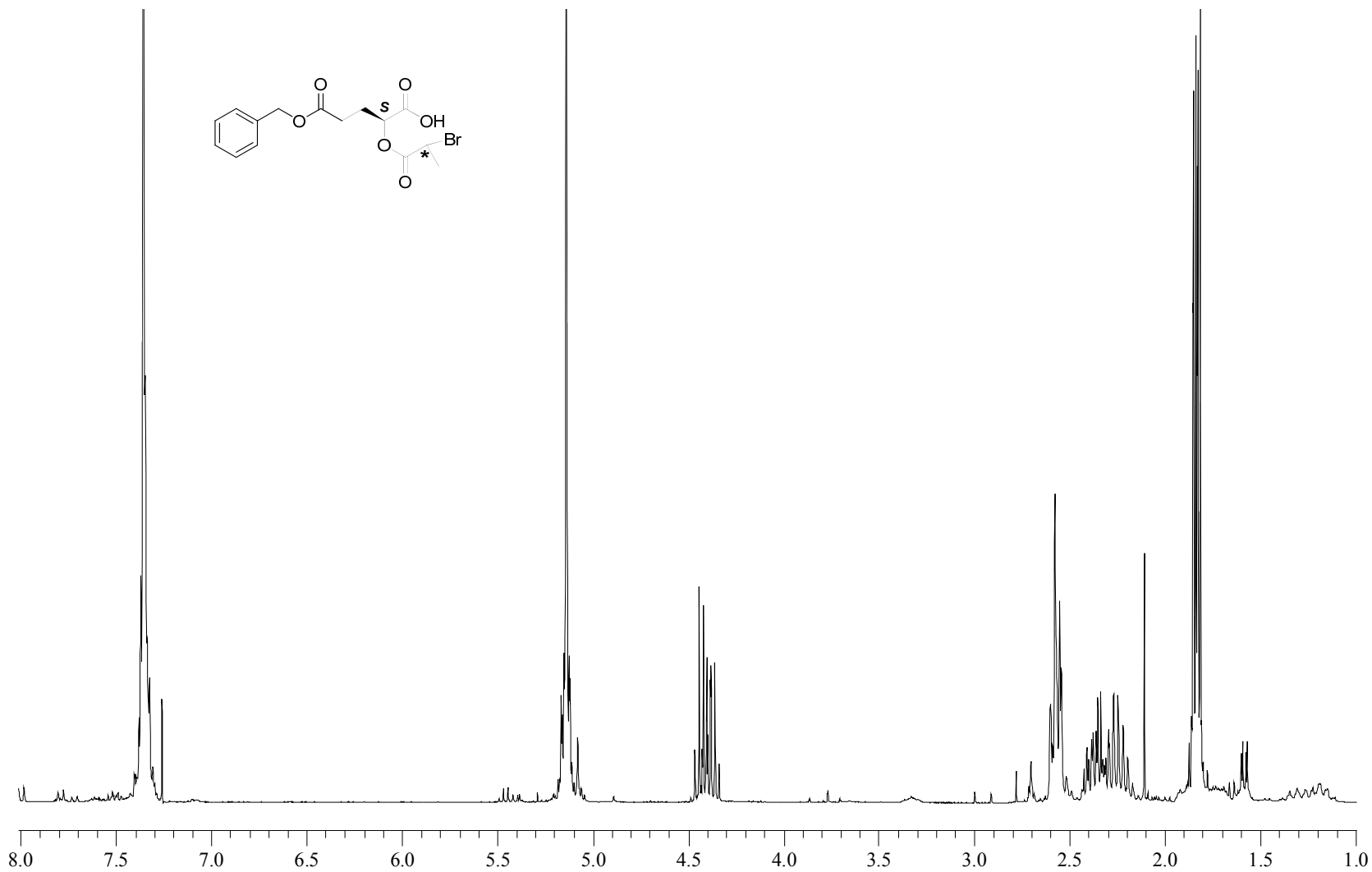


Figure B.8. ^1H NMR of 2-(2-Bromo-propionyloxy)pentanedioic acid 5-benzyl ester (**9**).

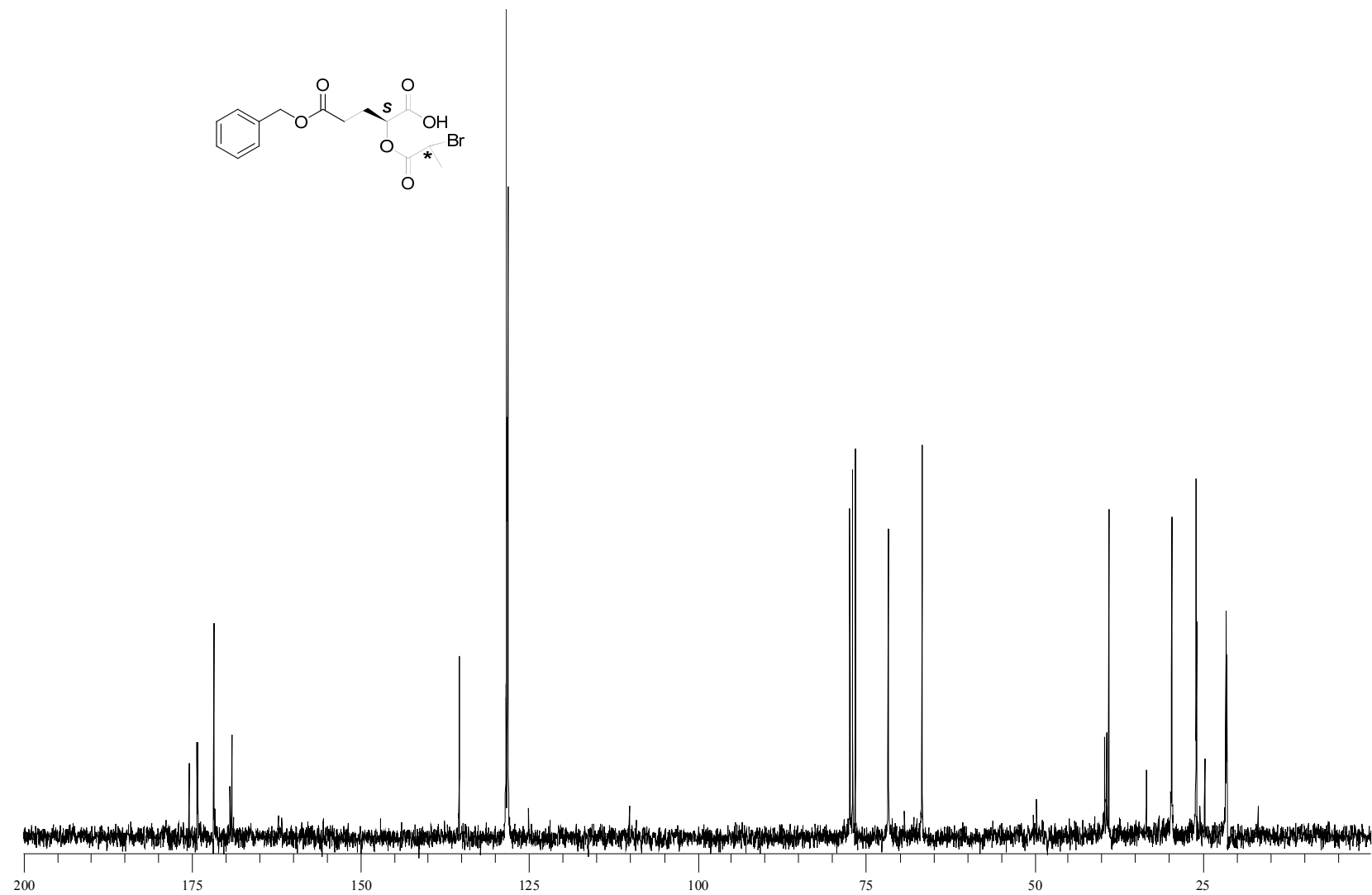


Figure B.9. ^{13}C NMR of 2-(2-Bromo-propionyloxy)pentanedioic acid 5-benzyl ester (9).

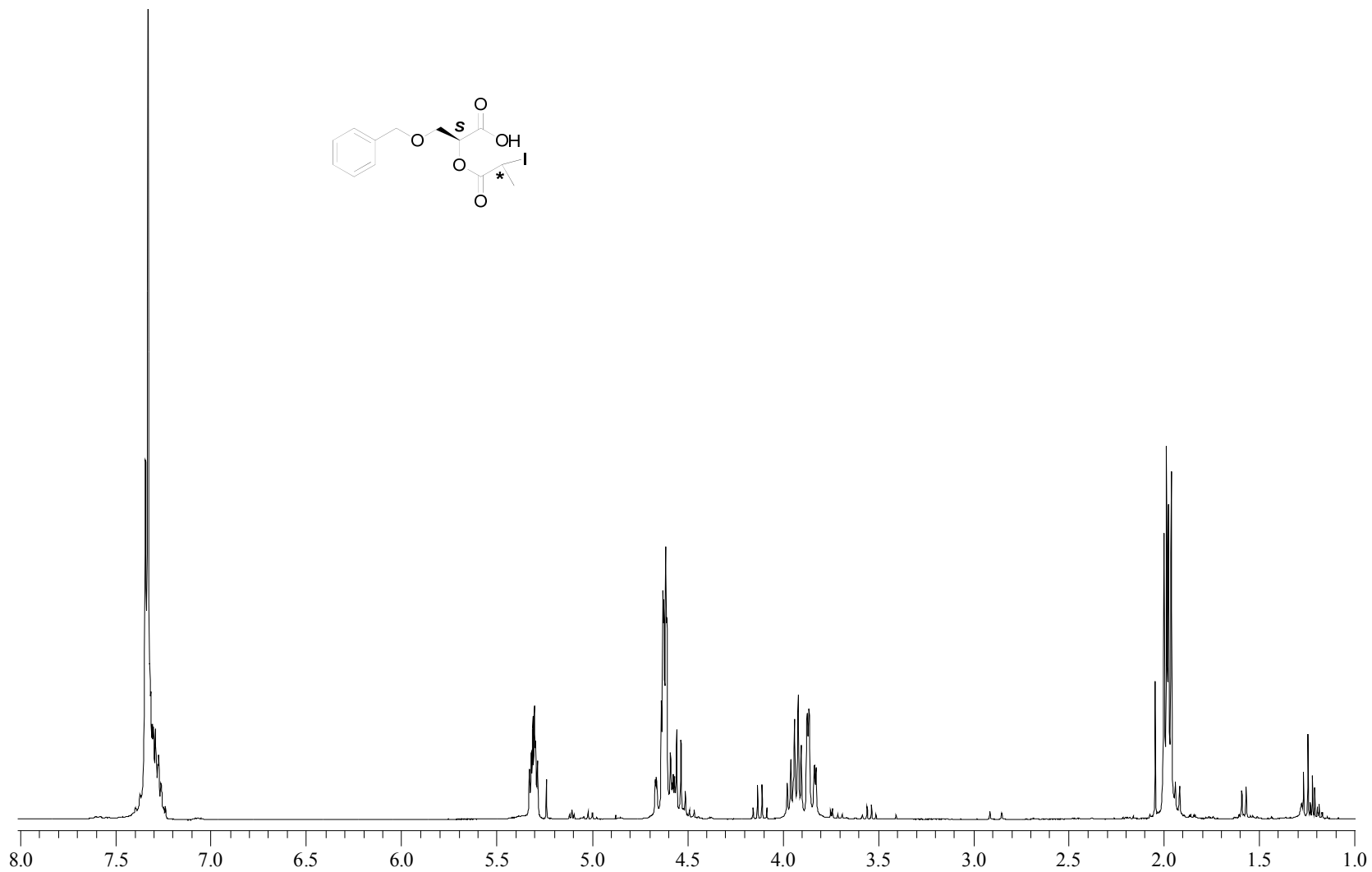


Figure B.10. ¹H NMR of α-iodocarboxylic acid intermediate (**10**). Spectrum contains residual EtOAc (4.1, 2.0, and 1.3 ppm).

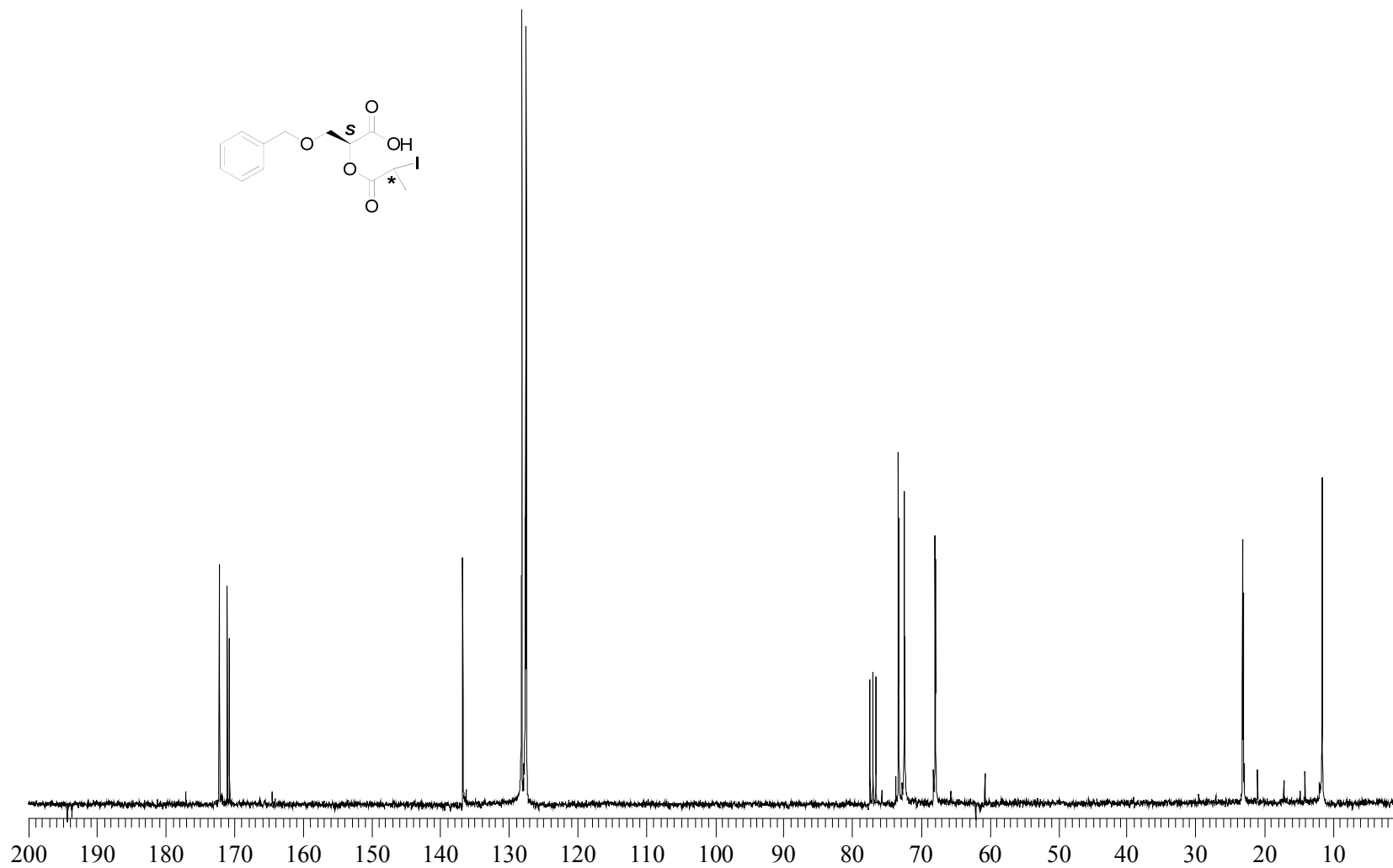


Figure B.11. ^{13}C NMR of α -iodocarboxylic acid intermediate (**10**).

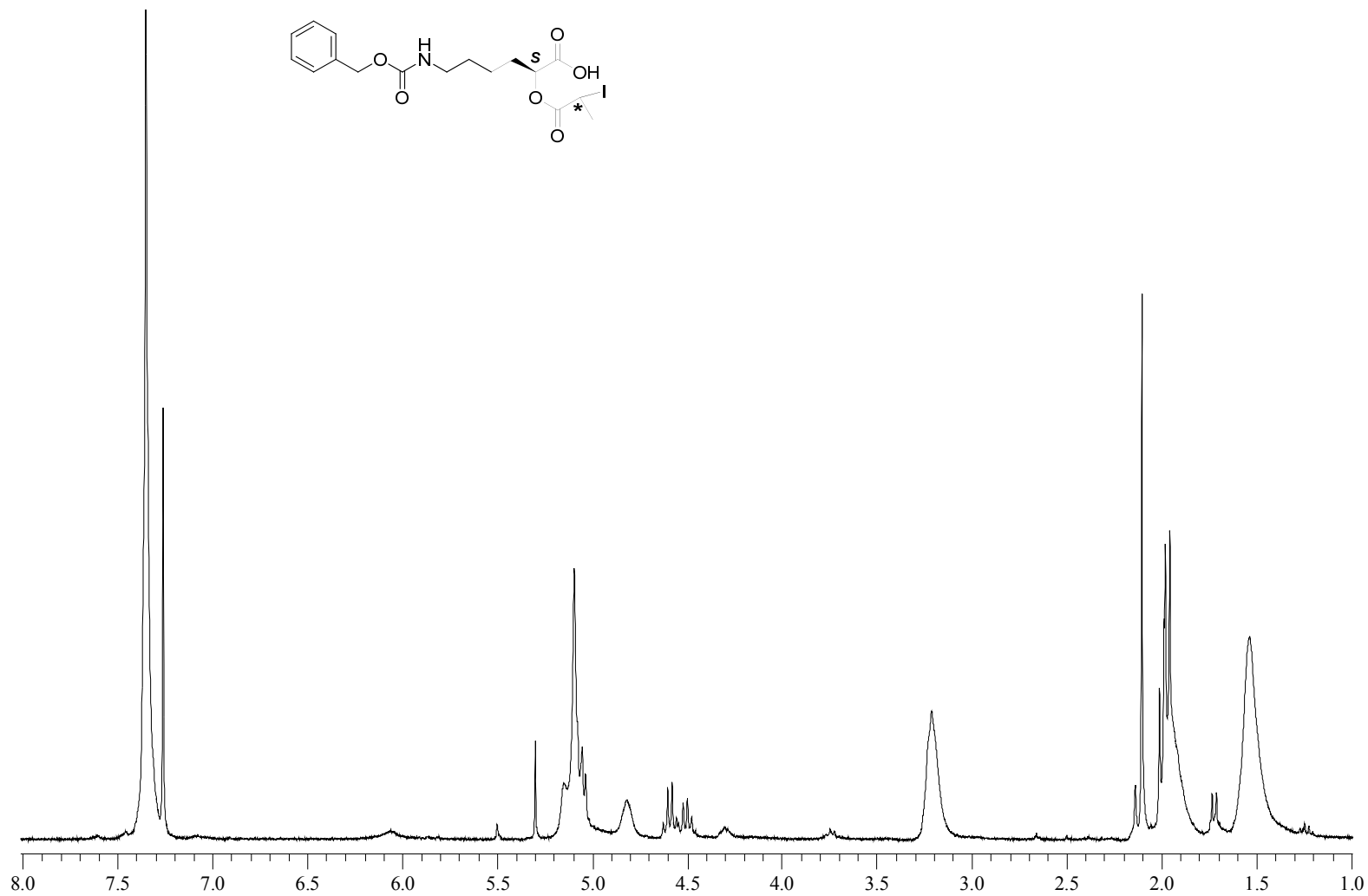


Figure B.12. ¹H NMR of α-iodocarboxylic acid intermediate (**11**).

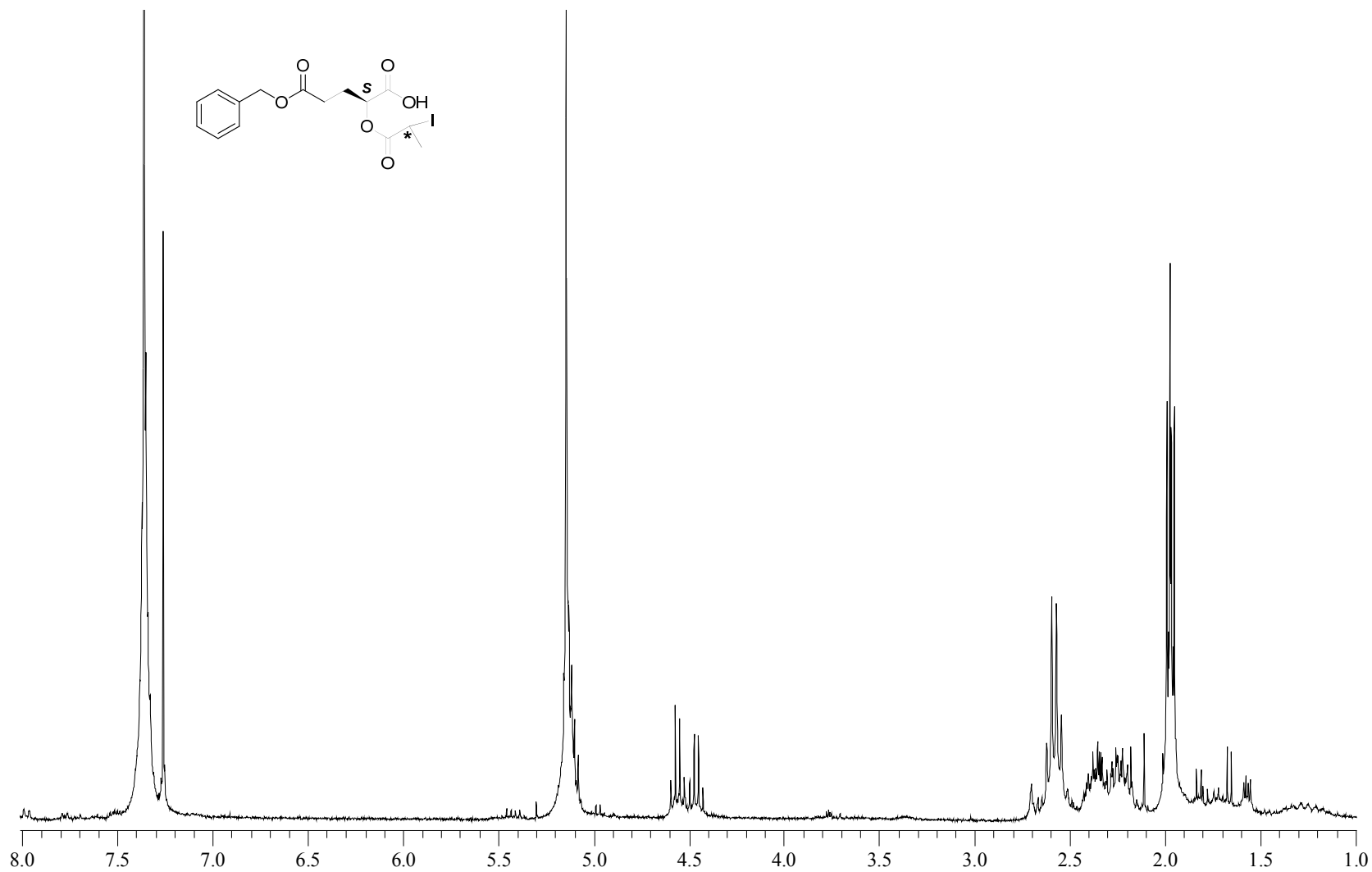


Figure B.13. ¹H NMR of α-iodocarboxylic acid intermediate (**12**).

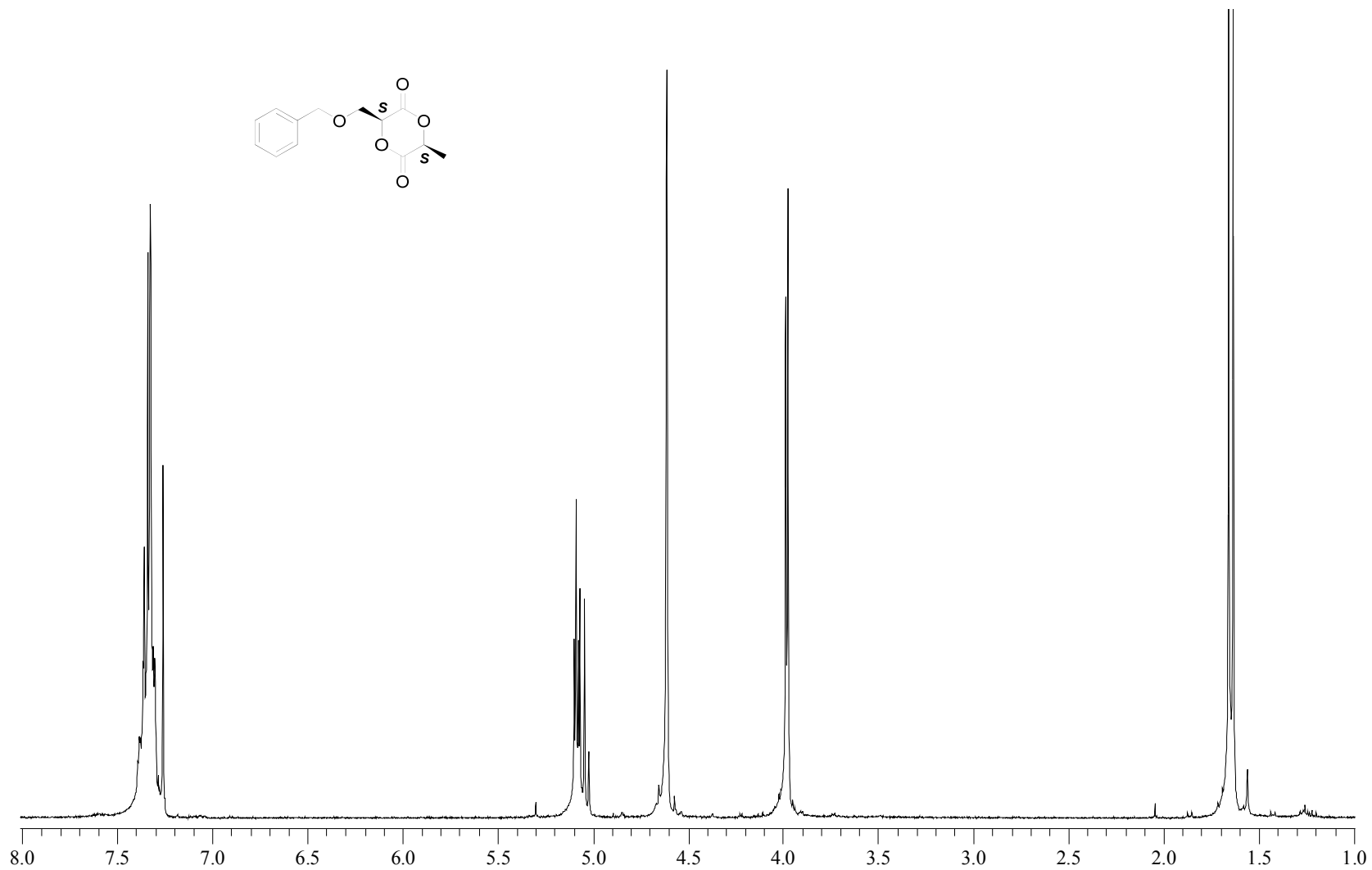


Figure B.14. ¹H NMR of 3-(Benzyloxymethyl)-6-methyl-1,4-dioxane-2,5-dione (**1**).

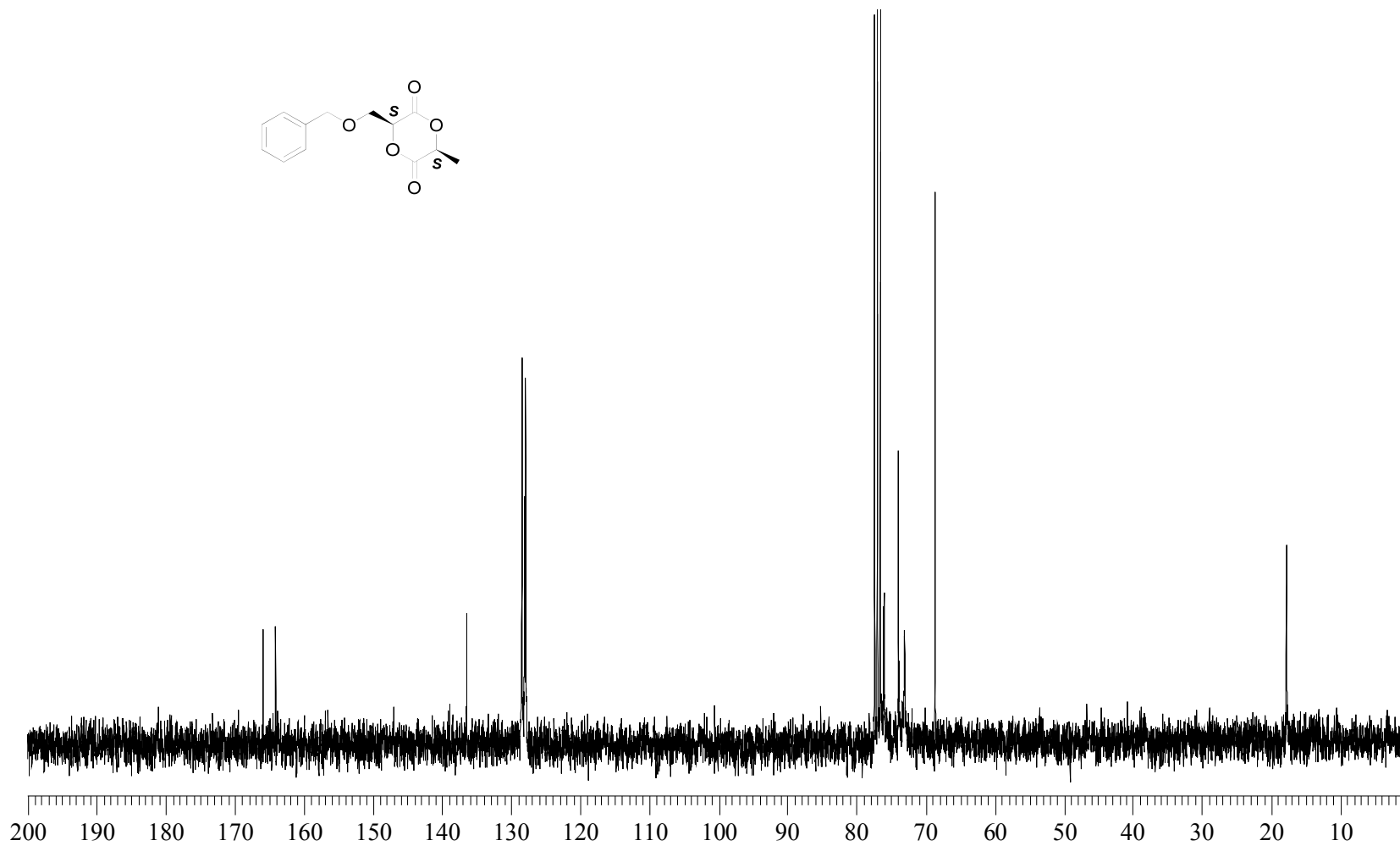


Figure B.15. ^{13}C NMR of 3-(Benzyloxymethyl)-6-methyl-1,4-dioxane-2,5-dione (**1**).

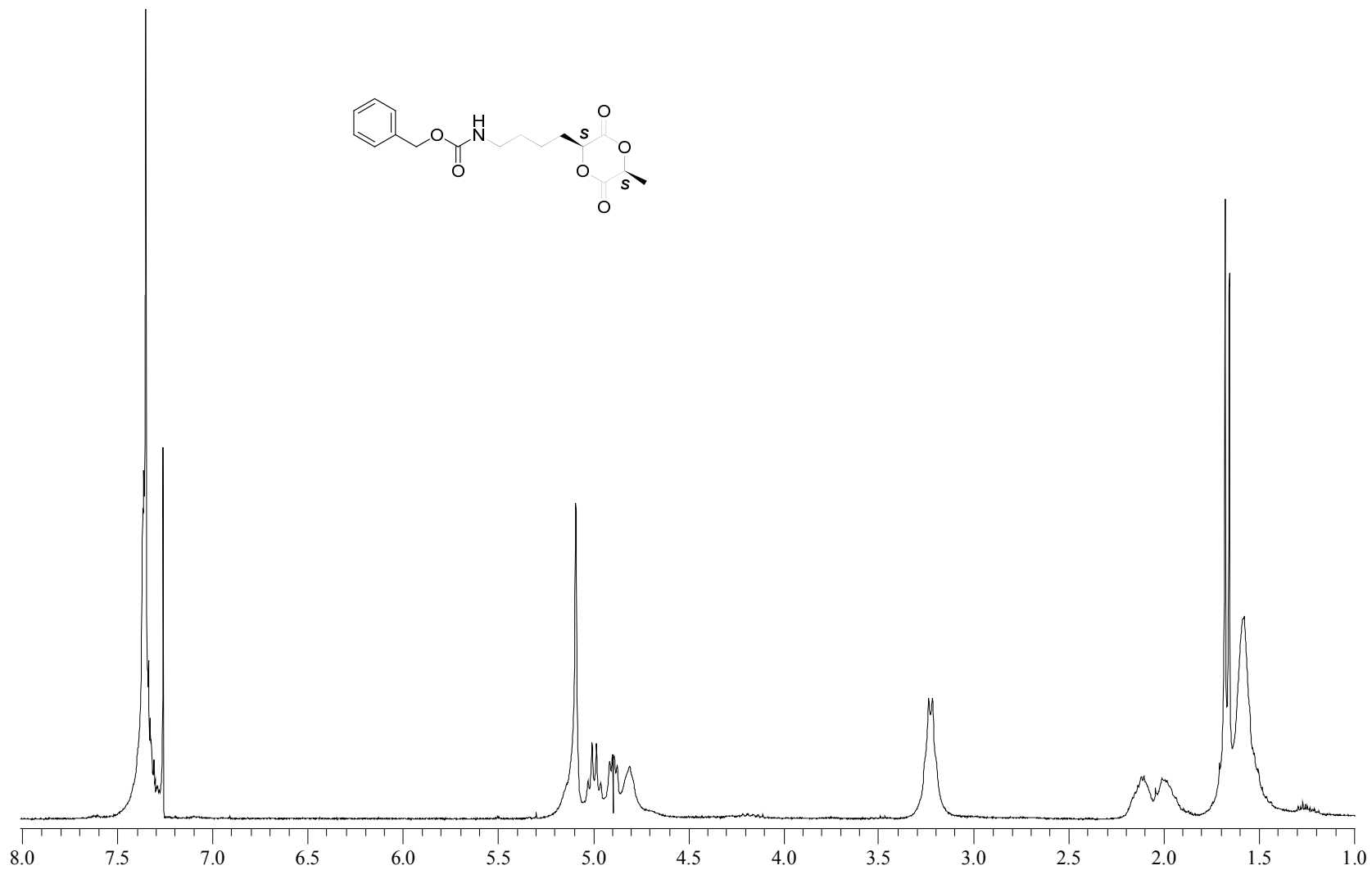


Figure B.16. ^1H NMR of Benzyl 4-(5-methyl-3,6-dioxo-1,4-dioxan-2-yl)butylcarbamate (2).

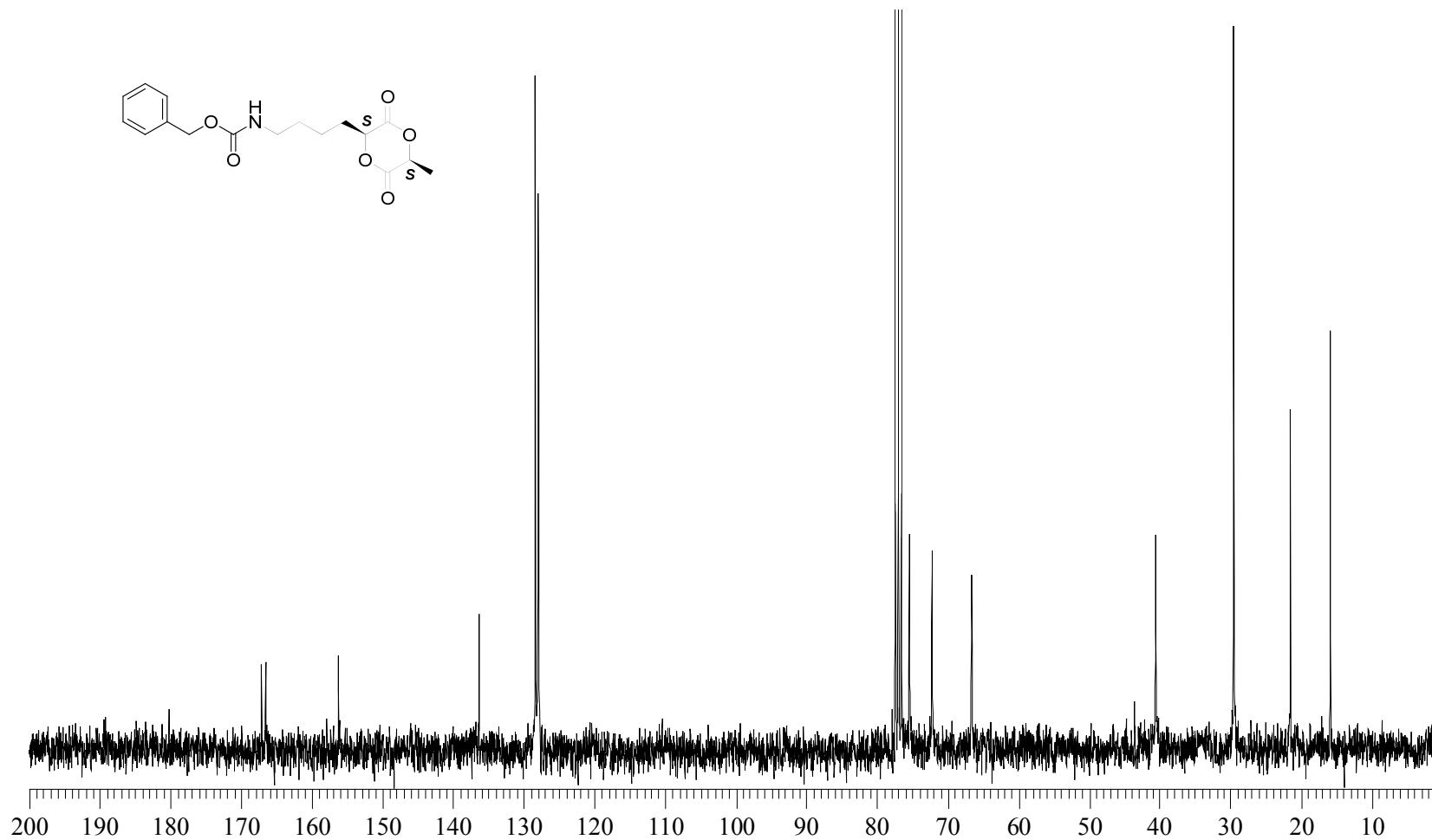


Figure B.17. ¹³C NMR of Benzyl 4-(5-methyl-3,6-dioxo-1,4-dioxan-2-yl)butylcarbamate (2).

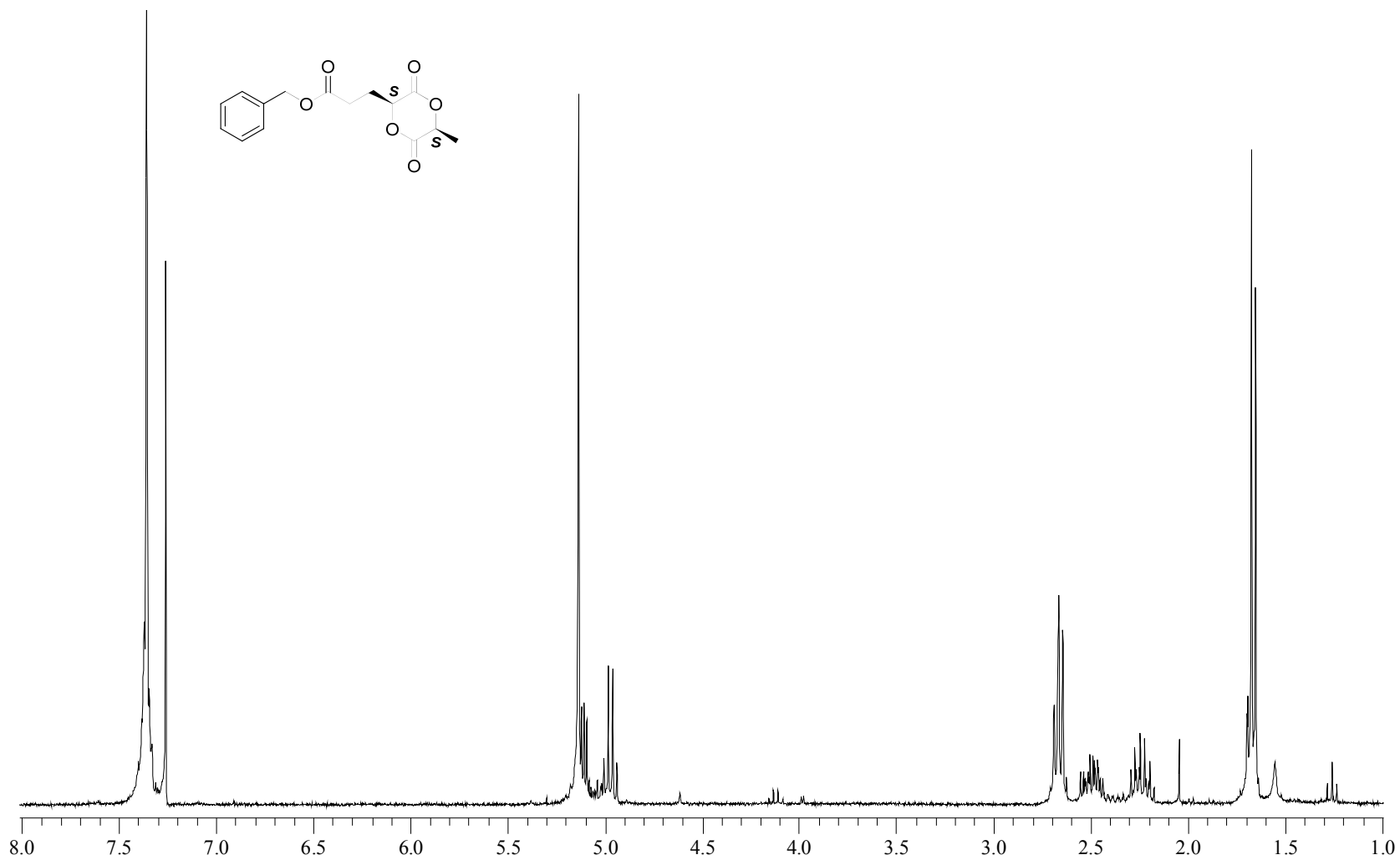


Figure B.18. ¹H NMR of Benzyl 3-(5-methyl-3,6-dioxo-1,4-dioxan-2-yl)propanoate (**3**). Spectrum contains residual EtOAc (4.1, 2.0, and 1.3 ppm).

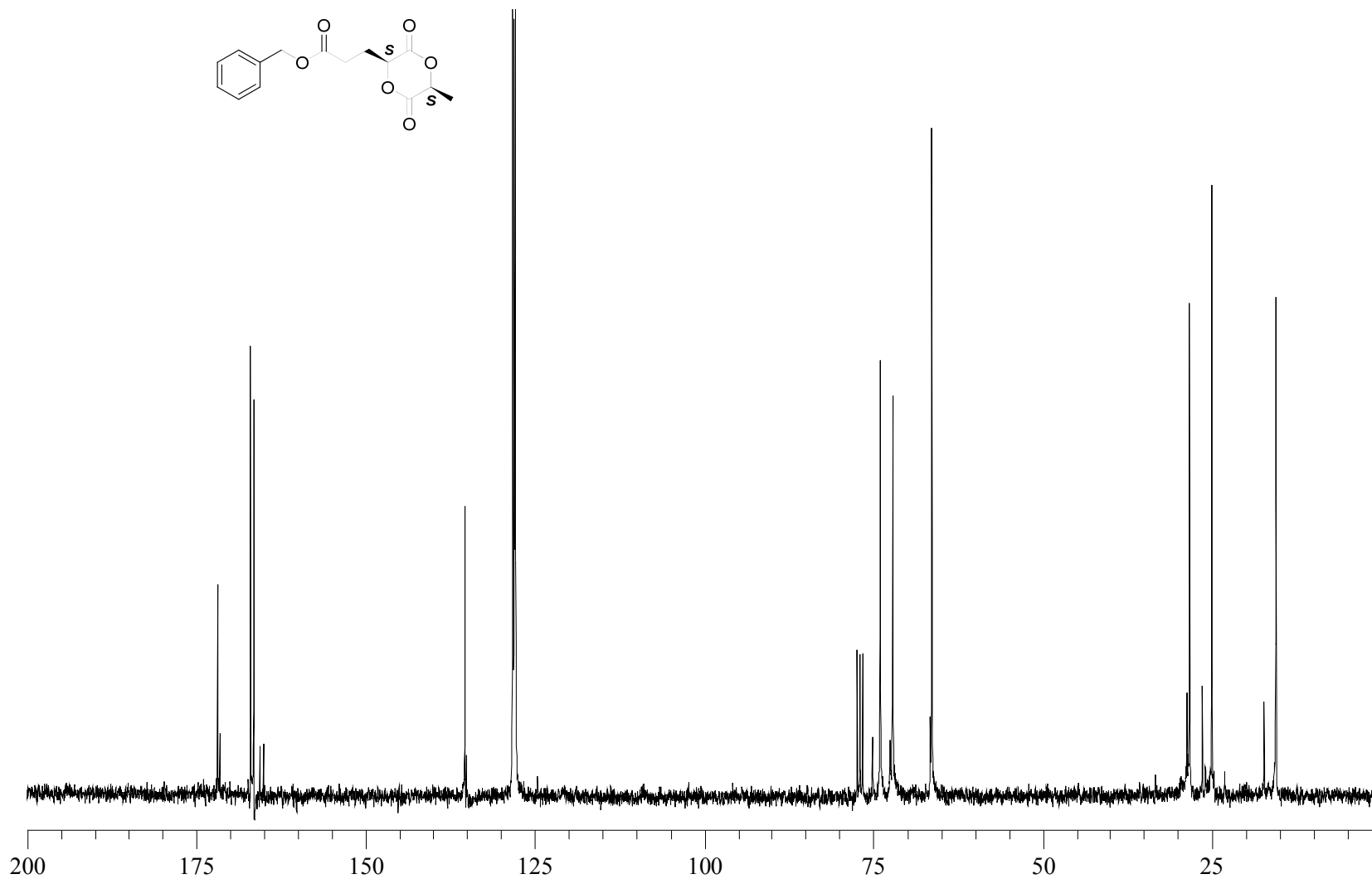


Figure B.19. ^{13}C NMR of Benzyl 3-(5-methyl-3,6-dioxo-1,4-dioxan-2-yl)propanoate (3).

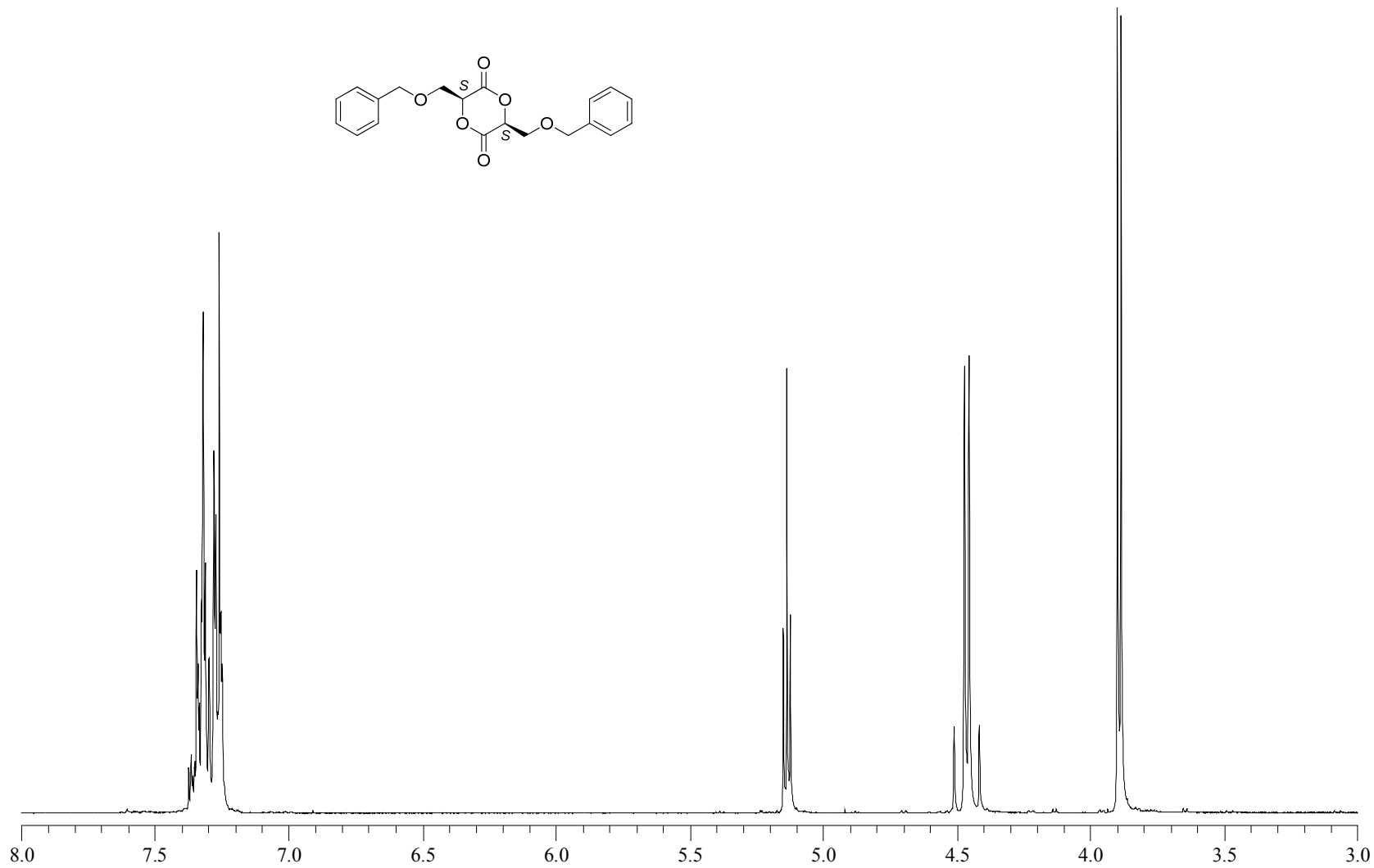
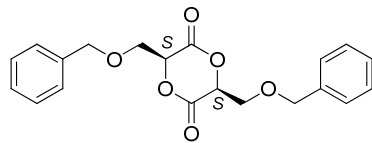


Figure B.20. ¹H NMR of (*S,S*)-3,6-(Benzyloxymethyl)-1,4-dioxane-2,5-dione (**2**).

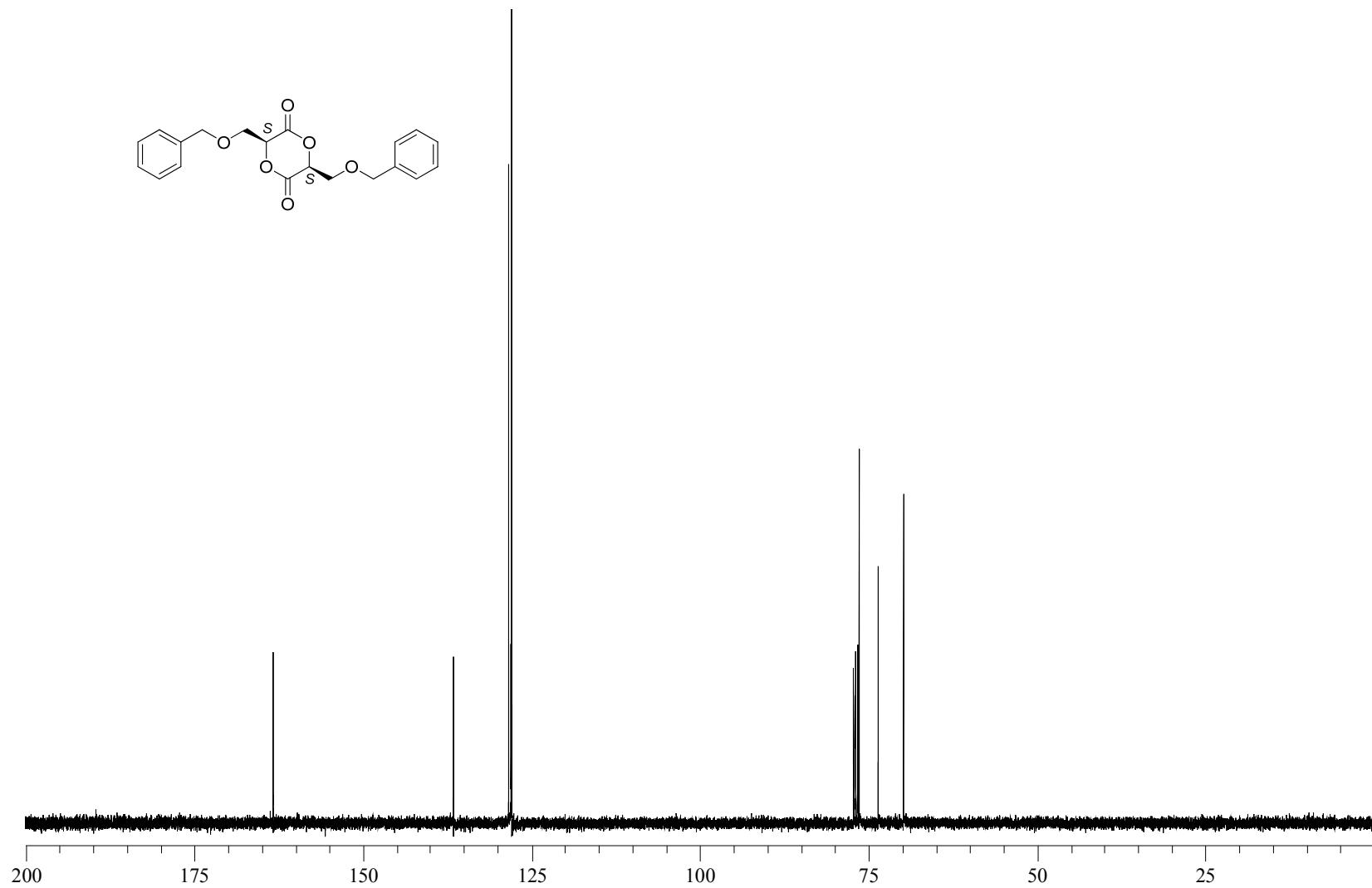


Figure B.21. ¹³C NMR of *(S,S)*-3,6-(Benzyloxymethyl)-1,4-dioxane-2,5-dione (**2**).

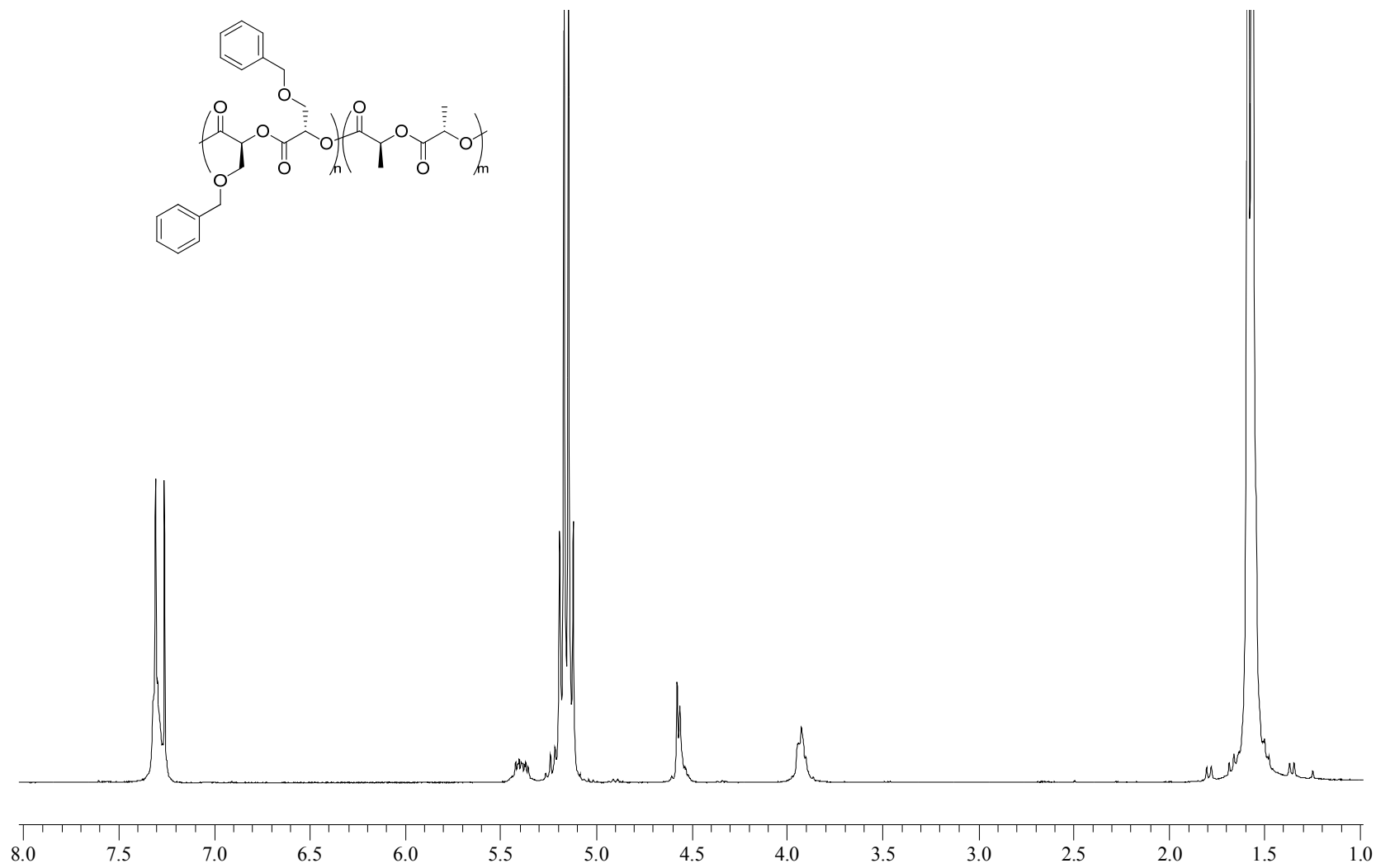


Figure B.22. ^1H NMR of dibenzyloxy-substituted PLA copolymer **3**.

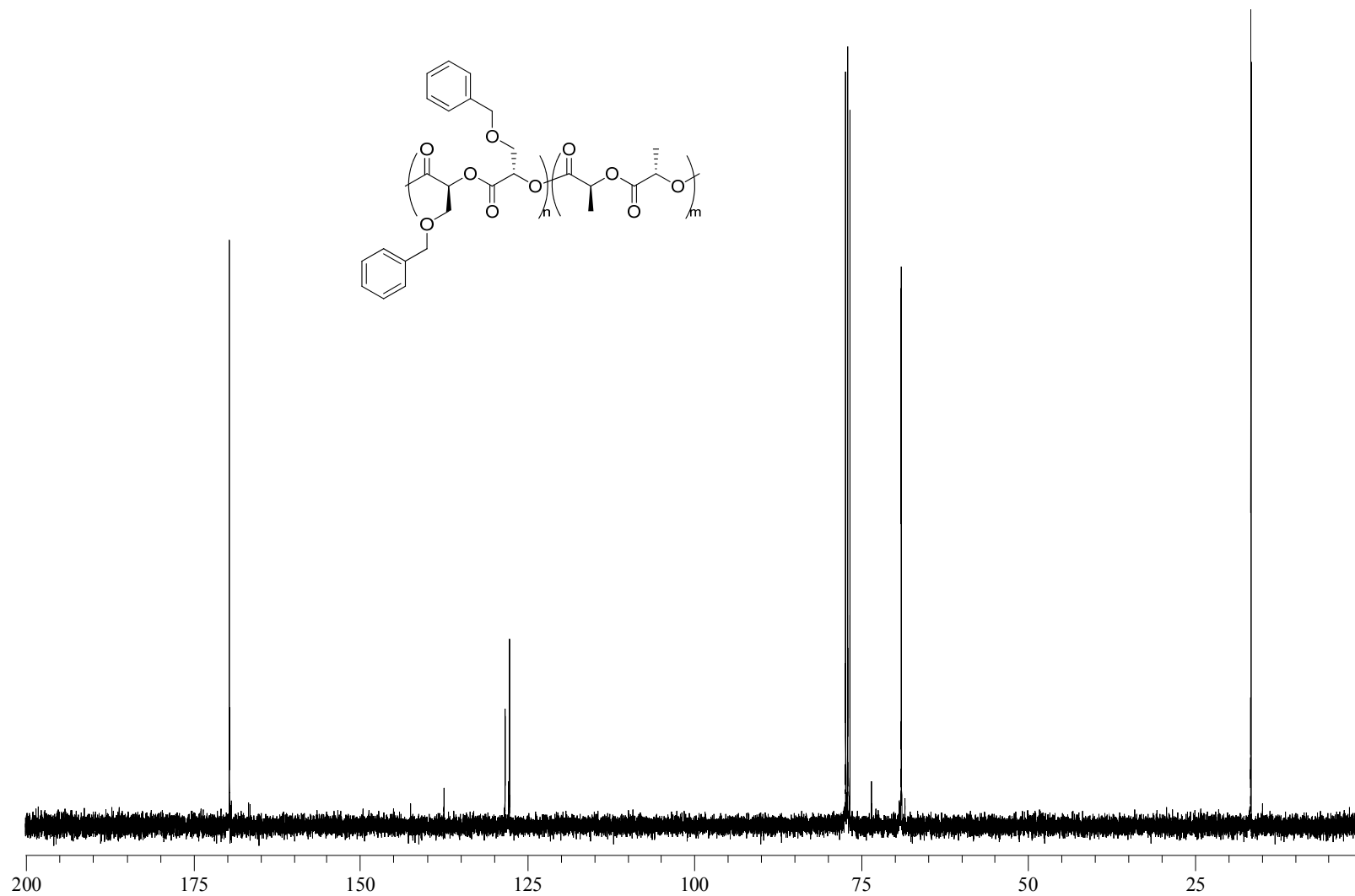


Figure B.23. ^{13}C NMR of dibenzyloxy-substituted PLA copolymer **3**.

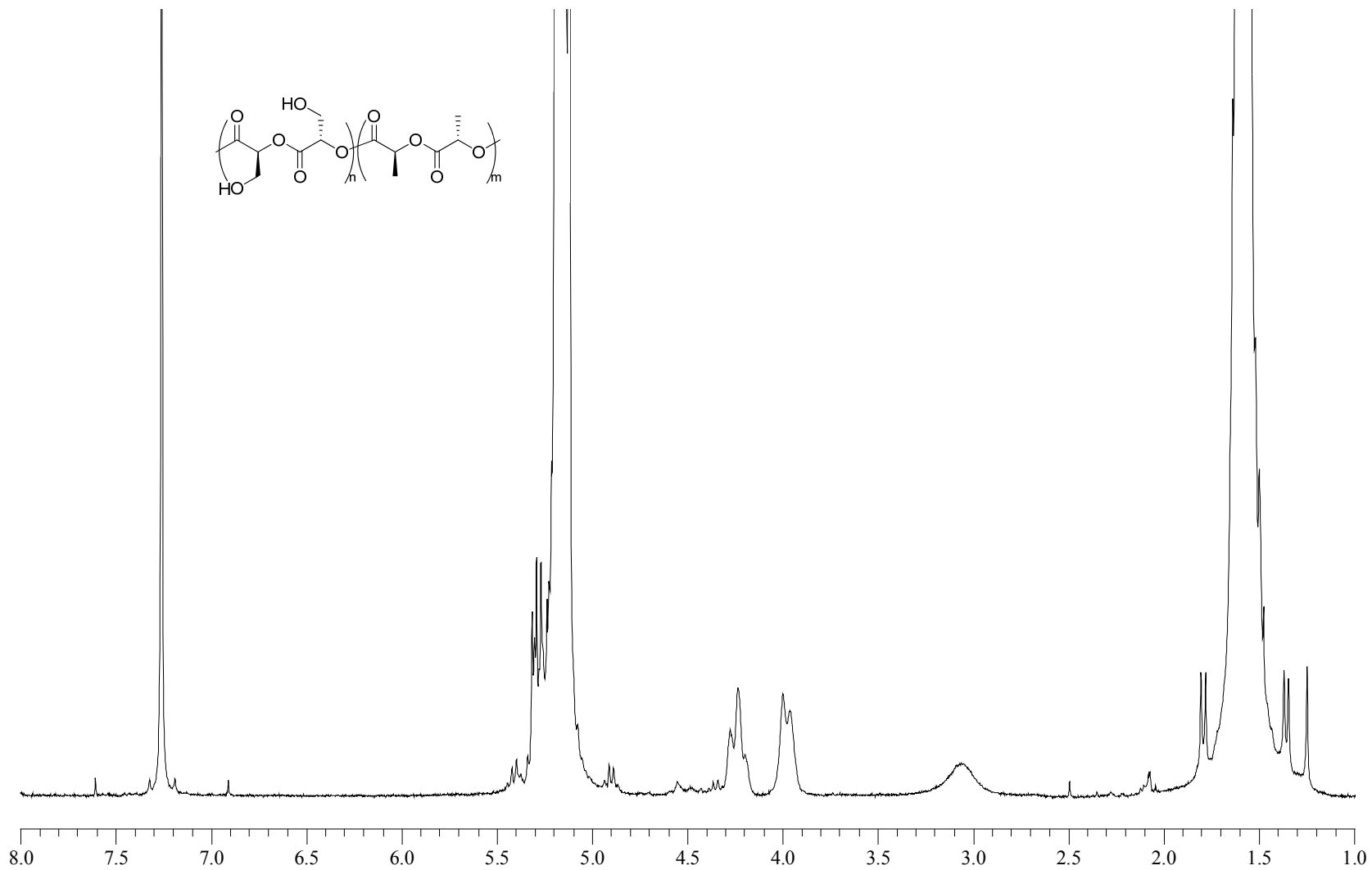


Figure B.24. ^1H NMR of hydroxy-bearing PLA copolymer 4.

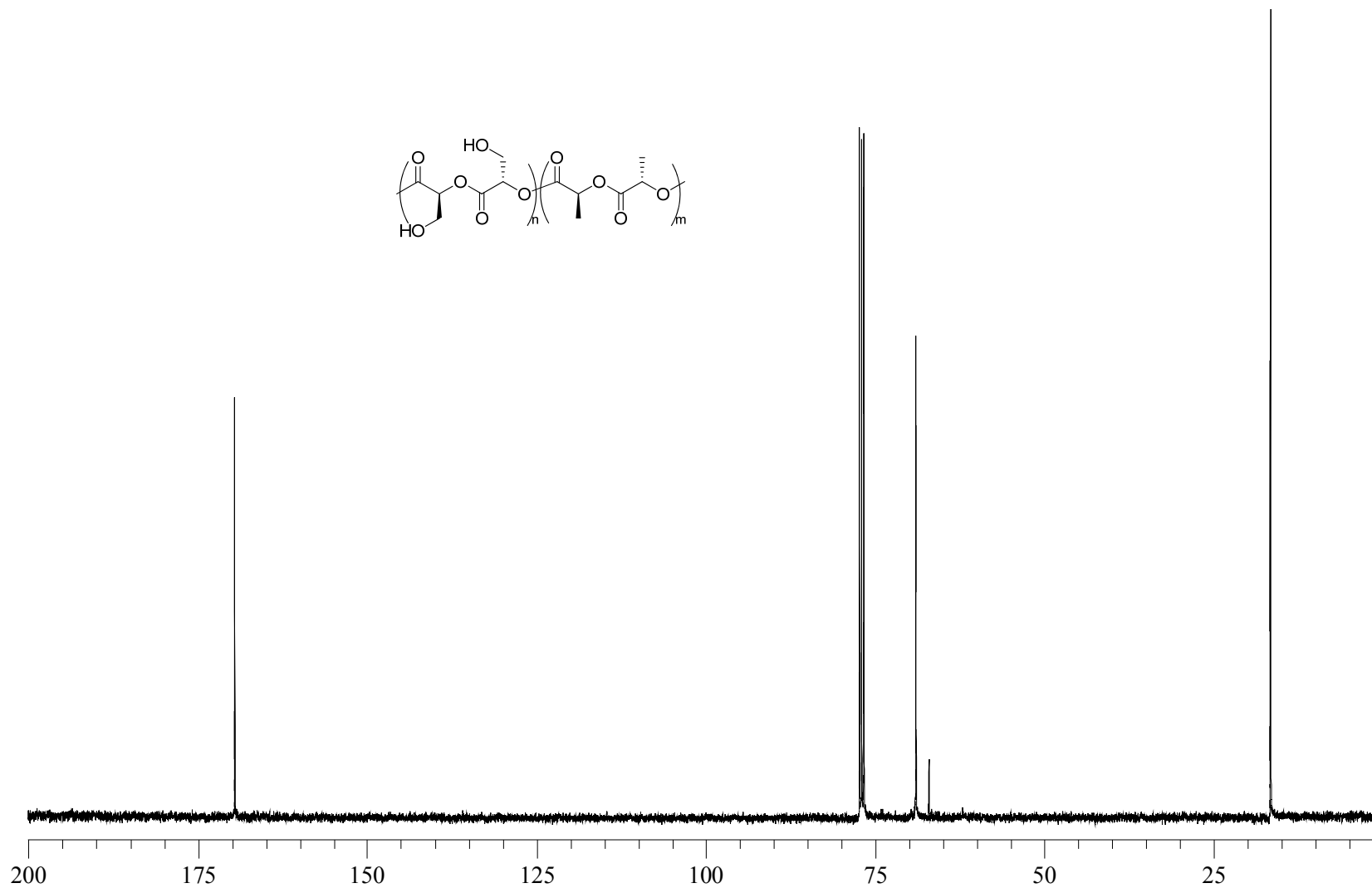


Figure B.25. ^{13}C NMR of hydroxy-bearing PLA copolymer 4.

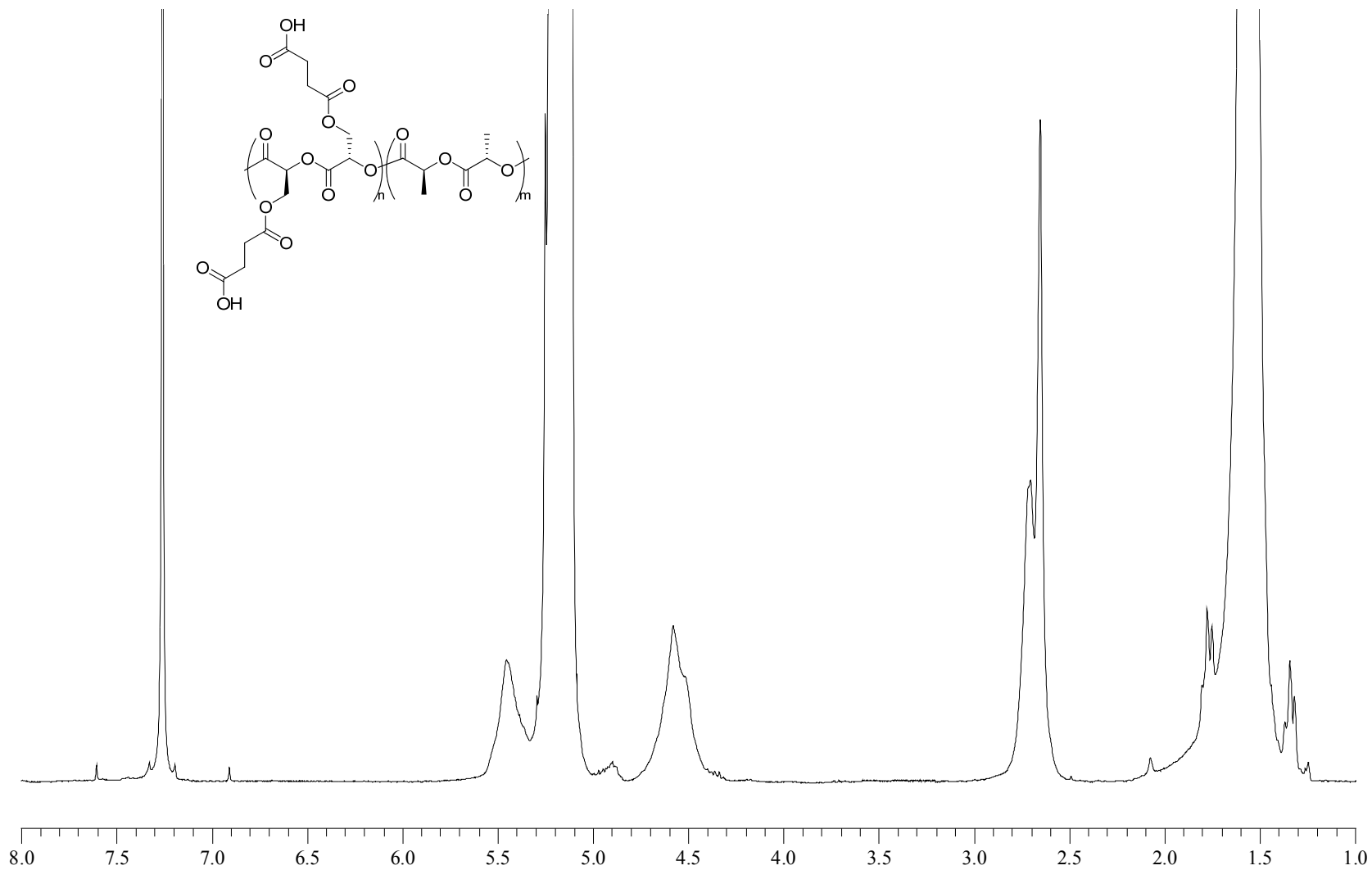


Figure B.26. ^1H NMR of succinic anhydride-modified PLA copolymer 5.

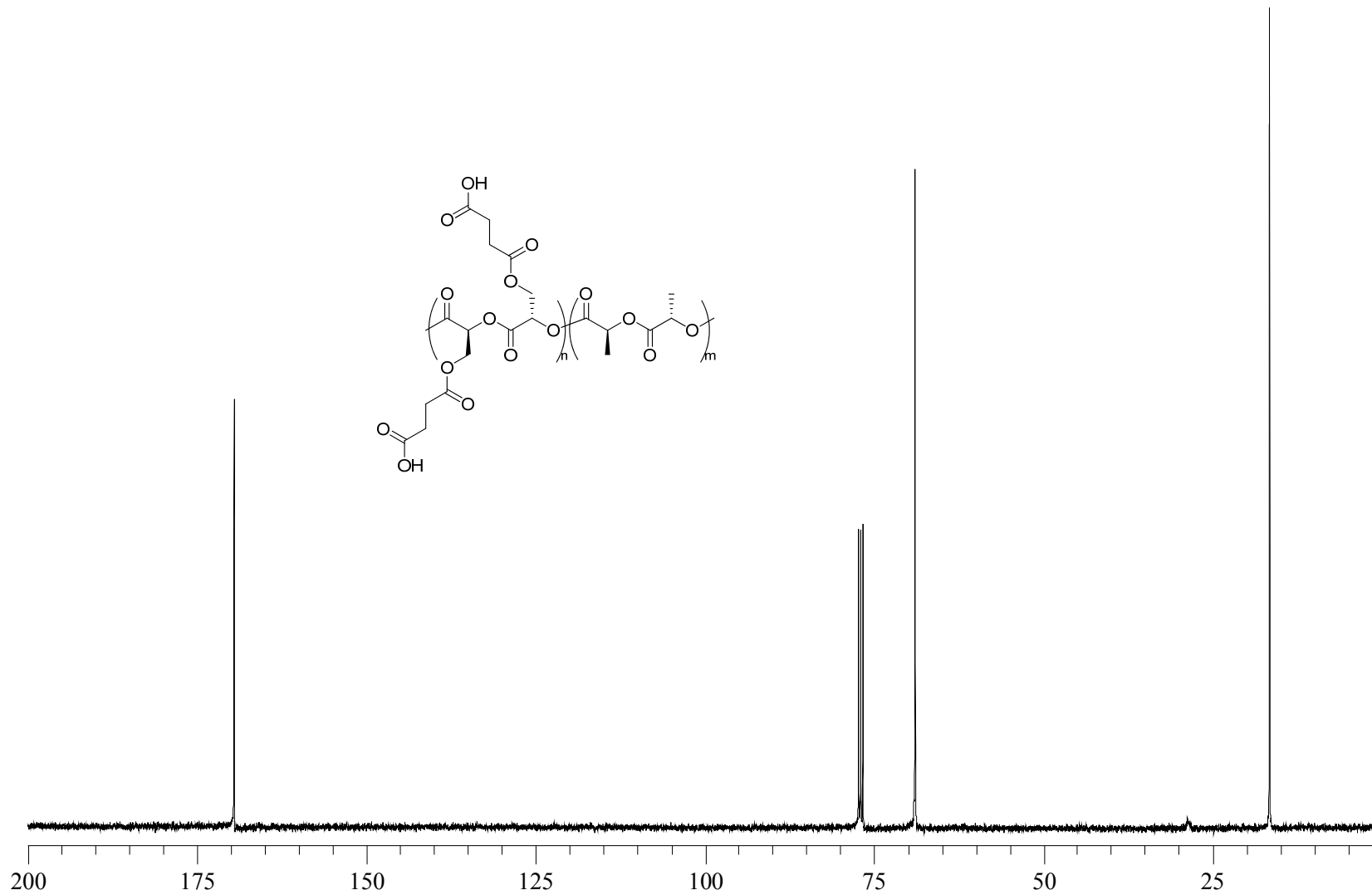


Figure B.27. ^{13}C NMR of succinic anhydride-modified PLA copolymer 5.

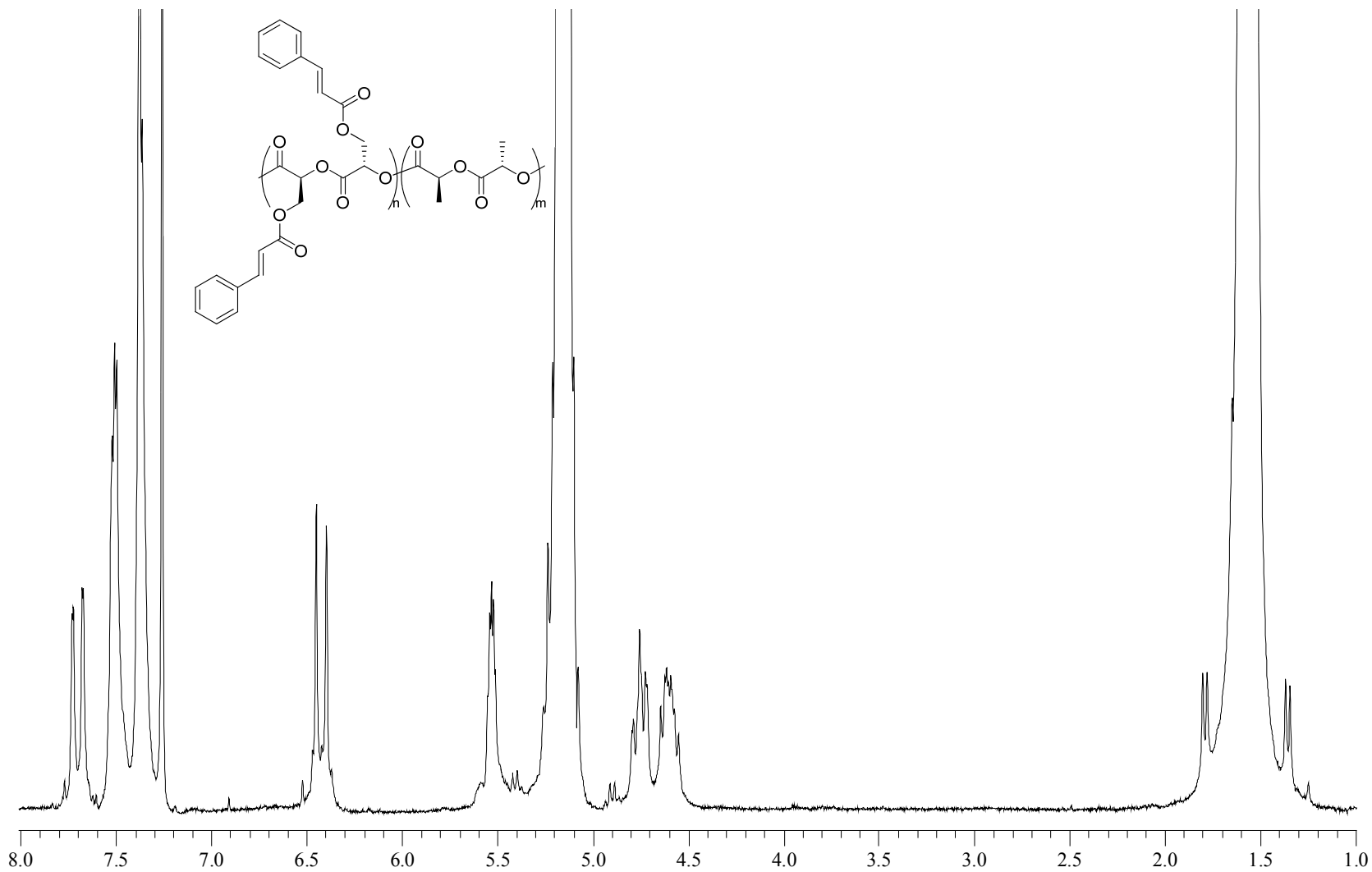


Figure B.28. ¹H NMR of cinnamate-modified PLA copolymer **5**.

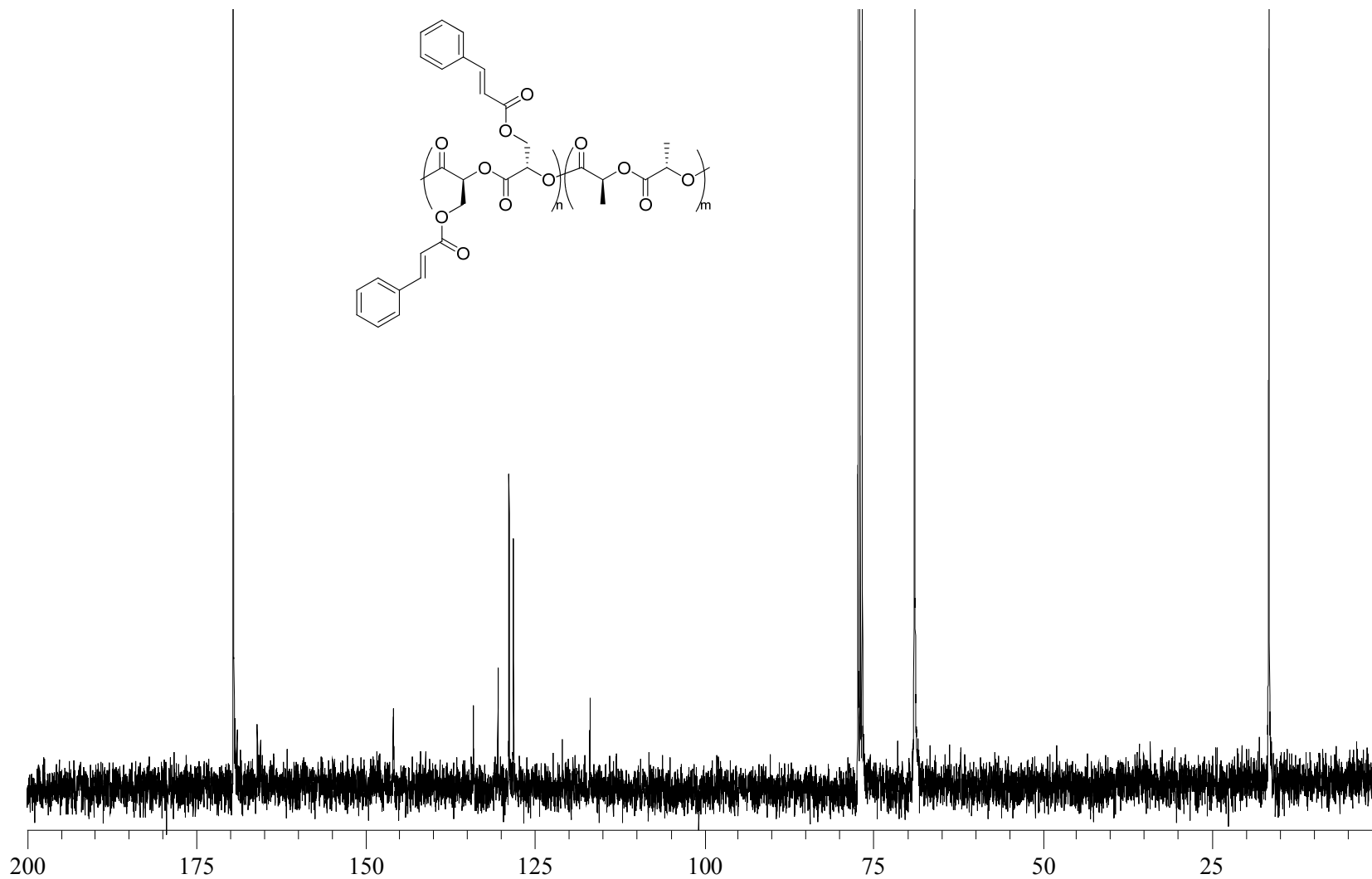


Figure B.29. ^{13}C NMR of cinnamate-modified PLA copolymer 5.

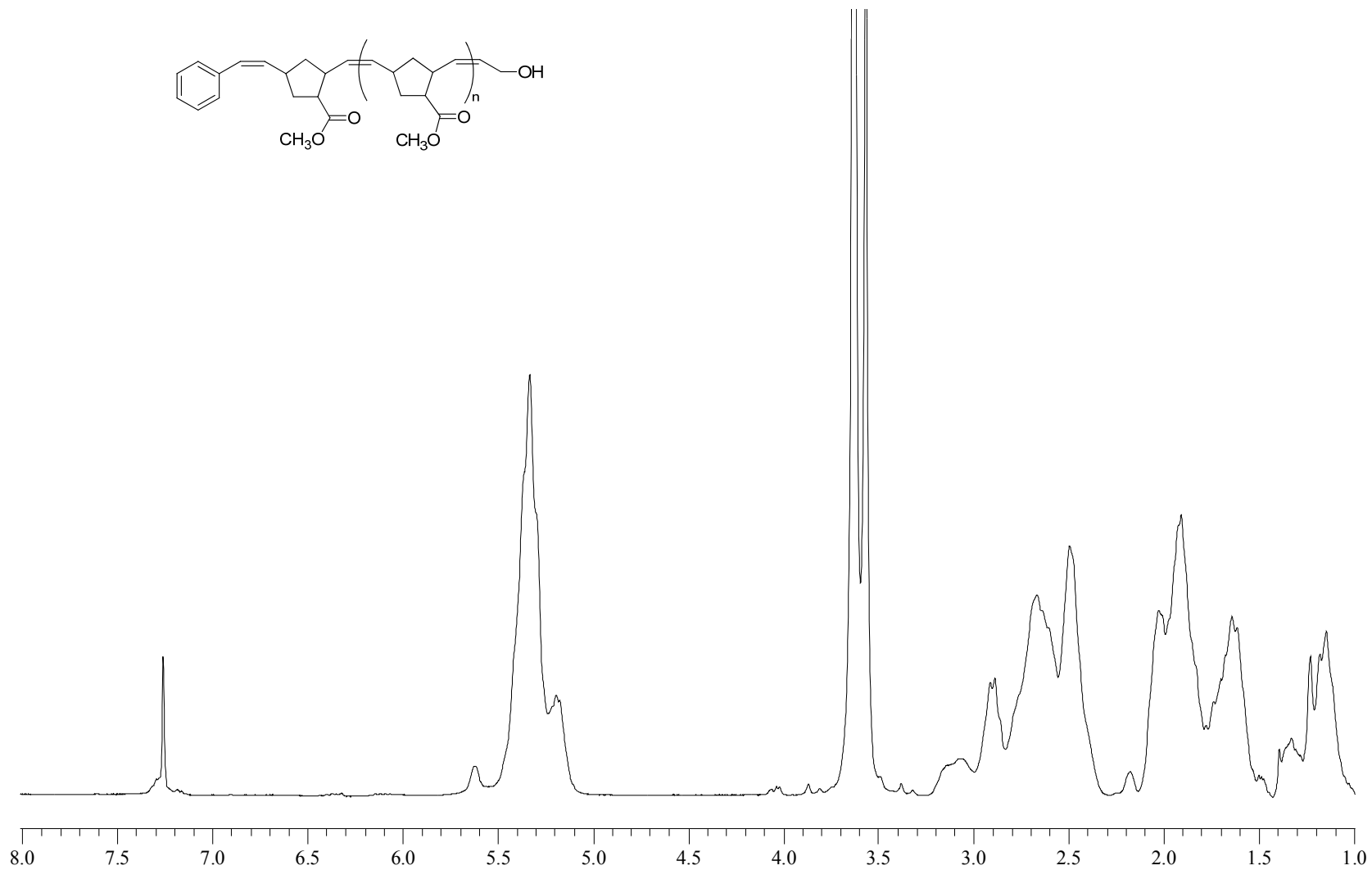


Figure B.30. ^1H NMR of hydroxyl-terminated PNb macroinitiator.

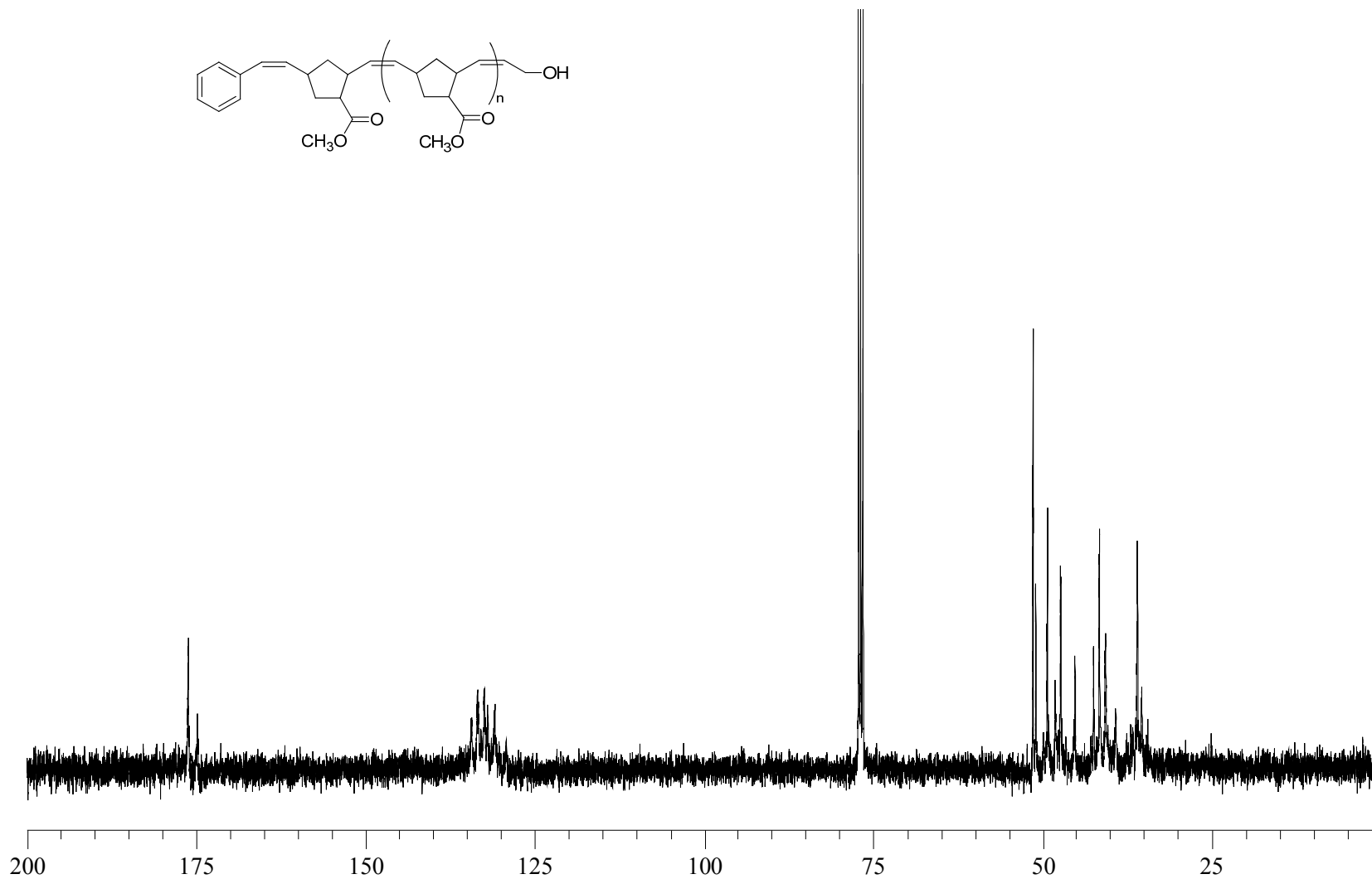


Figure B.31. ^{13}C NMR of hydroxyl-terminated PNb macroinitiator.

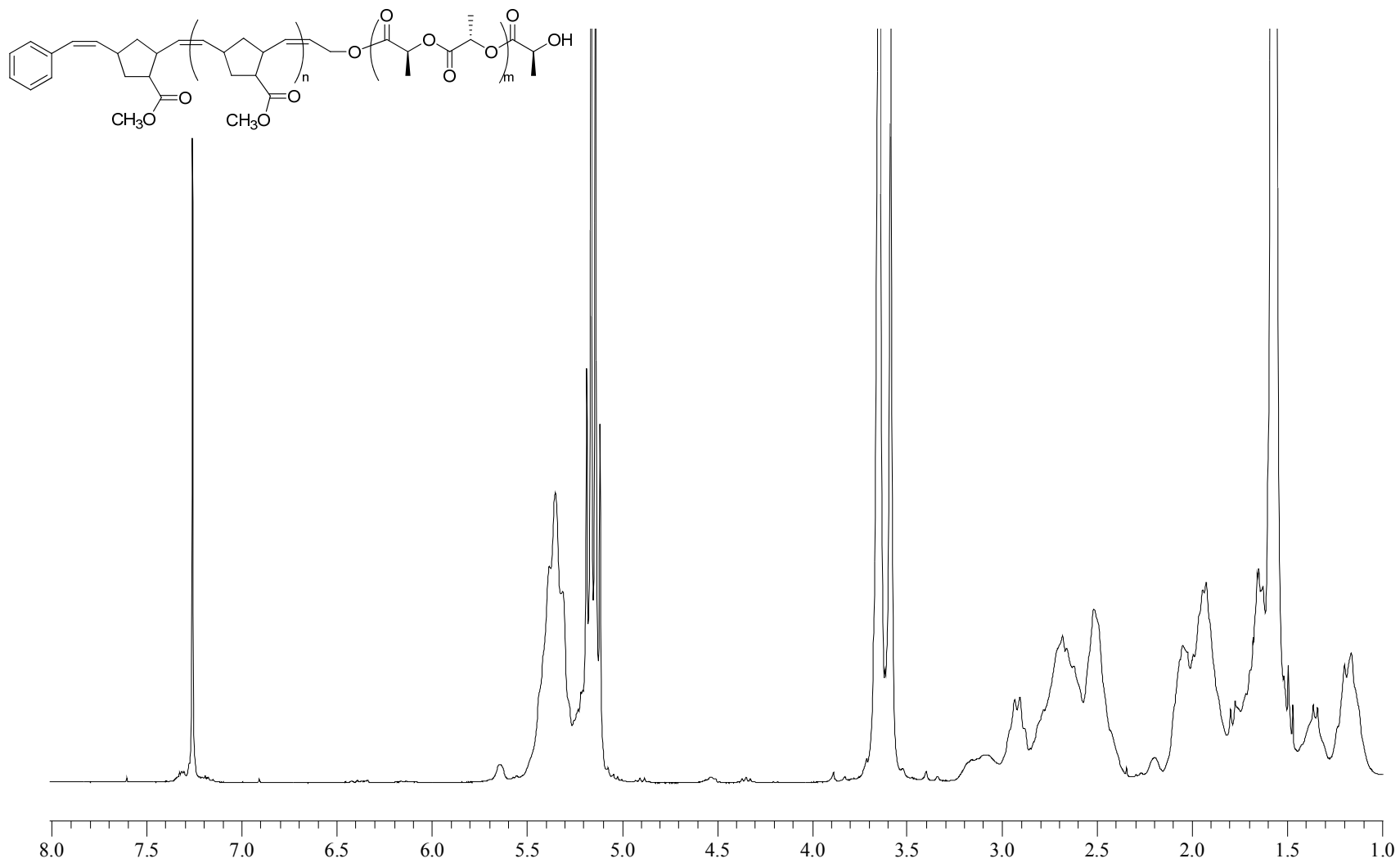


Figure B.32. ¹H NMR of PNb-*bl*-PLA diblock copolymer.

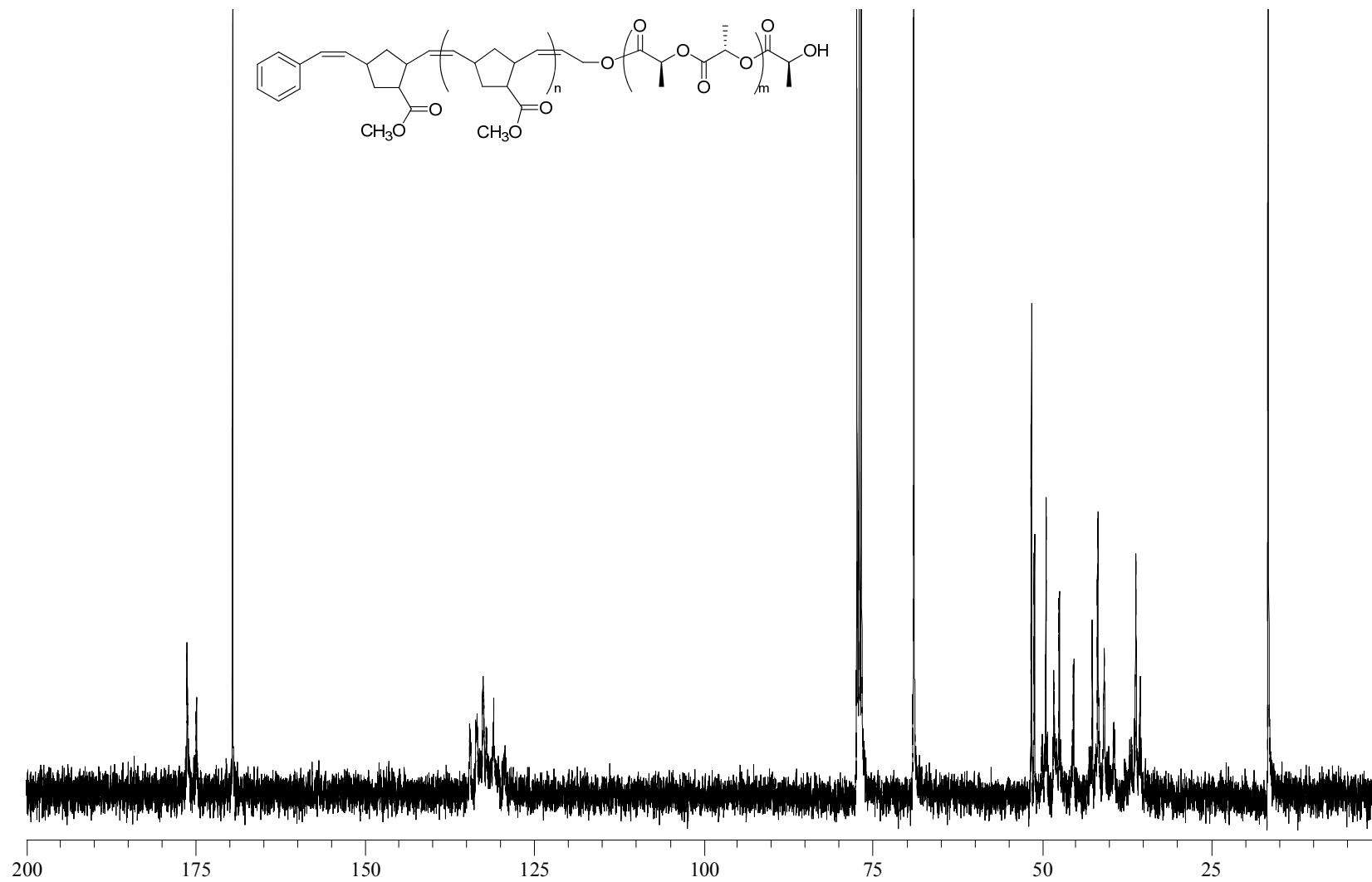


Figure B.33. ^{13}C NMR of PNB-*bl*-PLA diblock copolymer.

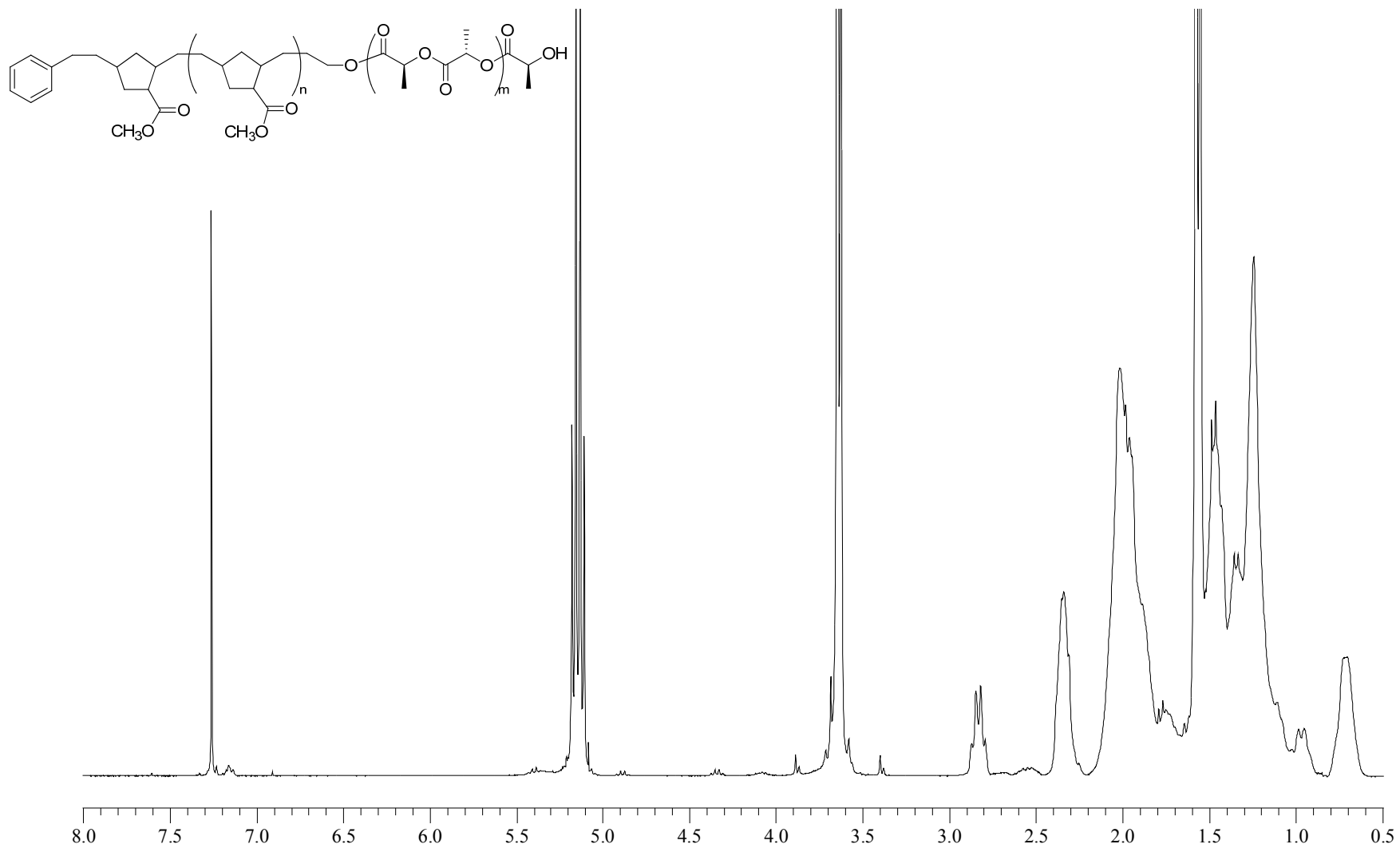


Figure B.34. ^1H NMR of hydrogenated PNb-*bl*-PLA diblock copolymer.

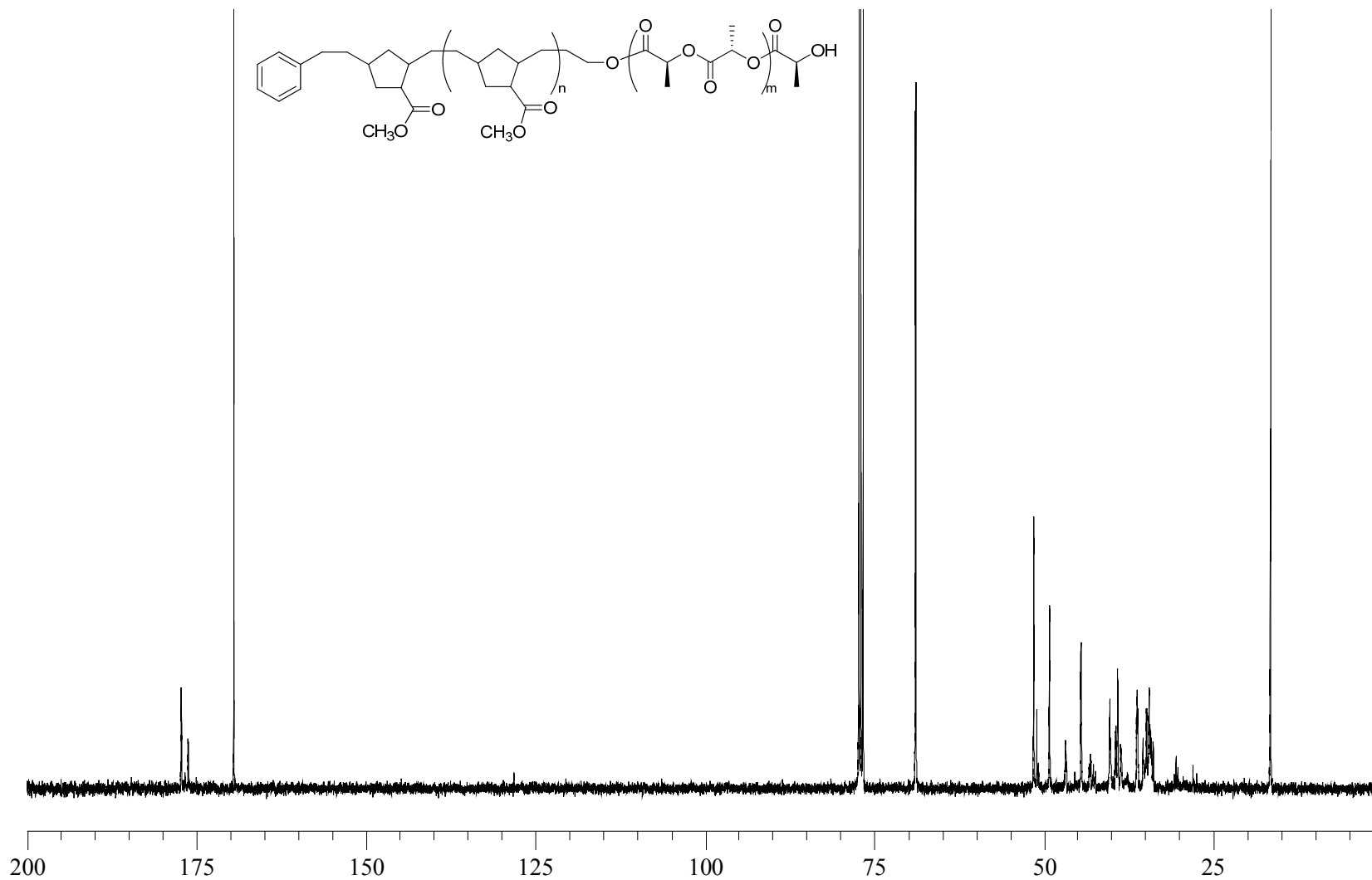


Figure B.35. ^{13}C NMR of hydrogenated PNb-*bl*-PLA diblock copolymer.

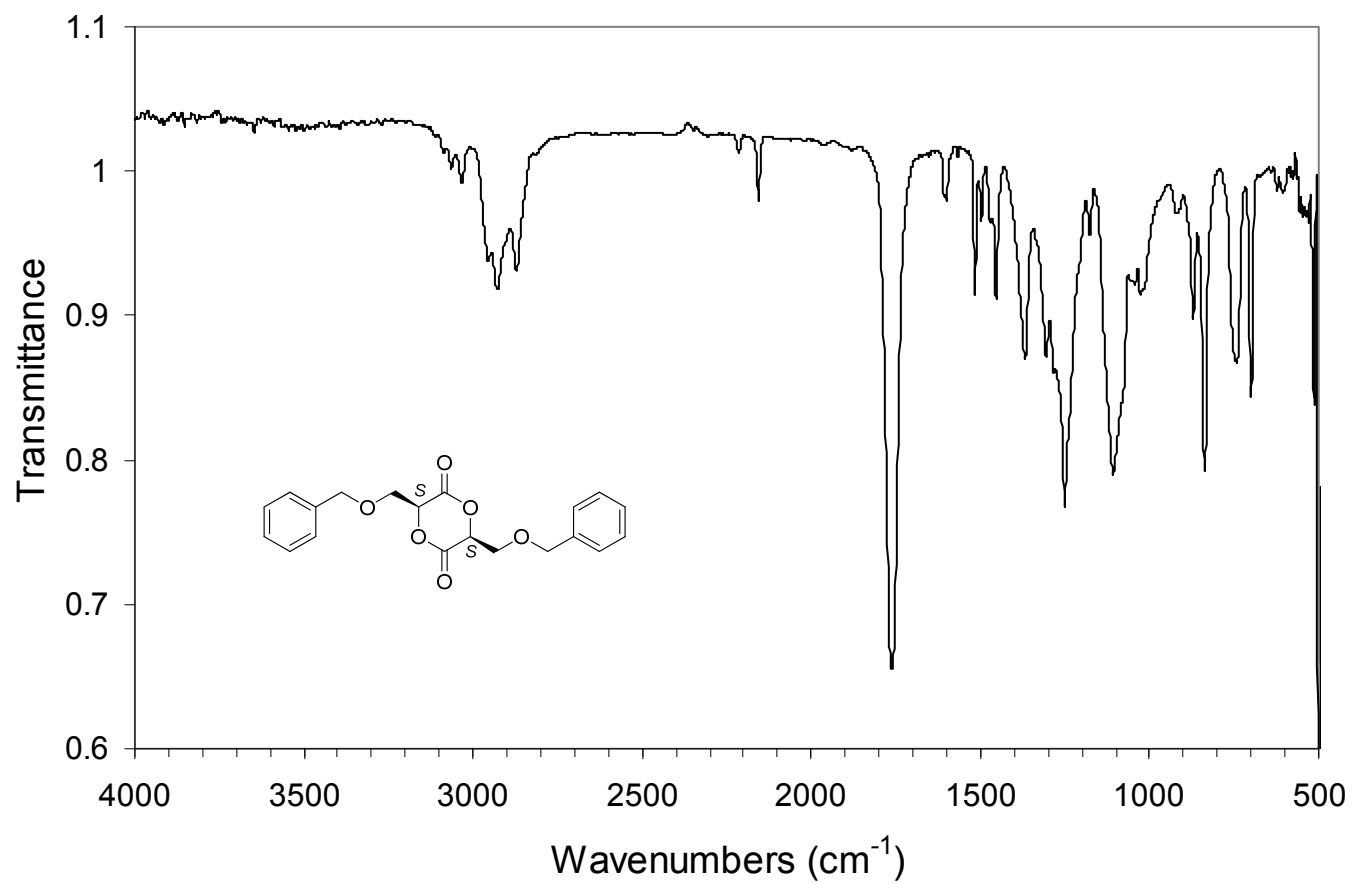


Figure B.36. ATR-IR spectra of (*S,S*)-3,6-(Benzyloxymethyl)-1,4-dioxane-2,5-dione (**2**).

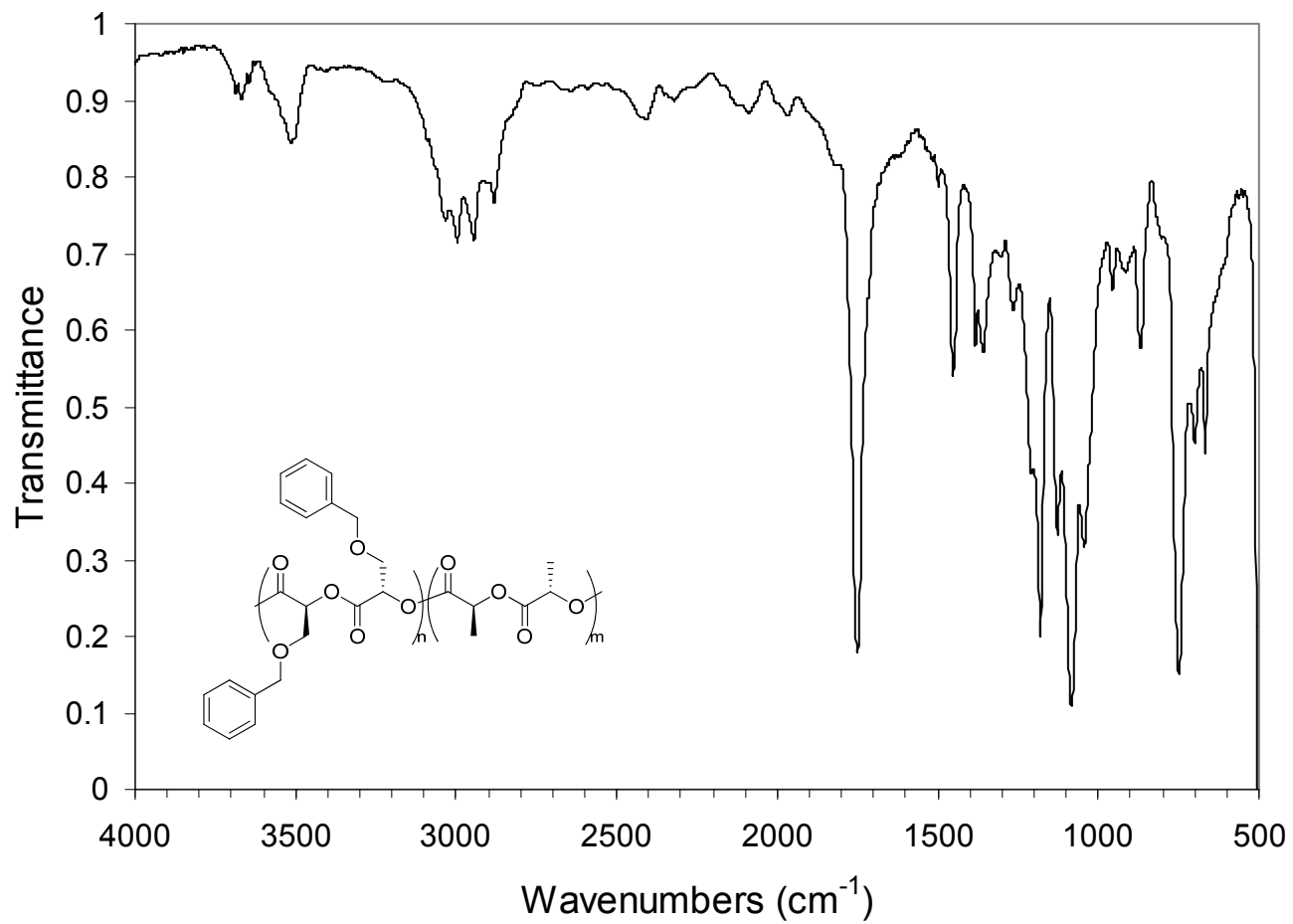


Figure B.37. ATR-IR spectra of dibenzoyloxy-substituted PLA copolymer **3**.

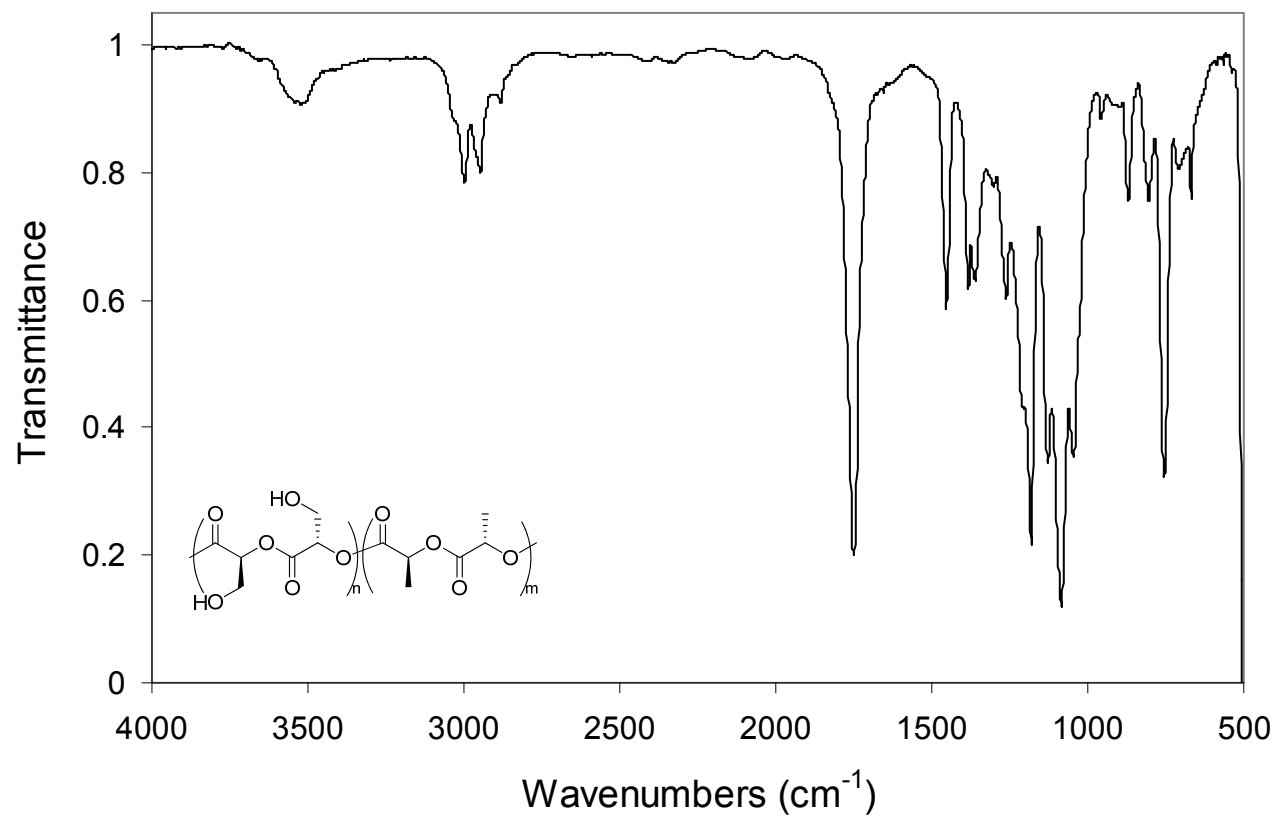


Figure B.38. ATR-IR spectra of hydroxy-bearing PLA copolymer 4.

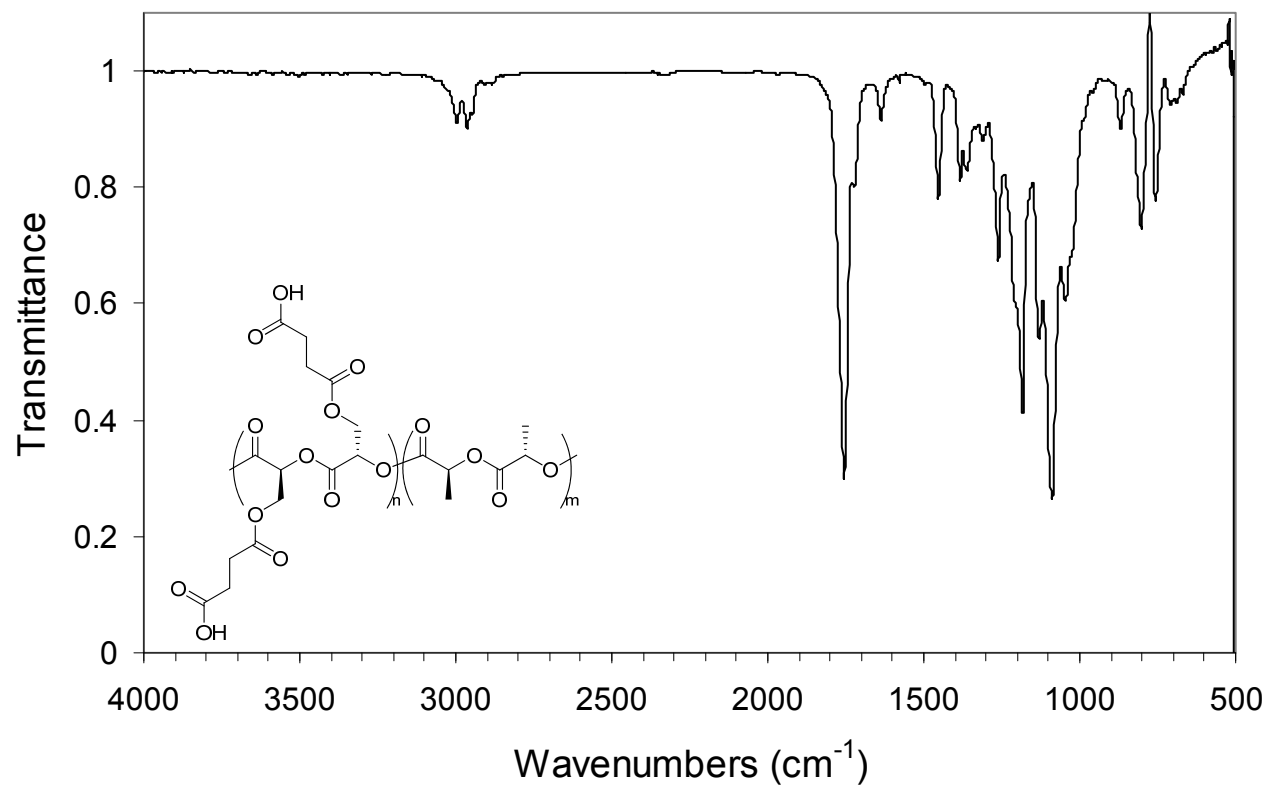


Figure B.39. ATR-IR spectra of succinic anhydride-modified PLA copolymer **5**.

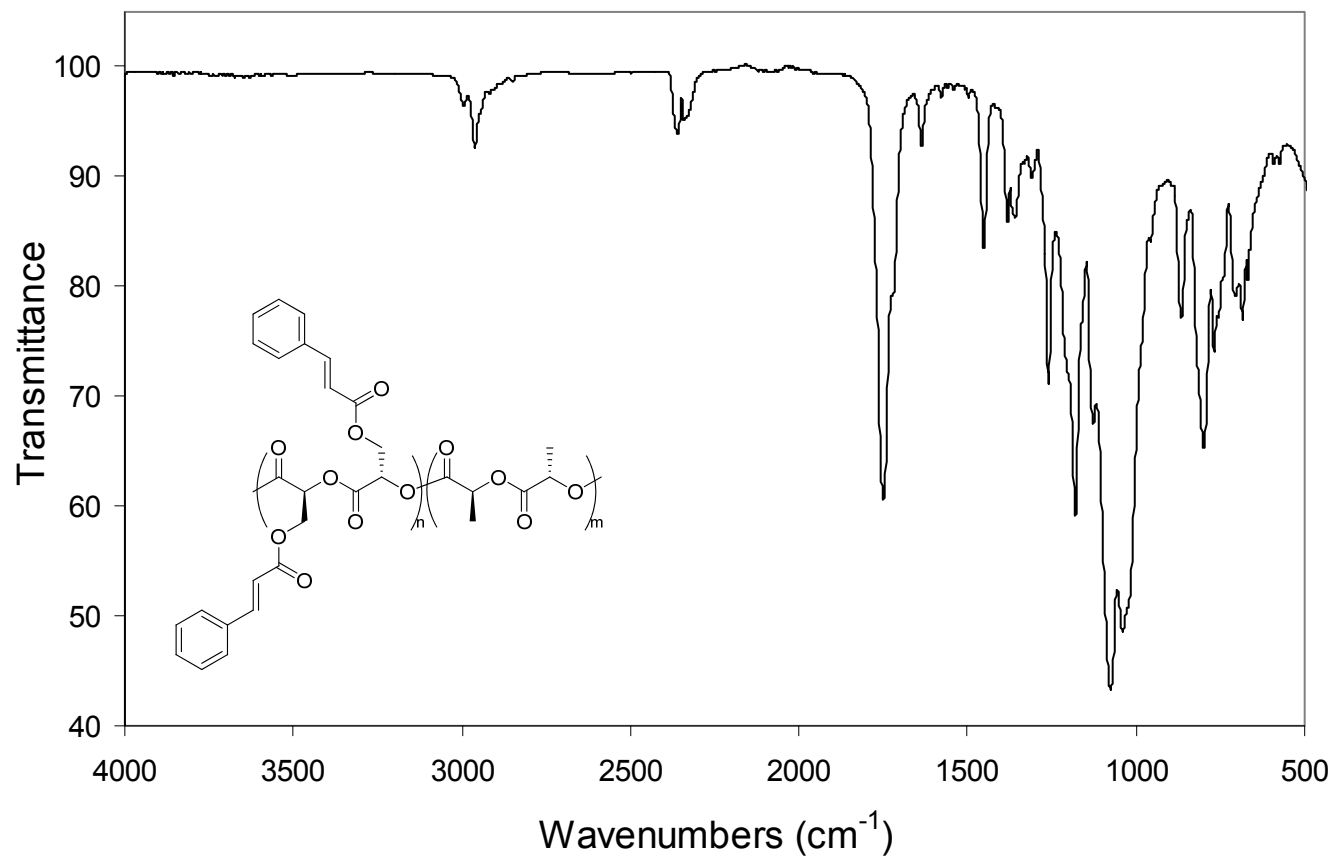


Figure B.40. ATR-IR spectra of cinnamate-modified PLA copolymer **5**.

VITA
DAVID E. NOGA

David Noga was born in Miami, Florida. He attended high school in Nashville, Tennessee, and received a B.S. in Chemistry from Middle Tennessee State University. In 2003, he began pursuing his doctorate degree in chemistry at Georgia Institute of Technology and started his work towards the synthesis of functional PLA copolymer scaffolds. He defended his thesis in June of 2008. When he is not working in the lab, he enjoys spending time with his wonderful wife, Jill, and their three turtles, George, Postal, and Silver.